COMPARING FORCE AND RATIO PROGRESSIONS FROM THE

BEHAVIORAL ECONOMIC UNIT PRICE EQUATION

BY

Shea Michelle Lemley

Submitted to the graduate degree program in the Department of Applied Behavioral Science and the Graduate Faculty of the University of Kansas in partial fulfillment of the requirements for the degree of Doctor of Philosophy

_____
Chair: David P. Jarmolowicz, Ph.D.

_____
Derek D. Reed, Ph.D., BCBA-D

_____
Vincent T. Francisco, Ph.D.

_____
Dean C. Williams, Ph.D.

_____
Stephen C. Fowler, Ph.D.

Date Defended: October 16, 2018

The Dissertation Committee for Shea Michelle Lemley

certifies that this is the approved version of the following dissertation:

Comparing Force and Ratio Progressions from the

Behavioral Economic Unit Price Equation

_____

Chair: David P. Jarmolowicz, Ph.D.

Date Approved: October 31, 2018

Abstract

In behavioral economic demand, the currently predominant conceptualization of unit price suggests that increasing lever weight or ratio requirement should result in equal changes in unit price and thus identical changes in consumption. Data from the few studies that have compared consumption under ratio progressions and force progressions tend to show differences in consumption across the two manipulations, even with unit price adjustments. These studies, however, failed to measure the broader operant class (i.e., subcriterion responses) and the force of individual responses, so the present experiments extend this work by using a force transducer to measure responding. In Experiment 1, six rats responded for sweetened condensed milk across ascending prices composed of ratio or force progressions equated based on unit price. Consistent with prior research, results showed consumption differed across progression types, with force progressions producing more inelastic consumption across low unit prices than ratio progressions. As force criterion increased, the proportion of subcriterion relative to total responses increased. Experiment 2 aimed to investigate how these subcriterion responses impacted the demand functions obtained from the force progressions. In Experiment 2, demand curves were obtained by yoking reinforcer-by-reinforcer to the total number of responses (i.e., subcriterion and criterion) per reinforcer delivery from the force progressions for each rat. Some similar patterns of consumption were observed across the force and yoked progressions, but deviations were noted. Convergence in consumption was assessed across several candidate alternatives to unit price, with the greatest convergence produced by measures of cumulative time integral of force per 0.05-ml unit of reinforcer and mean cumulative response duration per 0.05-ml unit of reinforcer.

Acknowledgements

I would like to thank the Society for the Advancement of Behavior Analysis for supporting this work with an Innovative Dissertation Research Grant.

Table of Contents

Introduction 1
Schedules of Reinforcement 1
Force 3
Force measurement. 3
Force as a dependent variable. 7
Force as an independent variable. 8
Force differentiation. 11
Reinforcer Magnitude. 14
Force and behavior regulation. 14
Behavioral Economics 16
Effort discounting. 17
Demand. 19
Modeling. 20
Aspects of demand. 24
Unit price. 26
Ratio progressions. 27
Reinforcer manipulations. 30
Time progressions. 32
Lever weight or force. 35
Purpose 39
Experiment 1 39
Method 39

Subjects. 39
Apparatus. 40
Procedure. 41
Experimental design. 43
Data Analysis 43
Operant analyses. 44
Behavioral economic analyses. 45
Price modifications. 45
Curve fitting. 48
Local elasticity analyses. 50
Statistical analyses. 50
Work data. 52
Results 53
Operant analyses. 55
Behavioral economic analyses. 64
Price modifications. 65
Individual curve fits. 68
Group curves. 76
Total work. 79
Discussion 81
Experiment 2 84
Method 84
Subjects. 84

Apparatus. 84
Procedure. 84
Experimental design. 85
Data Analysis 86
Operant analyses. 86
Behavioral economic analyses. 86
Results 87
Operant analyses. 89
Behavioral economic analyses. 93
Discussion 99
General Discussion 100
References 111
Tables 132
Appendices 216
A. Alternative Approaches to Analyzing Demand Data 216
B. Additional Analyses 224
C. Inconsistent Experiment 2 Consumption Data 280
D. Inconsistent Experiment 2 Response Rate Data 282
E. Email from ACU Facility Manager Describing Food Found after Cage Changes 283
F. Email from ACU Interim Director Detailing Dates of Cage Changes 284

List of Illustrative Materials

Table 1. Force measurement. 132

Table 2. Parameter values for demand curve assays..... 133

Table 3. Order of demand curve assays. 134

Table 4. Responses per reinforcer delivery in low reinforcer magnitude force progression. 135

Table 5. Responses per reinforcer delivery in high reinforcer magnitude force progression. 136

Table 6. Order of yoked assays. 137

Figure 1. Schematic illustrating force variations across time. 138

Figure 2. Sample demand curve and work function 139

Figure 3. Chamber schematic. 140

Figure 4. Consumption as a function of unit price across demand assays. 141

Figure 5. Consumption as a function of unit price in initial demand assays and replications. ... 142

Figure 6. Obtained mean peak force. 143

Figure 7. Peak force standard deviations. 144

Figure 8. Time integral of force for each response. 145

Figure 9. Response durations. 146

Figure 10. Proportion of subcriterion to total responses as a function of force criterion 147

Figure 11. Obtained ratio as a function of force criterion..... 148

Figure 12. Response rates from F-L and F-H progressions. 149

Figure 13. Response rates from R-L and R-H progressions. 150

Figure 14. Correlations between mean duration per response and mean cumulative time integral per reinforcer unit. 151

Figure 15. Correlations between mean duration per response and cumulative response duration per reinforcer unit. 152

Figure 16. Mean cumulative time integral of force per reinforcer unit and mean cumulative response duration per reinforcer unit. 153

Figure 17. IRT distributions from the F-L and R-L progressions for 1M. 154

Figure 18. IRT distributions from the F-H and R-H progressions for 1M. 155

Figure 19. IRT distributions from the F-L and R-L progressions for 2M. 156

Figure 20. IRT distributions from the F-H and R-H progressions for 2M. 157

Figure 21. IRT distributions from the F-L and R-L progressions for 3M. 158

Figure 22. IRT distributions from the F-H and R-H progressions for 3M. 159

Figure 23. IRT distributions from the F-L and R-L progressions for 4M. 160

Figure 24. IRT distributions from the F-H and R-H progressions for 4M. 161

Figure 25. IRT distributions from the F-L and R-L progressions for 1N. 162

Figure 26. IRT distributions from the F-H and R-H progressions for 1N. 163

Figure 27. IRT distributions from the F-L and R-L progressions for 2N. 164

Figure 28. IRT distributions from the F-H and R-H progressions for 2N. 165

Figure 29. Consumption as a function of unit price across various psychophysical scaling parameters. 166

Figure 30. Model comparisons using AICc for different price modifications. 167

Figure 31. Exponential demand curves fit to consumption as a function of unit price across all assessed prices, excluding prices with 0 consumption. 168

Figure 32. Exponential demand curves fit to consumption as a function of unit price across all assessed prices, including prices with 0 consumption (as 0.1). 169

Figure 33. Parameters and goodness-of-fit measures obtained from exponential demand curves fit to consumption as a function of the Hursh et al. (1988) unit price equation. 170

Figure 34. Local elasticity analysis for consumption as a function of unit price, sessions with 0 consumption excluded. 171

Figure 35. Local elasticity analysis for consumption as a function of unit price, sessions with 0 consumption included (as 0.1). 172

Figure 36. Slopes and P_{Max} as determined by local elasticity analyses. 173

Figure 37. Breakpoint comparisons based on unit price. 174

Figure 38. Exponential demand curves fit to consumption as a function of responses per reinforcer unit. 175

Figure 39. Exponential demand curves fit to consumption as a function of obtained unit price. 176

Figure 40. Exponential demand curves fit to consumption as a function of unit price adjusted with psychophysical scaling parameters. 177

Figure 41. Exponential demand curves fit to consumption as a function of obtained time integral of force per reinforcer unit. 178

Figure 42. Exponential demand curves fit to consumption as a function of mean cumulative response duration per reinforcer unit. 179

Figure 43. Derived parameters and goodness-of-fit measures for individual animals across different price conversions. 180

Figure 44. Results of AICc comparisons of single versus separate curves for each price conversion for each animal. 181

Figure 45. RMSE for a single curve and separate curves fit to each animal's progressions. 182

Figure 46. Exponential demand curves fit to aggregate consumption data as a function of unit price..... 183

Figure 47. Exponential demand curves fit to consumption data across different price modifications..... 184

Figure 48. Results of AICc comparisons for exponential demand curves fit to group consumption data. 185

Figure 49. Group RMSE for separate versus shared expontential demand curves with different price conversions. 186

Figure 50. Total work (criterion responses * force criterion) as a function of unit price. 187

Figure 51. Work function relating total responses and responses per reinforcer unit. 188

Figure 52. Work function based on obtained unit price..... 189

Figure 53. Work function based on psychophysical scaling adjustments of unit price. 190

Figure 54. Work function based on time integral of force. 191

Figure 55. Work function based on cumulative duration. 192

Figure 56. Schematic of yoking procedure. 193

Figure 57. Demand curves yoked to F-L progression by step. 194

Figure 58. Demand curves yoked to F-H progression by step. 195

Figure 59. Replications of demand curves yoked to original F-L and F-H progressions. 196

Figure 60. Demand curves yoked to replicated progressions by step. 197

Figure 61. Mean peak force as a function of step for yoked progressions. 198

Figure 62. Peak force standard deviation by step for yoked progressions..... 199

Figure 63. Time integral of force as a function of step for yoked progressions. 200

Figure 64. Mean duration per response as a function of step for yoked progressions..... 201

Figure 65. Response rate as a function of responses per reinforcer delivery for yoked progressions. 202

Figure 66. Correlations between mean duration per response and cumulative time integral of force per reinforcer unit for yoked progressions..... 203

Figure 67. Correlations between mean duration per response and cumulative response duration per reinforcer unit for yoked progressions. 204

Figure 68. Mean cumulative time integral of force per reinforcer unit and mean cumulative response duration per reinforcer unit as a function of responses per reinforcer unit. 205

Figure 69. Area under consumption curves across force and yoked progressions. 206

Figure 70. Single exponential demand curve fit to consumption as a function of unit price from all progressions from Experiment 1 and Experiment 2 for each animal..... 207

Figure 71. Single exponential demand curve fit to consumption as a function responses per reinforcer unit for all progressions from Experiment 1 and Experiment 2 for each animal. 208

Figure 72. Single exponential demand curve fit to consumption as a function of obtained unit price from all progressions for each animal from Experiment 1 and Experiment 2. 209

Figure 73. Single exponential demand curve fit to consumption as a function of unit price with psychophysical scaling parameter adjustments for all progressions for each animal from Experiment 1 and Experiment 2. 210

Figure 74. Single exponential demand curve fit to consumption as a function of cumulative time integral of force per reinforcer unit from all progressions for each animal from Experiment 1 and Experiment 2. 211

Figure 75. Single exponential demand curve fit to consumption as a function of cumulative response duration per reinforcerunit from all progressions for each animal from Experiment 1 and Experiment 2. 212

Figure 76. RMSE for a single exponential curve fit to each animal's data across all progressions for different price conversions. 213

Figure 77. Exponential curves fit to group Experiment 1 and Experiment 2 data across price modifications..... 214

Figure 78. Error from a single exponential curve fit to all rats' data from all Experiment 1 and Experiment 2 progressions for each price modification. 215

Figure A1. Consumption (ml) as a function of unit price (per ml) across demand assays. 216

Figure A2. Reinforcer deliveries as a function of cost per reinforcer delivery (FR x Force criterion) across demand assays. 217

Figure A3. Reinforcer deliveries as a function of unit price across demand assays. 218

Figure A4. Consumption as a function of cost per reinforcer delivery (FR x Force criterion) across demand assays 219

Figure A5. Comparisons using AICc of group data across different approaches to quantifying cost and benefit. 220

Figure A6. Normalized consumption as a function of normalized price, with consumption and price normalized based on consumption at first assessed price within each progression. 221

Figure A7. Normalized consumption as a function of normalized price, with consumption and price normalized based on consumption at first price within each reinforcer magnitude 222

Figure A8. Comparisons using AICc of group data across different normalization approaches 223

Figure B1. Peak force distributions from the R-L and F-L progressions for 1M. 224

Figure B2. Peak force distributions from the R-H and F-H progressions for 1M. 225

Figure B3. Peak force distributions from the R-L and F-L progressions for 2M. 226

Figure B4. Peak force distributions from the R-H and F-H progressions for 2M. 227

Figure B5. Peak force distributions from the R-L and F-L progressions for 3M. 228

Figure B6. Peak force distributions from the R-H and F-H progressions for 3M. 229

Figure B7. Peak force distributions from the R-L and F-L progressions for 4M. 230

Figure B8. Peak force distributions from the R-H and F-H progressions for 4M. 231

Figure B9. Peak force distributions from the R-L and F-L progressions for 1N. 232

Figure B10. Peak force distributions from the R-H and F-H progressions for 1N. 233

Figure B11. Peak force distributions from the R-L and F-L progressions for 2N. 234

Figure B12. Peak force distributions from the R-H and F-H progressions for 2N. 235

Figure B13. Cumulative response duration per reinforcer delivery, interreinforcement intervals, and difference..... 236

Figure B14. Mean duration per response as a function of responses per reinforcer unit. 237

Figure B15. Detailed cumulative record for 4M. 238

Figure B16. Detailed cumulative record for 2N. 239

Figure B17. Cumulative records for the F-L and R-L progressions for 1M. 240

Figure B18.Cumulative records for the F-H and R-H progressions for 1M. 241

Figure B19. Cumulative records for the F-L and R-L progressions for 2M. 242

Figure B20.Cumulative records for the F-H and R-H progressions for 2M. 243

Figure B21. Cumulative records for the F-L and R-L progressions for 3M. 244

Figure B22. Cumulative records for the F-H and R-H progressions for 3M. 245

Figure B23. Cumulative records for the F-L and R-L progressions for 4M. 246

Figure B24. Cumulative records for the F-H and R-H progressions for 4M. 247

Figure B25. Cumulative records for the F-L and R-L progressions for 1N. 248

Figure B26. Cumulative records for the F-H and R-H progressions for 1N..... 249

Figure B27. Cumulative records for the F-L and R-L progressions for 2N. 250

Figure B28. Cumulative records for the F-H and R-H progressions for 2N..... 251

Figure B29. Reinforcer units earned at first assessed unit price and first matched unit price.... 252

Figure B30. Consumption as a proportion of consumption in a comparison condition across unit prices. 253

Figure B31. Proportions for fitted parameters obtained from consumption as a function of unit price..... 254

Figure B32. Breakpoint comparisons based on unit price. 255

Figure B33. Proportions comparing derived parameters across different price conversions. 256

Figure B34. Peak force distributions for yoked progressions for 1M..... 257

Figure B35. Peak force distributions for yoked progressions for 2M..... 258

Figure B36. Peak force distributions for yoked progressions for 3M..... 259

Figure B37. Peak force distributions for yoked progressions for 4M..... 260

Figure B38. Peak force distributions for yoked progressions for 1N. 261

Figure B39. Peak force distributions for yoked progressions for 2N. 262

Figure B40. Cumulative response duration per reinforcer delivery and interreinforcement intervals. 263

Figure B41. Duration per response as a function of responses per reinforcer. 264

Figure B42. Detailed cumulative record for yoked progressions for 4M. 265

Figure B43. Detailed cumulative record for yoked progressions for 2N. 266

Figure B44. Cumulative record for yoked progressions for 1M. 267

Figure B45. Cumulative record for yoked progressions for 2M. 268

Figure B46. Cumulative record for yoked progressions for 3M. 269

Figure B47. Cumulative record for yoked progressions for 4M. 270

Figure B48. Cumulative record for yoked progressions for 1N. 271

Figure B49. Cumulative record for yoked progressions for 2N. 272

Figure B50. IRT distributions for 1M yoked progressions. 273

Figure B51. IRT distributions for 2M yoked progressions. 274

Figure B52. IRT distributions for 3M yoked progressions. 275

Figure B53. IRT distributions for 4M yoked progressions. 276

Figure B54.IRT distributions for 1N yoked progressions. 277

Figure B55.IRT distributions for 2N yoked progressions. 278

Figure B56. Proportions comparing force and yoked progression AUCs. 279

Figure C1. Inconsistent consumption data from the Y-F-L condition. 280

Figure C2. Inconsistent consumption data from the Y-F-H condition. 281

Figure D1. Inconsistent response rates. 282

Figure E1. Cage change observations. 283

Figure F1. Dates of cage changes. 284

Comparing Force and Ratio Progressions from the Behavioral Economic Unit Price Equation Introduction

Behavior analysis is concerned with the description, prediction, and control of behavior (Moore, 1981; Skinner, 1953). Critical to description, prediction, and control is the theoretical assumption–tested through extensive empirical investigation–that behavior is a function of its consequences (Catania, 1973; Ferster & Skinner, 1957; Moore, 2011; Skinner, 1953). Early research captured this observation in the law of effect, which states that those responses that produce satisfying consequences are more likely to be repeated, whereas those that produce dissatisfying consequences become less likely (Thorndike, 1898). Skinner sought to further develop general laws of behavior, and toward this end, he selected brief, discrete responses that permitted relatively easy measurement and control (Shull & Lawrence, 1998). From experimental arrangements with brief discrete responses, Ferster and Skinner (1957) examined how variations in the delivery of consequences (i.e., reinforcers) changed the temporal patterning of behavior absent other constraints.

Schedules of Reinforcement

Ferster and Skinner (1957) illustrated how various arrangements of reinforcer delivery, which they termed schedules of reinforcement, produced systematic patterns of responding. The most basic schedule arrangement consists of continuous reinforcement (CRF), in which every response is reinforced; by contrast, in extinction (EXT), the response-reinforcer contingency is terminated (Catania, 2013). On intermittent schedules only some responses are reinforced. The most basic intermittent schedules can be described by whether reinforcement is contingent on number of responses (i.e., ratio schedules) or the first response after a specified amount of time has elapsed (i.e., interval schedules; Ferster & Skinner, 1957). Fixed ratio (FR) schedules arrange

reinforcer delivery for a set number of responses, whereas variable ratio (VR) schedules program reinforcer delivery for a number of responses that averages to the schedule value (Ferster & Skinner, 1957). For example, a VR5 schedule might program reinforcer deliveries contingent on four, eight, and then three responses, averaging to five responses per reinforcer. Similarly, on a fixed interval (FI) schedule the first response after a set amount of time is reinforced, whereas on variable interval (VI) schedules, the first response after a variable amount of time, which averages to the schedule value, is reinforced (Ferster & Skinner, 1957).

Another type of intermittent schedule, differentiation schedules program reinforcement contingent on responses demonstrating a specific property (Zeiler, 1977). Common differentiation schedules include differential reinforcement of high (DRH) and low rates (DRL) of behavior, which program reinforcement for responses that occur within a certain time frame or separated by a minimum time period, respectively (Ferster & Skinner, 1957). For example, on a DRL 20-s schedule, only a response emitted 20 s or more after the previous response would be reinforced.

Responding produced by various schedules can be quantified in varying wats, including rate, interresponse time (IRT), and postreinforcement pause (PRP). Among the most common dimensions is rate of responding, calculated by dividing number of responses by the period of time in which they occurred. Similarly, IRT is the time between two discrete responses. The PRP (also called “preratio pause” or “between ratio pause"; Griffiths & Thompson, 1973) describes the time between a reinforcer delivery and the next response.

Schedules of reinforcement produce systematic patterns of responding. Ratio schedules tend to produce high rates of responding, relative to more moderate rates observed on interval schedules. In particular, FR schedules produce a “break and run” pattern in which high rates of

responding are followed by a pronounced PRP, whereas VR schedules tend to produce high and consistent rates of responding with no such pause. Similarly, FI schedules tend to produce a scallop pattern in which responding gradually increases toward the end of the interval, whereas VI schedules produce more consistent, yet relatively low rates.

Behavior analytic researchers have traditionally examined behavior under interval or ratio based schedules (Baum, 2002; Skinner, 1966), and other schedules and dimensions of responding have been less commonly manipulated. For example, contingencies can be programmed for response duration (Skinner, 1938), which is the length of time from the start to end of a response. Because experimental arrangements within behavior analysis have traditionally emphasized discrete responses (Baum, 2002), this dimension is less commonly examined (cf. Gulotta & Byrne, 2015; Peck & Byrne, 2016). Similarly, force is less commonly studied than rate (cf. Fowler, 1987; Mitchell & Brener, 1991).

Force

When a behavior operates on the environment, it exerts some degree of force across time (Fowler, 1987; Notterman & Mintz, 1965).The study of force draws from physics for definition and measurement. In physics, force is defined by change in states of rest or motion (Notterman & Mintz, 1965), and operational definitions of behavior similarly require "measurable change in at least one aspect of the environment" (Johnston & Pennypacker, 1980) and thus some emission of force (Notterman & Mintz, 1965). Force is commonly specified in grams (g), a unit of mass, but force may also be described in Newtons (N; kg-m/s^2; 101.9 g = 1 N), a measure of force or weight.

Force measurement. Force measurement or manipulation varies based on the experimental arrangement and apparatus used. Traditionally, operant studies have used standard

levers with weights that can be adjusted by changing the tension of a spring. The force required to depress many commonly available levers (e.g., Med Associates model ENV-110M) initially comes set at 25 g, but this requirement may be set as low as 15 g or as high as 100 g. With this apparatus, a response is defined as any contact with the lever whose force meets or exceeds the lever weight, closing an electronic switch (i.e., a binary response). Thus, a response is recorded if an electric switch is closed. By contrast, force transducers measure the forces emitted throughout the time course of an organism's response (Fowler, 1987; Notterman & Mintz, 1965).

Force transducers have several advantages over the traditional lever arrangements. First, force transducers are fixed or stationary, meaning that exteroceptive consequences (e.g., the audible click and spatial movement of a traditional lever) can be withheld or scheduled separately (Notterman & Mintz, 1965). Control over these consequences permits the examination of the effects of these consequences, as well as study of interoceptive consequences (Notterman & Mintz, 1965). Second, over time, researchers have moved the force transducer outside of the chamber (Fowler, 1987). With this modification, the operandum is accessible through a small opening, constraining the topographies with which the rat can depress the lever to a forelimb press (Fowler, 1987). Thus, although the response is still defined independent of topography, fewer topographical variations can be emitted. Third, force transducers are sensitive to a wide range of forces and can measure the force emitted throughout the time course of a response, including forces below the force requirement programmed in a reinforcement contingency (i.e., subcriterion responses; Notterman & Mintz, 1965). Such measurement allows for recording and calculating additional dimensions of each response.

Additional measurement is possible in experimental arrangements using force transducers (see Table 1). A threshold for response detection is programmed to filter noise resulting from

vibrations or electrical fluctuations (e.g., 4 g; Fowler, 1987; Notterman & Mintz, 1965). Because force occurs in time and varies within a single response, the force of every response is measured across any manipulation of the operandum, starting from the time a response force exceeds the threshold to the time the force drops below the threshold (see Figure 1). This results in a unique curve for every response, with force emission measured throughout the duration of the response. Additional measurements can then be determined for each response. The peak force of the response is defined as the maximum force obtained at any point during the response (Notterman & Mintz, 1965). The duration of each response is also measured; with a traditional lever arrangement, a response is a discontinuous event involving switch closure, so response duration is rarely collected (cf. Peck & Byrne, 2016). The time integral of force is the area under the force curve across the entire duration of the response (Notterman & Mintz, 1965). This measure is often discussed as effort because it approximates the total effort output of a given response (Fowler, 1987; Notterman & Mintz, 1965). The average force of a response is its time integral divided by its duration, resulting in the average force emitted at each point in time (Notterman & Mintz, 1965). Although measurement of response rate (i.e., responses/time) remains the same across the two arrangements, measurement of IRTs differs. In the traditional lever arrangement, an IRT is calculated from one switch closure to the next, whereas IRTs in the force literature are recorded from the time one response drops below threshold to the time another response exceeds the threshold (Fowler, 1987).

In research using force transducers, reinforcement contingencies can be programmed on any response force dimensions (e.g., peak force or time integral), in addition to those more commonly used in operant research (e.g., rate). For example, the closest analog to the traditional weighted lever arrangement involves establishing a peak force criterion; in this approach, any

response whose peak force exceeds the peak force criterion counts toward the reinforcement contingency (Notterman & Mintz, 1965). Other measures can be calculated from the additional dimensions of responding recorded by the force transducer. For example, average constant error (Slifkin, Mitchell, & Brener, 1995) indexes how much response force deviates from the programmed force contingency and is calculated by subtracting the peak force criterion from the mean peak force. Other studies have programmed contingencies on time integral of force (measured in gram-seconds and abbreviated g-s), either for a single response (Notterman & Mintz, 1965) or summed across multiple responses (Morefield, 1964; Notterman & Mintz, 1965).

Unlike the weighted lever, however, the force tranducer permits recording of every response, including those above, at, and below a programmed force criterion. Those responses that are below the force criterion but above the threshold are termed subcriterion responses. Miller (1970) suggested that different force criteria define different operant classes; changing force criteria, however, might also be viewed as selecting subclasses of the same operant response class (Catania, 1973; Zarcone, Chen, & Fowler, 2009). That is, subcriterion responses may be viewed as part of the broader operant class, defined by its functional rather than descriptive properties (Catania, 1973, 2013; Pinkston & Libman, 2017). Thus, the descriptive operant class includes only those responses for which consequences are arranged, but the functional operant class includes all of the responses generated by reinforcement, even those above or below the force programmed in the reinforcement contingency (Catania, 1973). Evidence for a range of forces comprising the same operant class comes from a study in which pigeons were trained to peck an illuminated key with elevated force (Cole, 1965). During an extinction condition, pigeons tended to emit the highest forces on keys of similar brightness, with

force of pecking decreasing as similarity to the original key decreased; the force generalization gradients produced under these conditions were consistent with those found for response rate (Cole, 1965).

Force as a dependent variable. A number of studies have used force transducers to evaluate changes in force emission as a function of other operant schedules. For example, Notterman (1959) found that rats' peak force was high and variable during acquisition on a CRF (i.e., FR1) schedule but later decreased and stabilized around twice the force threshold. Cole (1965) found that pigeons' time integral of force was low and relatively stable during acquisition.

On larger FR schedules, research suggests that force varies as a function of response location within the ratio run (Mintz, 1962; Notterman & Mintz, 1965; Pinkston & McBee, 2014); generally these patterns suggest lower peak force immediately after reinforcer delivery that either increases (Mintz, 1962) or forms a bitonic function, increasing across after the first response and then decreasing toward the end of the run (Pinkston & McBee, 2014). Procedural differences may account for these observed differences in force within ratio runs; Mintz (1962) reported data collected on the twelfth day of exposure to the schedule, whereas Pinkston and McBee (2014) reported data averaged across six days in which rate was determined to be stable. The patterns of force emission observed on FR schedules may serve a proprioceptive cueing function (Mintz, 1962; Notterman & Mintz, 1965; Pinkston & McBee, 2014), in which changes in response force aid in discriminating the FR contingency. Such variations are generally not seen on VR or VI schedules (Mintz, Samuels, & Barber, 1976; Notterman & Mintz, 1965), although Gollub and Lee (1966) found response force increased throughout the interval on a FI 60 s schedule (i.e., positively accelerated across the interval). Pinkston and McBee (2014) also found that IRTs

decreased toward the end of a ratio run (Pinkston & McBee, 2014). Higher peak forces are also unlikely to follow longer IRTs, and IRTs show more variability than response peak force immediately after reinforcer delivery (Notterman & Mintz, 1965). Using another experimental arrangement (not a force transducer) that permitted measurement of subcriterion responses, Skinner (1938) observed greater mean peak forces under FR2 than FR1 schedules of reinforcement (p. 318), and Mintz (1962) found greater force emission with longer sequences of unreinforced responses on FR schedules. Importantly, these findings together suggest that each response within a ratio is not identical, and that "effort costs" to the organism may vary across the ratio run (Pinkston & McBee, 2014). Such findings may have implications for arrangements in which price is manipulated using changing ratio requirements; the nominal change in ratio value may not describe the obtained changes in price.

During extinction, Skinner (1938) found that response force increased before dropping to very low levels, and he further indicated that changes in peak force were relatively independent of changes in rate. Consistent with these findings, Notterman (1959) reported that peak force increased during extinction, but Notterman also found that elevated peak force was persistent relative to rate increases during extinction. During training on a mult[1] FR1 EXT schedule, Notterman and Block (1960) found greater force emission in the extinction component. In the EXT component, elevated force emerged before rate of responding decreased and persisted even after rate decreased. The authors suggest that these initial differences may be attributed to an increase in force of responding after the change in schedule components.

Force as an independent variable. Although ratio and interval schedules are more commonly studied, operant psychologists have also conducted research manipulating force

[1] A multiple schedule is one in which two schedules alternate, and correlated stimuli are presented with the schedule in effect (Catania, 2013).

requirements. Many of these studies program differential reinforcement using weighted levers and show reductions in rate and increases in pausing, which some attribute to aversive properties of force (Alling & Poling, 1995; Chung, 1965). For example, across interval (Chung, 1965; Keehn, 1981) and ratio (Alling & Poling, 1995) schedules, researchers have found reductions in response rate with increasing force requirements. On ratio schedules, increasing the force requirement increases IRTs and PRPs (Adair & Wright, 1976; Alling & Poling, 1995; Miller, 1970). On two-component schedules, higher force requirements increased pausing to the first response on the component with the higher force requirement on both chained (Miller, 1970) and multiple schedules (Wade-Galuska, Perone, & Wirth, 2005), especially given a low-to-high force transition (Wade-Galuska et al., 2005). Although consistent across studies, these reductions in rate and increases in pausing only reflect changes in the temporal distribution of criterion responses. Because subcriterion responses were not recorded, conclusions about the aversiveness of force from these studies must be interpreted carefully. Effects of force contingencies on the entire operant class (i.e., subcriterion and criterion responses) can not be determined (Zarcone et al., 2009).

Findings from research using force transducers, however, are inconsistent with suggestions that force is aversive. For example, Zarcone, Chen, and Fowler (2007, 2009) found an increase in mice's overall rate of responding (i.e., rate calculated using both subcriterion and criterion responses) as peak force criteria increased on a CRF schedule, even as the rate of criterion responding decreased. Zarcone et al. (2009) suggested that as peak force criterion increased, patterns of responding resembled those obtained from intermittent schedules of reinforcement when the peak force requirement was within the organism's capacity. Once peak force began to exceed this capacity, however, responding tended to show signs of ratio strain or

extinction, even though the programmed ratio requirement remained FR1 (p. 270). Pinkston and Libman (2017) reported similar findings on FR5 schedules across a range of force criteria. Specifically, as force criteria increased, rates of criterion responding decreased but overall rates (including subcriterion and criterion) increased. A byproduct of this increase in subcriterion responses was an increase in the responses to reinforcer ratio (i.e., obtained ratio schedule; Pinkston & Libman, 2017, p. 81).

Relatedly, Pinkston and Libman (2017) noted greater latency from reinforcer delivery to the first criterion response at higher force criteria, but latency to the first response (criterion or subcriterion) was not different across force criteria. These results suggest longer PRPs observed in force experiments using weighted levers may be an artifact of a failure to measure subcriterion responses. Response duration also tends to increase as peak force increases, as more time is required to attain higher peak forces (Notterman & Mintz, 1965). Peak force also does not completely return to baseline after experience with high peak force criteria on interval (Gollub & Lee, 1966) and ratio schedules (Mitchell & Brener, 1991; Pinkston & Libman, 2017).

Reinforcement contingencies can also be arranged on time integral of force (Morefield, 1964; Notterman & Mintz, 1965). Morefield (1964) arranged for reinforcer delivery on a fixed effort schedule (i.e., on a fixed effort 30 g-s schedule, a single 30-g-s response would result in reinforcement, but so would five responses of 6 g-s). On this fixed effort schedule, the time integral of a series of responses accumulated until it met a set requirement (i.e., 30, 60, 120, and 240 g-s for four different groups of rats). Morefield found that number of responses per reinforcer increased as a monotonic function of increasing time integral requirement, but time integral (effort) per response increased in an asymptotic or bitonic fashion. Rats' PRPs also increased on this schedule, resulting in lower overall response rates and reinforcement rates as a

function of increasing time integral. In their investigations of fixed effort schedules, Notterman and Mintz (1965) similarly studied rats' responding on fixed effort schedules, also finding an increase in PRPs with increasing time-integral requirements. Additionally, they suggest that placing contingencies on time integral tended to result in a "sustained force response," in which both duration and peak force increased to meet the time integral contingency.

Force differentiation. Programming contingencies on response force requires the response form vary from instance to instance (Notterman & Mintz, 1965; Skinner, 1938). Skinner (1938) referred to the particular type of discrimination involved in changing the form of a response as differentiation (p. 309). Notterman and Mintz (1965) suggest that the key difference between discrimination and differentiation is whether the discriminative stimuli are exteroceptive (such as experimenter programmed cue lights) or interoceptive (e.g., proprioceptive, cutaneous, or kinesthetic stimuli produced by a response, p. 83). Through the procedure of differential reinforcement—wherein contingencies are programmed on some dimension of the force of the response—differentiation occurs as responses meeting the criterion are selected and become more likely, while those responses not meeting the criterion become less likely. Notterman and Mintz (1965) suggest that both exteroceptive and interoceptive stimuli are involved in force differentiation. Removal of proprioceptive stimuli via analgesia of rats' paws reduced the percentage of responses meeting force criterion but did not entirely abolish force differentiation (Notterman & Mintz, 1965). Addition of exteroceptive consequences (e.g., tone) improves differentiation, whether presented during (Notterman & Mintz, 1965) or immediately after (Slifkin & Brener, 1998) a response. The consequences produced by responses are essential for selection of response dimensions in differentiation.

Force differentiation schedules produce orderly effects on behavior. At lower force criteria, organisms tend to emit mean peak forces beyond the scheduled requirement, but at higher force criteria, more peak forces fall below the force criteria; Thus, as peak force criterion increases, the proportion of subcriterion to criterion responses tends to increase, even as the mean peak force of responding increases (Zarcone et al., 2009). These data are consistent with data observed on other response differentiation schedules (e.g., DRL; Sidman, 1955; Wilson & Keller, 1953). Moreover, mean peak force tends to increase as a linear function of peak force criterion, but with a slope less than one (Notterman & Mintz, 1965; Slifkin, Mitchell, & Brener, 1995). As peak force criterion increases, the frequency distribution of peak force tends to widen (Notterman & Mintz, 1965; Pinkston & Libman, 2017). Differentiation tends to improve across sessions at a set force criterion, with the proportion of responses meeting criterion increasing across sessions until it stabilizes (Mitchell & Brener, 1991; Notterman & Mintz, 1965). For example, Mitchell and Brener (1991) assessed rats' CRF performance across an increasing, parametric range of 10 peak force criteria, each of which was run for six consecutive sessions. The number of subcriterion responses increased with each increase in peak force criterion but decreased across the six sessions at that force value. Analyses revealed that mean peak force significantly increased within the first 20 reinforcer deliveries at each new criterion. Few other consistent changes were observed in operant measures (e.g., peak force, response duration, time to peak force within a response) across the six sessions at each force value.

Two common conceptualizations have related discrimination and strength of stimuli: Weber's law and Steven's power law. Weber's law suggests a logarithmic relation between the strength of a stimulus and its discrimination (Gibbon, 1977). In this conceptualization, the "just noticeable difference" (jnd) describes the smallest change in the magnitude of a stimulus capable

of being discriminated; dividing the jnd (i.e., necessary change in stimulus; ΔS) by the magnitude of the stimulus (S) results in the Weber ratio, ΔS/S (Gibbon, 1977). A measure proportional to the Weber ratio, the coefficient of variation is expressed as a ratio of response standard deviations to mean criterion values (Bizo, Chu, Sanabria, & Killeen, 2006). This treatment has also been extended to differentiation of response duration (Ferraro & Grilly, 1970) and response force (Mintz & Notterman, 1965; Notterman and Mintz, 1965). In force differentiation, Mintz (1965) suggested that the ratio of the standard deviations of the obtained peak forces to the peak force criterion (ΔF/F) provides an index of the relation between response variability and required magnitude of force that is comparable to the Weber ratio. Although Notterman and Mintz (1965) noted that increases in peak force standard deviation at higher force criteria are consistent with the relation between the jnd and stimulus magnitude, changes in peak force as a function of force criterion tend to fall below the changes predicted by Weber's law (Pinkston & Libman, 2017). Relatedly, Steven's power law posits a parabolic relation between stimulus strength and response strength (Staddon, 1978; Stevens, 1957) that takes the form

$$y = kx^s \qquad \text{Equation 1}$$

where y is the perceived magnitude of a stimulus x, k is a constant, and s is an exponent reflecting scaling of stimulus magnitude, which differs depending on the type of stimulus. From laboratory work with humans, the exponent for scaling force is generally suggested to be 1.7 (Stevens & Cain, 1970; Stevens & Mack, 1959), but has been reported to range from 0.8 to 2.0 (Jones, 1986). To my knowledge, however, no studies have determined an exponent for scaling force in rats.

Although programming a minimum peak force criterion requires differentiation of responding, researchers have also programmed force band criteria, which require the peak force

of a response to fall within a specified range with upper and lower bounds (Notterman & Mintz, 1965). Force band studies show that differentiation improves with experience of contingencies (Notterman & Mintz, 1965), that within band responding can be brought under stimulus control (Notterman & Mintz, 1962), and that responding can be differentiated across different topographies (i.e., plate press and chain pull; Kirkpatrick & Fowler, 1989).

Reinforcer Magnitude. Magnitude of reinforcement also impacts peak force differentiation. Fowler (1987) found that higher magnitude reinforcement results in lower peak forces. Relatedly, Di Lollo, Ensminger, and Notterman (1965) assessed the role of magnitude of reinforcement in a study using five groups of rats earning different numbers of pellets (1, 2, 3, 4, or 5) for each criterion response (8 g). In acquisition, groups receiving lower magnitude reinforcement produced higher peak forces that were further from the criterion force relative to forces produced by rats in the higher magnitude groups. When all groups were shifted to a three pellet condition, however, the previous low magnitude reinforcement groups showed reduced force variability and clustered around the criterion, whereas those groups that initially received more reinforcement increased force variability and temporarily increased their mean peak forces. Under conditions of force band differentiation, Harrell and Fowler (1977) found that rats receiving three pellets for each within-band response showed better band differentiation across sessions relative to those receiving fewer pellets (i.e., one or two). Together, these findings suggest that at the same force criteria, lower magnitude reinforcement should result in higher response peak force relative to responding maintained by higher magnitude reinforcement.

Force and behavior regulation. Interpreted from the behavior-regulation tradition, animals' responding under operant arrangements reflects a "compromise" between maintaining preferred levels of reinforcement (i.e., "equilibrium" measured during free access) given the

challenge of constraints imposed by the operant schedule (Timberlake, 1984, 1993; Timberlake & Peden, 1987). Thus, responding is a balance between the costs of responding and the aversiveness of loss of reinforcement (Timberlake & Peden, 1987, p. 36). Although response rate is commonly used to assess changes in the operant (i.e., instrumental) response and consumption response (Timberlake, 1984), other dimensions of responding (e.g., peak force) may also change to balance responding and reinforcer consumption. For example, Filion, Fowler, and Notterman (1970b) found that three different amounts of prefeeding had nonmonotonic but opposite effects on response rate and response differentiation (i.e., time integral of force); importantly, these adjustments interacted to maintain rats' reinforcement rates, suggesting that organisms may "compromise" in different ways in order to maximize access to reinforcers.

Other findings from the force literature may have implications for research concerned with the balance of responding and reinforcer consumption. Pinkston and McBee (2014) found that doubling the FR requirement (from FR10 to FR20) resulted in a less than two-fold increase in the time integral of force. These findings indicate a reduction in mean peak force per response, potentially supporting a conservation of energy conceptualization. Similarly, time integral tends to increase with increases in peak force criterion (Zarcone et al., 2009), but these increases are not necessarily proportional. For example, if an organism is already emitting peak forces above the peak force criterion, time integral of force would reflect this elevated force emission, and changing peak force criterion might not affect the peak force of responding.

Schwartz and Mintz (1980) studied humans' responding across a series of force band requirements. As the bands narrowed, more subcriterion responses were recorded, but at high narrow force bands, a greater proportion of responses fell below rather than above the band. The authors suggest that responses falling below band may be an artifact of the change in the force

band, which was narrowed by decreasing the upper bound. These findings, however, may reflect a tendency to conserve energy (Schwartz & Mintz, 1980). Similar patterns of responding have also been found in rats (Notterman & Mintz, 1965). Specifically, when force band contingencies (5-10 g and 15-20 g) were placed on response peak force, distributions peaked toward the lower end of the low force band and below the high force band (Notterman & Mintz, 1965). Force proportional reinforcement arrangements, a form of conjugate[2] schedule in which emission of greater forces earns higher magnitude reinforcement, similarly have implications for the regulatory approach. Filion, Fowler, and Notterman (1970a) initially failed to demonstrate force proportional reinforcement, but in a follow-up study, Fowler and Notterman (1974) compared force proportional reinforcement alone, a DRL schedule alone, and the two in combination. Their results suggested that the organism generally maintains its rate of reinforcement by increasing rate of responding; however, when this ability is limited, as in DRL schedules, the organism compensates by increasing force emission to earn greater magnitude reinforcement. Although behavior analysis has traditionally shown less interest in the balance of effort expenditure and reinforcer consumption (Mitchell & Brener, 1991), operant behavioral economic research has translated economic principles to specifically investigate consumption under conditions of constraint in operant arrangements.

Behavioral Economics

Behavioral economics is concerned with evaluating consumption within a system of constraint (Bickel, Green, & Vuchinich, 1995). In the behavior analytic tradition, behavioral economics includes two distinct approaches relevant to a discussion of effort: demand and

[2] A conjugate schedule is a CRF schedules that arranges for proportional increases in reinforcer delivery contingent on increases in some dimension of operant responding (e.g., intensity or rate; Lindsley, 1957; Rapp, 2008).

discounting. Demand assesses consumption as a function of increasing price (Hursh & Roma, 2016). By contrast, discounting assesses choice to determine preferences for a smaller reward with less constraint and a larger reward with greater constraint (e.g., greater delay or lower probability; Rachlin, 2006). Titration procedures permit researchers to determine the value of the smaller reward that is subjectively equal to the delayed or probabilistic larger reward. When subjective values are graphed as a function of the delay to their receipt (or odds against receipt in probability discounting), data are well fit by a hyperbolic function taking the form:

$$V = \frac{A}{1+kD}. \qquad \text{Equation 2}$$

In this equation, V is the subjective value of reward (A) given delay (D), and k is a fitted parameter reflecting the rate of discounting (Mazur, 1987).

Effort discounting. In addition to constraints of delay and probability, preference across differing effort conditions has also been examined in discounting arrangements wherein a smaller reward is available for less effort relative to a larger reward available for greater effort. For example, to assess effort discounting, Mitchell (1999, 2004) gave participants a hand dynamometer at baseline and asked them to squeeze with maximal effort for 10 s. Participants were then told that one of a series of hypothetical choices would be selected at random before choosing between low effort for less money and greater effort for more money; the value of the low effort reward was titrated across trials. Mitchell's effort discounting data were well fit by a hyperbolic model (see Equation 2), but very low effort discounting rates were obtained. Hartmann, Hager, Tobler, and Kaiser (2013) also gave participants an isometric hand dynamometer, but in addition to squeezing with maximal effort at baseline, participants were also required to squeeze the dynamometer at the low or high effort values chosen on each trial. Five of these trials were randomly selected at the end of the session for payout. Relative to

Mitchell, Hartmann et al. obtained greater discounting[3] as a function of effort; given the demonstrated correspondence between real and hypothetical rewards (Johnson & Bickel, 2002; Madden, Begotka, Raiff, & Kastern, 2003), such differences may suggest the importance of experiencing the effortful choices on each trial. In comparisons of different models fit to these estimated group indifference points, Hartmann et al. found that a quadratic model ($SV = a – k*Effort^2$; based on Steven's power law) provided superior fits over linear ($SV = a – k*Effort$) and hyperbolic models (see Equation 2) for their effort discounting data. It should be noted that these modeling approaches do not determine a unit price relating costs and benefits.

Grossbard and Mazur (1986) evaluated pigeons' preferences for reinforcers delivered contingent on FR schedule completion or after a delay using a procedure that adjusted delay or ratio using the pigeon's choices across trials. In this arrangement, pigeons chose longer delays relative to the mean ratio run duration, suggesting the effort required to complete the ratio impacted preference beyond completion time alone. Pigeons' responses during the delays were not recorded, but anecdotal observations suggested they engaged in few target responses but instead emitted a number of non-operanda behaviors. Such findings suggest that time to reinforcer delivery (i.e., "ratio run") is not the sole operative variable in a ratio schedule (Grossbard & Mazur, 1986; Herrnstein, 1964; Killeen, 1969; Neuringer & Schneider, 1968).

Other researchers have used hypothetical tasks to assess effort discounting. Sugiwaka and Okouchi (2004) assessed Japanese undergraduate's delay discounting using a standard task and effort discounting using a novel *furo* (Japanese bathtub) cleaning task in which students chose between a smaller monetary reward for no effort or a larger monetary reward for a given number of *furo* cleanings. Data from both the delay discounting and novel effort discounting tasks were

[3] Hartmann et al. (2013) did not obtain indifference points via titration but instead estimated them using logistic regression.

well fit by a hyperbolic discounting model, and participants discounted steeply in the effort task. Although the authors did not control for time to complete a cleaning in their *furo* cleaning task, delay and effort discounting were not correlated. Reed, DiGennaro Reed, Chok, and Brozyna (2011) presented a series of hypothetical choices about residential treatment programs to employees of a service organization. Participants chose between three alternatives: a single option, limited options, and extensive options. As the number of options in the extensive condition increased, participants' choices shifted away from this alternative, consistent with a "choice overload" (Iyengar & Lepper, 2000; Schwartz, 2004) effect. Patterns of choice were well fit by discounting models, suggesting participants may have been discounting due to the effort involved in considering multiple options, although the additional time required to assess more options cannot be ruled out.

Demand. Although effort has been examined using discounting procedure, behavioral economic demand procedures specifically manipulate the work (i.e., effort) required to obtain a reward. The ultimate goal of demand curve analyses is to provide a framework for evaluating and comparing reinforcer efficacy (Hursh & Silberberg, 2008). To this end, demand has been extended to study drugs of abuse in humans (Bickel, Marsch, & Carroll, 2000; Greenwald & Hursh, 2006; Johnson, Bickel, & Kirshenbaum, 2004) and non-humans (Christensen, Silberburg, Hursh, Roma, & Riley, 2008). These paradigms are also useful for assessing qualitative food preference in non-human animals (Foster, Sumpter, Temple, Flevill, & Poling, 2009), determining reinforcer efficacy in humans (Delmendo, Borrero, Beauchamp, & Francisco, 2009; Johnson & Bickel, 2006; Tustin, 1994), and informing public policy (Hursh & Roma, 2013; Reed, Hursh, Becirevic, Roma, & Hursh, 2016).

Behavioral economic demand quantifies consumption as a function of increasing constraints, relating these two dimensions as a ratio of costs to benefits (DeGrandpre, Bickel, Hughes, Layng, & Badger, 1993). Early conceptualizations of behavioral economic demand built on the traditional economic concepts of supply and demand by defining supply as reinforcers and demand as operant responding (Hursh, 1980, 1984; Rachlin, Green, Kagel, & Battalio, 1976). Thus, cost is defined as work to obtain a unit of reinforcement (Collier, Johnson, Hill, & Kaufman, 1986; Hursh, 1980, 1984). Hursh (1980) specified "it is essential that units of price and consumption be commensurate" (p. 229). That is, if "unit cost" is specified per ml of water, all quantities of consumption should be expressed as ml of water (Hursh, 1980, p. 230). Across a number of different reinforcers or commodities, consumption decreases in a systematic fashion as a function of increasing costs (Hursh, 2014a). Although demand paradigms have been extended to an analysis of humans' hypothetical consumption using hypothetical purchase tasks (HPTs; Jacobs & Bickel, 1999; Murphy & MacKillop, 2006; Murphy, MacKillop, Skidmore, & Pederson, 2009), the current review is focused on the operant demand literature.

Modeling. In traditional operant demand arrangements, the cost to obtain a unit of reinforcement increases across set periods of equal duration, and consumption (number of reinforcers earned at each price) is plotted as a function of price (Hursh, 1980). Curves are fit to these consumption data to model demand (see Figure 2). A major feature of demand curves are their elasticity, or the slope of demand (Hursh, 1980, 1984). Elasticity reflects an organism's "sensitivity to the cost-benefit ratio" to acquire a commodity (Hursh & Silberberg, 2008, p. 189), and demand curves traditionally are characterized by two phases: inelastic and elastic demand (Hursh, Raslear, Shurtleff, Bauman, & Simmons, 1988). In the inelastic portion (shown by the portion of the curve to left of the dotted line in the left panel of Figure 2), the organism is said to

defend its consumption, and consumption changes with a slope less than negative one (Hursh, 1980; Hursh & Silberberg, 2008). By contrast, in the elastic portion (shown to the right of the dotted line in the left panel of Figure 2), consumption begins to fall more rapidly, with a slope less than negative one (Hursh, 1980; Hursh & Silberberg, 2008). Demand curves showing both inelastic and elastic demand are said to have mixed elasticity (Bickel et al., 2000; Hursh, 1980).

Initially, a linear elasticity equation was proposed to model demand (Hursh, Raslear, Bauman, & Black, 1989; Hursh et al., 1988):

$$\log Q = \log L + b(\log P) - aP \ . \qquad \text{Equation 3}$$

In this equation, Q is the total consumption at a given price P, and L is observed consumption at the lowest price (Hursh et al., 1989; Hursh et al., 1988). Parameters b and a are the initial slope and acceleration in slope with increasing price, respectively. This dual-slope model captures two phases of demand, with the initial slope (b) expected to be near zero as "imperceptible" changes at low prices are not expected to change behavior relative to changes at higher prices, expressed by the a parameter (Hursh & Silberberg, 2008). (Note that in later versions of this equation [e.g., Hursh & Winger, 1995], log normal transformations were used.) Elasticity (E) can then be derived according to the formula:

$$E = b - aP \ . \qquad \text{Equation 4}$$

Hursh and Winger (1995) found that elasticity from this initial demand equation can not be reasonably compared given unadjusted differences in magnitude and potency; that is, without adjusting consumption and price for baseline (i.e., lowest price) values, the functional costs of each FR cannot be determined (Hursh & Winger, 1995, p. 383). They suggested a method for normalizing consumption by using consumption at the smallest FR [price] as a reference level from which to adjust both consumption and FR [price] across the range of the demand curve.

Thus, the number of reinforcer deliveries at the lowest price is set to 100, and all subsequent consumption values are expressed as a proportion of the number of reinforcers earned at the lowest price. Because initial consumption is set to 100 across demand curve manipulations, no comparisons can be made of level differences in consumption.

Although they recognize its predictive utility, Hursh and Silberberg (2008) suggest that the linear demand model (Equation 3) has a disadvantage in that no single fitted parameter accounts for the rate of change in elasticity; both parameters *b* and *a* are required. As a refinement, Hursh and Silberberg (2008) introduced an exponential model of demand:

$$\log_{10} Q = \log_{10} Q_0 + k(e^{-\alpha Q_0 C}) - 1 \, . \qquad \text{Equation 5}$$

In Equation 5, Q is consumption at price C. The k parameter is the range of consumption in $\log_{10}$ units. A number of additional observed or derived parameters describe different aspects of demand. Intensity, Q_0, is consumption at free price (i.e., when the commodity is available for free) and can be either observed or derived; if Q0 is derived, there are two free parameters (i.e., Q_0 and α), rather than one. Note that inclusion of Q_0 in the exponential component normalizes reinforcer consumption without separate calculations (Hursh & Silberberg, 2008). Demand elasticity is measured by the derived parameter α, which replaces the two slope parameters, *b* and *a*, from the linear model (Christensen, Silberburg, Hursh, Huntsberry, & Riley, 2008; Hursh & Silberberg, 2008). The single parameter for slope in the exponential model assumes consumption decreases as a constant, accelerating function of price. A lower α value is associated with greater reinforcing efficacy relative to a higher α value (Christensen, Silberburg, Hursh, Huntsberry, et al., 2008; Hursh & Silberberg, 2008).

Christensen, Silberburg, Hursh, Huntsberry, et al. (2008) describe two potential roles of this new equation: defining a good's reinforcing efficacy and providing an "equation presumed

to be isomorphic with the psychological processes by which animals scale goods" (p. 229). In an examination of this first role, Christensen et al. demonstrated the value of α in showing differences in consumption of food relative to cocaine. They note, however, that to determine the adequacy of the exponential model in scaling reinforcing efficacy, the most important evaluations are those showing that "the value of α for a good is largely invariant across manipulations of cost and reinforcement" (Christensen et al., 2008, p. 229).

Equation 5 requires transformation of raw data to $\log_{10}$ units, so values of zero for price or consumption can not be calculated. To remedy this issue, Koffarnus, Franck, Stein, and Bickel (2015) introduced an exponentiated version of Equation 5 to account for zero values in demand:

$$Q = Q_0 * 10^{k(e^{-\alpha Q_0 C}-1)} . \qquad \text{Equation 6}$$

The parameters from this equation are the same as those from Equation 5, but removing the log transformations means this equation incorporates data with zero values. Results from Koffarnus et al. suggest this equation shows better prediction and accounts for more variance when fitting datasets with zero consumption values from HPT datasets.

Additional parameters can be derived once demand has been modeled. Essential value, defined as rate of change in elasticity, (Hursh & Silberberg, 2008) can be derived by inputting the α and k values (from Equation 5 or Equation 6) using Hursh's (2014a) equation:

$$EV = \frac{1}{100\alpha k^{1.5}} . \qquad \text{Equation 7}$$

The point at which the demand curve switches from inelastic to elastic is P_{max}, and this is also typically the price at which total work reaches its maximum (Hursh & Winger, 1995). Moreover, Hursh and Winger suggest that a lower P_{Max} also suggests greater general elasticity (p. 381). Hursh (2014a) provided an equation for determining P_{max}:

$$P_{max} = \frac{0.083k+0.65}{Q_0 \alpha k^{1.5}} . \qquad \text{Equation 8}$$

Working under the assumption that he maximum response output, O_{max}, occurs at P_{max}, O_{max} can be calculated by multiplying price by predicted consumption at P_{max} (Hursh & Winger, 1995). Alternatively, O_{max} and P_{max} can be observed by identifying the highest number of responses in any session (O_{max}) and the point at which the local elasticity (i.e., slopes between subsequent data points) become greater than negative one (P_{max}). Of note, with observed values, the highest response output may not occur at P_{Max}. An additional, observed measure of demand, breakpoint is the last price point at which reinforcers are earned.

Aspects of demand. A number of variables may interact to impact consumption and responding within the behavioral economic demand framework. The observed and derived demand indices permit examination of how various manipulations impact different aspects of consumption (e.g., intensity versus elasticity). For example, mice with estrogen receptor knockout overeat in free feeding tasks, but demand assays demonstrated that these estrogen receptor knockout mice's demand was significantly more elastic across increasing prices than their control strain (Minervini, Rowland, Robertson, & Foster, 2015). In another example, Cassidy and Dallery (2012) found that nicotine administration reduced intensity of demand for food but not its elasticity.

Consistent with an economic tradition, a distinction is made between closed economies, in which all of the commodity (i.e, reinforcers) must be earned, and open economies in which some of the commodity is provided freely (Hursh, 1980). Traditional operant studies are conducted in open economies, in which a period of free access to food is provided after operant sessions, but closed economies maintain responding at greater prices (i.e., more responses per reinforcer) and show shorter pausing on longer FI or FR schedules relative to open economies

(Zeiler, 1999). As empirically demonstrated, elasticity of demand for a commodity increases as amount of free access increases (Greenwald & Hursh, 2006; Hursh et al., 1989; Imam, 1993).

Of note, most operant demand research with humans occurs in open economies (e.g., Bickel, DeGrandpre, Hughes, & Higgins, 1991; Johnson & Bickel, 2006; Johnson et al., 2004; Madden & Bickel, 1999). Greenwald and Hursh (2006), however, conducted a comparison of demand for hydromorphone using a progressive ratio (see Ratio progressions) task in which heroin-dependent individuals on an inpatient unit chose whether to complete increasing response requirements to earn hydromorphone or money. Supplemental hydromorphone either was (open economy) or was not (closed economy) available in addition to what was earned in the task. The open economy resulted in a greater reduction of choices for hydromorphone across increasing response requirements, suggesting demand was more inelastic in this open economy.

In everyday situations, organisms often have the opportunity to choose amongst varied commodities; concepts describing relations amongst different commodities are independence, substitutability, and complementarity. Independents are commodities whose supply and demand have no impact on each other (Green & Freed, 1993); an example might be jelly and cola; changes in the price of one would not impact consumption of the other. Substitutes are two commodities for which demand varies inversely, such that as price of one commodity increases and its consumption decreases, demand for the other commodity increases (Bickel, DeGrandpre, & Higgins, 1995; Hursh, 1980, 1984). Cola and root beer would likely be substitutes for many individuals. Specifically, if the price of cola increased, many individuals would purchase root beer instead, assuming the price of root beer remained unchanged. By contrast, demand for complements varies directly, and as demand for one increases, so does demand for the other

(Bickel, DeGrandpre, et al., 1995; Hursh, 1980, 1984). An example of likely complements are peanut butter and jelly; if the price of one increased, purchasing of both would likely decrease.

Reinforcer substitutability and complementarity have been empirically tested in the operant lab. Food and water have been shown to be complements (Hursh, 1978; Madden, Smethells, Ewan, & Hursh, 2007b). Other research suggests that substitutability depends on which commodity's availability is manipulated across both open and closed economies (Allison & Mack, 1982; Green & Freed, 1993; Rachlin & Krasnoff, 1983). When access to food is limited, water substitutes for food, but food does not substitute for water when access to water is restricted (Allison & Mack, 1982; Rachlin & Krasnoff, 1983). Substitution effects have been demonstrated between other commodities, such as food and fat (Madden, Smethells, Ewan, & Hursh, 2007a) or root beer and Tom Collins mix in rats (Rachlin et al., 1976); generalized tokens and food or water in pigeons (Andrade & Hackenberg, 2017); and cigarettes and nicotine gum (Shahan, Odum, & Bickel, 2000) or denicotinized cigarettes in humans (Johnson et al., 2004).

Unit price. In order to relate costs and benefits, work (i.e., cost per ratio completion) was related to reinforcers (i.e., benefit per ratio completion) in Hursh et al.'s (1988) unit price equation:

$$Unit\ Price = \frac{Ratio \times Lever\ Weigh}{Reinforcers \times Probability}. \qquad \text{Equation 9}$$

Total work (i.e., cost per session) was then defined as Total Responses × Lever Weight (Hursh et al., 1988; note that in a traditional weighted lever arrangement, subcriterion responses are not measured and thus could not be counted toward total responses in this equation), and total consumption (i.e., per session) was defined as FR Completions × Pellets per Completion × Probability. Plotting total consumption as a function of unit price typically produces a demand curve (see left panel of Figure 2; Hursh et al., 1988), and plotting total work as a function of unit

price tends to produce systematic bitonic work functions that increase across lower prices until reaching maximum response output (O_{Max}) and then decrease at higher prices (see right panel of Figure 2; Hursh et al., 1988).

From Equation 9, unit price can be adjusted by any combination of four different manipulations (ratio, lever weight, reinforcers, or probability of reinforcer delivery). Two predictions regarding consumption result from this conceptualization 1) total consumption should be the same across all combinations of benefits and constraints equated by unit price and 2) the same demand curve should describe total consumption plotted as a function of unit price, regardless of the combination of benefits and constraints making up each unit price (Bickel, DeGrandpre, Higgins, & Hughes, 1990; Hursh et al., 1988). Further, Hursh et al. (1988) predicted that work output plotted as a function of unit price should reveal a "unitary function" (i.e., work output that was superimposed across conditions; p. 421). Reanalysis of several prior studies using a unit price conceptualization revealed additional order in discrepant findings (DeGrandpre et al., 1993), and additional studies have specifically assessed behavioral economic demand based on unit price manipulations.

Ratio progressions. Demand research tends to use FR progressions as the price manipulation, given that they "simplify the definition of price as responses per reinforcer" (Hursh & Silberberg, 2008). In these studies, the FR requirement typically increases across some number of sessions, producing orderly decreases in consumption (Hursh, 2014a). Although early demand research collected data at each FR across several sessions (Hursh et al., 1988), demand curves in which each FR is assessed for just a single session produce demand curves with no differences from those requiring multiple sessions (i.e., rapid demand curve assay; Raslear,

Bauman, Hursh, Shurtleff, & Simmons, 1988; Tan & Hackenberg, 2015, but see Madden, Dake, Mauel, & Rowe, 2005 for differences when random ratio schedules were used).

Demand paradigms share some procedural similarities with progressive ratio (PR) arrangements, but demand parameters have shown inconsistent relations with PR measures. In PR procedures, the ratio requirement increases after some requirement is met (Hodos, 1961), generally within session after each reinforcer delivery (Hodos, 1961; Jarmolowicz & Lattal, 2010). The primary measure of reinforcing efficacy in PR arrangements is breakpoint, or the last ratio requirement completed before some predefined pausing criterion is met (e.g., no response for 15 min; Hodos, 1961). When PR data are obtained from independent PR procedures, PR measures (i.e., breakpoint and peak response output) do not consistently relate to demand indices (i.e., P_{max} and O_{max}) obtained from across session FR progressions in studies of food, fat, and water in rats (Madden et al., 2007a, 2007b). Similarly, in an experiment in which pigeons pecked keys to earn tokens exchanged for food, water or both, demand parameters obtained from an across session demand paradigm (i.e., intensity, elasticity, P_{max}, and O_{max}) differed across token types, but no differences were found on PR measures (Tan & Hackenberg, 2015). In a different approach, Foster, Temple, Cameron, and Poling (1997) plotted hens' reinforcement rate as a function of ratio size for data obtained from a PR procedure and an across session FR demand procedure. Demand curves were then fit to these data. Although reinforcement rate decreased as a function of ratio size across both procedures, FR schedules tended to produce higher breakpoints and more inelastic demand curves. By contrast, when PR and demand measures are derived from the same data (i.e., both from across session demand procedures), relations have been shown between PR breakpoint and P_{max} (Bickel & Madden, 1999; Johnson & Bickel, 2006) and between O_{max} and peak response output (Johnson & Bickel, 2006). Note that a demand

arrangement varies from a traditional progressive ratio schedule in that completing a given ratio increases the ratio requirement only in the progressive ratio arrangement (Jarmolowicz & Lattal, 2010). Additionally, the breakpoint in the demand paradigm is the price at which the organism fails to earn a minimum number of reinforcers, whereas in the progressive ratio requirement, the breakpoint is the last ratio completed prior to a predetermined period without a target response, which results in session lengths determined by the organism (Jarmolowicz & Lattal, 2010).

Given the FR series used in demand paradigms, no consistent differences in consumption have been found as a function of FR sequence[4] (i.e., ascending, descending, random) in non-humans (Foster, Blackman, & Temple, 1997; Raslear et al., 1988) or humans (Giordano, Bickel, Shahan, & Badger, 2001). Additionally, variations in step size, or the size of the progressions of FRs in the series, do not impact demand curves (Raslear et al., 1988). Relative to FR progressions, random ratio (RR) progressions produce different demand metrics. Madden, Dake, Mauel, and Rowe (2005) assessed consumption under increasing FR and RR progressions. In a condition assessing steady state responding at each price, the RR schedules resulted in greater inelasticity, higher P_{max}, and greater response output. A rapid demand curve assay also resulted in more inelastic demand and higher P_{max} in the RR condition relative to the FR for three of four subjects, although the absolute differences were less pronounced (Madden et al., 2005).

Although increasing the ratio requirement produces orderly reductions in consumption, authors have noted that response topography tends to shift with increasing ratio requirements (Allison, Buxton, & Moore, 1987; Bauman, 1991; Johnson & Collier, 1987; Zarcone et al., 2007) Bauman (1991) has suggested these shifts may serve to modify or decrease some aspects of the nominal cost of an increase in ratio value. The effects of topography on demand, however,

[4] For PR procedures, however, sequences affect breakpoints (Killeen, Posadas-Sánchez, Johansen, & Thrailkill, 2009)

remain relatively underexplored, limiting our understanding of behavior processes during behavioral economic demand. Arrangements that restrict topography, however, may control for this limitation. For example, an apparatus that restricts the topography of lever pressing to contact by a single forelimb (Fowler, 1987) may serve to reduce cost changes resulting from topography shifts.

Reinforcer manipulations. According to Equation 9, manipulations of the benefit component can include changes to reinforcer probability or magnitude. Relatively few studies have manipulated probability of reinforcement in demand studies using unit price conversions. Hursh et al. (1988) manipulated unit price using two probabilities of reinforcer delivery across a parametric range of ratio values. Across these arrangements, Hursh et al. found significant differences in the *b* parameter across reinforcer probability manipulations matched using the unit price equation. Similarly, in a concurrent progressive ratio arrangement in which probability of reinforcement decreased on one of the two components, Jarmolowicz, Sofis, and Darden (2016) found that allocation of responding across the two components was not well described by unit price. Adjusting the reinforcer component of unit price using a discounting model (see Equation 2), however, better accounted for rats' responding.

Manipulations of reinforcer magnitude based on unit price (Equation 9) are generally arranged across ratio progressions. Unit price predicts identical consumption across differing magnitudes, but studies yield mixed results. In closed economies, no significant differences were found in consumption obtained from ratio progressions across two magnitude manipulations (Cassidy & Dallery, 2012; Hursh et al., 1988). When matched unit prices are compared in open economies, however, studies with non-humans tend to show greater elasticity in higher magnitude conditions (Cassidy & Dallery, 2012; Foltin, 1994; Grant et al., 2014). Bickel et al.

(1991) found cigarette consumption at different magnitudes was idiosyncratic across humans responding in an open economy, and Delmendo et al. (2009) generally found similar – but not identical – consumption of edible items among children completing academic tasks for two different magnitudes of reward. Although these studies suggest economy effects on consumption by non-humans under different magnitude manipulations, such findings must be interpreted with caution because consumption across magnitudes in closed economies was not shown to be equivalent. Instead, these studies failed to demonstrate differences, thus the null hypothesis was not rejected.

Other demand arrangements have also been used to compare reinforcer magnitude manipulations. In concurrent demand arrangements, two commodities are concurrently available on separate operanda (i.e., concurrent demand), and the unit prices of each can be independently manipulated by varying ratio or magnitude. In these concurrent demand arrangements, pigeons always preferred lower FRs at matched unit prices (i.e., smaller magnitude reinforcer with lower work requirement; Foster & Hackenberg, 2004). Humans, however, tended to prefer larger magnitude rewards at smaller unit prices, only preferring lower FRs at higher unit prices (Madden, Bickel, & Jacobs, 2000).

Other researchers have used PR procedures with humans to create survival curves showing the proportion of participants continuing to work to earn a reward at a given unit price (Greenwald & Hursh, 2006; Henley, DiGennaro Reed, Reed, & Kaplan, 2016). Across two magnitude conditions in an open economy, lower magnitude monetary rewards resulted in higher breakpoints and more inelastic attrition (i.e., more participants continued working at higher unit prices; Henley et al., 2016); such findings suggest greater sensitivity to FR requirement relative to reward value at higher prices, consistent with findings of Madden, Bickel, and Jacobs (2000).

In participants working for hydromorphone, however, there were no significant differences across magnitude conditions in either open or closed economies (Greenwald & Hursh, 2006); note, however, that Greenwald and Hursh (2006) found no significant differences but did not test for statistical equivalence across magnitudes.

Using a novel within-session demand curve paradigm, Bentzley, Fender, and Aston-Jones (2013) obtained demand curves from an experimental preparation in which rats responded for cocaine across 11 increasing unit prices within a single 110-min session; the ratio requirement remained constant at FR1 while the unit price was increased by decreasing reinforcer magnitude. Consumption and response output were plotted as a function of unit price. The resulting curve appeared similar to those obtained from more traditional FR progressions. Stronger conclusions could have been made had they formally compared their findings to data obtained from a more traditional demand paradigm.

Time progressions. Because responses must occur in time, increasing the number of responses required for reinforcement also increases the length of time required to complete the ratio run. Thus, increasing the ratio requirement also indirectly increases the time to reinforcer delivery (Herrnstein, 1964; Killeen, 1969; Neuringer & Schneider, 1968). Although the findings of Grossbard and Mazur (1986; see Effort discounting section) suggest that ratio run duration was not the sole controlling variable in preference across two alternatives, in a paradigm in which organisms have a defined amount of time in which to earn reinforcers, ratio run durations may serve an important role in constraining consumption. That is, consumption may be particularly sensitive to run duration if the "budget" (i.e., time) is held constant across sessions, but the "price" (ratio run) increases (i.e., an uncompensated rather than compensated demand curve; Kagel, Battalio, Rachlin, & Green, 1981); similarly, the inter-trial interval (ITI) may

impact consumption more in a low relative to high reinforcer magnitude condition when session duration is fixed (Johnson & Bickel, 2006). In FR progressions in open economies, shorter sessions tend to produce more elastic demand (Foster, Kinloch, & Poling, 2011), and more elastic demand at the beginning relative to the end of operant sessions (McSweeney & Swindell, 1999).

Other researchers have more directly tested the effect of time costs on consumption by yoking to the duration of ratio runs. Bauman (1991) ran two manipulations to test the role of time in a closed economy demand arrangement: 1) a traditional demand curve condition obtained from increasing ratio values across sessions and 2) a yoked condition in which reinforcers were earned at the end of intervals yoked to the durations of the average response runs from the ratio condition. In the yoked condition, a response started the interval and a response at the end of the interval resulted in reinforcer delivery (i.e., response-initiated FI schedule, Shull, 1970). Bauman found marked overlap between the number of pellets consumed across the FR and yoked response-initiated FI conditions. Although the number of responses per reinforcer varied in the FI condition, fewer responses were generally emitted in the FI condition relative to FR condition, especially at larger ratios. Together, the similar patterns of consumption and fewer responses in the FI condition suggest that time – not ratio – was the major factor impacting consumption[5].

In other demand research, duration and delay have been manipulated. Peck and Byrne (2016) examined effects of response duration and signaled delays on consumption. In Experiment 1, rats earned sweetened condensed milk in 1-hr sessions with a fixed-duration requirement that doubled across sessions (0.5, 1, 2, 4, 8, 16, 32, 64, and 128 s); rats were

[5] Tsunematsu (2001) extended this work to pigeons and assessed consumption across FR and yoked response-initiated FI schedules in closed economies, but issues with the statistical analyses limit inferences that can be made from this research.

required to depress the lever for the entire duration (time did not accumulate across presses). In phase one of Experiment 2, increasing duration sessions were identical except that they ended after a 10-min breakpoint (i.e., after no responding of any duration). In phase two, these same animals earned reinforcers on a signaled delay procedure. Delays (1, 2, 4, 8, 16, 32, 64, and 128 s) increased across sessions that also ended after a 10-min breakpoint. Demand curves were not obtained from ratio progressions for comparison in either study. Manipulations showed that increasing durations and increasing delays reduced consumption and produced functions similar in form to traditional demand curves. Breakpoints were lower in the duration condition relative to the matched delay condition. Although such differences may suggest that the additional effort required to time lever duration may have contributed to differences between conditions, the signaling of the delays also may have served as conditioned reinforcement (Jarmolowicz & Lattal, 2013; Royalty, Williams, & Fantino, 1987; Zimmerman, Hanford, & Brown, 1967). Of note, responses of durations shorter than those programmed were recorded but not included in analyses. Taken together, these studies suggest that time-based constraints on reinforcer delivery produce demand curves that are similar to those produced by manipulations requiring greater levels of responding.

Although researchers have matched time to ratio duration from ratio progressions (i.e., Bauman, 1991), they did not include unit price manipulations to assess comprehensively the role of various costs and benefits in conjunction. Madden, Bickel, & Jacobs (2000) conducted a series of studies to test a simplified version of unit price (FR/A) for describing humans' cigarette consumption in a choice context. Choice data across options equal in unit price deviated from predictions in that at lower prices, individuals tended to prefer the higher magnitude option with a higher work requirement, whereas at higher unit prices, individuals preferred the lower FR and

lower magnitude option. These researchers added a parameter to reflect handling (Rapport, 1971) and incorporated the hyperbolic discounting model (see Equation 2) to modulate the value of rewards based on the time (i.e., ratio run) to their receipt. In the resulting equation

$$Uit\ Price = \frac{FR+H}{\frac{A}{1+kD}}, \qquad \text{Equation 10}$$

FR is the ratio value, *H* is handling cost, *A* is the amount of the reinforcer, *D* is the delay to reinforcer delivery, and *k* is a free parameter reflecting reinforcer devaluation due to delay. In this modified equation, only handling was added to the cost, whereas the benefit component was adjusted to reflect devaluation of the reinforcer because of delay, calculated as the time to complete the ratio run. These modifications resulted in predictions that were ordinally consistent with the patterns of responding observed for most participants. Foster and Hackenberg (2004) similarly found Equation 10 produced results consistent with the ordinal rankings of preference data from their pigeons working at equal unit prices when reinforcer magnitudes and FRs varied.

Lever weight or force. In the original unit price equation, the cost component included both responses and lever weight. Few studies, however, have directly manipulated the lever weight (or force) requirement in behavioral economic demand (Hursh et al., 1988; Nord, 2014; Sumpter, Temple, & Foster, 1999, 2004). In his introduction of the unit price concept, Hursh et al. (1988) obtained demand curves across eight groups of rats in a closed economy using the same FR progression (1, 15, 45, 90, 180, 360). The eight demand curves were comprised of all combinations of two lever weight values (0.265 and 0.530 N), two reinforcer magnitude conditions (1 and 2 pellets), and two probability conditions (0.5 and 1.0) probability manipulations, resulting in four demand curves obtained from each force condition.

When plotted as a function of ratio requirement, the consumption (reinforcers) and work data (responses) obtained from these eight manipulations differed in form. Plotting consumption

and work data (responses × lever weight [1 or 2]) as a function of unit price resulted in greater convergence, but two of the higher lever weight conditions visually deviated from the functions produced by other manipulation combinations. Consumption data from the high force, high reinforcer magnitude group (0.530 N, 2 pellets, 1.0 probability) deviated from a curve fit to control group (0.265 N, 1 pellet, 1.0 probability) consumption using the linear demand equation (see Equation 3). Additionally, when work data (responses × lever weight) were plotted as a function of unit price, two of the four high effort conditions (0.530 N, 2 pellets, 1.0 probability and 0.530 N, 2 pellets, 0.5 probability) deviated markedly from the group curve. In regards to these deviations, Hursh et al. (1988) noted that "the simple use of nominal lever weight as our measure of effort may have underestimated the functional change in effort" (p. 424). The only significant differences in IRTs and PRPs across conditions were noted across force manipulations. The IRTs were approximately double in the higher force conditions, and PRPs increased more rapidly as ratio requirement increased in the higher lever weight conditions relative to the lower lever weight conditions. The greater IRTs and PRPs observed in the higher force conditions may include periods in which subcriterion responses occurred because these were not recorded in the weighted lever arrangement used in this experiment. Moreover, including subcriterion responses may help to account for Hursh's suggestion of an underestimation of the changes in effort due to lever weight.

In an unpublished master's thesis Nord (2014), extended the work of Hursh et al. (1988) in an experiment in which she obtained demand curves across increasing FR requirements (5, 10, 18, 32, 56, 100, 180, 320, 560) at two force criteria: 5.6 g (.055 N) and 56 g (.55 N). Nord, however, used a force transducer to record the force of all responses, including subcriterion responses. She also included an additional yoked condition in which the force criterion was set at

5.6 g but the ratio requirement was set to the average number of total responses (i.e., subcriteron and criterion) per reinforcer for each FR value from the 56-g condition. Data obtained from the 5.6-g and 56-g conditions deviated from predictions based on unit price, with the 56-g criterion resulting in greater elasticity than the 5.6-g condition, rather than the identical elasticity values predicted by unit price (Nord, 2014).

Nord also examined total work using the Hursh et al (1988) equation (using peak force criterion for lever weight) and found marked differences across the force conditions. Removing subcriterion responses resulted in better convergence of the work functions from the different force conditions, particularly in the ascending portion of the work functions (i.e., at lower prices). Additionally, because the programmed peak force criterion tended to underestimate the forces actually emitted, Nord also analyzed work data using a unit price equation in which obtained mean peak force (i.e., typically the average force of criterion and subcriterion responses) was substituted for peak force criterion and multiplied by total criterion responses. Using mean peak force to calculate unit price resulted in better convergence across the progressions than force criterion for total work.

Aspects of Nord's (2014) analyses limit the conclusions that can be drawn from this study. Nord suggested that removing subcriterion responses resulted in greater convergence of work functions, but this may be an artifact of her calculation method. Total work was calculated by multiplying total responses (including subcriterion) by force criterion, even though subcriterion responses never met that force criterion, potentially overestimating work completed. Additionally, it is unclear whether subcriterion responses were included in calculations of mean peak force. If subcriterion responses were included, calculating unit price using mean peak force but excluding subcriterion responses form the response count also introduces potential analytic

problems, as the peak force of the subcriterion responses contributed to the mean peak force but not the ratio requirement. Further, data were never plotted as a function of step or obtained FR across the three conditions, so consumption data obtained from the yoked conditions were never directly compared with consumption in the sessions to which they were yoked. This analysis limits conclusions that can be drawn about the role of subcriterion responses in changing the shape of the functions obtained in the high force condition. Despite it being difficult to draw firm conclusions, this study suggests the value of using more sensitive force measurement in behavioral economic demand.

Few studies have examined parametric ranges of force values in demand arrangements. Sumpter et al. (1999) assessed hens' demand for grain using ratio and force progressions of door pushes. Force progressions generally resulted in curvilinear changes in consumption across increasing prices, whereas reductions in consumption from ratio values were linear. The shapes of the functions obtained from the FR and force progressions differed, and thus were not consistent with the predictions of the Hursh et al. (1988) unit price equation. Because the unit price analyses were post hoc, however, the force and ratio progressions were rarely matched at the same unit prices.

In a series of follow-up studies, Sumpter et al. (2004) assessed parametric ranges of force and ratio values matched by the Hursh et al. (1988) unit price equation. Two response topographies, key pecks and door pushes, were assessed. With the key peck manipulation, a limited range of forces was assessed, and no consistent effects of force on consumption were found. In the door push manipulation, however, seven unit prices were assessed with five force manipulations. Consumption was examined as a function of FR, force, and unit price, but findings were not consistent with the predictions of the Hursh et al. (1988) unit price equation.

Changes in consumption showed linear reductions for the FR progression but curvilinear reductions for the force progression. Thus, consumption for the same reinforcer was more inelastic in the force condition across low to moderate unit prices relative to matched prices in the FR manipulation. Sumpter et al. (2004) suggested the time required to complete the larger number of responses in the FR progressions was a critical factor influencing differences in the shape of the functions relating ratio, force, and consumption. Although their findings are broadly consistent with literature showing similar patterns of consumption across FR and time progressions, Sumpter et al. only counted responses sufficient to displace the door or key and did not record subcriterion responses or measure the actual peak force of any responses. Unanswered by these studies is the question of how organisms' actual responding to the force requirements relates to differences observed across the force and ratio demand progressions.

Purpose

The extant literature suggests differences in demand curve assays obtained from force and ratio progressions equated using unit price (Equation 9). This study aimed to further test the concept of unit price by obtaining demand curves from rats under increasing FR progressions and increasing force progressions that were matched according to unit price. A force transducer provided enhanced measurement of response dimensions, including the actual forces emitted per response and recording of both criterion and subcriterion responses.

Experiment 1

Method

Subjects. Subjects were six female Long Evans rats, approximately 205 days old and weighing approximately 210-230 g at the beginning of the experiment. Rats were identified by colored markings on their tails. All rats had prior experience working on ratio schedules of

reinforcement, and three rats (2M, 3M, and 2N) had prior experience on schedules wherein force requirement was manipulated. Rats were housed singly in a colony room with a 12hr:12hr light-dark cycle. Rats participated in operant sessions during the light portion of their daily cycle, and sessions took place 6-7 days per week at approximately the same time each day. Rats were maintained on 21-hr food restriction schedules. Rats earned a solution of sweetened condensed milk diluted with water (1 part milk : 2 parts water by volume) during 2-hr experimental sessions and then had access to rat chow for the remainder of each 3-hr food access period. This economy type could be considered closed in that sweetened condensed milk was not available outside of sessions (DeGrandpre et al., 1993), but given findings on the substitutability of food and a liquid fat solution (Madden et al., 2007a), this arrangement is likely best conceptualized as an open economy.

Apparatus. Experimental sessions were conducted in two identical, custom operant chambers (28×28×23 cm; see Figure 3) enclosed in sound-attenuating cabinets. Each chamber featured four Plexiglas walls held on stilts approximately 2 mm above a floor made of carbon fiber Nomex honeycomb wrapped in white contact paper; four force transducers were located under the floor at each corner of the chamber. A 14-V house light was located on a translucent panel on top of the Plexiglas chamber ceiling. The 20-cm chamber door was located on the front wall and on the wall to the right was the intelligence panel, where the response operandum and magazine were located. A 7×6-cm steel panel housed a 3×2.5-cm window. This window was located 5 cm above the floor, and an aluminum disk of 1.8-cm diameter covered a force transducer (the response operandum) located 1.5 cm beyond this window. The force threshold for a response was set to 4 g (.04 N). Prior to each session, the force transducer was calibrated to a reading of 0. Testing at the beginning and end of the experiment revealed no error at 5 g and up

to 1% error at 100 g (i.e., the force of a 100 g calibration weight was recorded as 100 g in one chamber and 101 g in the other chamber).

A 7×7-cm opening in the intelligence panel led to a 7×7×4 cm magazine alcove. A 1.8-cm diameter aluminum cup could be accessed through a 1.5-cm diameter opening in the floor located 2.4 cm into the magazine alcove. A peristaltic pump dispensed sweetened condensed milk (i.e., the reinforcer) into the cup, which held a maximum volume of approximately 7-8 ml; successive reinforcer deliveries could accumulate in the cup if the rat did not consume them immediately. Pumps were tested prior to each session to ensure milk dispensed. Testing at the beginning and end of the experiment revealed no discernible discrepancies in volume of reinforcer delivered across tests of the durations of pump activation used in this experiment.

Procedure. A variation of the procedure described by Raslear et al. (1988) for rapid demand curve assays was used to obtain demand curves. Two types of price progressions (ratio and force) were assessed across two reinforcer magnitude manipulations (low and high). A demand curve was obtained from each rat for each of four manipulations: low reinforcer magnitude increasing force requirement (F-L), low reinforcer magnitude increasing ratio requirement (R-L), high reinforcer magnitude increasing force requirement (F-H), and high reinforcer magnitude increasing ratio requirement (R-H). Unit prices were matched across the four demand curves (see Table 2), such that the work requirement (i.e., Ratio × Force Criterion) and reinforcer value (i.e., Magnitude × Probability) equated at each step in the demand curve when using Equation 9. After the first demand curve assay was obtained for each animal, relatively greater consumption was noted in the force relative to ratio progressions at low to moderate unit prices. Consumption in the ratio progressions also tended to reflect only the elastic portion, rather than inelastic and elastic portions, of the demand curve. Given these findings, five

additional lower unit prices were included for the R-L and R-H progressions (see Table 2) but were not matched in the force progressions.

A single session was devoted to each unit price for each demand curve manipulation. Although breakpoints are traditionally the price at which consumption is entirely suppressed, for this study, breakpoint was defined as the price at which rats' consumption was suppressed by 95% or more from consumption at the lowest matched price (i.e., unit price of 0.49) assessed in that demand curve. Each demand curve assay was terminated when rats met breakpoint. Order of demand curve manipulations was counterbalanced across rats, and each rat completed a replication of at least one demand curve assay (see Table 3). The first curve obtained from each rat was replicated, and additional replications were conducted at the end of the study for two rats who completed the five demand assays before the other four. A small camera mounted within the cabinet and above the intelligence panel video recorded most sessions (i.e., > 90%) for three rats (i.e., 2M, 4M, 2N).

For each response at or above threshold (i.e., 4 g [.04 N]; programmed to exclude readings resulting from vibrations or electrical variability), the time in session the response began, the interresponse time (IRT), duration of response, peak force, and time integral of force were recorded by the program (see Figure 1). Each demand assay featured both a peak force criterion and ratio requirement (see Table 2). Responses with a peak force between the force threshold and programmed peak force criterion were recorded but not counted toward the ratio requirement. Each response that met the programmed peak force criterion was counted toward the ratio requirement and was followed by a 0.1-s tone immediately after the response fell below the threshold. When the ratio requirement was satisfied, a relay click was presented, reinforcer delivery occurred, and a cue light above the magazine alcove was illuminated for the duration of

reinforcer delivery (i.e., pump activation of 0.91 s [low reinforcer magnitude 0.05 ml reinforcer delivery] or 1.82 s [high reinforcer magnitude 0.10 ml reinforcer delivery]). No consumption period was programmed, and any criterion responses emitted after a reinforcer delivery were counted toward the next ratio requirement.

All rats were placed on a FR5 schedule with a force criterion of 4 g (i.e., threshold) for at least three days prior to starting the experiment. To reduce carryover effects, rats were placed on this FR5 (4 g) procedure for at least three days between separate demand curve assays; rats continued with this procedure between assays until the number of reinforcers earned was no less than 90% of the number earned on this schedule prior to starting the experiment.

Experimental design. Consistent with prior demand research (e.g., Raslear et al., 1988), a parametric experimental design (Perone & Hursh, 2013) was used. Each demand assay consisted of an ascending sequence of unit prices for each of the four manipulations (i.e., F-L, F-H, R-L, R-H; see Table 2), and each price was assessed for a single day. Order of demand assays was counterbalanced across animals.

Data Analysis

The data analysis section has been divided into operant analyses and behavioral economic analyses. Several behavioral dependent variables (e.g., peak force and responses rate) were included in operant analyses, whereas the primary dependent variable in the behavioral economic analyses was total consumption per session, rather than number of ingestions, to be consistent with the conceptual underpinnings of behavioral economic demand (Bickel et al., 1990; Bickel et al., 2000; Hursh, 1980; Hursh et al., 1988) and the notions of unit price (Bickel et al., 1990; Hursh et al., 1988). Given potential differences in definitions of dependent variables across these two approaches (Hursh, Madden, Spiga, DeLeon, & Francisco, 2013), reinforcer delivery was

used to refer to a cycle of reinforcement (whether high or low reinforcer magnitude), and reinforcer unit was used to refer to 0.05 ml of the sweetened condensed milk-water solution (i.e., one reinforcer unit per reinforcer delivery in the low reinforcer magnitude condition but two reinforcer units per reinforcer delivery in the high reinforcer magnitude condition). Consumption was thus defined as number of 0.05-ml reinforcer units earned and was determined by multiplying reinforcer deliveries by number of 0.05-ml reinforcers per delivery[6].

Operant analyses. Individual analyses were performed to examine changes in each rat's behavior across all four demand assays.[7] To assess how response force changed as a function of changing contingencies, peak force means and standard deviations were calculated at each price. Mean peak force was determined by averaging the maximum peak force attained by all responses (i.e., criterion and subcriterion) in that session, and mean peak force was also determined separately for criterion responses. To estimate changes in effort expenditure across increasing ratio and force progressions, time integral of force was averaged per response at each price point. Mean duration of each response was determined for each session. Cumulative response duration per reinforcer unit was calculated by summing the duration (s) of all criterion and subcriterion responses for each reinforcer delivery and dividing by reinforcer units per delivery, and cumulative time integral per reinforcer unit was calculated by summing the time integral of force

[6] Other approaches to analyzing behavioral economic demand data can include plotting reinforcer deliveries as the dependent variable and cost per reinforcer delivery as the independent variable. Other approaches include normalizing consumption and price. Data from the present experiments have been graphed according to various conventions in Appendix A.

[7] Additional measures showing more granular changes are shown in Appendix B. These include peak force frequency distributions at each price, as well as for the first 10% and last 10% of responses within each session. Cumulative records were developed to visually assess patterns of temporal distribution of responses across increasing ratio and force requirements. Interreinforcment intervals (IRIs) and cumulative response durations per reinforcer delivery were determined. The IRI was the time (s) between consecutive reinforcer deliveries (thus time to first reinforcer delivery was excluded), and cumulative response duration was calculated by summing the duration (s) of all criterion and subcriterion responses for each reinforcer delivery. The difference between the cumulative response durations and IRIs was calculated for every reinforcer delivery (excluding the first reinforcer delivery) as a measure of total pausing (i.e., including IRTs and PRPs).

(g-s) of all criterion and subcriterion responses for each reinforcer delivery and dividing by reinforcer units per delivery.

Response rates at each price point were calculated for total (i.e., subcriterion and criterion) responding and separately for criterion and subcriterion responding. Because research has reported greater IRTs as a function higher force requirements in demand arrangements using weighted levers (Hursh et al., 1988), IRT frequency distributions were plotted for each session to visually assess changes as a function of increasing force requirements. For these frequency distributions, IRTs by opportunity were determined by dividing the number of IRTs in a 0.05-s bin by all IRTs of that duration or greater. All IRTs and criterion IRTs were plotted separately for force progressions to compare differences when examining only response meeting the force criterion. The IRT distributions plotted here include all times between responses, including times between responses that included a reinforcer delivery.

Behavioral economic analyses.

Price modifications. If differences emerged in the demand curves across the force and ratio progressions, attempts were made to bring greater convergence to consumption across the force and ratio progressions by modifying unit price. Consistent with the requirement that unit price and consumption be in "commensurate units" (Hursh, 1980, p. 229), each of these price modifications determined a unit price, or the price per 0.05-ml reinforcer unit; because Equation 9 has traditionally been referred to as unit price, for simplicity, these alternative calculations will be referred to as price modifications rather than unit prices. Consumption was quantified as number of 0.05-ml reinforcer units, consistent with a unit price approach. A price was determined for each session in each progression for every animal according to these candidate price modifications.

a) The number of obtained responses per reinforcer unit was determined by summing all criterion and subcriterion responses in each session and then dividing by total reinforcer units earned.

$$Responses\ per\ Reinforcer\ Unit = \frac{Total\ Responses}{Total\ 0.05ml\ Reinforcer\ Units\ Earned}. \quad \text{Equation 11}$$

b) A variation on unit price specified by Equation 9, obtained unit price was calculated for each session by multiplying the average number of responses (i.e., subcriterion + criterion) per reinforcer delivery by obtained mean peak force at that price (N; included both criterion and subcriterion responses; see Operant Analyses section) and dividing by 0.05-ml reinforcer units per delivery.

$$Obtained\ Unit\ Price = \frac{Responses\ per\ Delivery \times Mean\ Peak\ Force}{0.05ml\ Reinforcer\ Units\ per\ Completion}. \quad \text{Equation 12}$$

c) A psychophysical scaling adjustment of Hursh et al.'s (1988) unit price (Equation 9) was determined individually for each animal by adjusting the force criterion (N) component of Equation 9 using an exponent to reflect psychophysical scaling as suggested by Steven's power law (Equation 1), resulting in

$$Unit\ Price\ with\ a\ Psychophysical\ Scaling\ Parameter = \frac{Programmed\ Ratio \times Force\ Criterion^{s}}{0.05ml\ Reinforcer\ Units\ per\ Completion}, \quad \text{Equation 13}$$

wherein the ratio, force criterion, and number of reinforcer units per ratio completion were the programmed values for each session. For this adjustment, programmed—rather than obtained—values were used to be consistent with psychophysical scaling, which relates the perceived to the objective magnitude of the programmed stimuli (McKerchar, Green, & Myerson, 2010; Stevens, 1957). The *s* parameter was an exponent chosen for each rat through two steps, namely visual then quantitative analyses. For the first step, each rats' consumption data from all progressions

(i.e., F-L, F-H, R-L, and R-H; y-axis) were plotted as a function of prices (x-axis) produced by entering an *s* value into Equation 13. Convergence across a range of *s* values was visually assessed, and a series of values surrounding those that produced the greatest visual convergence was selected to be assessed via curve fitting. For the second step, a single curve was fit to consumption from all progressions at each *s* parameter for each animal. For this analysis, any fitted parameters were shared across progressions, and *k* values (if required by the best fitting model; see Curve Fitting) for each rat were calculated by log transforming that rat's total range of consumption (i.e., maximum consumption in any condition minus the minimum consumption in any condition). The total range of consumption was chosen for *k* for this analysis, consistent with the goal of finding the *s* value that minimized error of a shared curve fit to all progressions. For each rat, the *s* value that minimized RMSE and maximized R^2 was selected for subsequent analyses. If the same lowest RMSE and highest R^2 occurred across multiple *s* values (i.e., a tie), the absolute sum-of-squares was compared. If a tie remained after examining the absolute sum-of-squares, the middle value (given an odd number of tied values) or lowest value was selected for subsequent analyses.

d) Mean cumulative time integral of force per reinforcer was used as a price modification because time integral is a measure of effort (Fowler, 1987; Hursh et al., 2013; Notterman & Mintz, 1965). The time integral, or area under the force-time curve, was calculated within the program that presented stimuli and recorded responding. The time integrals (g-s) for all responses (subcriterion and criterion) at each price were summed, resulting in a cumulative time integral of force measure. This measure was then divided by number of reinforcer units earned at each price according to the equation:

$$Mean\ Cumulative\ Time\ Integral = \frac{\sum(\int F\mathrm{d}t)}{Total\ 0.05ml\ Reinforcer\ Units\ Earned}. \quad \text{Equation 14}$$

e) Mean cumulative response duration per reinforcer was calculated, given that Peck and Byrne (2016) demonstrated that increasing response duration requirements produced ratio-like demand curves. The durations of all responses (i.e., criterion and subcriterion) were summed for each reinforcer delivery in every session, and this cumulative response duration per reinforcer delivery measure was summed for all reinforcer deliveries at a given price. This value was then divided by the total number of 0.05-ml reinforcer units earned in that session according to the equation:

$$Mean\ Cumulative\ Duration = \frac{\sum(Cumulative\ Duration\ per\ Reinforcer\ Delivery)}{Total\ 0.05ml\ Reinforcer\ Units\ Earned}. \quad \text{Equation 15}$$

Curve fitting. Demand curves were fit to individual and group consumption data plotted using unit price (Equation 9) and price modifications that produced curvilinear functions (Equations 11-15). Linear (Equation 3) and exponential (Equation 5) models were compared[8] in GraphPad Prism version 7 using Akaike's information criterion with correction for small samples (AICc); AICc reports the likelihood that a given model provides a better fit, given different numbers of fitted parameters and non-nested models (Akaike, 1974). The model yielding the best fits across the largest number of datasets was used in subsequent analyses. For these comparisons, parameters *L*, *a*, and *b* were derived using the linear model. For fits using the exponential model, parameters Q_0 and α were derived. For models fit to individual rat's data, the *k* value was constrained to each rat's mean range of consumption across all progressions in log units, and for curves fit to group data, the *k* value was constrained to the log-transformed mean range of consumption across all progressions for all rats. Because α is dependent on the range of

[8] Although subsequent versions of the linear demand equation featured log-normal transformations (e.g., Hursh & Winger, 1995), the initial equation featured log transformations (Hursh et al., 1989). Because a log transformation facilitated comparison between the linear and exponential models, the initially reported log transformations was used.

consumption (*k*) used in the exponential equation, problems arise in comparing α if different *k* values are used (Hursh & Silberberg, 2008). Although Hursh (2014b) indicated that small *k* values (between 1 to 5) should not impact α, Foster et al. (2009) found that adjusting *k* values from 2 to 3 (log units) resulted in changes in both the magnitude and ranking of α values across commodities. In the present experiment, maximum consumption within subject varied by up to 0.95 log units (i.e., 2.0 to 2.95 log units) across conditions (largely due to differences in consumption at the first unit price assessed; see Table 2. Given concerns about the effects of *k* on curve fits and parameters, the averaged range of consumption in log units was used for each animal.

For models fit to individual rat's data based on unit price, curves were fit to consumption data (i.e., total reinforcer units at each price) when those prices with 0 consumption were excluded (i.e., 0 consumption occurred in 4 datasets; one dataset each for 3M, 4M, 1N, and 2N; one F-L progression and three F-H progressions) and when 0.1 was substituted for 0 consumption to allow plotting on log axes. Because other price modifications (Equations 11-12, 14-15) were dependent on calculating a price per reinforcer unit, fits to data excluding 0 consumption were used in comparisons of price modifications.

The best fitting model was fit in GraphPad Prism version 7, which was used to derive parameters (i.e., α and Q_0) and goodness of fit measures (i.e., RMSE and R^2) for all progressions. Additional parameters (i.e., P_{Max} and O_{Max}) were calculated using a freely available Excel tool (Kaplan & Reed, 2014). Curves fit using this model were compared using AICc (rather than sum-of-squares F-tests) because this approach provides likelihood estimates for both approaches considered, rather than relying on statistical hypothesis testing, which only permits rejection of the null hypothesis. For individual curves, AICc was used to determine whether a single curve or

separate curves were more appropriate across progressions for each rat. For group curves, AICc was used to determine whether a single curve or separate curves were more appropriate overall and for all progression comparisons (i.e., FL-RL, FH-RH, FL-RL, FH-RH, FL-RH, and FH-RL).

Local elasticity analyses. Model fit was evaluated using R^2 and RMSE, and plots of residuals were visually analyzed for systematic over or under deviation (McDowell, Calvin, & Klapes, 2016). If any datasets were not well fit (e.g., $R^2 < .7$, systematic deviations in residuals) by the best fitting model when consumption was plotted as a function of unit price (Hursh et al., 1988), local elasticities were determined for each rat's consumption in every progression based on the unit price equation. To determine local elasticities, untransformed consumption data were plotted on log-log axes, and log-log slopes were calculated between each sequential pair of data points in all conditions for each animal. These slopes were examined, and the first data points with a slope less than negative one (i.e., more negative than negative one) were selected for determining P_{Max}, unless visual analysis suggested this slope was due to a single, nonsystematic data point, in which case the data points surrounding the next slope that was less than negative one were selected. The price of P_{Max} was then estimated by averaging the unit prices from the two consecutive data points with log-log slope less than negative one. Consumption for each curve then was divided into two sections: elastic (slope from the first price assessed to the first point at P_{Max}) and inelastic (slope from the second point at P_{Max} to the breakpoint); these analyses were conducted with prices with zero consumption excluded and with zero consumption coded as 0.1. Linear regression was then used to determine the slope of each segment to permit comparison across progression types.

Statistical analyses. Additional statistical analyses were conducted using GraphPad Prism version 7. Because of the small sample sizes, tests of normality could be underpowered

(Razali & Wah, 2011), so non-parametric statistical tests were conducted. These included Spearman's Rho for correlations, Wilcoxon signed-ranks tests for paired comparisons, and Friedman's tests as an alternative to one-way repeated measures ANOVA. Sample size for the present experiment was determined based on conventions in the experimental analysis of behavior rather than from power analysis, and given issues with post-hoc power analyses (Hoenig & Heisey, 2001; Levine & Ensom, 2001), no power analyses were conducted for the current data. With a sample size of six, the Wilcoxon test only permits testing for significance at an *alpha* level of .05 for a two-tailed test (Wilcoxon, Katti, & Wilcox, 1975); thus, these tests were not corrected for multiple comparisons.

To further evaluate the findings from individual curve fits, parameters (i.e., α, Q_0, P_{Max} and O_{Max}) and goodness-of-fit measures (i.e., R^2 and RMSE) produced from all price modifications were tested for difference using Wilcoxon signed-ranks tests across the primary force and ratio comparisons (i.e., FL-RL and FH-RH). Breakpoints (i.e., first price with 95% or greater suppression of consumption) were compared only for unit price; breakpoints were not compared using other price modifications because most of these modifications required a reinforcer delivery, which did not occur in all conditions for all animals. Given the small sample sizes, these tests were not corrected for multiple comparisons.

To supplement the AICc comparisons, Friedman's test (non-parametric alternative to one-way repeated measures ANOVA) were conducted to compare RMSE produced by group curves across different price conversions. Given the exploratory nature of these tests, post-hoc results were conducted using Dunn's tests and reported with and without corrections for multiple comparisons.

Work data. The most common approach to quantifying work is to plot response output (i.e., total number of responses) as a function of unit price (Bickel, Madden, & DeGrandpre, 1997; Madden et al., 2000; Madden et al., 2005), but studies using this approach have not manipulated force or lever weight. Consistent with the procedures of Hursh et al. (1988) for quantifying work when a lever weight manipulation was used (see Unit price), total work was calculated by multiplying criterion responses × force criterion for each price. Several of the modifications of unit price were attempted for consumption data (see Price modifications) were also applied to quantifying total work output.

a) Total responses were determined by summing all responses (i.e., criterion and subcriterion) in each session and plotting them as a function of responses per reinforcer unit at each price.
b) Obtained total work was calculated by multiplying total responses (i.e., criterion and subcriterion) by mean peak force (N; including criterion and subcriterion responses) in each session and plotting as a function of obtained unit price.
c) The psychophysical scaling parameter adjustment of work was based on the Hursh et al. (1988) quantification of work and was determined by adjusting the force criterion (N) using the selected *s* parameter at each price for each animal, and then multiplying the adjusted force criterion by the programmed ratio. Total work adjusted by the psychophysical scaling parameter was plotted as a function of the ssychophysical scaling parameter adjusted unit price.
d) Mean cumulative time integral per reinforcer (g-s) was determined by summing time integral of force across all responses (i.e., criterion and subcriterion) and plotting as a function of mean time integral of force per reinforcer unit.

e) Mean cumulative duration per reinforcer was determined by summing all response durations (i.e., criterion and subcriterion) and plotting as a function of mean cumulative duration per reinforcer unit.

These plots of work data were assessed for visual convergence.

Results

All six rats completed at least four demand curve assays: low reinforcer magnitude increasing force (F-L), low reinforcer magnitude increasing ratio (R-L), high reinforcer magnitude increasing force (F-H), and high reinforcer magnitude increasing ratio (R-H). Additionally, four rats completed a replication of a single assay, and two rats completed replications of two different demand assays. Three replications were obtained for the F-L assay, two for the F-H assay, two for the R-L assay, and one for the R-H assay. Different numbers of price points were required for each rat to reach breakpoint (i.e., 95% suppression of consumption at the lowest price). If a rat's first progression was R-L (1N and 2N) or R-H (3M), the rat first completed a demand assay starting from unit price 0.49 through the breakpoint, and then the five lower unit prices (i.e., 0.05-0.44) in that condition were assessed following a three-day washout period. Other rats (1M, 2M, 4M) completed the ratio demand assays beginning at unit price 0.05 with no washout period between any prices within the ratio progression.

Consistent with the prediction that total consumption should be the same at unit prices equated by Equation 9, Figure 4 shows consumption (y-axis; number of 0.05-ml reinforcer units; see Data Analysis) as a function of unit price (price per 0.05-ml reinforcer unit; x-axis) calculated using Hursh et al. (1988) unit price for the F-L progression (closed squares and dot-dashed lines), F-H progression (open squares and dotted lines), R-L progression (closed circles

and solid lines), and R-H progression (open circles and dashed lines)[9]. To determine mean consumption across rats, zeroes were imputed for consumption at prices beyond the defined breakpoint for each rat, and mean consumption at each price point was calculated for each progression. The top panel shows group means, and the six lower panels show data from each animal. All animals showed systematic decreases in number of 0.05-ml reinforcer units earned as a function of increasing unit price. Note that Figure 4 shows consumption (i.e., FR completions × magnitude). A common alternative entails plotting reinforcer deliveries (i.e., FR completions) as a function of cost (i.e., FR × Force criterion; see Figure A2); this alternative approach depicts stratification of demand intensity across magnitudes. The α parameters derived for each progression type from these two approaches are identical, but the Q_0 parameters differ. Figure A2 shows stratification reflecting a magnitude effect, such that across a range of low costs per reinforcer delivery, there are more reinforcer deliveries in the low reinforcer magnitude condition relative to the high reinforcer magnitude condition. Consumption also hits a breakpoint at lower costs in the low reinforcer magnitude condition relative to the high reinforcer magnitude condition. By contrast, plotting consumption as a function of unit price (Figure 4) does not show this magnitude effect but permits testing two predictions of unit price: that consumption is the same at matched unit prices and that a single demand curve (i.e., the same derived α and Q_0) describes all the progression types.

Marked visual differences were noted in the shapes of the mean and individual curves obtained from the F-L and F-H progressions relative to those obtained for the R-L and R-H conditions. Relative to the R-L progressions, the F-L progressions tended to show greater consumption (i.e., more inelastic) across a range of low to moderate prices for both mean and

[9] Additionally, Figure A1 in Appendix A shows consumption (in ml) plotted as a function of unit price per ml; note the functions are the same whether plotted based on 0.05 ml or total ml.

individual animal data. The F-H progressions also tended to produce more inelastic demand at lower prices than the R-H curves, though this effect was pronounced for only four of the six animals (1M, 3M, 4M, and 2N). For four animals, breakpoints were visually lower in the F-H relative to F-L progression (1M, 2M, 4M, and 2N).

To visually assess reliability of consumption patterns for each progression type, consumption data from within-subject demand assay replications were plotted as a function of unit price in Figure 5. Across all panels, larger symbols show the initial demand assays and smaller symbols show the replications. Functions generally took a similar form across original and replication data, and only minor deviations were noted across replications. Because only some animals completed replications of each progression type (see Table 3), analyses in Experiment 1 included only data from the initial progression of each type (i.e., F-L, F-H, R-L, and R-H) for each animal.

Operant analyses. The peak force criterion was increased as a method of increasing price; to analyze changes in force across increasing force or ratio requirements of the demand assays, obtained mean peak force (i.e., average peak force of all subcriterion and criterion responses) and peak force standard deviations (i.e., standard deviations of the peak forces of all subcriterion and criterion responses) were calculated for every price point for each progression. Figure 6 shows mean peak force (y-axis) as a function of peak force criterion (left column; x-axis) or fixed ratio requirement (right column; x-axis) for individual animals (separate rows). Larger symbols show mean peak force of all responses, and smaller symbols show mean peak force of only criterion responses. Lines fit to the peak force of all responses as a function of peak force criterion (force progressions) and ratio requirement (ratio progressions) are shown at the bottom of each panel. Error bars show one SEM, and when error bars are not shown, error was

too small to be plotted with the data points. Most animals showed systematic increases in mean peak force as a function of increasing peak force criterion. In the force progressions, mean peak force changed as a function of force criterion with a slope less than one (range: 0.551-0.088 [highest slope was from 4M's F-H progression and lowest was from 1M's F-H progression]). For three rats, the slope in one condition was markedly higher than in the other (1M and 1N in the F-L progression and 3M in the F-H progression), and two rats showed high slopes in both conditions (4M and 2N). One rat (2M) showed relatively low slopes in both conditions. Additionally, mean peak force was elevated at the first price point in the second force progression (whether F-L or F-H) relative to the first force progression for three of six animals (1M, 4M, and 2N). Mean peak force was lower at the first price point in the second progression for one animal (2M), and mean peak force was similar at the first price point in both force progressions for two animals (1N and 3M). Three animals reached similar peak force criteria across the F-L and F-H progressions before reaching the defined breakpoint (2M, 4M, and 1N), whereas three animals reached higher peak force criteria in the F-H progression (1M, 3M, and 2N). Two animals attained relatively higher force criteria in the second force progression experienced (3M and 2N). In the ratio progressions, most animals showed relatively minimal increases in mean peak force across ratio requirements (i.e., slopes less than 0.11), with the exception of 2N, who showed marked increases in in the R-L progression. Moderately increasing slopes across increasing ratio requirement were observed for 2M in the F-L progression and 3M in the F-H progression. Across ratio and force progressions, there were no consistent differences across high and low reinforcer magnitude conditions.

Prior research has indicated that peak force variability corresponds with changes in peak force (Notterman & Mintz, 1965; Pinkston & Libman, 2017). Peak force standard deviations

were plotted to determine if this finding was replicated in the current study. Figure 7 shows mean peak force standard deviation (g; y-axis) as a function of peak force criterion (left column; x-axis) or fixed ratio requirement (right column; x-axis) for individual animals (separate rows). Peak force standard deviations tended to increase as mean peak force (see Figure 6) increased. In the ratio progressions, peak force standard deviations tended to be relatively stable across increasing ratio requirements, but with clear increases observed for 1N and 2N, consistent with increases in their mean peak force in the ratio progressions. In the force conditions, most animals show an increase in peak force standard deviation as mean peak force increased, though this was not pronounced for 1M and 2M. Across ratio and force progressions, there were no consistent differences across high and low reinforcer magnitude conditions.

The time integral of force is considered a measure of effort (Notterman & Mintz, 1965) and may be useful as a measure of price in behavioral economic demand (Hursh et al., 2013), so changes in time integral of force across force criteria and ratio requirements were evaluated. Figure 8 shows the mean time integral of force (y-axis) as a function of force criterion (x-axis; left column) and fixed ratio (x-axis; right column). The F-L and F-H progressions are shown by closed and open squares, respectively, and the R-L and R-H progressions are shown by closed and open circles, respectively. Error bars show one SEM, and when error bars are not shown, error was too small to be plotted with the data points. As peak force criterion increased, time integral tended to increase across the F-L and F-H progressions. Patterns across force progressions and animals were generally similar to those observed for mean peak force. Time integral tended to remain relatively flat across the ratio progressions, though time integral increased in in the R-L progressions for 2M and 2N, and 3M and 1N showed some increase in

the R-H progressions. Across ratio and force progressions, there were no consistent differences across high and low reinforcer magnitude conditions.

Response duration increases as response peak force increases (Fowler, 1987). Therefore, mean response duration, which isolates the time-related changes in time integral of force (Notterman & Mintz, 1965), were calculated to assess changes in duration across changing response requirements. Figure 9 shows mean response duration (y-axis) as a function of force criterion (left panels) or ratio requirement (right panels) for individual animals (rows). Error bars show one SEM, and when error bars are not shown, error was too small to be plotted with the data points. Across increasing force criteria, most animals' response duration increased. For 1M, increases were not pronounced, and for 2M, increases in duration tended to appear at only higher force criteria. Increases in response duration tended to correspond with increases in mean peak force (see Figure 6) and mean time integral of force (see Figure 8). No consistent differences were noted across animals as a result of reinforcer magnitude condition. Two animals (1M and 4M) showed relatively greater duration in the F-H condition relative to F-L, while one animal (2M) showed greater durations in the F-L relative to F-H condition. Changes in duration as a function of increasing ratio requirement were less consistent, with no clear differences discernible across reinforcer magnitude conditions. In some progressions, some animals showed greater response duration with increasing FR (2N, F-L for 2M, F-H for 3M), but some showed decreasing duration with small increases in ratio requirement that then flattened or increased (1M, 3M F-L, 4M, 1N F-H). In other conditions, some animals showed no consistent differences as a function of FR (2M F-H and 1N F-L). There were no consistent magnitude differences noted in response duration across animals. Two animals (3M and 4M) had relatively greater duration in

the R-H condition relative to R-L, while three animals (2M, 1N, and 2N) showed greater durations in the R-L relative to R-H condition.

Elevated force criteria result in changes in characteristics of responding (i.e., peak force, time integral of force, duration) and are associated with an increase in the proportion of subcriterion to total responses (Mitchell & Brener, 1991; Notterman & Mintz, 1965; Zarcone et al., 2009). These subcriterion responses, which have not been measured in most previous demand research (e.g., Hursh et al., 1988; Sumpter et al., 1999, 2004; cf. Nord, 2014), may contribute to changes in consumption as a function of increasing force criteria. Figure 10 shows the proportion of total to subcriterion responses (y-axis) as a function of force criterion (x-axis) for the F-L (closed squares) and F-H (open squares) progressions overall in the left column. The proportion for the first 10% of responses (closed, up triangles) and last 10% of responses (open, down triangles) in each session is shown for the F-L progressions (center panel) and F-H progressions (right panel). Individual animals are shown in rows. As force criteria increased, all animals showed an increasing proportion of subcriterion to total responses. Although for most animals this proportion tends to increase relatively consistently, 3M and 4M show a flat or decreasing proportion of subcriterion responses at midrange force criteria before the proportion of subcriterion responses increased again at higher force criteria. More moderate slopes (i.e., slopes less than 0.01) were also noted in the F-H progressions for 3M and 2N and in both force the F-L and F-H progressions for 4M. For all animals, in the last session in each force progression (i.e., the breakpoint or the session in which consumption was reduced by at least 95% of the first price point), at least 75% of total responses were subcriterion. For most animals, no consistent differences in proportion of subcriterion responses were noted across the first 10% of responses relative to the last 10% of responses, but 1N tended to show a greater proportion of

subcriterion responses in the last 10% of responses in session in both the F-L and F-H progressions. By contrast, 4M tended to have a greater proportion of subcriterion responses in the first 10% relative to last 10% of responses in each session.

Because the ratio requirement was held constant at 10 criterion responses in the force progressions, one effect of the increasing proportion of subcriterion to total responses could be an increase in the obtained ratio (Pinkston & Libman, 2017), which is not accounted for in the programmed ratio requirement component of unit price. Thus, responses per reinforcer delivery (i.e., subcriterion and criterion) was determined for each reinforcer delivery at every price point. Figure 11 shows the range (shaded area) and median number of responses per reinforcer delivery across all prices (x-axes) in the F-L (left panels) and F-H (right panels) progressions. Table 4 shows data from the F-L progression, and Table 5 shows the F-H progression. The mean number of responses per reinforcer delivery and standard deviation are shown across the force progressions for each rat (separate columns). The obtained ratio tended to increase as the force criterion—and unit price—increased.

As force criteria increase, rates of criterion responses decrease, whereas rates of the overall functional operant class increase (Pinkston & Libman, 2017). To examine changes in response rates, rates were plotted for all responses, criterion, and subcriterion responses at each force criterion and ratio requirement. Figure 12 shows responses per minute (y-axis) as a function of force criterion (x-axis) for the F-L (left panel) and F-H (right panel) progressions for individual animals (rows). Closed squares show the total response rates (for subcriterion and criterion responses), closed circles show criterion response rates, and open circles show subcriterion responses rates. Generally, total response rates tended to increase then decrease. These patterns are also reflected in subcriterion response rates, which showed a similar but more

marked increase before decreasing. By contrast, criterion response rates tended to decrease with every increase in force criteria.

Figure 13 shows responses per minute (y-axis) as a function of fixed ratio requirement (x-axis) for the R-L (left panel) and R-H (right panel) progressions for individual animals (rows). Closed squares show the total response rates (for subcriterion and criterion responses), closed circles show criterion response rates (i.e., responses with peak force greater than 5 g), and open circles show subcriterion responses rates (i.e., responses with peak force between the 4-g threshold and 5 g). Generally, total response rates tended to increase then decrease. These patterns are also reflected in criterion response rates, which are nearly identical to the overall responses rates. Relatively few subcriterion responses were observed, and rates for the subcriterion responses remained very low but typically showed a slight increase then decrease.

Time integral of force (Hursh et al., 2013) and duration (Peck & Byrne, 2016) have been considered as price manipulations in demand paradigms. Conceptually, cumulative measures of duration and time integral could increase through changes in the responses themselves (e.g., elevated response duration) or through greater numbers of responses. To assess the potential contribution of response duration to cumulative time integral of force, Spearman's Rho correlations between response duration and cumulative time integral of force per reinforcer unit were determined in each progression type for each rat. Figure 14 shows regression lines fit to mean cumulative time integral of force per reinforcer unit (y-axis) plotted as a function of mean duration per response (x-axis). Shown are Spearman's Rho correlation coefficients for the ratio progressions (left column) and force progressions are plotted (right) column. In the force progressions, the mean duration of response was positively related to mean cumulative time integral of force per reinforcer unit for most animals, with the exception of 2N's progressions

and 1N's F-H progression. For these animals, mean cumulative time integral of force per reinforcer unit tended to increase as mean response duration increased, but these relations were not significant. Relations were more varied in the ratio progressions, with half of the animals showing no significant relations (1M, 4M, and 1N). The other three animals (2M, 3M, 2N) had one or more positive relations between mean duration of response and mean cumulative time integral of force per reinforcer unit, and for 3M's R-L progression, mean duration of response was negatively related to mean cumulative time integral of force per reinforcer unit.

To assess the potential association of response duration with cumulative response duration per reinforcer unit, Spearman's Rho correlations were determined in each progression type for each rat. Figure 15 shows regression lines fit to mean cumulative response duration per reinforcer unit (y-axis) as a function of mean duration per response (x-axis). Spearman's Rho correlations are shown for the ratio progressions (left column) and force progressions (right column). In the force progression, most animals showed a positive relation between mean duration of response and mean cumulative duration of responding per reinforcer unit. For 2N's progressions, 2M's F-L progression, and 1N's F-H progression, however, mean cumulative response duration per reinforcer unit was not significantly related to mean response duration. In the ratio progressions, half of the animals showed no significant relations (1M, 4M, and 1N). The other three animals (2M, 3M, 2N) had one or more positive relations between mean duration of response and mean cumulative response duration per reinforcer unit, but for 3M's R-L progression, mean cumulative duration of responding per reinforcer unit was negatively related to mean duration of response.

Cumulative time integral of force and cumulative response duration per reinforcer unit were plotted as a function of responses per reinforcer unit to visually assess the potential

association between number of responses and these cumulative measures. Figure 16 shows mean cumulative time integral of force per reinforcer unit (y-axis; left column) and mean cumulative response duration per reinforcer unit (y-axis; right column) as a function of responses per reinforcer unit (x-axis) across all progressions (i.e., F-L, R-L, F-H, and R-H) for each animal (rows). Across all progressions, mean cumulative time integral of force per reinforcer unit and mean cumulative response duration per reinforcer unit tended to increase as number of responses per reinforcer increased. Functions relating cumulative time integral of force per reinforcer unit and responses per reinforcer unit were generally linear when plotted on log—log axes. Some animals showed reasonable convergence across the progression types, but marked divergence was observed for 3M, 4M, and 2N. For 3M and 4M, mean cumulative time integral per reinforcer unit was elevated in the force relative to ratio progressions when plotted as a function of responses per reinforcer unit. By contrast, 2N showed elevated cumulative time integral in the F-H and R-L progressions. For most animals, the functions relating cumulative duration and responses per reinforcer unit were linear and quite similar, but divergence was noted across progression types for some animals, especially 3M and 4M.

In previous demand research, greater IRTs were obtained in elevated lever weight conditions relative to lower lever weight conditions (Hursh et al., 1988). One possibility is that the elevated IRTs observed by Hursh et al. (1988) could be explained by unmeasured subcriterion responses, which increased with greater force criteria in the current experiment. Given the more granular measurement available with the force transducer, changes in IRTs across force criteria were assessed by plotting IRT distributions for times between consecutive criterion responses, as well as times between consecutive responses when subcriterion and criterion responses were examined. Figure 17 through Figure 28 show IRT by opportunity

distributions for each of the four progressions for all six animals. Figure 17, Figure 19, Figure 21, Figure 52, Figure 54, and Figure 27 show the R-L and F-L progressions, and Figure 18, Figure 20, Figure 22, Figure 24, Figure 26, and Figure 28 show the R-H and F-H progressions for 1M, 2M, 3M, 4M, 1N, and 2N, respectively. The x-axis shows 0.05-s IRT bins, and the y-axis shows the proportion of IRT opportunities (i.e., IRTs in that bin divided by all IRTs greater than or equal to that bin). The thin gray bars show the distribution of all IRTs (subcriterion and criterion), while the black data path shows the distributions of IRTs for only criterion responses. For most animals, the IRTs for all responses show a clear peak around 0.25 s at low prices for all progressions (F-L, R-L, R-H, F-H). For 2M, however, IRT distributions did not show clear peaks, and her distributions were wider and flatter across all price points (see Figure 19 and Figure 20). Few consistent differences in overall IRT distributions were observed between increasing ratio requirements and force criteria. With increasing prices, some animals showed a slight widening of the overall force IRT distributions and relatively higher peaks in the ratio IRT distributions. These are most pronounced for 3M's R-L and F-L progressions, but can also be observed for 4M's high reinforcer magnitude progressions. At low force criteria, few differences are visible between the distributions for criterion and all IRTs. As force criteria increased, however, the proportion of shorter criterion IRTs decreases markedly relative to all IRTs for most animals.

Behavioral economic analyses. Visual comparison of Figure 4 suggested differences in consumption between the force and ratio comparisons. Because no universally accepted statistical tests were available to compare consumption across prices and progression types (i.e., no nonparametric alternative to two-way repeated measures ANOVA), Wilcoxon tests were used to compare consumption across progression types at each price point. Zeroes were imputed for

consumption at prices beyond the defined breakpoint in each progression, and tests on consumption across price comparisons using Wilcoxon tests revealed significant differences in consumption between the F-L/R-L progressions from prices 0.98 to 2.94, the F-H/R-H progressions from prices 0.98 to 1.96, the F-L/F-H progressions at price 2.94, the F-L/R-H progressions from prices 1.47 to 2.94, and the R-L/F-H progressions from prices 0.98 to 1.47. There were no significant differences in consumption between the R-L/R-H progressions at any prices.

Price modifications. Given the visual and statistical differences in consumption at matched unit prices across the different progression types, various price modifications were calculated in an attempt to bring greater convergence to the consumption data. Specifically, these analyses allowed for an initial assessment of variables potentially controlling consumption across progression types. Whether these variables helped account for consumption was determined by the likelihood of a single curve providing a better fit to all data across progression types (i.e., AICc comparisons) relative to a single curve, as well as by relatively lower error resulting from fitting a single curve to all progression types across price modifications. Several of these modifications entailed using obtained measures of cost or effort for each session: obtained responses per reinforcer unit, obtained unit price per reinforcer unit, mean cumulative time integral of force per reinforcer unit, and mean cumulative duration of responding per reinforcer unit.

Psychophysical scaling parameter adjustments were obtained by modifying unit price by applying an exponent to the force criterion component of unit price across all prices assessed (see Equation 13). Figure 29 shows consumption (y-axis) as a function of unit price with psychophysical scaling parameter transformations (x-axis) for individual animals (separate

columns). Each row shows adjustment by a different *s* exponent (i.e., 0.9 to 0.55 in 0.05 increments); smaller exponents reflect a relatively lower "cost" of increasing force criteria relative to increasing FR requirements. Modifications of unit price were calculated according to Equation 14 across a range of *s* values, which were visually assessed for convergence across progressions. Values within the range of 0.9 to 0.55 were judged as bringing greater visual convergence relative to values outside this range. For each rat, a curve was then fit to all progressions (i.e., F-L, F-H, R-L, and R-H) at each *s* value; for these comparisons, the *k* values for each rat were constrained to that rat's log-transformed total range of consumption (i.e., 1M: 2.9, 2M: 2.96, 3M: 2.77; 4M: 2.98; 1N: 2.89; 2N: 2.87), and the Q_0 and α parameters were shared. The exponent that produced the most marked visual convergence was then determined separately for each animal by comparing R^2 and RMSE. The *s* value that produced the lowest RMSE and highest R^2 was selected for each animal. When the lowest RMSE and highest R^2 occurred across multiple *s* values (i.e., a tie; see 1M, 2M, 1N, and 2N), the absolute sum-of-squares was compared, which resolved the tie for 1M. For 2N, the middle *s* value was selected from amongst three with identical fit and error. For 2M and 1N, the lower of the two *s* values with the best fit was selected. These quantitative comparisons also confirmed the visual analysis, in that measures of fit and error tended to be worse at the extremes of the range examined (0.9 and 0.55) relative to interior values (i.e., 0.85 to 0.6). An asterisk on the figure judged as most converged for each animal denotes the *s* parameter used in subsequent analyses. Across animals, exponents ranged from 0.8 (2M) to 0.6 (3M).

After calculating price modifications, AICc comparisons were used to determine whether the linear or exponential model provided the better fit to the most datasets across price modifications and thus should be used in subsequent analyses. Because unit price and the price

modifications were compared using AICc and RMSE, the model yielding the better fits was chosen for subsequent analyses as both of these measures (AICc and RMSE) reflect the fit of the chosen model to the data. Figure 62 shows results of the AICc comparisons in each price modification (rows; unit price, responses per reinforcer unit, obtained unit price, psychophysical scaling adjustment of unit price, cumulative time integral of force per reinforcer unit, and cumulative duration of responding per reinforcer unit) across different progressions (sub-rows; F-L, R-L, F-H, R-H) for each animal (columns). Filled circles show greater likelihood of the exponential model, and open circles show a greater likelihood of the linear model. Relative preference is shown by circle size, and blanks show indifference (i.e., likelihoods between 40-60%). For these comparisons, prices in which no reinforcer deliveries were earned are excluded, and the *k* value for each rat was constrained to its average range of consumption in log units (i.e., 1M 2.7, 2M 2.68, 3M 2.67, 4M 2.79, 1N 2.74, 2N 2.61). Other parameters (i.e., Q_0 and α for the exponential model and *L, a,* and *b* for the linear model) were unconstrained. Overall, the exponential model was preferred in 70.8% of cases in which model selection was differentiated (i.e., minimum 60% likelihood of preferred model)[10]. For most price modifications, the exponential model was preferred, with exceptions for the unit price equation and unit price with psychophysical scaling parameter adjustments, which produced similar numbers of cases for both the linear and exponential models. Given the relatively greater number of cases for which the exponential model produced a better fit, this model was used for all subsequent analyses.

[10] For unit price, when consumption was entered as 0.1 for prices in which no reinforcers were earned, the likelihood of the linear model for 3M's F-H progression dropped to 77%; for 4M's F-H progression, the model shifted from undifferentiated to 65% likelihood of linear; and for 2N's F-H progression, the likelihood shifted to 99% likelihood of the exponential model from having too few datapoints to determine a preferred model. For 1N's F-H model, there were still too few datapoints to determine a preferred model.

Individual curve fits. A prediction of the unit price equation is that the same curves should describe consumption plotted as a function of unit price (Hursh et al., 1988), so curves were fit to consumption data as a function of unit price to compare derived parameters and goodness-of-fit measures. Because demand is plotted in log-log units, sessions without consumption can not be evaluated; alternative approaches include excluding 0 consumption or substituting a small number for 0 (i.e., 0.1; Koffarnus et al., 2015). Price points with 0 consumption occurred only in force progressions (i.e., 3M's F-L, 4M's F-H, 1N's F-H, and 2N's F-H progressions), potentially biasing results for these analyses if data with 0 consumption were excluded. The price modifications, however, were obtained from operant data and could not be calculated in sessions without a reinforcer delivery. To be conservative, analyses of consumption as a function of unit price were conducted with 0 consumption coded as 0.1 to help account for these potential biases, and also with consumption excluded to be consistent with the analyses used for the price modifications. Figure 31 shows exponential demand curves fit to consumption as a function of unit price for individual rats; all assessed prices are included here except those in which zero reinforcer deliveries were earned. Figure 32 shows exponential demand curves fit to consumption as a function of unit price for individual rats with all assessed prices included; if no reinforcer deliveries were earned at a given price, 0.1 was substituted for 0 (i.e., 3M's F-L, 4M's F-H, 1N's F-H, and 2N's F-H progressions). For these curves, k was constrained to each rats' average range of consumption in log units (i.e., 1M 2.7, 2M 2.68, 3M 2.67, 4M 2.79, 1N 2.74, 2N 2.61), and Q_0 and α were derived. Across both figures, closed circles and solid lines show R-L progressions, open circles and dashed lines show R-H progressions, closed squares and dot-dashed lines show F-L progressions, and open squares and dotted lines show F-H progressions. Inset panels show residuals. Across animals, residuals tended to show systematic deviation, with

over then under deviations. Curves were well fit to data from the R-L (R^2: *Mdn* = .94, range = .91-.98; RMSE: *Mdn* = 0.125, range = 0.089-0.26) and R-H (R^2*: Mdn* = .97, range = .94-.98; RMSE: *Mdn* = 0.105, range = 0.093-0.13) progressions. When prices with no consumption were excluded, fits were poor to moderate in the F-L (R^2: *Mdn* = .78, range = .57-.93; RMSE: *Mdn* = 0.205, range = 0.12-0.41) and F-H (R^2*: Mdn* = .67, range = .4-.79; RMSE: 0.31, range = 0.2-0.49) progressions. When prices with no consumption were included, fits remained poor to moderate in the F-L (R^2*: Mdn* = .76, range = .45-.93; RMSE: *Mdn* = 0.24, range = 0.14-0.65) and F-H (*R2: Mdn* = .43, range = .4-.79; RMSE: 0.655, range = 0.35-1.2) progressions.

Figure 33 shows derived parameters and goodness-of-fit measures obtained from fitting the exponential model to consumption as a function of unit price without (left panel) and with prices with 0 consumption (right panels). When prices with no consumption were excluded, comparisons of the F-L and R-L progressions revealed significant differences between the conditions on α (W = 21, p = .03), P_{Max} (W = -21, p = .03), and O_{Max} (W = -21, p = .03), such that the F-L progressions had higher P_{Max} and O_{Max} and lower α. There were no significant differences in Q_0 (W = -7, p = .56) across these progressions. Although RMSE and R^2 values generally suggested worse fits in the F-L relative to R-L conditions, these differences were not statistically significant (RMSE: W = -9, p = .40; R^2: W = 17, p = .09). These results did not change when prices with no consumption were included and coded as 0.1.

Comparisons of the F-H and R-H progressions when 0 consumption data were excluded showed significantly lower α (W = 21, p = .03) and higher O_{Max} (W = -21, p = .03) in the F-H relative to R-H progressions. There were no differences in P_{Max} (W = -15, p = .16) or Q_0 (W = -19, p = .06). There were also significant differences in R^2 (W = 21, p = .03) and RMSE (W = -21, p = .03), with the exponential model producing significantly worse fits to the F-H relative to R-

H progressions. When the 0 consumption data were included (coded as 0.1), the derived parameters α ($W = 17$, $p = .09$) and O_{Max} ($W = -15$, $p = .16$) were no longer significantly different between the F-H and R-H comparisons, but Q_0 ($W = -21$, $p = .03$) was significantly greater in the F-H progression. There were still no significant differences in P_{Max} ($W = 3$, $p = .84$), and the differences in R^2 ($W = 21$, $p = .03$) and RMSE ($W = -21$, $p = .03$) remained significant.

The systematic deviations in residuals and significant differences in fit between the F-H and R-H progressions suggest interpretation of the derived parameters from these models should be interpreted with caution. Thus, local elasticity analyses, in which slopes between successive data points were assessed to determine the point of P_{Max} (see Local elasticity analyses), were also conducted on these data. Specifically, these analyses were conducted with 0 consumption excluded (see Figure 34) and included (coded as 0.1; see Figure 35). For these figures, consumption is along the y-axis and unit price is along the x-axis with different progressions in columns and individual animals in rows. Data points outlined in red show the points selected as P_{Max} (i.e., generally the first two data points with a slope less than negative one), and red log-log lines show the slopes of the elastic and inelastic portion of each curve. The P_{Max} value displayed on each panel is the average of the two prices associated with the slope less than negative one. For some animals, visual analysis suggested the first points selected as P_{Max} were not consistent with the overall changes in consumption across the function (i.e., a single parameter was inconsistent). For these conditions, the first price point selected as P_{Max} is shown in gray text, and the next data points with a slope less than negative one were used to determine the point of P_{Max}.

Figure 36 shows slopes of the inelastic portion of each curve (first panel), slopes for the elastic portion of each curve when 0 consumption points were excluded (second panel) and

included (third panel), and the points of P_{Max} (bottom panel). There were no significant differences in the slopes of the inelastic portions of the curves comparing F-L and R-L (W = -11, p = .31) or F-H and R-H (W = -11, p = .31) progressions. Comparisons of the slopes of the elastic portion of the curves were consistent regardless of whether 0 consumption was excluded or included, with no significant differences when comparing the F-L and R-L (W = 13, p = .22) progressions but significantly greater slopes in the F-H relative to R-H (W = 21, p = .03) progressions. Significant differences were found in P_{Max} when comparing the F-L and R-L (W = 21, p = .03) and F-H and R-H (W = 21, p = .03) progressions, such that the F-L and F-H progressions resulted in greater P_{Max} than the R-L and R-H progressions, respectively.

Breakpoints, another measure obtained from the demand assays, were also compared for differences; note that the breakpoint was defined as 95% or greater suppression of consumption from the first matched price (i.e., unit price 0.49). Figure 37 shows unit price breakpoints across the four price progressions with medians and IQRs. Wilcoxon signed-rank tests revealed significantly higher breakpoints in the F-L relative to R-L progressions (W = -21, p = .03) but no significant differences between the F-H and R-H progressions (W = -9, p = .41).

Given the differences in demand plotted as a function of unit price across various demand measures, other price modifications were attempted to bring greater convergence across progression types. Whether these variables helped account for consumption was determined by assessing the likelihood of a single curve providing the best fit to the data across progression types (i.e., from AICc comparisons) and through comparisons of the RMSE resulting from fitting a single curve to all progression types across price modifications. Exponential curves were fit to consumption in each progression type for all rats as a function of each price modification. Figure 38 through Figure 42 show exponential curves fit to individual rats' consumption data as a

function of the price modifications of responses per reinforcer unit (Figure 38), obtained unit price (Figure 39), unit price with psychophysical scaling adjustments (Figure 40), mean cumulative time integral of force per reinforcer unit (Figure 41), and mean cumulative duration of responding per reinforcer unit (Figure 42). In all figures, closed circles and solid lines show R-L progressions, open circles and dashed lines show R-H progressions, closed squares and dot-dashed lines show F-L progressions, and open squares and dotted lines show F-H progressions. Inset panels show residuals. Generally, there were few systematic deviations in residuals across the different price modifications, but deviations were noted when consumption was plotted as a function of the psychophysical scaling parameter modifications of unit price and when consumption was plotted as a function of mean cumulative duration of responding per reinforcer unit. Relative to the Hursh et al. (1988) unit price equation (Equation 9), these price modifications generally improved the fits of the exponential model to the force progressions, and visual analysis suggested greater convergence across the progression types using these modifications.

Figure 38 shows consumption as a function of responses per reinforcer unit. For this price modification, the exponential model generally fit the data well across the F-L (R^2*: Mdn* = .84, range = .7-.96; RMSE: *Mdn* = 0.18, range = 0.09-0.3), F-H (R^2*: Mdn* = .98, range = .62-1; RMSE: *Mdn* = 0.08, range = 0.02-0.29), R-L (R^2*: Mdn* = .95, range = .89-.98; RMSE: *Mdn* = 0.125, range = 0.089-0.23), and R-H (R^2*: Mdn* = .97, range = .94-.98; RMSE: *Mdn* = 0.11, range = 0.09-0.13) progressions. Plotting consumption as a function of responses per reinforcer unit resulted in moderate visual convergence across most rats, with the exception of 4M, who showed minimal convergence.

Figure 39 shows consumption as a function of obtained unit price. In these graphs, the exponential model generally fit the data well across the F-L (R^2*: Mdn* = .94, range = .91-.97; RMSE: *Mdn* = 0.12, range = 0.08-0.19), F-H (R^2*: Mdn* = .98, range = .83-.99; RMSE: *Mdn* = 0.07, range = 0.05-0.19), R-L (R^2*: Mdn* = .94, range = .91-.97; RMSE: *Mdn* = 0.13, range = 0.1-0.17), and R-H (R^2*: Mdn* = .96, range = .94-.98; RMSE: *Mdn* = 0.12, range = 0.08-0.13) progressions. In these graphs, marked visual convergence across progression types was found for most animals, with the exception of 3M.

Figure 40 shows consumption as a function of unit price with psychophysical scaling parameter adjustments, and in these graphs, moderate visual convergence across progression types was found for all animals. In these graphs, the exponential model generally fit the data well across the R-L (R^2*: Mdn* = .94, range = .91-.98; RMSE: *Mdn* = 0.11, range = 0.09-0.16) and R-H (R^2*: Mdn* = .97, range = .94-.98; RMSE: *Mdn* = 0.10, range = 0.09- 0.12) progressions. By contrast, fits were moderate to poor for the F-L (R^2*: Mdn* = .71, range = .52-.85; RMSE: *Mdn* = 0.26, range = 0.16-0.43) and F-H (R^2*: Mdn* = .6, range = .34-.73; RMSE: *Mdn* = 0.55, range = 0.22-0.40) progressions.

Figure 41 shows consumption as a function of mean time integral of force and in these graphs, marked visual convergence across progression types was found for most animals, with the exception of 3M and 4M. In these graphs, the exponential model generally fit the data well across the R-L (R^2*: Mdn* = .96, range = .94-.98; RMSE: *Mdn* = 0.12, range = 0.08-0.16), R-H (R^2*: Mdn* = .97, range = .95-.98; RMSE: *Mdn* = 0.11, range = 0.08-0.13), F-L (R^2*: Mdn* = .95, range = .9-0.96; RMSE: *Mdn* = 0.1, range = 0.07-0.17), and F-H (R^2*: Mdn* = .98, range = .83-.99; RMSE: *Mdn* = 0.08, range = 0.05-0.19) progressions.

Figure 42 shows consumption as a function of mean duration of responding, and in these graphs, marked visual convergence across progression types was found for most animals, with the exception of 2N. In these graphs, the exponential model generally fit the data well across the R-L (R^2*: Mdn* = .96, range = .94-.99; RMSE: *Mdn* = 0.13, range = 0.06-0.16) and R-H (R^2*: Mdn* = .97, range = .97-.98; RMSE: *Mdn* = 0.09, range = 0.08-0.1) progressions. The exponential model fit the data moderately well to well in the F-L (R^2*: Mdn* = .94, range = .77-.97; RMSE: *Mdn* = 0.13, range = 0.07-0.27) and F-H (R^2*: Mdn* = .96, range = .74-.99; RMSE: *Mdn* = 0.09, range = 0.05-0.29) progressions.

The derived parameters and goodness-of-fit measures were compared for differences, consistent with the analyses conducted on the parameters from curves fit to unit price. Figure 43 shows derived demand parameters and goodness-of-fit measures for individual animals across different price conversions. Curves fit to consumption as a function of unit price with psychophysical scaling parameter adjustments yielded significant differences in some derived parameters and goodness-of-fit measures. Specifically, Q_0 was significantly higher in the F-H relative to R-H progression (W = -21, p = .03), R^2 was significantly lower in the F-L relative to R-L (W = 21, p = .03) and F-H relative R-H progressions (W = 21, p = .03), and RMSE was significantly higher in the F-H relative to R-H progressions (W = -21, p = .03). With the psychophysical scaling parameter adjustments, there were no significant differences in α or P_{Max} (all p > .06), and there were no significant differences between the F-L and R-L progressions for Q_0 or RMSE (all p > .06). There were no significant differences in the primary force-ratio comparisons (F-L vs R-L and F-H vs R-H) for any of the other measures (α, Q_0, P_{Max}, R^2, RMSE; all p > .06) across the other price conversions (responses per reinforcer unit, obtained unit price,

mean cumulative time integral of force per reinforcer unit, and mean cumulative duration of responding per reinforcer unit).

To increase confidence in the findings, AICc tests were used to assess whether consumption across the progressions at each price modification was better described by a single exponential curve or separate exponential curves. Relative preference for a single curve would suggest relatively greater likelihood of that price modification accounting for consumption across progression types. Figure 44 shows results of AICc tests for each rat comparing a single curve versus separate curves across all progression types (i.e., F-L, R-L, F-H, R-H) for unit price and the five price modifications. Black circles show greater likelihood of a single curve for all progressions, and white circles show greater likelihood of separate curves for each progression type. Size shows relative likelihood, and blanks show indifference (i.e., likelihood of preferred model between 50-60%). For unit price, separate curves were most likely for all rats. For the responses per reinforcer unit measure, separate curves were more likely for four rats, a single curve was more likely for one rat, and the AICc comparison resulted in relative indifference for one rat. For the time integral measure, separate curves were more likely for four of the six rats. For duration and obtained unit price a single curve was more likely for four of the six rats. For unit price with psychophysical scaling parameter adjustments, a single curve was preferred for five of six animals, but these results should be interpreted with caution given the significant differences in RMSE found for curves fit to the psychophysical scaling adjustments. That is to say, these AICc likelihood estimates do not indicate goodness-of-fit of a single curve, but relative preference for a single curve given the error produced by separate curves.

The AICc comparisons evaluate relative fit of single versus separate curves, so RMSE was determined to assess absolute fit of a single curve fit to each rat's data. Figure 45 shows

RMSE for single (top panel) and separate (bottom panels) curves fit to each animal's progressions (i.e., F-L, R-L, F-H, R-H) across unit price and the five price modifications. In the top panel, gray open circles show RMSE for each animal, and in the bottom panels closed circle show R-L progressions, open circles show R-H progressions, closed squares show F-L progressions, and open squares show F-H progressions. A Friedman's test on RMSE produced by fitting a single curve at each price revealed a significant main effect ($\chi^2 = 21.39$, $p > .001$). Given the exploratory nature of these analyses, post-hoc tests were conducted with and without correction for multiple comparisons. Post-hoc Dunn's tests without correction revealed significantly greater RMSE in the single curve fit to consumption as a function of unit price relative to responses per reinforcer unit (Rank sum difference = 14, $p = .03$, adjusted $p = .46$), but this did not remain significant after correcting for multiple comparisons. Unit price with psychophysical scaling parameter adjustments also showed higher RMSE than obtained price (Rank sum difference = -13.5, $p = .04$, adjusted $p = .56$) and the cumulative duration measure (Rank sum difference = 16, $p = .01$, adjusted $p = .20$), but this comparison also did not remain significant after correcting for multiple comparisons. After correcting for multiple comparisons, results showed that the unit price equation produced greater RMSE than the obtained unit price (Rank sum difference = 22.5, $p < .001$ adjusted $p = .008$), cumulative time integral (Rank sum difference = 19.5, $p = .003$, adjusted $p = .04$), and cumulative duration (Rank sum difference = 25, $p < .001$, adjusted $p = .002$) price modifications.

Group curves. Curves were also fit to group data across three approaches to aggregation to supplement the findings derived from individual data. Figure 46 shows three different aggregation approaches for plotting group consumption data: means (top left panel), medians (top right panel), and all group data (middle left panel). The group data approach fit curves to all

non-zero data points from all animals, rather than fitting curves to means or medians. Price modifications (see Equation 12 through 16) were individualized for each animal. Most price modifications—with the exception of the psychophysical scaling parameter adjustment—were obtained from operant data, and the x-coordinates were not the same across animals, preventing the calculation of means or medians for group curve fits. To be most consistent with the approach used to aggregate data in the other price modifications, the group data approach was selected for all analyses.

For curves fit to group data, k was set to 2.70, which was determined by taking the average range of consumption across all animals and progressions then log transforming. The closed circles and solid lines show R-L progressions, open circles and dashed lines show R-H progressions, closed squares and dot-dashed lines show F-L progressions, and open squares and dotted lines show F-H progressions. Inset panels show residuals. The bottom panel shows RMSE for a single curve fit to all progression types (black stars) and separate curves fit to the group data across progression types (gray open circles) for these different aggregation methods. Consistent with the findings from the individual analyses, group residuals tended to show systematic deviations. The group RMSE of separate curves also tended to vary widely within each aggregation approach. Single curve RMSE was generally similar across the aggregation approaches and was lowest for the curve fit to median data and highest for the curve fit to the group data approach.

Figure 47 shows curves fit to group data across different price modifications. Closed circles and solid lines show R-L progressions, open circles and dashed lines show R-H progressions, closed squares and dot-dashed lines show F-L progressions, and open squares and dotted lines show F-H progressions. Inset panels show residuals. The top left panel shows unit

price, the top right panel shows responses per reinforcer unit, the middle left panel shows obtained unit price, the middle right panel shows unit price with psychophysical scaling parameter adjustments, the bottom left panel shows cumulative time integral per reinforcer unit, and the bottom right panel shows cumulative duration per reinforcer unit. Residuals generally showed systematic deviations. Visual analyses suggested the price modifications plotted here showed greater convergence relative to unit price.

To quantitatively examine convergence at the group level, AICc comparisons were also conducted to assess the likelihood of a single curve describing the data for each price modification; relative preference for a single curve would suggest relatively greater likelihood of that price modification accounting for consumption across progression types. Figure 51 shows AICc comparisons of single versus separate curves for group data at each price modification (rows). Columns show results of AICc comparisons for all progressions in a condition and the results of comparisons across pairs of progression types. Black circles show greater likelihood of a single curve, and white circles show greater likelihood of separate curves for the different progressions. Size shows relative preference, and blanks show indifference (i.e., likelihood between 50-60%). For three price modifications—obtained unit price, psychophysical scaling parameter adjustment of unit price, and cumulative duration per reinforcer unit—a single curve was more likely than separate curves when fitting to the data across all progression types (i.e., F-L, R-L, F-H, R-H). By contrast, separate curves better described the data across the four progression types for unit price, responses per reinforcer unit, and time integral of force per reinforcer unit. For unit price and the price modifications of responses per reinforcer unit and time integral of force per reinforcer unit, separate curves were generally more likely than individual curves for most comparisons. For obtained unit price, a single curve was more likely

for three comparisons, including overall, while separate curves were preferred for three comparisons. By contrast, for psychophysical scaling parameter adjustments to unit price, single curves were preferred for all comparisons except FL-RH, wherein separate curves were preferred. Similarly, for cumulative duration per reinforcer unit, single curves were preferred for all comparisons except FH-RH, which was indifferent.

Because AICc comparisons evaluate relative fit of single versus separate curves, RMSE was determined to assess absolute fit of a single curve for all rats' data at each price modification. Figure 49 shows RMSE for group curve fits, with gray open circles showing RMSE for a separate curve for each progression and black stars showing RMSE for a single curve fit to all group progressions. A Friedman's test on RMSE of the separate curves for each progression at the different price modifications revealed a significant main effect ($\chi^2 = 13.51$, $p = .019$). Post-hoc Dunn's tests without correction revealed significantly greater RMSE in the single curve fit to consumption as a function of unit price relative to the cumulative duration price conversion (Rank sum difference = 13.5, $p = .011$, adjusted $p = .161$), but this did not remain significant after correcting for multiple comparisons. Unit price with psychophysical scaling parameter adjustments also showed higher RMSE than the responses per reinforcer unit (Rank sum difference = -12, $p = .011$, adjusted $p = .350$) and cumulative duration measures (Rank sum difference = 15.5, $p = .023$, adjusted $p = .051$), but these comparisons also did not remain significant after correcting for multiple comparisons. No post-hoc comparisons remained significant after correcting for multiple comparisons. Visual analyses suggested that the RMSE for a single curve was lowest for consumption plotted as a function of cumulative duration.

Total work. To assess the prediction that a unitary function should describe total output as a function of unit price (i.e., work output should be superimposed across progression types),

work data were plotted as a function of unit price and visually assessed for deviations. Figure 50 shows a unit price approach to quantifying work; in this figure, work data (y-axis) are calculated by multiplying the number of criterion responses by the force criterion (N) at each unit price (x-axis). The top panel shows group means, and the six lower panels show data from each animal. All animals showed an increase in total work output at lower prices and then a decreasing trend at higher prices. Marked visual differences tended to emerge in the shapes of the mean curves obtained from the F-L and F-H progression relative to those obtained for the R-L and R-H conditions, with visual analysis suggesting greater work was performed in the force progressions (F-L and F-H) relative to the ratio progressions (R-L and R-H) at mid to high unit prices overall and for most animals.

Given these differences, Figure 51 through Figure 55 show various methods of quantifying work (y-axis) as a function of price (x-axis) across the four progressions for individual animals (separate panels). Group means are shown for work using unit price (Figure 50, but group means are not shown for the price modifications because the obtained data resulted in different prices across rats.

Because deviations were noted in the work curves obtained for unit price, work curves were also plotted for the price modifications. Figure 51 shows total response output (number of criterion and subcriterion responses; y-axis) as a function of total responses per reinforcer unit (criterion and subcriterion responses; x-axis). Visually, this approach to quantifying price and work brought greater convergence across progression types for two animals (2M and 1N) relative to the functions produced by unit price (see Figure 50), but these data overall were only moderately converged. In Figure 52, obtained work (total responses times mean peak force; y-axis) is plotted as a function of obtained unit price (mean responses per reinforcer delivery time

mean peak force divided by reinforcer units per delivery). Visual analysis suggested that obtained work generally converged across price progressions for most animals, though some divergence was visible in the force progressions for 3M and 1N. In Figure 53 obtained work adjusted by a psychophysical scaling parameter (y-axis) is plotted as a function of unit price adjusted by a psychophysical scaling parameter (x-axis). The psychophysical scaling adjustments brought general convergence to the work data for most animals. Figure 54 shows total time integral of force (y-axis) as a function of mean time integral of force per reinforcer delivery. Relative to the unit price work functions, greater visual convergence was seen across progressions, but the force functions tend to deviate to some degree for 3M, 4M and 1N. Figure 55 shows total cumulative response duration (y-axis) as a function of mean cumulative response duration per reinforcer unit (x-axis). Although greater convergence was noted relative to the original unit price work curves, deviations were found across magnitude progressions for 1M and 1N and across the ratio and force progressions for 4M.

Discussion

To my knowledge, this is the first study to fit the exponential demand model to both ratio and force progressions. Differences in consumption, curve fits, and work curves were obtained when comparing ratio and force progressions. Specifically, consumption tended to be higher across a range of low to moderate unit prices in the force relative to ratio progressions. When exponential demand curves were fit to consumption as a function of unit price, fits were generally worse in the force relative to ratio progressions, though this was significant only for high reinforcer magnitude comparisons. Although the worse fits prompt caution, derived parameters varied across force and ratio progressions, and separate curves also better described the force and ratio progressions across individual and group-level analyses. Additional support of

these findings is provided by local elasticity analyses that produced different elastic slopes across the F-H/R-H comparisons and different points of P_{Max} across F-L/R-L and F-H/R-H comparisons. Visual analysis of total work (i.e., total responses × force criterion) plotted as a function of unit price also suggested clear deviations across force and ratio progressions.

Such findings are broadly consistent with the results of Sumpter at al. (1999, 2004), who found differences in consumption between ratio and force progressions. Sumpter et al. suggested the results they obtained were due to the greater time requirements in the ratio relative to force progressions, but their use of a weighted door arrangement limited the data collected the actual force of responses, as well as the presence of subcriterion responses.

To address the limitation of the weighted door arrangement used by Sumpter et al. (1999, 2004), a force transducer was used in the current study to program force requirements and measure responding across ratio and force progressions; to my knowledge, this is the first study to use such measurement across force and ratio progressions in behavioral economic demand. This enhanced measurement revealed additional details about the effects of the programmed cost requirements on rats' responding, outcomes that can not be recorded using traditional weighted operanda arrangements. First, rats' patterns of force differentiation varied within and across animals. Markedly better force differentiation was observed for some animals relative to others, and some rats showed enhanced force differentiation in one of the force progressions relative to another. Second, a number of other changes accompanied changes in response peak force, including greater force variability, longer response durations, and elevated time integral of force. Of note, IRT distributions generally did not vary markedly between the ratio and force progressions or across increasing force criteria when times between all responses (i.e., criterion and subcriterion) were examined. When times between only criterion responses were calculated,

however, the proportion of shorter IRTs dropped markedly. Such findings regarding longer criterion IRTs at higher force criteria are generally consistent with the findings of Hursh et al. (1988), who noted greater IRTs in their higher lever weight conditions. The current data suggest such elevated IRTs may be due to subcriterion responses occurring between criterion responses, as cumulative records show subcriterion responses tended to occur in between criterion responses and more often at higher force values. These data suggest that the elevated IRTs obtained from weighted levers may be an artifact of that measurement approach. Finally, as force criteria increased, relatively more subcriterion responses were emitted. Including these subcriterion responses in analyses of response rates revealed an increasing then decreasing trend in total rates, rather than the only decreasing trend in rates of criterion responses.

Given the differences in consumption across ratio and force progressions plotted as a function of unit price, several candidate price modifications were analytically evaluated in an attempt to bring greater convergence to the consumption and work data across progression types. When examined visually, all price modifications brought relatively more convergence to graphs of consumption and work relative to unit price, but when curves were fit to consumption, three price modifications significantly reduced RMSE relative to unit price: obtained unit price, cumulative duration of responding per reinforcer unit, and time integral of force per reinforcer unit. Across qualitative comparisons, two measures brought the most marked visual convergence to the data across progression types: obtained unit price and cumulative duration of responding per reinforcer unit. Of note, the obtained unit price, cumulative time integral of force, and cumulative duration price modifications were possible only because of the data collection permitted by the force transducer. Subcriterion responses were a critical component of these price modifications, as responses with peak force below the force criterion (i.e., subcriterion)

increased the obtained ratio (Pinkston & Libman, 2017) and thus total time and effort spent responding. Experiment 2 was undertaken to evaluate the role of obtained responses per reinforcer unit on consumption to control for fluctuations in obtained ratio due to variability in force differentiation.

Experiment 2

Consistent with results reported by Sumpter et al. (1999 2004), ratio and force progressions produced different patterns of consumption across increasing price points. The force transducer, however, permitted additional measurements. For example, increasing proportions of subcriterion responses (Figure 10) and number of responses per reinforcer delivery (Table 4 and Table 5) were found with higher peak force criteria. These results raise the question of whether decreases in consumption found across increasing price points were due to the force criteria themselves or a byproduct of the force criteria, the higher number of total responses per reinforcer delivery. Experiment 2 aimed to address this question by obtaining demand curves yoked to the total number of responses (criterion and subcriterion) per reinforcer delivery from the force progressions in Experiment 1.

Method

Subjects. The same six animals from Experiment 1 participated in Experiment 2. At the beginning of Experiment 2, their weights were between 240 and 290 g, and they were between 290 to 305 days old.

Apparatus. The same apparatus from Experiment 1 were used in Experiment 2.

Procedure. Demand curves were obtained by yoking to responses (criterion and subcriterion) per reinforcer delivery at each price point for the F-L and F-H progressions from Experiment 1 (see Figure 56). Specifically, the number of responses was determined for each

reinforcer delivery from Experiment 1, and responses per reinforcer delivery was yoked reinforcer delivery by reinforcer delivery. Thus, the ratio requirement for each reinforcer delivery in Experiment 2 was determined from the number of responses required for the corresponding reinforcer delivery from the force progression, creating a VR schedule for each session (see Table 4 and Table 5 for means indicating the VR schedule value). This procedure created a finite number of ratio requirements for each yoked session. If the rat's reinforcer deliveries in the yoked condition exceeded the number of reinforcer deliveries from the force condition, the ratio requirements repeated from the beginning of the sequence. For one animal (2N), an additional progression was obtained by yoking to the mean responses per reinforcer delivery (rather than reinforcer delivery by reinforcer delivery). For each yoked demand assay, the peak force criterion was set to the threshold (i.e., 4 g), so every recorded response counted toward the ratio requirement and no subcriterion responses were recorded. Every response was followed by a 0.1-s tone immediately after the response peak force dropped below threshold. The response that satisfied the ratio requirement was also followed by a relay click, illumination of the cue light above the magazine alcove, and the delivery of sweetened condensed milk (i.e., 0.05 ml [0.91-s pump activation] for the assay yoked to the F-L progression or 0.10ml [1.82-s pump activation] for the assay yoked to the F-H progression). Consistent with the procedures from Experiment 1, each price point was assessed during a single 2-h session.

Experimental design. As in Experiment 1, different independent variable values were assessed at each session. In the present study, however, the independent variable manipulation was responses per reinforcer delivery, determined by yoking to number of responses per reinforcer delivery across progressions in Experiment 1 (see Figure 56). For each animal, two primary yoked progressions were assessed: yoked F-L (Y-F-L, the curve yoked to the obtained

ratio values from the F-L progression) and yoked F-H (Y-F-H, the curve yoked to the obtained ratio values from the F-H progression). The order of yoked progressions (i.e., Y-F-L or Y-F-H) was counterbalanced across rats, and within each yoked progression, sessions were assessed in the same order as the corresponding force progressions prices to which they were yoked. Additionally, yoked curves were assessed from the replications from Experiment 1 after the primary curves (Y-F-L and Y-F-H) were obtained.

Data Analysis

Operant analyses. The same operant analyses conducted in Experiment 1 were conducted with data obtained from yoked curves in Experiment 2. Deviations were noted in both consumption and operant data (see Appendices C and D), with deviations across animals occurring on some of the same dates. Based on observations (see Appendix E), it seemed likely that a veterinary technician had been providing animals with supplementary feedings, so nonsystemtic data from the dates the tech worked (see Appendix F) were excluded from all operant and behavioral economic analyses.

Behavioral economic analyses. The first objective of Experiment 2 was to assess differences in consumption data between the F-L and Y-F-L progressions and the F-H and Y-F-H progressions. Consumption (total 0.05-ml reinforcer units) was plotted as a function of step and visually analyzed across the force and yoked progressions for each animal. Consumption was also compared using area under the curve (AUC). Consumption for each animal in each condition was first normalized by expressing consumption at each step as a proportion of consumption at the first step in that assay (Hursh & Winger, 1995). The AUC was then calculated for each assay using the summed trapezoid method (Amlung, Yurasek, McCarty,

MacKillop, & Murphy, 2015; Myerson, Green, & Warusawitharana, 2001), and these AUC measures were compared using Wilcoxon tests.

The second objective of Experiment 2 was to determine which price modifications from Experiment 1 (i.e., responses per reinforcer unit, obtained unit price, unit price with psychophysical scaling adjustments, mean cumulative time integral of force per reinforcer unit, and mean cumulative duration of responding per reinforcer unit) brought greater relative convergence across all of the Experiment 1 and Experiment 2 progressions (i.e., R-L, R-H, F-L, F-H, Y-F-L, and Y-F-H). Toward this end, consumption data were plotted as a function of the price modifications from Experiment 1.

A single demand curve was fit to each animal's consumption data from the Experiment 1 and Experiment 2 progressions using the exponential model of demand, which provided the best fits from Experiment 1. Relative convergence across price modifications was assessed using two approaches. First, RMSE was compared across price modifications using Friedman's tests conducted in Graphpad Prism with corrected and uncorrected Dunn's tests for post-hoc comparisons. Second, data scatter was visually judged to assess correspondence of data around a single function for each animal.

Group data across animals were also plotted as a function of the price modifications. A single exponential demand curve was fit to group data from all animals across all progressions (i.e., R-L, R-H, F-L, F-H, Y-F-L, and Y-F-H) for each price modification. The 95% prediction bands around each group curve were plotted as a measure of variation. Relative convergence across price modifications was assessed using RMSE, as well as visual judgement of data scatter and prediction bands.

Results

To visually assess consumption across the force and yoked progressions, consumption was plotted as a function of step. Figure 57 shows consumption data (y-axis; number of 0.05-ml reinforcer units) plotted as a function of step (x-axis) from the F-L progressions (Experiment 1; black filled squares and dot-dashed lines) with yoked curves (gray filled diamonds and dot-dashed lines) obtained from yoking to responses per reinforcer delivery at each step. Figure 58 shows consumption data (y-axis; number of 0.05-ml reinforcer units) plotted as a function of step (x-axis) from the F-H progressions (Experiment 1; black open squares and dotted lines) with yoked curves (gray open diamonds and dotted lines) obtained from yoking to responses per reinforcer delivery at each step. Visual analysis suggested similarity in the functions obtained from the force and yoked progressions for some animals, but relatively greater consumption was obtained in the yoked progressions, especially for 3M and 4M. For these animals, consumption across the force and yoked progressions was similar across the lower steps in the progressions and showed a similar decreasing trend; at the higher steps, however, consumption rose in the yoked progression and remained elevated over that in the force progressions.

Consumption was also plotted for replications. Figure 59 shows consumption data (y-axis; number of 0.05-ml reinforcer units) plotted as a function of step (x-axis) from the replicated F-L progressions (Experiment 1; black closed squares and dot-dashed lines) and F-H progressions (Experiment 1; black open squares and dotted lines) with yoked curves (diamonds) obtained from yoking to responses per reinforcer delivery at each step. Figure 60 shows consumption data (y-axis; number of 0.05-ml reinforcer units) plotted as a function of step (x-axis) from the replicated F-L progressions (Experiment 1; black closed squares and dot-dashed lines) and F-H progressions (Experiment 1; black open squares and dotted lines) with yoked curves (diamonds) obtained from yoking to responses per reinforcer delivery at each step. As

with consumption in the first exposure to each progression, functions were similar across the force and yoked conditions.

Operant analyses. In Experiment 1, most animals showed changes in peak force across increasing force criteria. In Experiment 2, the peak force criterion (i.e., 4 g) was not changed across steps. If obtained mean peak force did not systematically increase across steps, this would increase confidence that the patterns of consumption obtained were due to the yoked ratios, rather than increases in mean peak force. To assess whether mean peak force changed across steps in the yoked progressions, mean peak force was determined for each step. Figure 61 shows mean peak force (g; y-axis) plotted as a function of step for Yoked F-L (closed gray diamonds) and Yoked F-H (open gray diamonds) progressions for all animals (separate panels). The SEM was calculated for each step in both progressions, but error was too small to be plotted with data points. The red, horizontal reference line shows the peak force criterion (4 g; same as threshold). The inset panels show the same data but with y-axes scaled to only the yoked progressions for each animal. For most animals, mean peak force does not vary markedly as a function of step. For 1M, however, mean peak force tends to decrease across both the F-L and F-H the progressions, and 1N's mean peak force increased in the F-H progression. For most animals, mean peak force in the Experiment 2 yoked progressions started at a similar level as mean peak force in the first price of the Experiment 1 force progressions, but in the yoked progressions, mean peak force remained low, while the mean peak force in the force progressions tended to increase. Mean peak force in the Experiment 1 ratio progressions tended to be similar (2M R-H, 4M, 1N, 2N R-H) or higher (1M, 2M R-L, 3M, 2N R-L) than mean peak force in the Experiment 2 yoked progressions. No consistent differences were found based on reinforcer magnitude condition, but some rats tended to show higher mean peak forces in the Y-F-L progression (2M

and 3M), whereas others tended to show higher mean peak forces in the Y-F-H progression (1M and 1N). Of note, these were the first yoked progressions experienced for these four animals.

Peak force standard deviations increased with changing peak force in Experiment 1, so peak force standard deviations were also assessed in the yoked progressions. Figure 62 shows peak force standard deviations (g; y-axis) plotted as a function of step for Yoked F-L (closed gray diamonds) and Yoked F-H (open gray diamonds) progressions for all animals (separate panels). Generally, peak force standard deviation remained relatively low and stable across steps, but with clear increases for 1N, consistent with her increasing mean peak force.

Mean time integral of force generally increased with increasing peak force in Experiment 1, so mean time integral was determined for the yoked progressions. Figure 63 shows the mean time integral of force (g-s; y-axis) as a function of step for the Yoked F-L (closed gray diamonds) and Yoked F-H (open gray diamonds) progressions for all animals (separate panels). The SEM was calculated for each step in both progressions, but error was too small to be plotted with data points. Inset panels show the same data but with axes scaled only to the yoked progressions. Time integral of force tends to remain consistent across steps, with a slight increase seen in 1N's F-H progression. The time integrals from the Experiment 2 yoked progressions tended to be similar for four animals (2M, 4M, 1N, and 2N) and lower for two animals (1M and 3M) relative to time integral data from Experiment 1 ratio progressions. The time integrals from the Experiment 1 force progressions tended to be higher than the time integrals from the Experiment 2 yoked progressions, especially as force criterion increased. For some animals (1M, 2M, and 1N), however, the force and yoked time integrals were similar across one or both conditions. No consistent differences were observed across reinforcer magnitude conditions, but

consistent with findings from mean peak force in the yoked progressions, several animals tended to show higher time integrals of force in the first progression experienced (1M, 3M, 4M).

Mean response duration generally increased in the Experiment 1 force progressions, and mean response durations were calculated for the yoked progressions for comparison. Figure 64 shows mean response duration (s; y-axis) plotted as a function of step for Yoked F-L (closed gray diamonds) and Yoked F-H (open gray diamonds) progressions for all animals (separate panels). Inset panels show the same data but with axes scaled only to the yoked progressions. The SEM was calculated for each step in both progressions, and where error bars are not shown, the error was too small to be plotted with the data points. Generally, no systematic changes were noted in response duration as a function of step. For 1M, however, a slight decrease was seen across steps. Mean response duration across the yoked progressions tended to be lower than in the force progressions, with exceptions noted for the F-L progressions for 1M and 1N. Mean response duration in the Experiment 1 ratio progressions tended to be similar (2M R-H, 4M R-L, 1N R-H, 2N R-H) or higher (1M, 2M R-L, 3M, 4M R-H, 1N R-L, 2N R-L) than mean response duration in the Experiment 2 yoked progressions. No consistent differences were observed across reinforcer magnitude conditions, but similar to findings from mean peak force and mean time integral in the yoked progressions, several animals tended to show elevated response durations in the first progression experienced (1M, 3M, 4M).

In Experiment 1, response rates generally showed an increasing then decreasing trend across the ratio and force progressions if all responses (subcriterion and criterion) were evaluated, so trends were also evaluated across the yoked progressions. Figure 65 shows total response rate (per minute; y-axis) as a function of mean responses per reinforcer delivery for the Yoked F-L (left panels) and Yoked F-H (right panels) progressions for all animals (rows).

Closed squares show the total response rates; because the peak force criterion was set to the threshold, no subcriterion responses were recorded and criterion response rates were the same as the total rates. Trends in response rates varied across progressions and animals, and rates were generally more variable than in Experiment 1. As responses per reinforcer delivery increased, response rates increased then decreased for some progressions (1M F-L and F-H; 2M F-H; 4M F-L, and 1N F-H). Several progressions showed increasing response rates (3M F-L and F-H and 4M F-H), and one progression showed a decreasing trend (2M F-L). Responses rates in other progressions were undifferentiated (1N F-L and 2N F-L and F-H).

Two cumulative measures—mean cumulative time integral of force per reinforcer unit and mean cumulative response duration per reinforcer unit—were evaluated as candidate price modifications in Experiment 1. Generally, these cumulative measures increased as numbers of responses increased across progression types, and given that response duration was associated with these cumulative measures in the Experiment 1 force progressions, these relations were also analyzed for the yoked progressions. Figure 66 shows trend lines and Spearman's Rho correlations between mean duration per response (x-axis) and mean cumulative time integral of force per reinforcer unit (y-axis) for the yoked progressions. The only significant relation was found for 1M, who showed a positive relation between mean duration per response and mean cumulative time integral of force per reinforcer unit in the Y-F-L progression. For the other animals, there were no significant relations between mean duration per response and mean cumulative time integral of force per reinforcer unit.

Figure 67 shows trend lines and Spearman's Rho correlations between mean duration per response (x-axis) and mean cumulative response duration per reinforcer unit (y-axis) for the yoked progressions. For most animals, there were no significant relations between mean duration

per response and mean cumulative response duration per reinforcer unit. The only significant relation was found for 1M, who showed a positive relation between mean duration per response and mean cumulative response duration per reinforcer unit.

Figure 68 shows mean cumulative time integral of force per reinforcer unit (y-axis; left column) and mean cumulative response duration per reinforcer unit (y-axis; right column) as a function of responses per reinforcer unit (x-axis) for each animal (rows). Shown are the ratio and force progressions from Experiment 1 and the yoked progression from Experiment 2. Consistent with the findings from Experiment 1, cumulative time integral and cumulative duration tended to increase as responses per reinforcer increased.

Behavioral economic analyses. Figure 69 shows the area under the consumption curves plotted as a function of step, after normalizing to consumption at the first step in each progression. For most animals, the AUCs reflect relatively lower consumption in the force relative to yoked progressions, which is broadly consistent with visual deviations noted between the force and yoked progressions. A Wilcoxon test, however, revealed no significant differences in the AUCs between the F-L and Y-F-L progressions ($W = 15$, $p = .156$) or F-H and Y-F-H progressions ($W = 17$, $p = .094$).

Given visual discrepancies noted in consumption across the force and yoked progressions, consumption from all progressions (i.e., F-L, R-L, F-H, R-H, Y-F-L, Y-F-H) was plotted as a function of unit price and the five price modifications from Experiment 1 to determine which might bring the most convergence across progression types. In each of Figure 70 through Figure 75, a single exponential curve fit is to each animal's consumption data from all Experiment 1 and Experiment 2 progressions plotted as a function of unit price and price modifications: responses per reinforcer unit, obtained unit price, unit price with psychophysical

scaling adjustments, cumulative time integral per reinforcer unit, and cumulative duration per reinforcer unit. A shared exponential curve was fit to all progressions for each animal at each price modification to examine RMSE. For these fits, *k* was constrained for each animal to its maximum range of consumption in log units (1M 2.90, 2M 2.96, 3M 2.77, 4M 2.98, 1N 2.98, 2N 2.87); this range of consumption was calculated for each rat by subtracting the minimum non-zero number of reinforcer units earned in any progression from the maximum number or reinforcer units earned in any condition and then log transforming. Shared α and Q_0 parameters were derived for each animal.

Figure 70 shows consumption data from all the Experiment 1 and Experiment 2 progressions plotted as a function of unit price (see Equation 9) for individual animals (separate panels). Closed circles show R-L progressions, open circles show R-H progressions, closed squares show F-L progressions, open squares show F-H progressions, closed gray diamonds show Y-F-L progressions, and open gray diamonds show Y-F-H progressions. A single exponential demand curve was fit to all progressions for each animal and is shown by a solid black line. Inset panels show residuals. When plotted by unit price, the yoked progressions tend to resemble the Experiment 1 ratio progressions rather than the Experiment 1 force progressions, and there were marked areas of divergence. Curves were relatively poorly fit to each animal's data (R^2*: Mdn* = .67, range = .42-.73; RMSE: *Mdn* = 0.31, range = 0.25-0.36). Consistent with the findings from Experiment 1, residuals showed systematic deviations.

Figure 71 shows consumption data from all Experiment 1 and Experiment 2 progressions plotted as a function of responses per reinforcer unit (see Equation 11) for individual animals (separate panels). Closed circles show R-L progressions, open circles show R-H progressions, closed squares show F-L progressions, open squares show F-H progressions, closed gray

diamonds show Y-F-L progressions, and open gray diamonds show Y-F-H progressions. A single exponential demand curve was fit to all progressions for each animal and is shown by a solid black line. Inset panels show residuals. Data were moderately converged, with the yoked progressions generally falling along the same data paths as Experiment 1 force and ratio progressions for most animals. For 3M and 4M, however, the yoked progressions most resembled the ratio progression data. Curves were moderately well fit to most rats' data (R^2: *Mdn* = .815, range = .7-.91; RMSE: *Mdn* = 0.195, range = 0.1-0.27). Residuals showed minor systematic deviation for most animals, with more marked deviation for 3M and 4M.

Figure 72 shows consumption data from all Experiment 1 and Experiment 2 progressions plotted as a function of obtained unit price (see Equation 12) for individual animals (separate panels). Closed circles show R-L progressions, open circles show R-H progressions, closed squares show F-L progressions, open squares show F-H progressions, closed gray diamonds show Y-F-L progressions, and open gray diamonds show Y-F-H progressions. A single exponential demand curve was fit to all progressions for each animal and is shown by a solid black line. Inset panels show residuals. Data converged reasonably well on a single function, and curves were moderately well fit to each animal's data (R^2: *Mdn* = .895, range = .83-.93; RMSE: *Mdn* = 0.165, range = 0.13-0.21). Residuals generally did not deviate systematically.

Figure 73 shows consumption data from all the Experiment 1 and Experiment 2 progressions plotted as a function of unit price with psychophysical scaling adjustments (see Equation 13) for individual animals (separate panels). Closed circles show R-L progressions, open circles show R-H progressions, closed squares show F-L progressions, open squares show F-H progressions, closed gray diamonds show Y-F-L progressions, and open gray diamonds show Y-F-H progressions. A single exponential demand curve was fit to the progressions for

each animal and is shown by a solid black line. Inset panels show residuals. Some divergence was observed across progressions for most animals, but the yoked data points fell along the paths of the Experiment 1 progressions. Curve fits were moderate to poor (R^2: *Mdn* = .79, range = .6-.84; RMSE: *Mdn* = 0.255, range = 0.16-0.3), and there were systematic deviations of residuals.

Figure 74 shows consumption data from all the Experiment 1 and Experiment 2 progressions plotted as a function of mean time integral of force per reinforcer unit (see Equation 14) for individual animals (separate panels). Closed circles show R-L progressions, open circles show R-H progressions, closed squares show F-L progressions, open squares show F-H progressions, closed gray diamonds show Y-F-L progressions, and open gray diamonds show Y-F-H progressions. A single exponential demand curve was fit to the progressions for each animal and is shown by a solid black line. Inset panels show residuals. Generally, the yoked progressions tended to converge with the Experiment 1 progressions, but for 3M, yoked data points tended to lie below those from Experiment 1. With the exception of 3M and 4M, curves were well fit for most animals, (R^2: *Mdn* = .9, range = .72-.96; RMSE: *Mdn* = 0.17, range = 0.11-0.22), and there were minor systematic deviations of residuals.

Figure 75 shows consumption data from all the Experiment 1 and Experiment 2 progressions plotted as a function of mean cumulative duration of responding per reinforcer unit unit (see Equation 15) for individual animals (separate panels). Closed circles show R-L progressions, open circles show R-H progressions, closed squares show F-L progressions, open squares show F-H progressions, closed gray diamonds show Y-F-L progressions, and open gray diamonds show Y-F-H progressions. A single exponential demand curve was fit to all of the progressions for each animal and is shown by a solid black line. Inset panels show residuals. The yoked data points tended to converge well with data from Experiment 1 progressions. Curves

were generally well fit to each animal's data (R^2: *Mdn* = .92, range = .85-.95; RMSE: *Mdn* = 0.14, range = 0.11-0.18), but minor systematic deviation of residuals was observed.

Generally, price modifications that produce the greater convergence should yield lower RMSE, so RMSE was compared from the single curves fit to each rat's data across the price modifications. Figure 76 shows RMSE for a single curve fit to each animal's consumption across all Experiment 1 and Experiment 2 progressions for unit price and the five price modifications. Gray open circles show RMSE for each animal, and lines and error bars show medians and IQRs. A Friedman's test revealed a significant main effect ($\chi^2 = 23.1$, $p = .003$). Post-hoc Dunn's tests without correction revealed significantly greater RMSE in the single curve fit to consumption as a function of unit price relative to responses per reinforcer unit (Rank sum difference = 14, $p = .03$, adjusted $p = .46$) and obtained unit price (Rank sum difference = 18.5, $p = .004$, adjusted $p = .06$), but these did not remain significant after correcting for multiple comparisons. Cumulative duration per reinforcer unit had lower RMSE than unit price with psychophysical scaling parameter adjustments (Rank sum difference = 19, $p = .003$, adjusted $p = .05$) and responses per reinforcer unit (Rank sum difference = 14, $p = .04$, adjusted $p = .46$), but these results did not remain significant after correction. After correcting for multiple comparisons, the unit price equation produced greater RMSE than the cumulative time integral (Rank sum difference = 20.5, $p = .002$, adjusted $p = .02$) and cumulative duration (Rank sum difference = 28, $p < .001$, adjusted $p = .002$) price modifications.

To lend additional confidence to the findings, curves were also fit to the group data across all animals and progression types. Figure 77 shows exponential curves fit to group data from all Experiment 1 and Experiment 2 progressions across price modifications. Closed circles show R-L progressions, open circles show R-H progressions, closed squares show F-L

progressions, open squares show F-H progressions, gray closed diamonds show Y-F-L progressions, and open gray diamonds show Y-F-H progressions. The gray shaded regions show 95% prediction bands. Inset panels show residuals. Visually, the price modification of cumulative response duration per reinforcer unit produced the most marked convergence, but responses per reinforcer unit; obtained unit price, and cumulative time integral of force per reinforcer unit also brought greater convergence to the data relative to the Hursh et al., (1988) unit price. The 95% prediction bands, which show the area within which 95% of additional data points are predicted to fall, were consistent with the trends noted in the visual analysis. Specifically, the prediction bands for the cumulative duration measure were smaller than those for other price modifications and unit price, though the largest prediction bands were found for the Hursh et al. (1988) unit price and unit price with psychophysical scaling parameter price modification.

To assess the absolute fit of a single curve to the group data across all progressions for each price modification. RMSE was determined. Figure 78 shows RMSE from an exponential curve fit to all progressions from all rats for each respective price modification (x-axis). The black stars show RMSE from a single curve fit to all rats' data from all progressions for each price modification. Across conditions, RMSE ranged from 0.19 (i.e., cumulative duration per reinforcer unit) to 0.40 (i.e., the Hursh et al. [1988] unit price equation). Similar RMSE was produced by the curves fit to unit price and unit price with the psychophysical scaling parameter adjustment (i.e., 0.40 and 0.37, respectively). Similar RMSE (i.e., 0.27-0.29) was also produced by the obtained ratio, obtained unit price, and cumulative time integral of force per reinforcer unit price modifications. The lowest RMSE was obtained from the cumulative duration measure, which was approximately 30% to 50% lower than the RMSE in any other price modification.

Discussion

Although the yoked progressions produced functions that appeared similar to the force progressions from Experiment 1 in cases, visual discrepancies were noted for several animals, and most animals showed slightly greater consumption in the yoked progressions relative to the force progressions, though these differences were not significant. If consumption was the same in the force and yoked progressions, it would suggest that responses per reinforcer unit solely accounted for the differences in consumption across the ratio and force progressions. The current findings, however, prompts consideration of factors beyond number of responses per reinforcer unit that may have influenced consumption between the yoked and force progressions.

Generally, peak force, time integral, and response duration were lower in the yoked progressions relative to the force progressions. Although response rates tended to be similar across the force and yoked progressions for most animals, response rates were generally higher in the yoked progressions for 3M and 4M. Notably, the cumulative response duration per reinforcer unit measure, which was affected by both number and duration of responses, showed a distinct impact of the lower response durations for 3M and 4M. Differences in operant behavior across the force and yoked progressions suggest measures of responding beyond responses per reinforcer unit and the programmed force criteria may influence consumption in demand.

Because visual differences were observed in the yoked and force progressions, the same price modifications from Experiment 1 were attempted to determine which price modifications, if any, might bring convergence to all progressions from Experiment 1 and Experiment 2. Because consumption in the yoked progressions did not conform to a prototypical demand curve shape, a single curve was fit to consumption data across all progressions for each animal. Consistent with findings from Experiment 1, cumulative duration per reinforcer unit appeared to

bring more convergence to the consumption data than other price modifications. Plotting consumption as a function of cumulative duration and cumulative time integral per reinforcer unit significantly reduced RMSE compared to plotting consumption as a function of unit price (Hursh et al., 1988). All three of these measures accounted for time, but not effort, suggesting time costs may be a critical factor influencing consumption in behavioral economic demand.

General Discussion

Data from the current experiments failed to support the unit price conceptualization that suggests increasing force or ratio requirement should produce identical changes in consumption. These findings suggest that the unit price variables manipulated in the current experiments—ratio requirement, force criterion, and reinforcer magnitude—were not the factors controlling consumption, at least as related in the Hursh et al. (1988) equation. When matched by the Hursh et al. (1988) unit price equation, progressions composed of parametric ranges of force or ratio requirements produced different curves when fit by the exponential model of demand. These differences were consistent with the findings of Sumpter et al. (1999, 2004), who found force progressions produced relatively more inelastic demand at lower unit prices. Moreover, Hursh et al. (1988) identified deviations in consumption across high force relative to low force requirement ratio progressions. The current experiments, however, obtained additional operant data using a force transducer that permitted additional analyses of differences across ratio and force progressions.

The force transducer permitted recording of subcriterion responses—those responses with a peak force below the force criterion specified for reinforcement. One effect of these subcriterion responses is changing the obtained ratio (Pinkston & Libman, 2017). In Experiment 2, programming ratio requirements using the obtained ratios from the force progressions resulted

in visual differences in consumption functions. These data suggest that the obtained ratios did not sufficiently account for the functions obtained in the force progressions—even when yoking reinforcer delivery by reinforcer delivery to control for fluctuations resulting from variability in force differentiation. Although obtained ratio was held constant across the force and yoked progressions, other operant measures differed between the force and yoked progressions for some animals (e.g., time integral of force and response duration).

Analytically accounting for price per reinforcer unit using other changes in operant behavior (i.e., the price modifications), however, brought greater convergence to the consumption data across progression types relative to unit price. Relative degree of convergence varied across the price modifications. The addition of a scaling parameter to the force criterion of the Hursh et al. (1988) unit price equation generally brought the consumption data closer together across progression types; the individual functions, however, generally maintained different shapes, suggesting that changes in costs associated with increasing force or ratio requirements may not be related through simple exponentiation of the force criterion. Although AICc comparisons suggested a single curve provided a relatively better fit across progression types, RMSE tended to be elevated relative to the other price modifications. This elevated RMSE associated with the psychophysical scaling modification, combined with the different shapes of functions across progression types, suggests other price modifications, which were calculated from the operant data, better accounted for consumption across progression types. Plotting consumption as a function of responses per reinforcer unit, which was calculated using criterion and subcriterion responses, brought greater convergence to the consumption data relative to unit price for most rats. Across the Experiment 1 progression types, greater deviations tended to be noted from force progressions with relatively greater peak force slopes and more moderate

slopes for proportion of subcriterion to total responses across increasing force criteria. In Experiment 2, the yoked progressions for these rats with high peak force and moderate subcriterion to total slopes generally fell along the Experiment 1 ratio, rather than force, progressions; for the other rats, however, responses per reinforcer generally accounted for consumption across the ratio progressions. Together these findings suggest that for animals with less force differentiation and a more rapid increase in subcriterion responses, the obtained ratio generally accounted for the consumption obtained, whereas for animals with better force differentiation, other variables influenced consumption. Calculating an obtained unit price—entering responses per reinforcer unit and mean peak force calculated from the operant data into the Hursh et al. (1988) equation—generally resulted in visual convergence of the consumption data across progression types for most rats in Experiment 1. In Experiment 2, several rats' consumption in the yoked progressions fell below the consumption data from the Experiment 1 progressions when plotted as a function of obtained price. Although less marked than differences in other price modifications, the differences in consumption across progression types suggests that more granular measures, beyond the mean peak force and number of responses captured by unit price, influenced consumption.

Two other price modifications—cumulative time integral of force per reinforcer unit and cumulative duration of responding per reinforcer unit—generally brought marked convergence to the consumption data, with cumulative duration of responding per reinforcer unit bringing the greatest convergence across all price modifications attempted in Experiment 1 and Experiment 2. Response duration was a key component of the calculation of both of these price modifications. The cumulative time integral and cumulative duration measures could increase both through greater numbers of responses and through changes in dimensions of the responses. Specifically,

as force criteria increased in Experiment 1, both peak force and duration of responding increased. Response duration measures solely changes in duration, whereas time integral–the area under the force-time curve–could be impacted by both changes in peak force and duration (Fowler, 1987; Notterman & Mintz, 1965). In the present experiments, mean duration per response tended to relate to both cumulative time integral per reinforcer unit and cumulative duration per reinforcer unit in the force progressions, suggesting that changes in duration may have contributed to both price modifications.

Although Hursh et al. (2013) indicated that effort expended per reinforcer, which could be quantified as time integral of force, could be used to quantify cost, to my knowledge, no studies have manipulated time integral of force in behavioral economic demand. The results of the present experiments suggest potential advantages of this approach, which approximates energy expenditure (Fowler, 1987; Notterman & Mintz, 1965), over the traditional definition of unit price (Hursh et al., 1988). Future studies should further evaluate time integral of force as a candidate measure of cost in behavioral economic demand.

That plotting consumption as a function of cumulative duration per reinforcer unit brought the greatest convergence across progression types highlights the likely influence of time constraints on consumption. These findings are broadly consistent with data from Peck and Byrne (2016), who obtained demand curves by increasing response duration per reinforcer unit. Differences between these two investigations should be noted, however, as Peck and Byrne required a single response of a criterion duration, whereas in the present experiments, the durations of all responses were summed. Of note, the convergence across price modifications affected by time could be related to session length, as session length was relatively short and held constant (i.e., an ordinary or uncompensated demand curve; Kagel et al., 1981). Given the

fixed session durations, future research might replicate the present experiment across varied session lengths to address this issue. Although both the cumulative duration and cumulative time integral of force measures analytically brought convergence to the demand functions across progression types, the relative impact of duration versus effort in influencing consumption in demand paradigms should be experimentally evaluated to better isolate controlling factors.

Altogether, these findings have broader implications for behavioral economic demand. Christensen et al. (2008) indicated an important test of the exponential model of demand is whether α is the same across different types of costs (e.g., force versus ratio); data from the present experiment failed to achieve this marker, with differences in both fit and derived parameters observed across ratio and force progressions when consumption was plotted as a function of unit price. Other price modifications, however, brought relatively greater convergence to the data from ratio and force progressions.

Bickel et al. (2000) suggested that behavioral economics is more appropriate for the behavior maintaining, rather than behavior strengthening, effects of reinforcement. The behavior strengthening effects of reinforcement are associated with behavior in transition states (Bickel et al., 2000), and both the ratio and force progressions were obtained from transition – rather than steady – state behavior. Prior research has shown FR progressions under steady state criteria tend to produce qualitatively similar demand curves to those produced in transition states (Madden et al., 2005). Force differentiation, however, requires selection of specific response topographies (Notterman & Mintz, 1965) and thus may show greater variability in transition states relative to changing ratio requirement. Consistent with this possibility, worse fits were obtained in the force progressions. Although the force progressions produced curves that were different from the ratio

progressions, future studies should evaluate whether force curves would be better fit by behavioral economic demand models under steady state conditions.

Findings from the present study are generally consistent with the force transducer literature. As force criteria increase, both the proportion of subcriterion responses (Mitchell & Brener, 1991; Pinkston & Libman, 2017; Zarcone, Chen & Fowler, 2007, 2009) and response peak force (Notterman & Mintz, 1965; Mitchell & Brener, 1991; Pinkston & Libman, 2017; Zarcone, Chen & Fowler, 2007, 2009) increased, and results of the present study were consistent with these findings. Rats' peak force of responding increased as peak force criteria increased in the force progressions, whereas peak force in the ratio and yoked progressions showed few consistent or robust changes. Similarly, duration, which has been shown to increase with increasing peak force (Notterman & Mintz, 1965), and time integral of force—a composite measure of response force and duration (Fowler, 1987; Notterman & Mintz, 1965)—showed similar increases in the force progressions but not in the ratio or yoked progressions. Consistent with findings from Zarcone, Chen & Fowler (2007, 2009), rats' total rates of responding in the force progressions tended to increase with increasing force criteria, even as criterion response rates decreased. Regardless of progression type, there was no clear effect of reinforcer magnitude on peak force, a finding that is inconsistent with other research (Di Lollo et al., 1965; Fowler, 1987). The procedures of the current experiment, in which force criterion increased each day, may have contributed to these findings.

Results of the present experiments may have implications for addressing problems of social significance. For example, response effort manipulations have been used to reduce problem behaviors, such as hand mouthing, through use of braces that increase the effort required for elbow flexion. Braces resulted in reductions in hand mouthing while the braces were

worn, but mouthing was often not entirely suppressed (Wallace, Iwata, Zhou, & Goff, 1999; Zhou, Goff, & Iwata, 2000). Findings from the present experiments may suggest that more forceful responses could be selected, potentially requiring more intrusive interventions over time as individuals grow stronger. Although rats' rates of criterion responses decreased as the force criterion increased in the current experiments, their mean peak force generally increased, indicating selection of more forceful response topographies. Assuming findings from the current experiments generalize to a treatment context, these data suggest careful consideration of factors such as degree of effort and response suppression when considering response effort interventions. The present findings could also inform interventions to improve pro-health behavior. For example, Hursh et al. (2013) suggest that the results of Madden et al. (2005), in which RR schedules maintained relatively greater consumption than FR schedules matched by unit price, have implications when the goal of an intervention is increasing behavior, such as with exercise. Similarly, results of the current experiments may suggest that increasing intensity (e.g., incline of a treadmill), rather than amount (e.g., number of steps), of exercise could improve adherence and fitness-related positive health outcomes. Further, such an approach may be facilitated by the increasing availability of technology that could detail frequency and intensity-related data in real world settings. Implications could be explored in future translational research.

Additional challenges of the current study should be addressed by future research. The sample size of these experiments was relatively small ($N = 6$), and based on this sample size, statistical comparisons (e.g., tests of normality) were potentially underpowered. Although the nonparametric Wilcoxon tests were not corrected for multiple comparisons and are susceptible to Type I error, these results are included given the exploratory nature of these analyses. The lowest

ratio requirement in the force progression was FR10, and the first five prices in the ratio progressions were not matched to data in the force progressions. Even though the force requirement was lower than in most weighted lever arrangements, the relatively high ratio requirement in the force conditions likely influenced the shapes of the demand curves. The steps and step size for this experiment were chosen based on pilot research, but given the role of force differentiation in the force progressions, step size likely influenced the functions obtained. Although research using ratio progressions has not found differences as a result of sequence or step size (Giordano et al., 2001; Raslear et al., 1988), future research should evaluate the role of step size and sequence (i.e., ascending, descending, random) in force progressions. Sessions with no consumption, which were excluded from the price modification analyses, occurred more often in force progressions. Unfortunately, because the planned price modifications used obtained data based on number of reinforcer units earned, these sessions could not be included in these analyses.

For the purposes of these experiments, reinforcer delivery was used to refer to a single cycle of reinforcement, and reinforcer unit referred to 0.05-ml of sweetened condensed milk solution; the dependent variable was total consumption. Such an approach is generally consistent with the definition of consumption in the Hursh et al. (1988) introduction of unit price; recommendations that price and consumption be in commensurate units (Hursh, 1980). Of note, these calculations of unit price (cost/number of reinforcer units per reinforcer delivery) and consumption (i.e., total number of reinforcer units) assume a scalar relation between changes in behavior and changes in reinforcer magnitude (Wade-Galuska, Galuska, Winger, & Woods, 2007). How other aspects of the reinforcement context (e.g., stimulus control or conditioned reinforcement associated with eating; Epstein, Dearing, Temple, & Cavanaugh, 2008) might

impact this arrangement should be explored by future research. The reinforcer in this study was a liquid, food reinforcer delivered within an open economy. Other questions, such as how ratio and force progressions might differ with other commodities—such as drugs that may impact force differentiation—or in closed economies should be explored by future research. The rats gained weight over the course of the experiment, but these changes were not accounted for in analyses. Rats were weighed after session each day, consistent with the conventions of the lab in which the study was conducted. Their weights varied markedly, however, based on the volume of milk consumed in session, limiting use of these data in analytically controlling for weight.

A number of limitations are related to potential history effects, especially given that force differentiation is a learning process (Skinner, 1938), and the proportion of criterion responses decreases with exposure to that criterion (Mitchell & Brener, 1991; Notterman & Mintz, 1965). Rats had different histories prior to the experiment, with some having experience with changing force criteria. Rats also experienced the progression types in different orders, and rats' mean peak force may not return to baseline levels after experience with a high force criterion (Pinkston & Libman, 2017). Although reversibility or irreversibility of response force was not directly evaluated in the current experiments, potential evidence of history effects may be seen in the relatively elevated peak forces found in the ratio relative to yoked progressions for some animals and in 1M's elevated peak force after experience with the F-L progression. Future studies might more directly account for potential order effects. Such procedural issues limit the generality of the findings. Additionally, a limited number of replications were conducted per progression type. Although replications generally resembled the first run data, force differentiation may have been impacted by exposure, as two rats attained higher force criteria in their second force progression.

Relatedly, how these progressions might differ if a stability criterion was imposed at each step also remains to be explored.

Finally, no consumption period was programmed in the present experiments. Although every response was eligible to satisfy the reinforcement contingency, marked response overruns were noted for multiple animals. To avoid making assumptions about reinforcer consumption periods, the IRT distributions included times between all responses, including those with a reinforcer delivery. The overruns may also be a result of the reinforcer delivery apparatus, in which rats could "save" the sweetened condensed milk-water solution across multiple deliveries. Although the opportunity to store reinforcers is common with the pellet magazines used in much rat research, other demand studies that have delivered liquid reinforcers to rats (e.g., Peck & Byrne, 2016) have used dippers. Dippers have a limited reinforcer consumption period, similar to the hoppers used in demand research with pigeons (e.g., Tan & Hackenberg, 2015) and hens (e.g., Sumpter et al., 2004). Given that data from this experiment suggest a role of time costs in demand, future research should examine effects of consumption periods and limited holds on demand.

In conclusion, although a unit price conceptualization suggests that increasing force or ratio requirement should produce identical changes in consumption, data form the current experiments failed to support this hypothesis. Enhanced measurement with a force transducer permitted analysis of the effects of changes in operant behavior. Experimentally controlling for responses per reinforcer unit, which was influenced by both programmed ratio and subcriterion responses—resulted in similar consumption functions only for some rats. Exploring other ways of quantifying costs analytically, however, showed marked convergence across price modifications affected by time: cumulative time integral of force per reinforcer unit, cumulative

duration of responding per reinforcer unit, and mean IRI per reinforcer unit. Although the relative roles of time integral and duration should be experimentally determined by future research, these findings generally lend tentative support to hypotheses that time may be a pivotal variable controlling consumption in behavioral economic demand (Bauman, 1991; Hursh et al., 1988).

References

Adair, E. R., & Wright, B. A. (1976). Behavioral thermoregulation in the squirrel monkey when response effort is varied. *Journal of Comparative and Physiological Psychology, 90*(2), 179-184. doi:10.1037/h0077197

Akaike, H. (1974). A new look at the statistical model identification. *IEEE Transactions on Automatic Control, 19*(6), 716-723. doi:10.1109/TAC.1974.1100705

Alling, K., & Poling, A. (1995). The effects of differing response-force requirements on fixed-ratio responding of rats. *Journal of the Experimental Analysis of Behavior, 63*(3), 331-346. doi:10.1901/jeab.1995.63-331

Allison, J., Buxton, A., & Moore, K. E. (1987). Rats' responses to molar and local schedule constraints. *Animal Learning & Behavior, 15*(4), 360-367. doi:10.3758/BF03205041

Allison, J., & Mack, R. (1982). Polydispsia and autoshaping: Drinking and leverpressing as substitutes for eating. *Animal Learning & Behavior, 10*(4), 465-475. doi:10.3758/BF03212286

Amlung, M., Yurasek, A. M., McCarty, K. N., MacKillop, J., & Murphy, J. G. (2015). Area under the curve as a novel metric of behavioral economic demand for alcohol. *Experimental and Clinical Psychopharmacology, 23*(3), 168-175. doi:10.1037/pha0000014

Andrade, L. F., & Hackenberg, T. D. (2017). Substitution effects in a generalized token economy with pigeons. *Journal of the Experimental Analysis of Behavior, 107*(1), 123-135. doi:10.1002/jeab.231

Baum, W. M. (2002). From molecular to molar: A paradigm shift in behavior analysis. *Journal of the Experimental Analysis of Behavior, 78*(1), 95-116. doi:10.1901/jeab.2002.78-95

Bauman, R. (1991). An experimental analysis of the cost of food in a closed economy. *Journal of the Experimental Analysis of Behavior, 56*(1), 33-50. doi:10.1901/jeab.1991.56-33

Bentzley, B. S., Fender, K. M., & Aston-Jones, G. (2013). The behavioral economics of drug self-administration: A review and new analytical approach for within-session procedures. *Psychopharmacology (Berlin), 226*(1), 113-125. doi:10.1007/s00213-012-2899-2

Bickel, W. K., DeGrandpre, R. J., & Higgins, S. T. (1995). The behavioral economics of concurrent drug reinforcers: A review and reanalysis of drug self-administration research. *Psychopharmacology (Berlin), 118*(3), 250-259. doi:10.1007/BF02245952

Bickel, W. K., DeGrandpre, R. J., Higgins, S. T., & Hughes, J. R. (1990). Behavioral economics of drug self-administration. I. Functional equivalence of response requirement and drug dose. *Life Sciences, 47*(17), 1501-1510. doi:10.1016/0024-3205(90)90178-T

Bickel, W. K., DeGrandpre, R. J., Hughes, J. R., & Higgins, S. T. (1991). Behavioral economics of drug self-administration. II. A unit-price analysis of cigarette smoking. *Journal of the Experimental Analysis of Behavior, 55*(2), 145-154. doi:10.1901/jeab.1991.55-145

Bickel, W. K., Green, L., & Vuchinich, R. E. (1995). Behavioral economics. *Journal of the Experimental Analysis of Behavior, 64*(3), 257-262. doi:10.1901/jeab.1995.64-257

Bickel, W. K., & Madden, G. J. (1999). A comparison of measures of relative reinforcing efficacy and behavioral economics: Cigarettes and money in smokers. *Behavioral Pharmacology, 10*(6-7), 627-637. doi:10.1097/00008877-199908001-00023

Bickel, W. K., Madden, G. J., & DeGrandpre, R. J. (1997). Modeling the effects of combined behavioral and pharmacological treatment on cigarette smoking: Behavioral-economic analyses. *Experimental and Clinical Psychopharmacology, 5*(4), 334-343. doi:10.1037/1064-1297.5.4.334

Bickel, W. K., Marsch, L. A., & Carroll, M. E. (2000). Deconstructing relative reinforcing efficacy and situating the measures of pharmacological reinforcement with behavioral economics: a theoretical proposal. *Psychopharmacology (Berlin), 153*(1), 44-56. doi:10.1007/s002130000589

Bizo, L. A., Chu, J. Y. M., Sanabria, F., & Killeen, P. R. (2006). The failure of Weber's law in time perception and production. *Behavioural Processes, 71*(2-3), 201-210. doi:10.1016/j.beproc.2005.11.006

Cassidy, R. N., & Dallery, J. (2012). Effects of economy type and nicotine on the essential value of food in rats. *Journal of the Experimental Analysis of Behavior, 97*(2), 183-202. doi:10.1901/jeab.2012.97-183

Catania, A. C. (1973). The concept of the operant in the analysis of behavior. *Behaviorism, 1*(2), 103-116. Retrieved from http://www.jstor.org/stable/27758804

Catania, A. C. (2013). *Learning* (5th Edition ed.). Cornwall-On-Hudson, NY: Sloan Publishing.

Christensen, C. J., Silberburg, A., Hursh, S. R., Huntsberry, M. E., & Riley, A. L. (2008). Essential value of cocaine and food in rats: Tests of the exponential model of demand. *Psychopharmacology (Berlin), 198*(2), 221-229. doi:10.1007/s00213-008-1120-0

Christensen, C. J., Silberburg, A., Hursh, S. R., Roma, P. G., & Riley, A. L. (2008). Demand for cocaine and food over time. *Pharmacology, Biochemistry and Behavior, 91*(2), 209-216. doi:10.1016/j.pbb.2008.07.009

Chung, S. (1965). Effects of effort on response rate. *Journal of the Experimental Analysis of Behavior, 8*(1), 1-7. doi:10.1901/jeab.1965.8-1

Cole, J. L. (1965). Force gradients in stimulus generalization. *Journal of the Experimental Analysis of Behavior, 8*(4), 231-241. doi:10.1901/jeab.1965.8-231

Collier, G. H., Johnson, D. F., Hill, W. L., & Kaufman, L. W. (1986). The economics of the law of effect. *Journal of the Experimental Analysis of Behavior, 46*(2), 113-136. doi:10.1901/jeab.1986.46-113

DeGrandpre, R. J., Bickel, W. K., Hughes, J. P., Layng, M. P., & Badger, G. J. (1993). Unit price as a useful metric in analyzing effects of reinforcer magnitude. *Journal of the Experimental Analysis of Behavior, 60*(3), 641-666. doi:10.1901/jeab.1993.60-641

Delmendo, X., Borrero, J. C., Beauchamp, K. L., & Francisco, M. T. (2009). Consumption and response output as a function of unit price: Manipulation of cost and benefit components. *Journal of Applied Behavior Analysis, 42*(3), 609-625. doi:10.1901/jaba.2009.42-609.

Di Lollo, V., Ensminger, W. D., & Notterman, J. M. (1965). Response force as a function of amount of reinforcement. *Journal of Experimental Psychology, 70*(1), 27-31. doi:10.1037/h0022062

Epstein, L. H., Dearing, K. K., Temple, J. L., & Cavanaugh, M. D. (2008). Food reinforcement and impulsivity in overweight children and their parents. *Eating Behaviors, 9*(3), 319-327. doi:10.1016/j.eatbeh.2007.10.007

Ferraro, D. P., & Grilly, D. M. (1970). Response differentiation: A psychophysical method for response produced stimuli. *Perception & Psychophysics, 7*(4), 206-208. doi:10.3758/BF03209359

Ferster, C. B., & Skinner, B. F. (1957). *Schedules of reinforcement*. Englewood Cliffs, NJ: Prentice Hall.

Filion, R. D., Fowler, S. C., & Notterman, J. M. (1970a). Effort expenditure during proportionally reinforced responding. *Quarterly Journal of Experimental Psychology, 22*(3), 398-405. doi:10.1080/14640747008401913

Filion, R. D., Fowler, S. C., & Notterman, J. M. (1970b). Some effects of prefeeding and training upon rate and precision of bar-pressing response. *Journal of Comparative and Physiological Psychology, 73*(2), 328-333. doi:10.1037/h0030236

Foltin, R. W. (1994). Does package size matter? A unit-price analysis of "demand" for food in baboons. *Journal of the Experimental Analysis of Behavior, 62*(2), 293-306. doi:10.1901/jeab.1994.62-293

Foster, T. A., & Hackenberg, T. D. (2004). Unit price and choice in a token-reinforcement context. *Journal of the Experimental Analysis of Behavior, 81*(1), 5-25. doi:10.1901/jeab.2004.81-5

Foster, T. M., Blackman, K. A., & Temple, W. (1997). Open versus closed economies: Performance of domestic hens under fixed-ratio schedules. *Journal of the Experimental Analysis of Behavior, 67*(1), 67-89. doi:10.1901/jeab.1997.67-67

Foster, T. M., Kinloch, J., & Poling, A. (2011). The effects of session length on demand functions generated using FR schedules. *Journal of the Experimental Analysis of Behavior, 95*(3), 289-304. doi:10.1901/jeab.2011.95-289

Foster, T. M., Sumpter, C. E., Temple, W., Flevill, A., & Poling, A. (2009). Demand equations for qualitatively different foods under fixed-ratio schedules: A comparison of three data conversions. *Journal of the Experimental Analysis of Behavior, 92*(3), 305-326. doi:10.1901/jeab.2009.92-305

Foster, T. M., Temple, W., Cameron, B., & Poling, A. (1997). Demand curves for food in hens: Similarity under fixed-ratio and progressive-ratio schedules. *Behavioural Processes, 39*(2), 177-185. doi:10.1016/S0376-6357(96)00051-4

Fowler, S. C. (1974). A minicomputer system for recording the dynamic properties of individual operant responses. *Behavior Research Methods & Instrumentation, 6*(2), 288-292. doi:10.3758/BF03200345

Fowler, S. C. (1987). Force and duration of operant response as dependent variables in behavioral pharmacology. In T. Thompson, P. B. Dews, & J. E. Barrett (Eds.), *Advances in behavioral pharmacology (Vol 6): Neurobehavioral pharmacology* (pp. 83-127). Hillside, NJ: Erlbaum.

Fowler, S. C., & Notterman, J. M. (1974). Reinforcement rate and force proportional reinforcement. *Learning and Motivation, 5*(1), 80-91. doi:10.1016/0023-9690(74)90039-3

Gibbon, J. (1977). Scalar expectancy theory and Weber's law in animal timing. *Psychological Review, 84*(3), 279-325. doi:10.1037/0033-295X.84.3.279

Giordano, L. A., Bickel, W. K., Shahan, T. A., & Badger, G. J. (2001). Behavioral economics of human drug self-administration: Progressive ratio versus random sequences of response requirements. *Behavioral Pharmacology, 12*(5), 343-347. doi:10.1097/00008877-200109000-00005

Gollub, L. R., & Lee, R. M. (1966). Response force under fixed-interval reinforcement. *Psychonomic Science, 4*(1), 9-10. doi:10.3758/BF03342148

Grant, A. A., Foster, T. M., Temple, W., Jackson, S., Kinloch, J., & Poling, A. (2014). Reinforcer magnitude and demand under fixed-ratio schedules with domestic hens. *Behavioural Processes, 103*, 199-210. doi:10.1016/j.beproc.2013.12.013

Green, L., & Freed, G. L. (1993). The substitutability of reinforcers. *Journal of the Experimental Analysis of Behavior, 60*(1), 141-158. doi:10.1901/jeab.1993.60-141

Greenwald, M. K., & Hursh, S. R. (2006). Behavioral economic analysis of opioid consumption in heroin-dependent individuals: Effects of unit price and pre-session drug supply. *Drug and Alcohol Dependence, 85*(1), 35-48. doi:10.1016/j.drugalcdep.2006.03.007

Griffiths, R. R., & Thompson, T. (1973). The post-reinforcement pause: A misnomer. *The Psychological Record, 23*(2), 229-235. doi:10.1007/BF03394160

Grossbard, C. L., & Mazur, J. E. (1986). A comparison of delays and ratio requirements in self-control choice. *Journal of the Experimental Analysis of Behavior, 45*(3), 305-315. doi:10.1901/jeab.1986.45-305

Gulotta, K. B., & Byrne, T. (2015). A progressive-duration schedule of reinforcement. *Behavioural Processes, 121*, 93-97. doi:10.1016/j.beproc.2015.10.022

Harrell, J. V., & Fowler, S. C. (1977). Amount of reinforcer and differentiation of response force. *Bulletin of the Psychonomic Society, 10*(5), 358-360. doi:10.3758/BF03329359

Hartmann, M. N., Hager, O. M., Tobler, P. N., & Kaiser, S. (2013). Parabolic discounting of monetary rewards by physical effort. *Behavioural Processes, 100*, 192-196. doi:10.1016/j.beproc.2013.09.014

Henley, A. J., DiGennaro Reed, F. D., Reed, D. D., & Kaplan, B. A. (2016). A crowdsourced nickel-and-dime approach to analog OBM research: a behavioral economic framework for understanding workforce attrition. *Journal of the Experimental Analysis of Behavior, 106*(2), 134-144. doi:10.1002/jeab.220

Herrnstein, R. J. (1964). Secondary reinforcement and rate of primary reinforcement. *Journal of the Experimental Analysis of Behavior, 7*(1), 27-36. doi:10.1901/jeab.1964.7-27

Hodos, W. (1961). Progressive ratio as a measure of response strength. *Science, 134*(3483), 943-944. doi:10.1126/science.134.3483.943

Hoenig, J. M., & Heisey, D. M. (2001). The abuse of power: The pervasive fallacy of power calculations for data analysis. *The American Statistician, 55*(1), 19-24. doi:10.1198/000313001300339897

Hursh, S. R. (1978). The economics of daily consumption controlling food- and water-reinforced responding. *Journal of the Experimental Analysis of Behavior, 29*(3), 475-491. doi:10.1901/jeab.1978.29-475

Hursh, S. R. (1980). Economic concepts for the analysis of behavior. *Journal of the Experimental Analysis of Behavior, 34*(2), 219-238. doi:10.1901/jeab.1980.34-219

Hursh, S. R. (1984). Behavioral economics. *Journal of the Experimental Analysis of Behavior, 42*(3), 435-452. doi:10.1901/jeab.1984.42-435

Hursh, S. R. (2014a). Behavioral economics and the analysis of consumption and choice. In F. K. McSweeney & E. S. Murphy (Eds.), *The Wiley Blackwell handbook of operant and classical conditioning* (pp. 275–305). Hoboken, NJ: Wiley.

Hursh, S. R. (2014b). *Generalized Essential Value*. Paper presented at the Society for the Quantitative Analyses of Behavior, Chicago, IL.

Hursh, S. R., Madden, G. J., Spiga, R., DeLeon, I. G., & Francisco, M. T. (2013). The translational utility of behavioral economics: The experimental analysis of consumption and choice. In G. J. Madden (Ed.), *APA handbook of behavior analysis: Vol. 2. Translating principles into practice* (pp. 191-124). Washington, DC: American Psychological Association.

Hursh, S. R., Raslear, T. G., Bauman, R., & Black, H. (1989). The quantitative analysis of economic behavior with laboratory animals. In K. G. Grunert & F. Ölander (Eds.), *Understanding Economic Behaviour* (Vol. 11). Dordrecht: Springer.

Hursh, S. R., Raslear, T. G., Shurtleff, D., Bauman, R., & Simmons, L. (1988). A cost-benefit analysis of demand for food. *Journal of the Experimental Analysis of Behavior, 50*(3), 419-440. doi:10.1901/jeab.1988.50-419

Hursh, S. R., & Roma, P. G. (2013). Behavioral economics and empirical public policy. *Journal of the Experimental Analysis of Behavior, 99*(1), 98-124. doi:10.1002/jeab.7

Hursh, S. R., & Roma, P. G. (2016). Behavioral economics and the analysis of consumption and choice. *Managerial and Decision Economics, 37*(4-5), 224-238. doi:10.1002/mde.2724

Hursh, S. R., & Silberberg, A. (2008). Economic demand and essential value. *Psychological Review, 115*(1), 186-198. doi:10.1037/0033-295X.115.1.186

Hursh, S. R., & Winger, G. (1995). Normalized demand for drugs and other reinforcers. *Journal of the Experimental Analysis of Behavior, 64*(3), 373-384. doi:10.1901/jeab.1995.64-373

Imam, A. A. (1993). Response-reinforcer independence and the economic continuum: A preliminary analysis. *Journal of the Experimental Analysis of Behavior, 59*(1), 231-243. doi:10.1901/jeab.1993.59-231

Iyengar, S. S., & Lepper, M. R. (2000). When choice is demotivating: Can one desire too much of a good thing? *Journal of Personality and Social Psychology, 79*(6), 995-1006. doi:10.1037/0022-3514.79.6.995

Jacobs, E. A., & Bickel, W. K. (1999). Modeling drug consumption in the clinic using simulation procedures: Demand for heroin and cigarettes in opioid-dependent outpatients. *Experimental and Clinical Psychopharmacology, 7*(4), 412-426. doi:10.1037/1064-1297.7.4.412

Jarmolowicz, D. P., & Lattal, K. A. (2010). On distinguishing progressively increasing response requirements for reinforcement. *The Behavior Analyst, 33*(1), 119-125. doi:10.1007/BF03392207

Jarmolowicz, D. P., & Lattal, K. A. (2013). Delayed reinforcement and fixed-ratio performance. *Journal of the Experimental Analysis of Behavior, 100*(3), 370-395. doi:10.1002/jeab.48

Jarmolowicz, D. P., Sofis, M. J., & Darden, A. C. (2016). Concurrent progressive ratio schedules: Effects of reinforcer probability on breakpoint and response allocation. *Behavioural Processes, 128*, 103-107. doi:10.1016/j.beproc.2016.04.012

Johnson, D. F., & Collier, G. (1987). Caloric regulation and patterns of food choice in a patchy environment: The value and cost of alternative foods. *Physiology & Behavior, 39*(3), 351-359. doi:10.1016/0031-9384(87)90234-4

Johnson, M. W., & Bickel, W. K. (2002). Within-subject comparison of real and hypothetical money rewards in delay discounting. *Journal of the Experimental Analysis of Behavior, 77*(2), 129-146. doi:10.1901/jeab.2002.77-129

Johnson, M. W., & Bickel, W. K. (2006). Replacing relative reinforcing efficacy with behavioral economic demand curves. *Journal of the Experimental Analysis of Behavior, 85*(1), 73-93. doi:10.1901/jeab.2006.102-04

Johnson, M. W., Bickel, W. K., & Kirshenbaum, A. P. (2004). Substitutes for tobacco smoking: a behavioral economic analysis of nicotine gum, denicotinized cigarettes, and nicotine-containing cigarettes. *Drug and Alcohol Dependence, 74*(3), 253-264. doi:10.1016/j.drugalcdep.2003.12.012

Johnston, J. M., & Pennypacker, H. S. (1980). *Strategies and tactics of human behavioral research*. Hillsdale, NJ: Lawrence Erlbaum Associates.

Jones, L. A. (1986). Perception of force and weight: Theory and research. *Psychological Bulletin, 100*(1), 29-42. doi:10.1037/0033-2909.100.1.29

Kagel, J. H., Battalio, R. C., Rachlin, H., & Green, L. (1981). Demand curves for animal consumers. *The Quarterly Journal of Economics, 96*(1), 1-15. doi:10.2307/2936137

Kaplan, B. A., & Reed, D. D. (2014). Essential value, Pmax, and Omax automated calculator [spreadsheet application]. Retrieved from: http://hdl.handle.net/1808/14934.

Keehn, J. D. (1981). Choice of equal effects with unequal efforts: A way to quantify the law of least effort. *Bulletin of the Psychonomic Society, 17*(3), 166-168. doi:10.3758/BF03333700

Killeen, P. (1969). Reinforcement frequency and contingency as factors in fixed-ratio behavior. *Journal of the Experimental Analysis of Behavior, 12*(3), 391-395. doi:10.1901/jeab.1969.12-391

Killeen, P. R., Posadas-Sánchez, D., Johansen, E. B., & Thrailkill, E. A. (2009). Progressive ratio schedules of reinforcement. *Journal of Experimental Psychology, 35*(1), 35-50. doi:10.1037/a0012497

Kirkpatrick, M. A., & Fowler, S. C. (1989). Operant force-band differentiation by rats using two different response topographies. *Bulletin of the Psychonomic Society, 27*(1), 52-54. doi:10.3758/BF03329895

Koffarnus, M. N., Franck, C. T., Stein, J. S., & Bickel, W. K. (2015). A modified exponential behavioral economic demand model to better describe consumption data. *Experimental and Clinical Psychopharmacology, 23*(6), 504-512. doi:10.1037/pha0000045

Levine, M., & Ensom, M. H. H. (2001). Post hoc power analysis: An idea whose time has passed? *Pharmacotherapy, 21*(4), 405-409. doi:10.1592/phco.21.5.405.34503

Lindsley, O. R. (1957). Operant behavior during sleep: A measure of depth of sleep. *Science, 126*(3286), 1290-1291. doi:10.1126/science.126.3286.1290

Madden, G. J., Begotka, A. M., Raiff, B. R., & Kastern, L. L. (2003). Delay discounting of real and hypothetical rewards. *Experimental and Clinical Psychopharmacology, 11*(2), 139-145. doi:10.1037/1064-1297.11.2.139

Madden, G. J., & Bickel, W. K. (1999). Abstinence and price effects on demand for cigarettes: A behavioral-economic analysis. *Addiction, 94*(4), 577-588. doi:10.1046/j.1360-0443.1999.94457712.x

Madden, G. J., Bickel, W. K., & Jacobs, E. A. (2000). Three predictions of the economic concept of unit price in a choice context. *Journal of the Experimental Analysis of Behavior, 73*(1), 45-64. doi:10.1901/jeab.2000.73-45

Madden, G. J., Dake, J. M., Mauel, E. C., & Rowe, R. R. (2005). Labor supply and consumption of food in a closed economy under a range of fixed- and random-ratio schedules: tests of unit price. *Journal of the Experimental Analysis of Behavior, 83*(2), 99-118. doi:10.1901/jeab.2005.32-04

Madden, G. J., Smethells, J. R., Ewan, E. E., & Hursh, S. R. (2007a). Tests of behavioral economic assessments of relative reinforcer efficacy: Economic substitutes. *Journal of the Experimental Analysis of Behavior, 87*(2), 219-240. doi:10.1901/jeab.2007.80-06

Madden, G. J., Smethells, J. R., Ewan, E. E., & Hursh, S. R. (2007b). Tests of behavioral economic assessments of relative reinfrocer efficacy II: Economic complements. *Journal of the Experimental Analysis of Behavior, 88*(3), 355-367. doi:10.1901/jeab.2007.8-355

Mazur, J. E. (1987). An adjusting procedure for studying delayed reinforcement. In M. L. Commons, J. E. Mazur, J. A. Nevin, & H. Rachlin (Eds.), *Quantitative analyses of*

behavior: Vol. 5. The effect of delay and of intervening events on reinforcement value (Vol. 5, pp. 55-73). Hillsdale, NJ: Erlbaum.

McDowell, J. J., Calvin, O. L., & Klapes, B. (2016). A survey of residual analysis and a new test of residual trend. *Journal of the Experimental Analysis of Behavior, 105*(3), 445-458. doi:10.1002/jeab.208

McKerchar, T. L., Green, L., & Myerson, J. (2010). On the scaling interpretation of exponents in hyperboloid models of delay and probability discounting. *Behavioural Processes, 84*(1), 440-444. doi:10.1016/j.beproc.2010.01.003

McSweeney, F. K., & Swindell, S. (1999). Behavioral economics and within-session changes in responding. *Journal of the Experimental Analysis of Behavior, 72*(3), 355-371. doi:10.1901/jeab.1999.72-355

Miller, L. K. (1970). Some punishing effects of response force. *Journal of the Experimental Analysis of Behavior, 13*(2), 215-220. doi:10.1901/jeab.1970.13-215

Minervini, V., Rowland, N. E., Robertson, K. L., & Foster, T. C. (2015). Role of estrogen receptor-a on food demand elasticity. *Journal of the Experimental Analysis of Behavior, 103*(3), 553-561. doi:10.1002/jeab.149

Mintz, D. E. (1962). Force of response during ratio reinforcement. *Science, 138*(3539), 516-517. doi:10.1126/science.138.3539.516

Mintz, D. E. (1965). Force differentiation in human subjects. *Psychonomic Science, 2*(1-12), 289-290. doi:10.3758/BF03343459

Mintz, D. E., Samuels, R. M., & Barber, N. G. (1976). Force and rate relations in respoding during variable-interval reinforcement. *Journal of the Experimental Analysis of Behavior, 26*(3), 387-393. doi:10.1901/jeab.1976.26-387

Mitchell, S. H. (1999). Measures of impulsivity in cigarette smokers and non-smokers. *Psychopharmacology (Berlin), 146*(4), 455-464. doi:10.1007/PL00005491

Mitchell, S. H., & Brener, J. (1991). Energetic and motor responses to increasing force requirements. *Journal of Experimental Psychology: Animal Behavior Processes, 17*(2), 174-185. doi:10.1037/0097-7403.17.2.174

Moore, J. (1981). On mentalism, methodological behaviorism, and radical behaviorism. *Behaviorism, 9*(1), 55-77. Retrieved from http://www.jstor.org/stable/27758972

Moore, J. (2011). Behaviorism. *The Psychological Record, 61*(3), 449-464. doi:10.1007/BF033

Morefield, M. A. (1964). *A fixed effort schedule of reinforcement (Unpublished doctoral dissertation)*. Princeton University. Princeton, NJ.

Murphy, J. G., & MacKillop, J. (2006). Relative reinforcing efficacy of alcohol among college student drinkers. *Experimental and Clinical Psychopharmacology, 14*(2), 219-227. doi:10.1037/1064-1297.14.2.219

Murphy, J. G., MacKillop, J., Skidmore, J. R., & Pederson, A. A. (2009). Reliability and validity of a demand curve measure of alcohol reinforcement. *Experimental and Clinical Psychopharmacology, 17*(6), 396-404. doi:10.1037/a0017684

Myerson, J., Green, L., & Warusawitharana, M. (2001). Area under the curve as a measure of discounting. *Journal of the Experimental Analysis of Behavior, 76*(2), 235-243. doi:10.1901/jeab.2001.76-235

Neuringer, A. J., & Schneider, B. A. (1968). Separating the effects of interreinforcement time and number of interreinforcement responses. *Journal of the Experimental Analysis of Behavior, 11*(6), 661-667. doi:10.1901/jeab.1968.11-661

Nord, C. M. (2014). *The behavioral economics of effort (Unpublished master's thesis).* (Master of Science), University of North Texas, Denton, TX.

Notterman, J. M. (1959). Force emission during bar pressing. *Journal of Experimental Psychology, 58*(5), 341-347. doi:10.1037/h0042801

Notterman, J. M., & Mintz, D. E. (1962). Exteroceptive cueing of response force. *Science, 135*(3508), 1070-1071. doi:10.1126/science.135.3508.1070

Notterman, J. M., & Mintz, D. E. (1965). *Dynamics of response*. New York: John Wiley & Sons, Inc.

Peck, S., & Byrne, T. (2016). Demand in rats responding under duration-based schedules of reinforcement. *Behavioural Processes, 128*, 47-52. doi:10.1016/j.beproc.2016.04.002

Perone, M., & Hursh, D. E. (2013). Single-case experimental designs. In G. J. Madden (Ed.), *APA handbook of behavior analysis* (Vol. 1: Methods and Principles, pp. 107-126): American Psychological Association.

Pinkston, J. W., & Libman, B. M. (2017). Aversive functions of response effort: Fact or artifact? *Journal of the Experimental Analysis of Behavior, 108*(1), 73-96. doi:10.1002/jeab.264

Pinkston, J. W., & McBee, L. N. (2014). Force dynamics in fixed-ratio schedules. *Behavioural Processes, 103*, 112-116. doi:10.1016/j.beproc.2013.11.005

Rachlin, H. (2006). Notes on discounting. *Journal of the Experimental Analysis of Behavior, 85*(3), 425-435. doi:10.1901/jeab.2006.85-05

Rachlin, H., Green, L., Kagel, J. H., & Battalio, R. C. (1976). Economic demand theory and psychological studies of choice. In G. H. Bower (Ed.), *The psychology of learning and choice: Advances in research and theory* (Vol. 10, pp. 129-152). New York: Academic Press.

Rachlin, H., & Krasnoff, J. (1983). Eating and drinking: An economic analysis. *Journal of the Experimental Analysis of Behavior, 39*(3), 385-404. doi:10.1901/jeab.1983.39-385

Rapp, J. T. (2008). Conjugate reinforcement: A brief review and suggestions for applications to the assessment of automatically reinforced behavior. *Behavioral Interventions, 23*(2), 113-136. doi:10.1002/bin.259

Rapport, D. J. (1971). An optimization model of food selection. *The American Naturalist, 105*(946), 575-587. doi:10.1086/282746

Raslear, T. G., Bauman, R. A., Hursh, S. R., Shurtleff, D., & Simmons, L. (1988). Rapid demand curves for behavioral economics. *Animal Learning & Behavior, 16*(3), 330-339. doi:10.3758/BF03209085

Razali, N. M., & Wah, Y. B. (2011). Power comparisons of Shapiro-Wilk, Kolmogorov-Smirnov, Lilliefors and Anderson-Darling tests. *Journal of Statistical Modeling and Analytics, 2*(1), 21-33.

Reed, D. D., DiGennaro Reed, F. D., Chok, J., & Brozyna, G. A. (2011). The "tyranny of choice": Choice overload as a possible instance of effort discounting. *The Psychological Record, 61*(4), 547-560. doi:10.1007/BF03395776

Reed, D. D., Hursh, S. R., Becirevic, A., Roma, P. G., & Hursh, S. R. (2016). Toward quantifying the abuse liability of ultraviolet tanning: A behavioral economic approach to tanning addiction. *Journal of the Experimental Analysis of Behavior, 106*(1), 93-106. doi:10.1002/jeab.216

Royalty, P., Williams, B. A., & Fantino, E. (1987). Effects of delayed conditioned reinforcement in chain schedules. *Journal of the Experimental Analysis of Behavior, 47*(1), 41-56. doi:10.1901/jeab.1987.47-41]

Schwartz, B. (2004). *The paradox of choice: Why more is less*. New York: Ecco Press.

Schwartz, G. E., & Mintz, D. E. (1980). Force differentiation in human subjects: Effects of criterion range and level. *Perceptual and Motor Skills, 51*(2), 575-581. doi:10.2466/pms.1980.51.2.575

Shahan, T. A., Odum, A. L., & Bickel, W. K. (2000). Nicotine gum as a substitute for cigarettes: a behavioral economic analysis. *Behavioral Pharmacology, 11*(1), 71-79. doi:10.1097/00008877-200002000-00008

Shull, R. L. (1970). A response-initiated fixed-interval schedule of reinforcement. *Journal of the Experimental Analysis of Behavior, 13*(1), 13-15. doi:10.1901/jeab.1970.13-13

Shull, R. L., & Lawrence, P. S. (1998). Reinforcement schedule performance. In K. A. Lattal & M. Perone (Eds.), *Handbook of research methods in operant behavior*. New York: Plenum Press.

Sidman, M. (1955). Technique for assessing the effects of drugs on timing behavior. *Science, 122*(3176), 925. doi:10.1126/science.122.3176.925

Skinner, B. F. (1938). *The behavior of organisms: An experimental analysis*. Oxford, England: Appleton-Century.

Skinner, B. F. (1953). *Science and human behavior*. New York, NY: Macmillan Publishing.

Skinner, B. F. (1966). What is the experimental analysis of behavior? *Journal of the Experimental Analysis of Behavior, 9*(3), 213-218. doi:10.1901/jeab.1966.9-213

Slifkin, A. B., & Brener, J. (1998). Control of operant response force. *Journal of Experimental Psychology: Animal Behavior Processes, 24*(4), 431-438. doi:10.1037/0097-7403.24.4.431

Slifkin, A. B., Mitchell, S. H., & Brener, J. (1995). Variation of isometric response force in the rat. *Journal of Motor Behavior, 27*(4), 375-381. doi:10.1080/00222895.1995.9941725

Staddon, J. E. R. (1978). Theory of behavioral power functions. *Psychological Review, 85*(4), 305-320. doi:10.1037/0033-295X.85.4.305

Stevens, J. C., & Cain, W. S. (1970). Effort in isometric muscular contractions related to force level and duration. *Perception & Psychophysics, 8*(4), 240-244. doi:10.3758/BF03210214

Stevens, J. C., & Mack, J. D. (1959). Scales of apparent force. *Journal of Experimental Psychology, 58*(5), 405-413. doi:10.1037/h0046906

Stevens, S. S. (1957). On the psychophysical law. *Psychological Review, 64*(3), 153-181. doi:10.1037/h0046162

Sugiwaka, H., & Okouchi, H. (2004). Reformative self-control and discouting of reward value by delay or effort. *Japanese Psychological Research, 46*(1), 1-9. doi:10.1111/j.1468-5884.2004.00231.x

Sumpter, C. E., Temple, W., & Foster, T. M. (1999). The effects of differing response types and price manipulations on demand measures. *Journal of the Experimental Analysis of Behavior, 71*(3), 329-354. doi:10.1901/jeab.1999.71-329

Sumpter, C. E., Temple, W., & Foster, T. M. (2004). Comparing demand functions when different price manipulations are used: Does unit price help? *Learning & Behavior, 32*(2), 202-212. doi:10.3758/BF03196021

Tan, L., & Hackenberg, T. D. (2015). Pigeons' demand and preference for specific and generalized conditioned reinforcers in a token economy. *Journal of the Experimental Analysis of Behavior, 104*(3), 296-314. doi:10.1002/jeab.181

Thorndike, E. L. (1898). Animal intelligence: An experimental study of the associative processes in animals. *Psychological Monographs: General and Applied, 2*(4), i-109. doi:10.1037/h0092987

Timberlake, W. (1984). Behavior regulation and learned performance: Some misapprehensions and disagreements. *Journal of the Experimental Analysis of Behavior, 41*(3), 355-375. doi:10.1901/jeab.1984.41-355

Timberlake, W. (1993). Behavior systems and reinforcement: An integrative approach. *Journal of the Experimental Analysis of Behavior, 60*(1), 105-128. doi:10.1901/jeab.1993.60-105

Timberlake, W., & Peden, B. F. (1987). On the distinction between open and closed economies. *Journal of the Experimental Analysis of Behavior, 48*(1), 35-60. doi:10.1901/jeab.1987.48-35

Tsunematsu, S. (2001). Effort- and time-cost effects on demand curves for food by pigeons under short session closed economies. *Behavioural Processes, 53*(1-2), 47-56. doi:10.1016/S0376-6357(00)00147-9

Tustin, R. D. (1994). Preference for reinforcers under varying schedule arrangements: A behavioral economic analysis. *Journal of Applied Behavior Analysis, 27*(4), 597-606. doi:10.1901/jaba.1994.27-597

Wade-Galuska, T., Galuska, C. M., Winger, G., & Woods, J. H. (2007). Aspartame demand in rhesus monkeys: Effects of volume and concentration manipulations. *Behavioural Processes, 74*(1), 71-78. doi:10.1016/j.beproc.2006.09.015

Wade-Galuska, T., Perone, M., & Wirth, O. (2005). Effects of past and upcoming response-force requirements on fixed-ratio pausing. *Behavioural Processes, 68*(1), 91-95. doi:10.1016/j.beproc.2004.10.001

Wallace, M. D., Iwata, B. A., Zhou, L., & Goff, G. A. (1999). Rapid assessment of the effects of restraint on self-injury and adaptive behavior. *Journal of Applied Behavior Analysis, 32*(4), 525-528. doi:10.1901/jaba.1999.32-525

Wilcoxon, F., Katti, S. V., & Wilcox, R. A. (1975). Critical values and probability levels for the Wilcoxon rank sum test and the Wilcoxon signed rank test. In H. L. Harter & D. B. Owen (Eds.), *Selected tables in mathematical statistics* (Vol. 1). Providence, RI: Mathematical Society.

Wilson, M. P., & Keller, F. S. (1953). On the selective reinforcement of spaced responses. *Journal of Comparative and Physiological Psychology, 46*(3), 190-193. doi:10.1037/h0057705

Zarcone, T. J., Chen, J., & Fowler, S. C. (2009). Effects of differing response-force requirements on food-maintained responding in C57Bl/6J mice. *Journal of the Experimental Analysis of Behavior, 92*(2), 257-274. doi:10.1901/jeab.2009.92-257

Zarcone, T. J., Chen, R., & Fowler, S. C. (2007). Effects of differing response-force requirements on food-maintained responding in CD-1 mice. *Journal of the Experimental Analysis of Behavior, 88*(3), 381-393. doi:10.1901/jeab.2007.88-381

Zeiler, M. (1977). Schedules of reinforcement: The contolling variables. In W. K. Honig & J. E. R. Staddon (Eds.), *Handbook of operant behavior* (pp. 201-232). Englewood Cliffs, NJ: Prentice-Hall.

Zeiler, M. D. (1999). Reversed schedule effects in open and closed economies. *Journal of the Experimental Analysis of Behavior, 71*(2), 171-186. doi:10.1901/jeab.1999.71-171

Zhou, L., Goff, G. A., & Iwata, B. A. (2000). Effects of increased response effort on self-injury and object manipulation as competing responses. *Journal of Applied Behavior Analysis, 33*(1), 29-40. doi:10.1901/jaba.2000.33-29

Zimmerman, J., Hanford, P. V., & Brown, W. (1967). Effects of conditioned reinforcement frequency in an intermittent free-feeding situation. *Journal of the Experimental Analysis of Behavior, 10*(4), 331-340. doi:10.1901/jeab.1967.10-331

Table 1. Force measurement. **Tables**

Term	Definition
Threshold	The force required (grams) to record a response; reduces recording of fluctuations in force measurement due to vibrations and fluctuations in airflow
Peak force	The maximum force (grams) of a response
Time integral of force	Area under the force-time curve (grams/s^2); referred to as effort
Duration	Time from when a responses surpasses threshold to the time a response falls below threshold
Interresponse time (IRT)	Time from when one response drops below threshold to the time the next response surpasses threshold
Average force	Time integral of force divided by the duration of the response
Peak force criterion	The peak force required (grams) for a response to be included in the reinforcement contingency
Subcriterion response	Responses whose peak force falls between the threshold and peak force criterion
ΔF/F	The standard deviation of the mean peak force divided by the peak force criterion

Table 2. Parameter values for demand curve assays.

Unit Price	Low Reinforcer Magnitude								High Reinforcer Magnitude							
	Increasing Force				Increasing Ratio				Increasing Force				Increasing Ratio			
	FR	Force g (N)	S^{R+} ml (units)	*P*	FR	Force g (N)	S^{R+} ml (units)	*P*	FR	Force g (N)	S^{R+} ml (units)	*P*	FR	Force g (N)	S^{R+} ml (units)	*P*
0.05					**1**	5 (0.049)	.05 (1)	1.0	10				**2**	5 (0.049)	.10 (2)	1.0
0.15					**3**	5 (0.049)	.05 (1)	1.0	10				**6**	5 (0.049)	.10 (2)	1.0
0.25					**5**	5 (0.049)	.05 (1)	1.0	10				**10**	5 (0.049)	.10 (2)	1.0
0.34					**7**	5 (0.049)	.05 (1)	1.0	10				**14**	5 (0.049)	.10 (2)	1.0
0.44					**9**	5 (0.049)	.05 (1)	1.0	10				**18**	5 (0.049)	.10 (2)	1.0
0.49	10	**5 (0.049)**	.05 (1)	1.0	**10**	5 (0.049)	.05 (1)	1.0	10	**10 (0.098)**	.10 (2)	1.0	**20**	5 (0.049)	.10 (2)	1.0
0.98	10	**10 (0.098)**	.05 (1)	1.0	**20**	5 (0.049)	.05 (1)	1.0	10	**20 (0.196)**	.10 (2)	1.0	**40**	5 (0.049)	.10 (2)	1.0
1.47	10	**15 (0.147)**	.05 (1)	1.0	**30**	5 (0.049)	.05 (1)	1.0	10	**30 (0.294)**	.10 (2)	1.0	**60**	5 (0.049)	.10 (2)	1.0
1.96	10	**20 (0.196)**	.05 (1)	1.0	**40**	5 (0.049)	.05 (1)	1.0	10	**40 (0.392)**	.10 (2)	1.0	**80**	5 (0.049)	.10 (2)	1.0
2.45	10	**25 (0.245)**	.05 (1)	1.0	**50**	5 (0.049)	.05 (1)	1.0	10	**50 (0.490)**	.10 (2)	1.0	**100**	5 (0.049)	.10 (2)	1.0
2.94	10	**30 (0.294)**	.05 (1)	1.0	**60**	5 (0.049)	.05 (1)	1.0	10	**60 (0.588)**	.10 (2)	1.0	**120**	5 (0.049)	.10 (2)	1.0
3.43	10	**35 (0.343)**	.05 (1)	1.0	**70**	5 (0.049)	.05 (1)	1.0	10	**70 (0.686)**	.10 (2)	1.0	**140**	5 (0.049)	.10 (2)	1.0
3.92	10	**40 (0.392)**	.05 (1)	1.0	**80**	5 (0.049)	.05 (1)	1.0	10	**80 (0.785)**	.10 (2)	1.0	**160**	5 (0.049)	.10 (2)	1.0
4.41	10	**45 (0.441)**	.05 (1)	1.0	**90**	5 (0.049)	.05 (1)	1.0	10	**90 (0.883)**	.10 (2)	1.0	**180**	5 (0.049)	.10 (2)	1.0
4.90	10	**50 (0.490)**	.05 (1)	1.0	**100**	5 (0.049)	.05 (1)	1.0	10	**100 (0.981)**	.10 (2)	1.0	**200**	5 (0.049)	.10 (2)	1.0
5.39	10	**55 (0.539)**	.05 (1)	1.0	**110**	5 (0.049)	.05 (1)	1.0	10	**110 (1.079)**	.10 (2)	1.0	**220**	5 (0.049)	.10 (2)	1.0
5.88	10	**60 (0.588)**	.05 (1)	1.0	**120**	5 (0.049)	.05 (1)	1.0	10	**120 (1.177)**	.10 (2)	1.0	**240**	5 (0.049)	.10 (2)	1.0
6.37	10	**65 (0.637)**	.05 (1)	1.0	**130**	5 (0.049)	.05 (1)	1.0	10	**130 (1.275)**	.10 (2)	1.0	**260**	5 (0.049)	.10 (2)	1.0
6.86	10	**70 (0.686)**	.05 (1)	1.0	**140**	5 (0.049)	.05 (1)	1.0	10	**140 (1.373)**	.10 (2)	1.0	**280**	5 (0.049)	.10 (2)	1.0
7.35	10	**75 (0.735)**	.05 (1)	1.0	**150**	5 (0.049)	.05 (1)	1.0	10	**150 (1.471)**	.10 (2)	1.0	**300**	5 (0.049)	.10 (2)	1.0
7.85	10	**80 (0.784)**	.05 (1)	1.0	**160**	5 (0.049)	.05 (1)	1.0	10	**160 (1.570)**	.10 (2)	1.0	**320**	5 (0.049)	.10 (2)	1.0
8.34	10	**85 (0.834)**	.05 (1)	1.0	**170**	5 (0.049)	.05 (1)	1.0	10	**170 (1.667)**	.10 (2)	1.0	**340**	5 (0.049)	.10 (2)	1.0
8.83	10	**90 (0.883)**	.05 (1)	1.0	**180**	5 (0.049)	.05 (1)	1.0	10	**180 (1.863)**	.10 (2)	1.0	**360**	5 (0.049)	.10 (2)	1.0
9.32	10	**95 (0.932)**	.05 (1)	1.0	**190**	5 (0.049)	.05 (1)	1.0	10	**190 (1.961)**	.10 (2)	1.0	**380**	5 (0.049)	.10 (2)	1.0
9.81	10	**100 (0.981)**	.05 (1)	1.0	**200**	5 (0.049)	.05 (1)	1.0	10	**200 (2.059)**	.10 (2)	1.0	**400**	5 (0.049)	.10 (2)	1.0

Table note: Unit price (calculated per 0.05-ml reinforcer; shaded column) for each of four demand curve assays: low reinforcer magnitude increasing force (F-L), low reinforcer magnitude increasing ratio (R-L), high reinforcer magnitude increasing force (F-H), and high reinforcer magnitude increasing ratio (R-H). Increasing response requirement within each assay is denoted in bold text. Consistent with Hursh et al. (1988), unit price is calculated from Lever Weight (Force criterion) in Newtons.

Table 3. Order of demand curve assays.

Rat	*1*	*Rep*	*2*	*3*	*4*	*Rep*
1M	F-L	F-L	R-H	F-H	R-L	—
2M	F-L	F-L	R-L	R-H	F-H	F-H
3M	R-H	R-H	F-L	F-H	R-L	—
4M	F-H	F-H	R-H	R-L	F-L	—
1N	R-L	R-L	F-H	F-L	R-H	—
2N	R-L	R-L	R-H	F-L	F-H	F-L

Table note. Demand curve assay order (columns) detailed for each rat (rows). Replications are denoted by "Rep." Demand curve assays include: increasing force, low reinforcer magnitude (F-L); increasing ratio, low reinforcer magnitude (R-L); increasing force, high reinforcer magnitude (F-H); and increasing ratio, high reinforcer magnitude (R-H).

Table 4. Responses per reinforcer delivery in low reinforcer magnitude force progression.

Unit Price	Force (g)	1M		2M		3M		4M		1N		2N	
		Mean	SD	Mean	SD	Mean	SD	Mean	SD	Mean	SD	Mean	SD
0.49	5	10.5	0.85	11.1	1.14	10.1	0.33	10.2	0.73	11.0	1.23	12.4	2.19
0.98	10	12.2	2.14	12.9	1.86	10.5	0.87	10.7	1.10	13.3	3.08	26.8	7.32
1.47	15	12.7	2.34	15.4	3.36	11.2	1.57	11.9	1.86	15.4	4.17	25.7	7.10
1.96	20	14.3	3.64	15.1	3.19	12.7	2.72	13.2	2.50	18.5	6.22	31.8	12.06
2.45	25	15.9	4.03	17.0	4.90	18.8	6.41	16.0	4.52	21.2	7.72	32.8	13.38
2.94	30	18.2	4.83	21.3	5.85	21.5	8.96	17.2	6.42	22.5	7.41	40.3	14.00
3.43	35	23.6	8.29	23.0	6.97	25.6	8.88	20.3	8.63	25.7	11.03		
3.92	40	28.7	11.62	33.0	11.43	31.5	12.86	25.2	10.09	33.2	16.60		
4.41	45	50.5	30.43	37.0	11.91	35.6	18.34	20.7	9.93	40.2	24.26		
4.90	50	39.0	18.42	35.3	15.52	45.5	17.19	23.2	12.16	43.7	20.38		
5.39	55	42.5	19.74	31	*	42.0	17.91	20.9	13.91	83.8	78.03		
5.88	60	56.9	30.09			48.2	17.98	19.8	12.78				
6.37	65	54.2	30.62			40.7	12.77	17.9	7.92				
6.86	70	103.7	60.25			33.5	10.03	19.5	6.02				
7.35	75							19.7	7.00				
7.85	80							31.0	13.11				
8.34	85							20.4	5.14				
8.83	90							56.3	36.12				
9.32	95							49.4	17.63				
9.81	100												

Table note:

* Only one reinforcer delivery in this session (not included in yoking.)

— No reinforcer deliveries in this session (not included in yoking.)

Table 5. Responses per reinforcer delivery in high reinforcer magnitude force progression.

Unit Price	Force (g)	1M		2M		3M		4M		1N		2N	
		Mean	SD	Mean	SD	Mean	SD	Mean	SD	Mean	SD	Mean	SD
0.49	10	10.5	0.88	15.6	3.33	12.8	3.07	13.8	3.36	14.3	3.86	16.7	3.95
0.98	20	11.1	1.19	25.5	7.98	12.6	3.16	18.6	5.64	19.7	6.92	23.8	5.32
1.47	30	12.2	2.08	43.7	17.09	13.7	3.90	32.2	20.16	37.0	14.89	29.6	7.82
1.96	40	15.3	3.38	60.7	22.10	16.4	6.05	32.7	29.45	104.8	72.33	33.4	10.75
2.45	50	18.7	6.12	99.1	30.31	23.0	7.24	20.1	12.50	—	—	26.8	9.18
2.94	60	25.2	8.15	138	*	41.3	9.79	20.8	13.12			—	—
3.43	70	36.9	12.37			42.9	11.38	21.6	8.44				
3.92	80	80.6	60.71			30.0	11.97	30.7	10.70				
4.41	90					25.8	9.03	44.8	24.37				
4.90	100					21.1	7.15	56.4	18.64				
5.39	110					31.0	22.29	—	—				
5.88	120					22.5	6.51						
6.37	130					23.6	6.19						
6.86	140					25.7	7.06						
7.35	150					26.7	12.93						
7.85	160					69.8	48.82						
8.34	170					79	*						
8.83	180												
9.32	190												
9.81	200												

Table note:

* Only one reinforcer delivery in this session (not included in yoking.)

— No reinforcer deliveries in this session (not included in yoking.)

Table 6. Order of yoked assays.

Rat	*1*	*2*	*Rep 1*	*Rep 2*	*Rep 3*	*Rep 4*
1M	Y-F-H	Y-F-L	Y-F-L-R	Y-F-H-2		
2M	Y-F-L	Y-F-H	Y-F-H-R	Y-F-L-R	Y-F-L-2	
3M	Y-F-L	Y-F-H	Y-F-L-2			
4M	Y-F-L	Y-F-H	Y-F-H-R			
1N	Y-F-H	Y-F-L	Y-F-L-2	Y-F-H-2		
2N	Y-F-H	Y-F-L	Y-F-L-R	Y-F-H-M	Y-F-L-R-2	Y-F-L2

Table note. Yoked assay order (columns) detailed for each rat (rows). Assays were yoked to the force progression, low reinforcer magnitude (Y-F-L) and force progression, high reinforcer magnitude (Y-F-H) conditions from Experiment 1. Replications are shown in the "Rep" columns. Replicated assays were yoked to Experiment 1 replications (shown by R), and the yoked progressions (columns 1 and 2) were replicated (shown by 2). For 2N, the Y-F-H condition was repeated using means rather than reinforcer-by-reinforcer ratio values (Y-F-H-M; Rep 2).

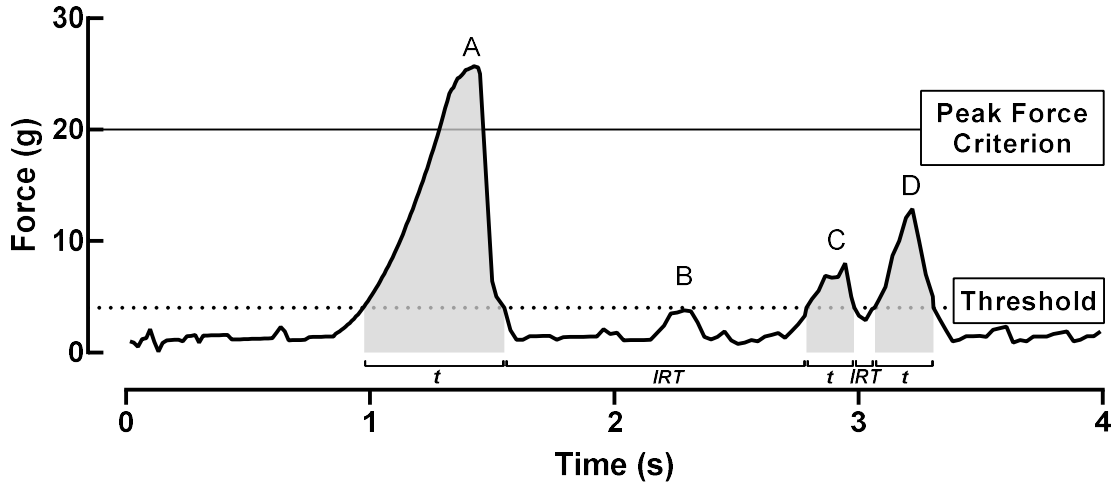

Figure 1. Schematic illustrating force variations across time. Response threshold is shown by the dotted line (shown at 4 g, as in the present experiment), and the peak force criterion is shown by the solid line (20 g here, but varied across conditions in the present experiment). Responses A, C, and D surpass the response threshold and are recorded, whereas B is subthreshold and is not recorded. The recorded portion of each response (above threshold) is shown by the shaded region. The duration of each response (*t*) is shown beneath the figure, as are IRTs. Note that if responses were counted based on switch closure, response durations would not be recorded and would be included in the IRTs. Only response A meets the peak force criterion and would qualify in the reinforcement contingency. Responses C and D are subcriterion responses and would not be recorded in a traditional weighted lever arrangement (Schematic adapted from Fowler, 1974; Notterman & Mintz, 1965)

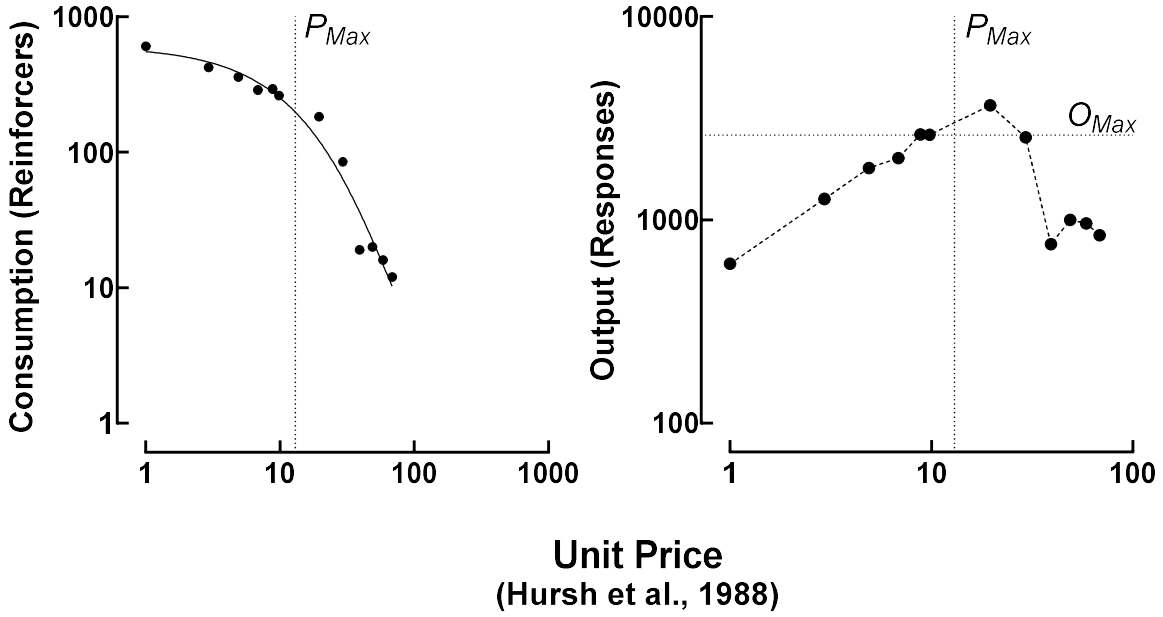

Figure 2. Sample demand curve and work function (data from Experiment 1 graphed as unit price per mL). The left panel shows a demand curve with consumption (y-axis) plotted as a function of unit price (x-axis). Individual data points show number of reinforcers earned at a given price. The solid line shows the best fit curve using the Hursh and Silberburg (2008) exponential model of demand. The left panel shows a work function with work output (number of responses; y-axis) plotted as function of unit price (x-axis). The vertical dotted line on each panel show the derived value of P_{max}, or the price of maximum work, and this is also the point at which the demand curve (left panel) shifts from inelastic (left portion of demand curve with slope less than one) to elastic (right portion of demand curve with slope greater than one). The horizontal dashed line on the right panel shows the derived O_{max}, or maximum response output.

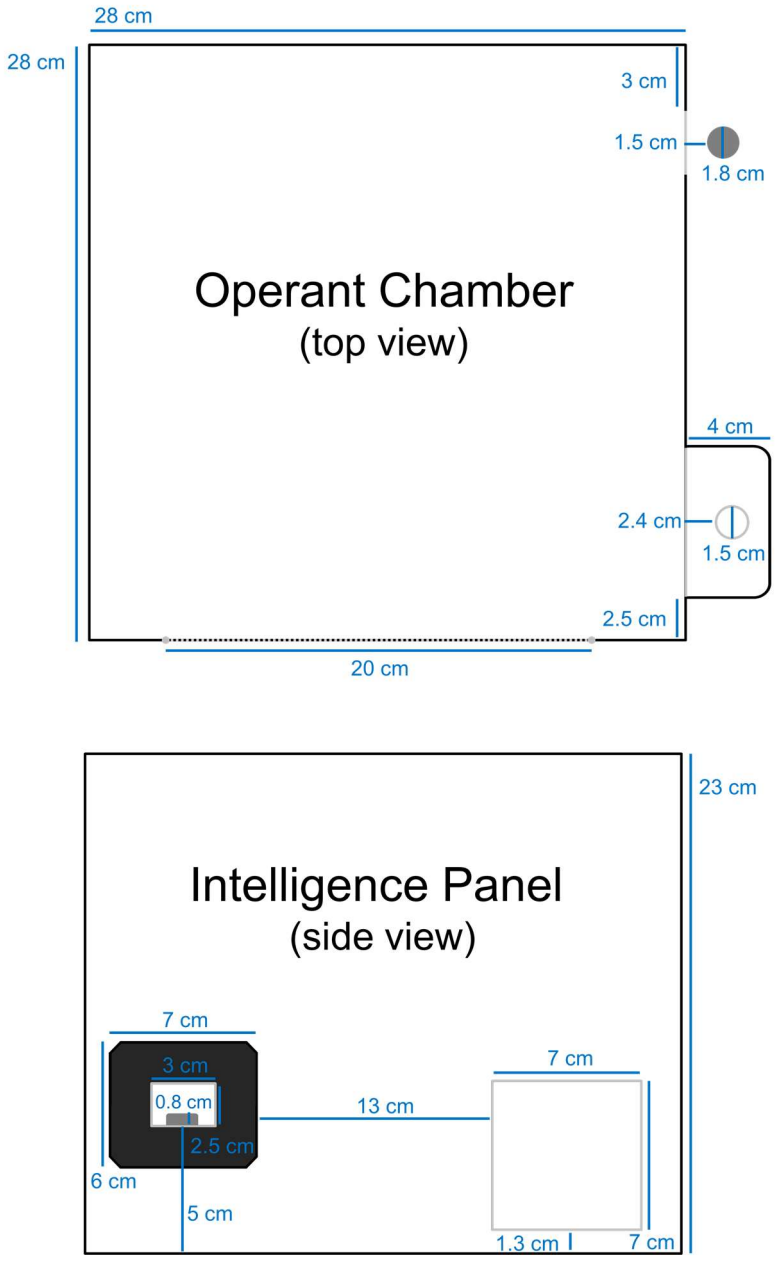

Figure 3. Chamber schematic. Blue lines and text show dimensions. Top panel shows operant chamber. gray solid lines show openings in chamber wall, and gray dashed line shows location of chamber door. Open gray circle is cutout for rats to access reinforcer cup, and filled gray circle shows response operandum. Bottom panel shows intelligence panel. gray solid lines show openings in chamber wall. Dark rectangle shows steel panel on chamber wall with cutout for access to response operandum, which is shown as the filled gray disc.

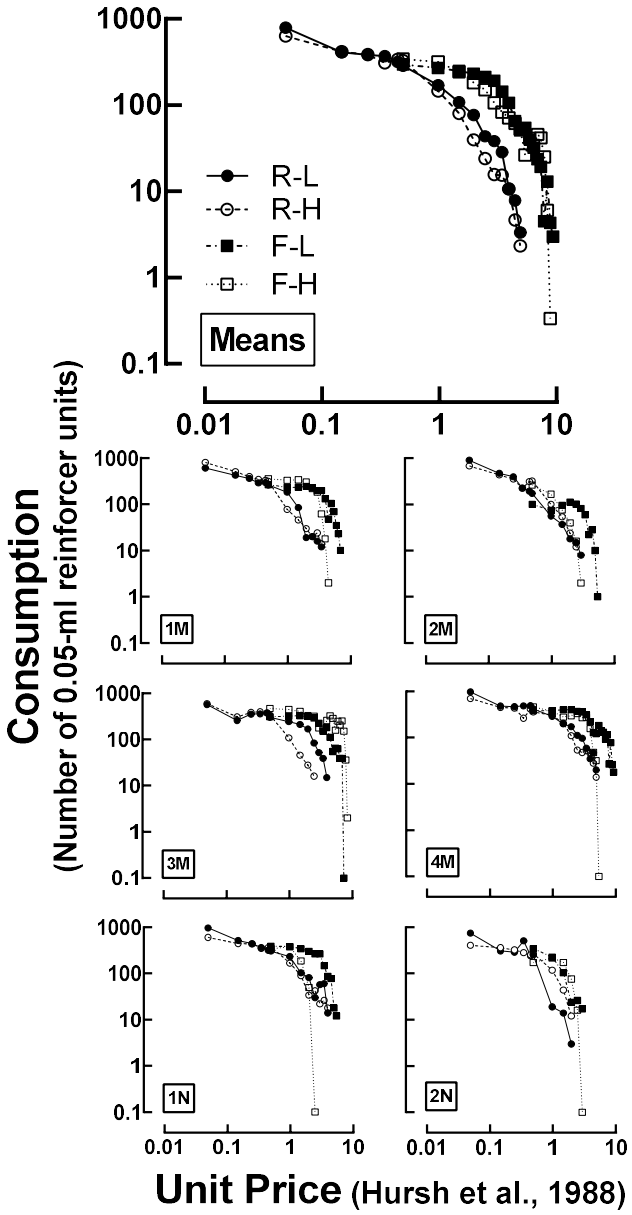

Figure 4. Consumption as a function of unit price across demand assays. Top panel shows means, and six lower panels show data from individual rats (subject codes at lower left). Closed circles and solid lines show R-L progressions, open circles and dashed lines show R-H progressions, closed squares and dot-dashed lines show F-L progressions, and open squares and dotted lines show F-H progressions.

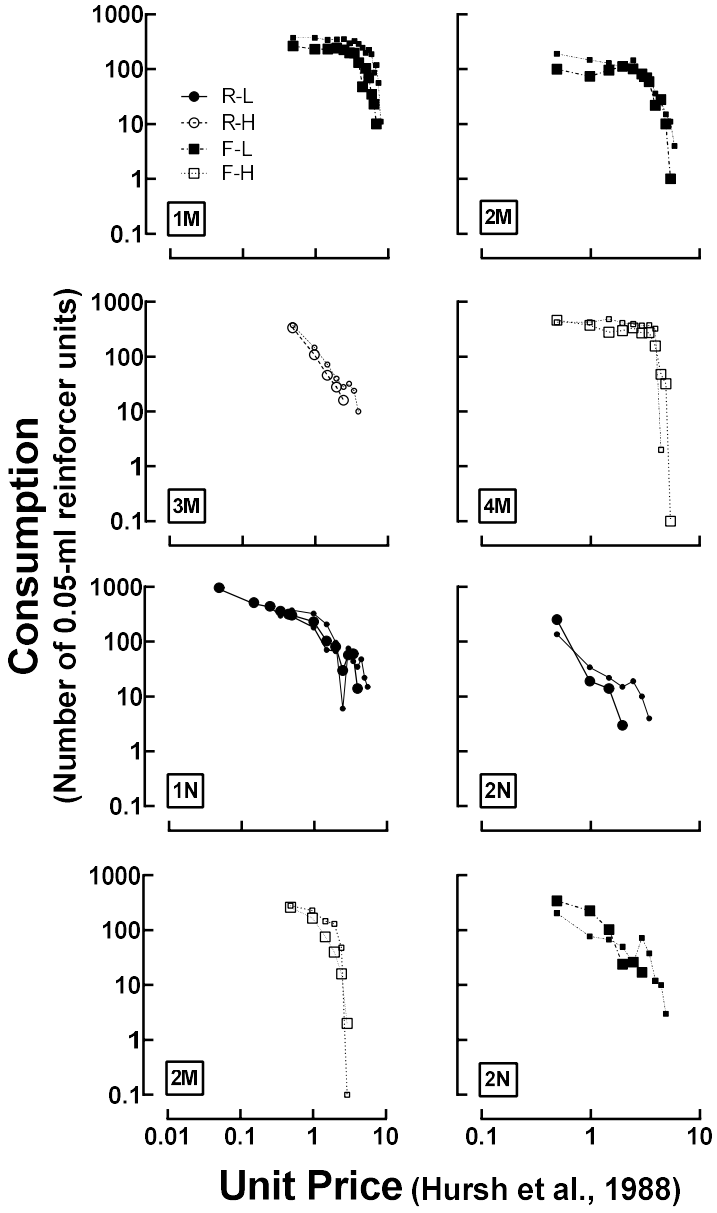

Figure 5. Consumption as a function of unit price in initial demand assays and replications. Each panel shows an initial demand assay (large symbols) and a replication (open symbols). Subjects codes are in lower left corner (note bottom panel shows additional replications for 2M and 2N). Closed circles and solid lines show R-L progression, open circles and dashed lines shows R-H progression, closed squares and dot-dashed lines show F-L progression, and open squares and dotted lines show F-H progression.

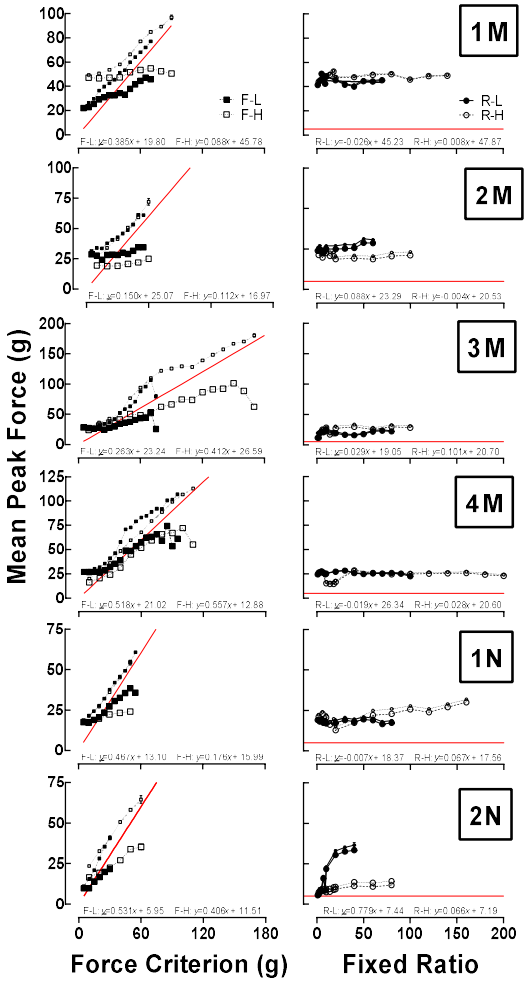

Figure 6. Obtained mean peak force. Left column shows mean peak force (g) as a function of force criterion, and right column shows mean peak force as a function of programmed fixed ratio requirement with individual subjects in rows. Closed circles and solid lines show R-L progressions, open circles and dashed lines show R-H progressions, closed squares and dot-dashed lines show F-L progressions, and open squares and dotted lines show F-H progressions. Smaller symbols show mean peak force of only criterion responses. The solid red reference lines show the obtained mean peak force that would match the force criterion. Equations show formula of lines fit to the peak force of all responses (i.e., criterion and subcriterion). Error bars show one SEM; error bars that are not shown were too small to be plotted.

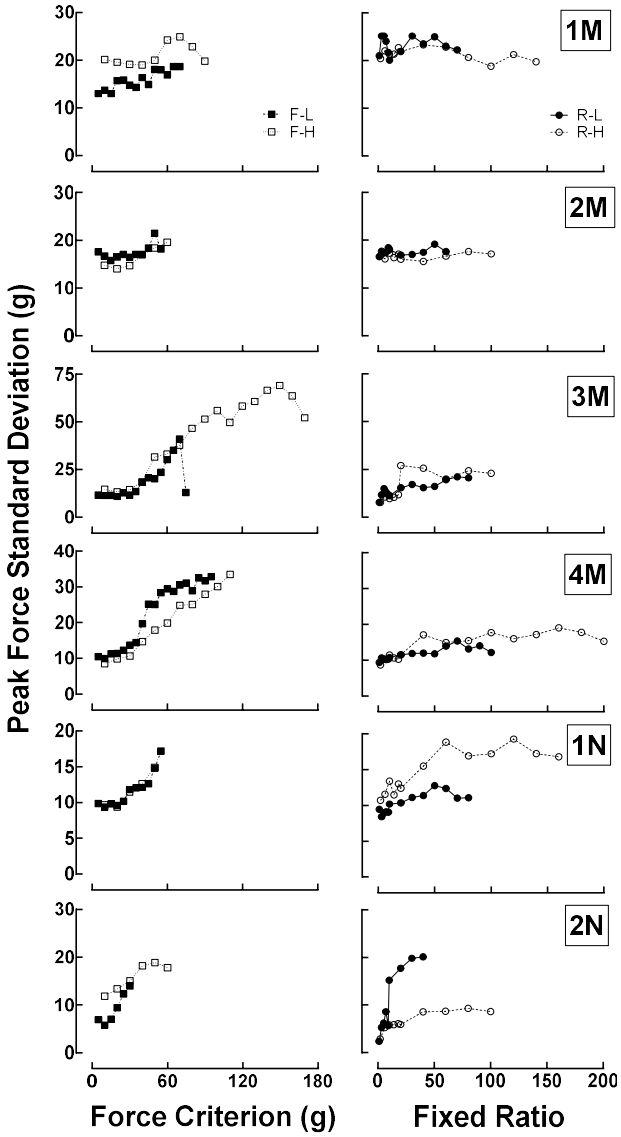

Figure 7. Peak force standard deviations. Peak force standard deviation (g) is plotted along the y-axis as a function of force criterion (left column x-axis) programmed fixed ratio requirement (right column x-axis). Each row shows data from a different subject (subject codes in upper right corner). Closed circles and solid lines show R-L progressions, open circles and dashed lines show R-H progressions, closed squares and dot-dashed lines show F-L progressions, and open squares and dotted lines show F-H progressions. Error bars show one SEM; error bars that are not shown were too small to be plotted.

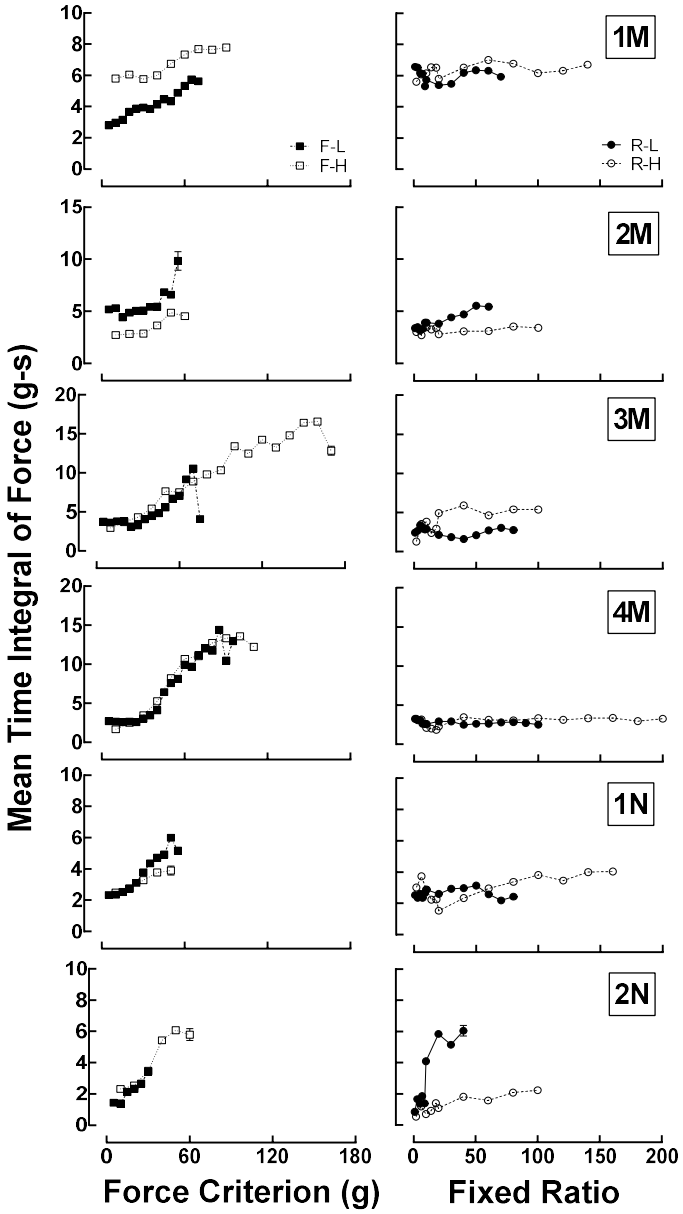

Figure 8. Time integral of force for each response. Mean time integral of force per response (g-s) as a function of force criterion (left column) and programmed fixed ratio requirement (right column) for individual subjects (rows). Closed circles and solid lines show R-L progressions, open circles and dashed lines show R-H progressions, closed squares and dot-dashed lines show F-L progressions, and open squares and dotted lines show F-H progressions.

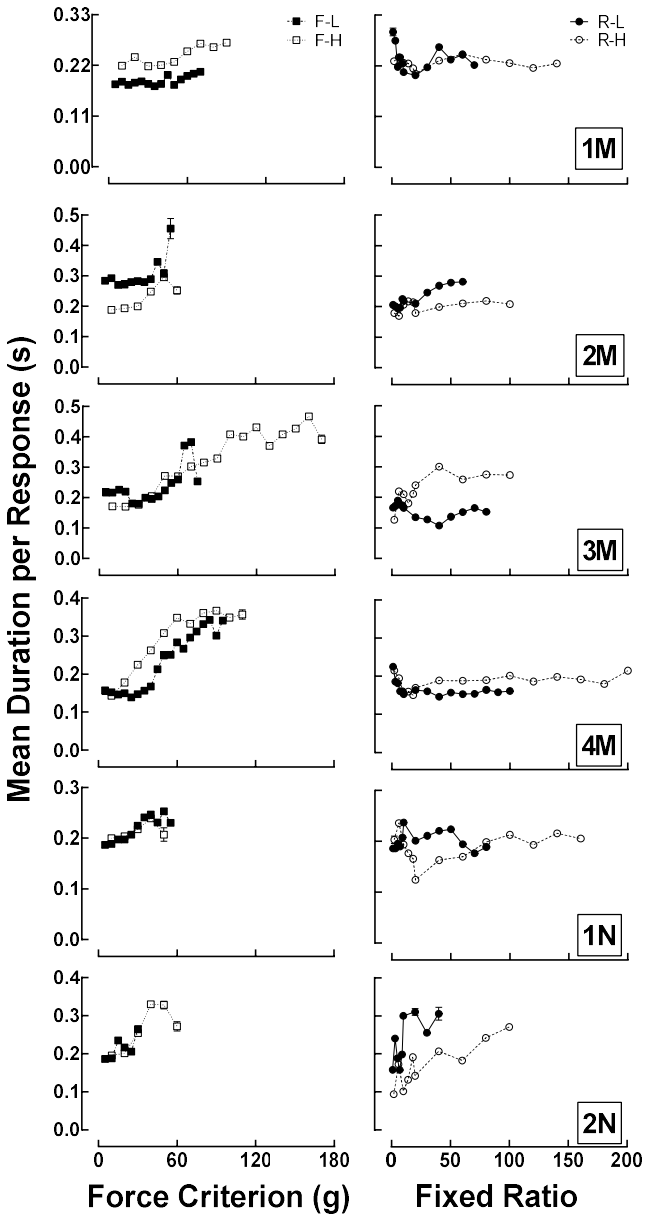

Figure 9. Response durations. Mean duration per response (s) as a function of force criterion (left column) and programmed fixed ratio requirement (right column) for individual subjects (rows). Closed circles and solid lines show R-L progressions, open circles and dashed lines show R-H progressions, closed squares and dot-dashed lines show F-L progressions, and open squares and dotted lines show F-H progressions. Error bars show one SEM; error bars that are not shown were too small to be plotted.

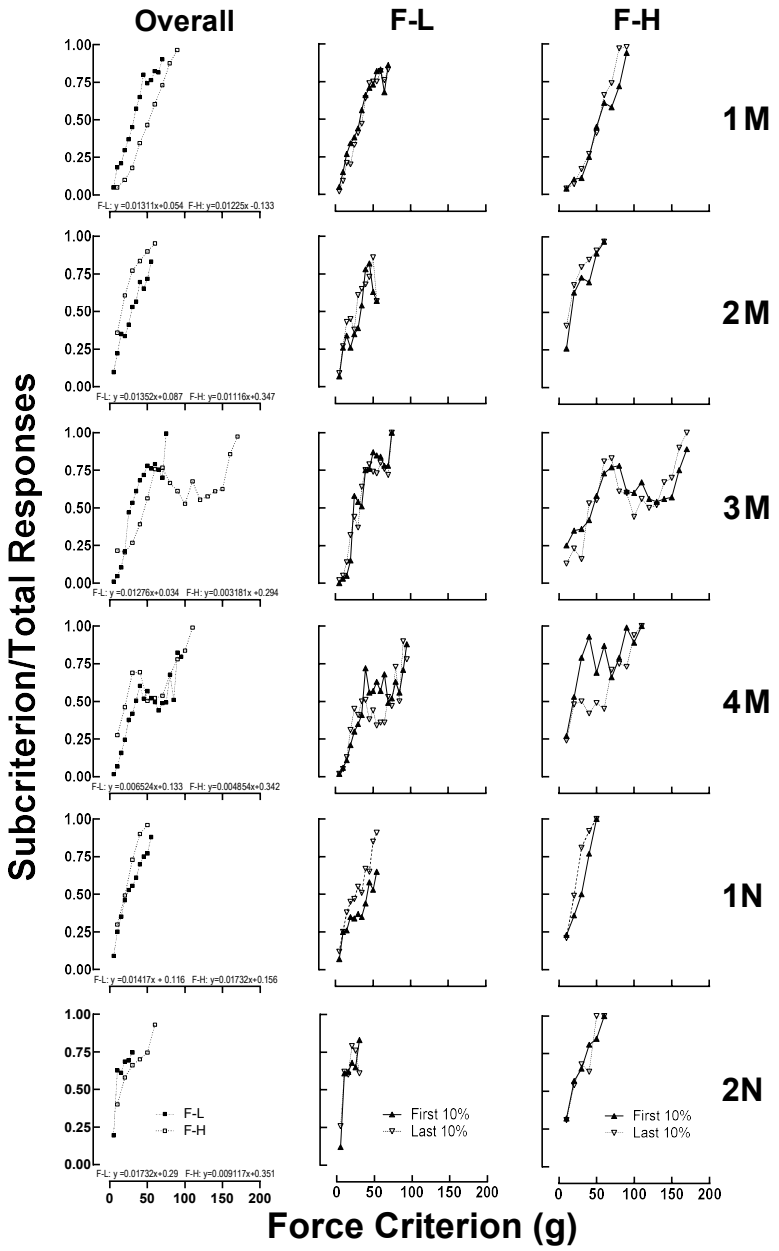

Figure 10. Proportion of subcriterion to total responses as a function of force criterion for individual subjects (rows). The left column shows proportion for entire session; closed squares and dot-dashed lines show F-L progression, and open squares and dotted lines show F-H progression. Proportions are also shown for the first 10% of responses in session (closed, upright triangles and solid lines) and last 10% of responses in session (open, upside-down triangles and dashed lines) for the F-L progression (middle column) and F-H progression (right column).

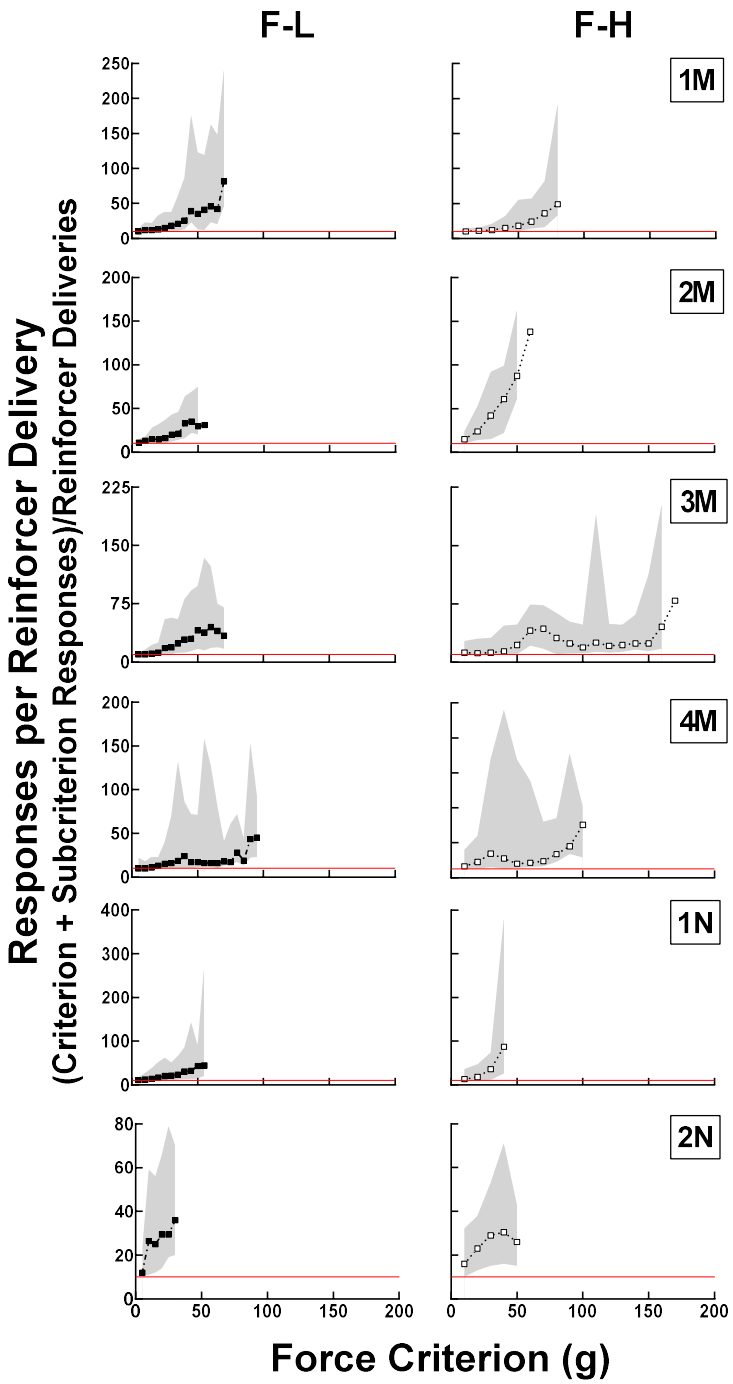

Figure 11. Obtained ratio as a function of force criterion. Data paths show the median obtained ratio for the F-L (closed squares, left column) and F-H (open squares, right column) progressions for each animal. Gray shaded regions show the range of minimum to maximum obtained ratio, and the red reference line shows the programmed ratio (FR10).

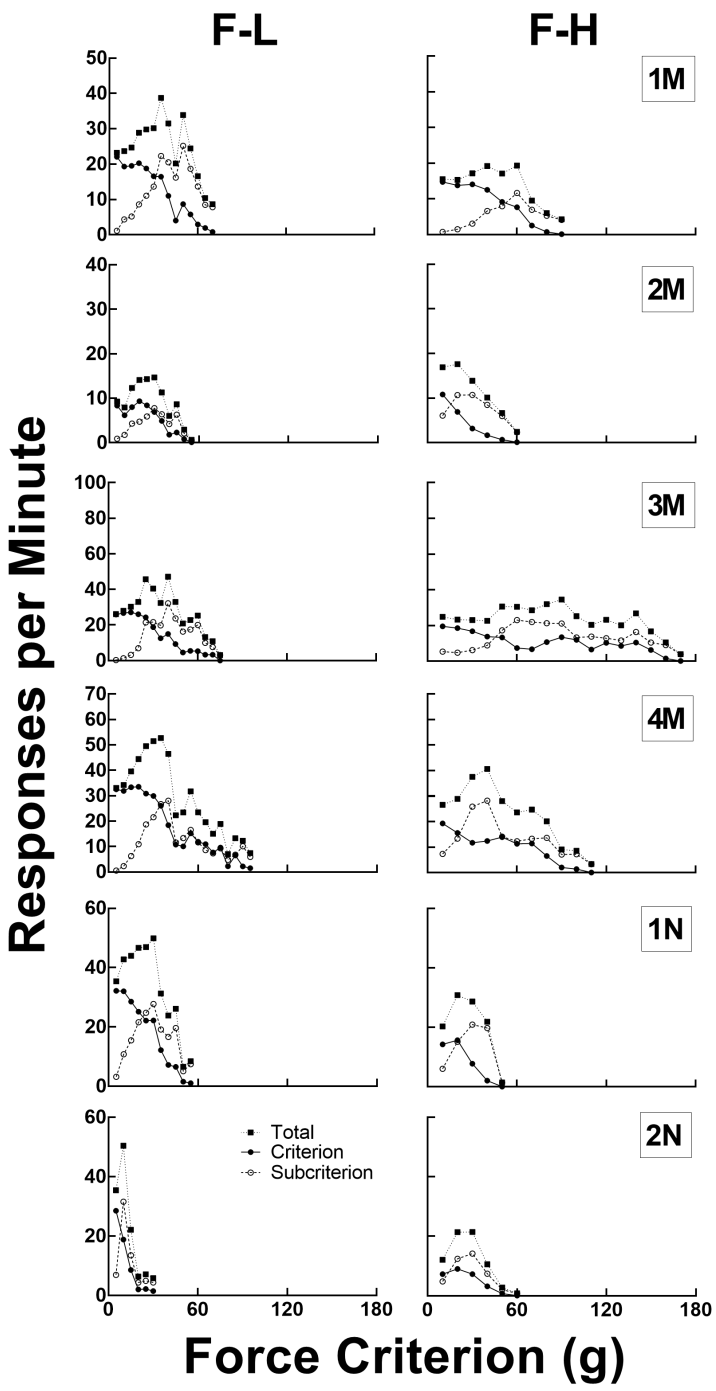

Figure 12. Response rates from F-L and F-H progressions. Response rates (y-axis) across force criteria (x-axis) for F-L (left column) and F-H (right column) progressions for individual animals (rows). Closed squares and dotted lines show total response rate, open circles and solid data paths show criterion response rates, and open circles and dashed lines show subcriterion rates.

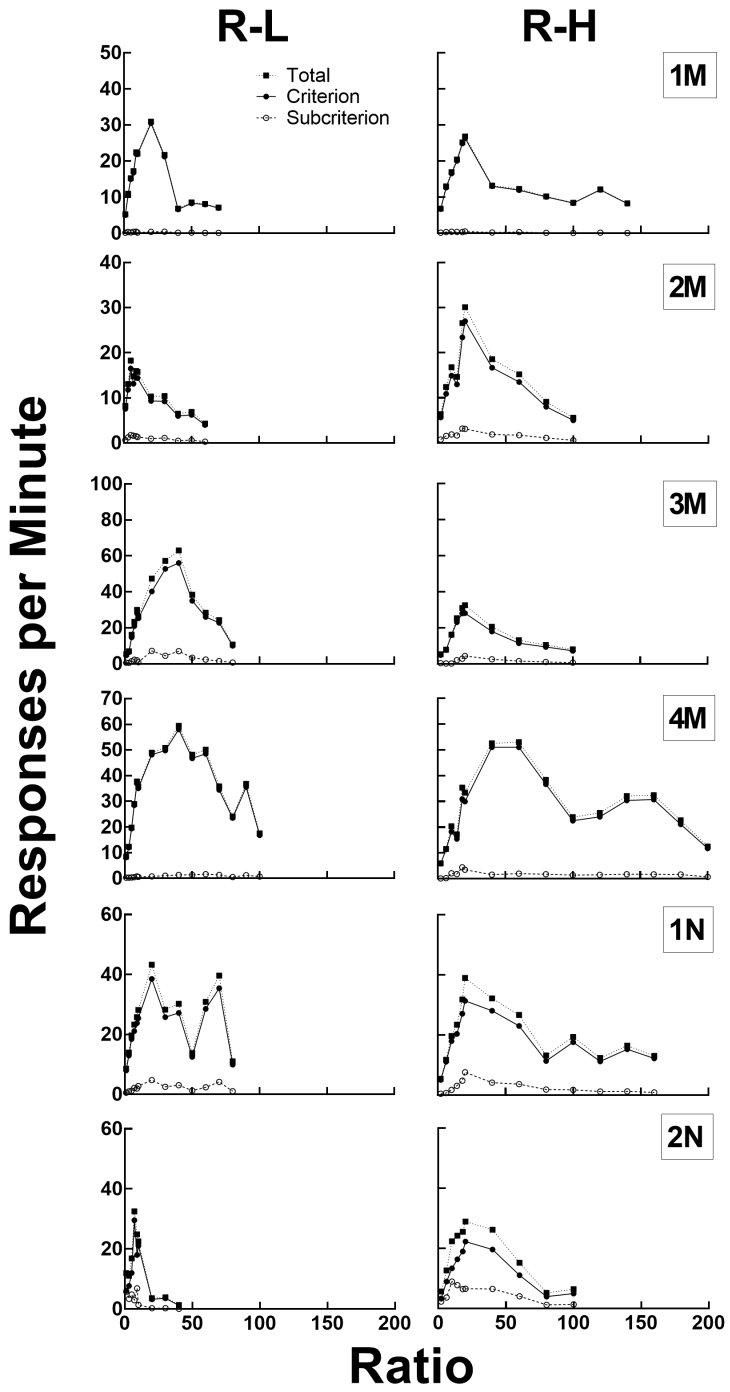

Figure 13. Response rates from R-L and R-H progressions. Response rates (y-axis) across programmed FR (x-axis) for R-L (left column) and R-H (right column) progressions for individual animals (rows). Closed squares and dotted paths show total rates, open circles and solid data paths show criterion rates, and open circles and dashed lines show subcriterion rates.

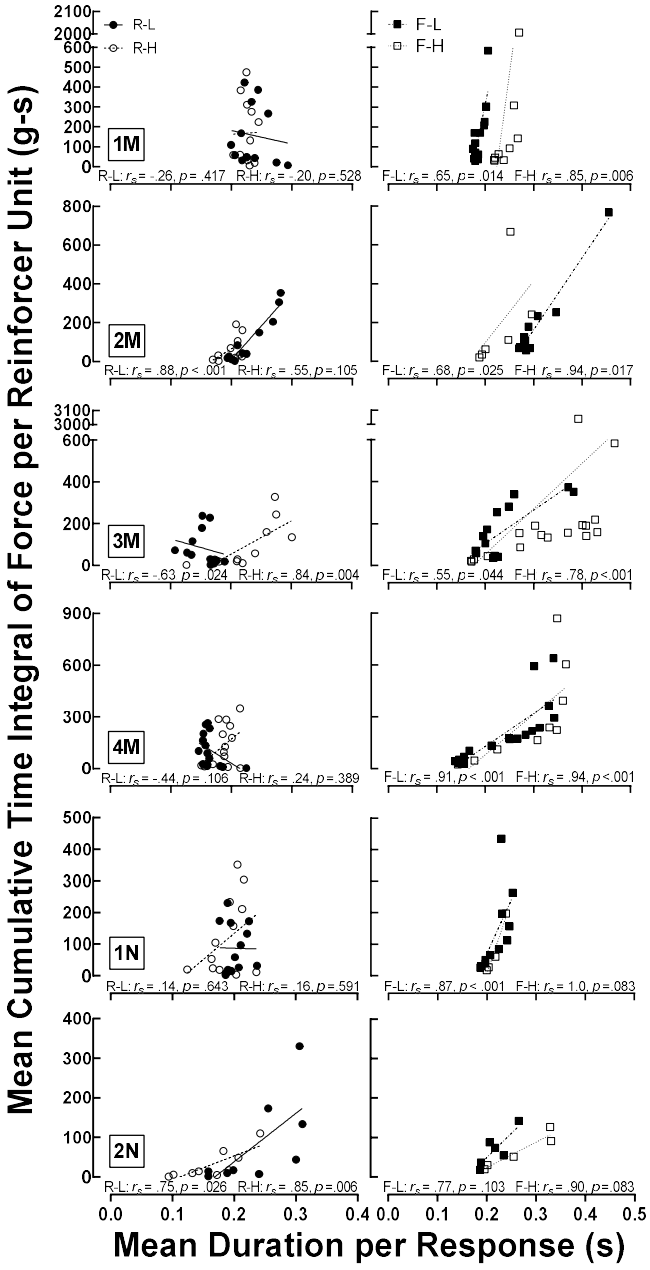

Figure 14. Correlations between mean duration per response and mean cumulative time integral per reinforcer unit. Mean duration per response is shown along the x-axis, and cumulative time integral of force per reinforcer is along the y-axis. Closed circles and solid lines show R-L progressions, open circles and dashed lines show R-H progressions, closed squares and dot-dashed lines show F-L progressions, and open squares and dotted lines show F-H progressions.

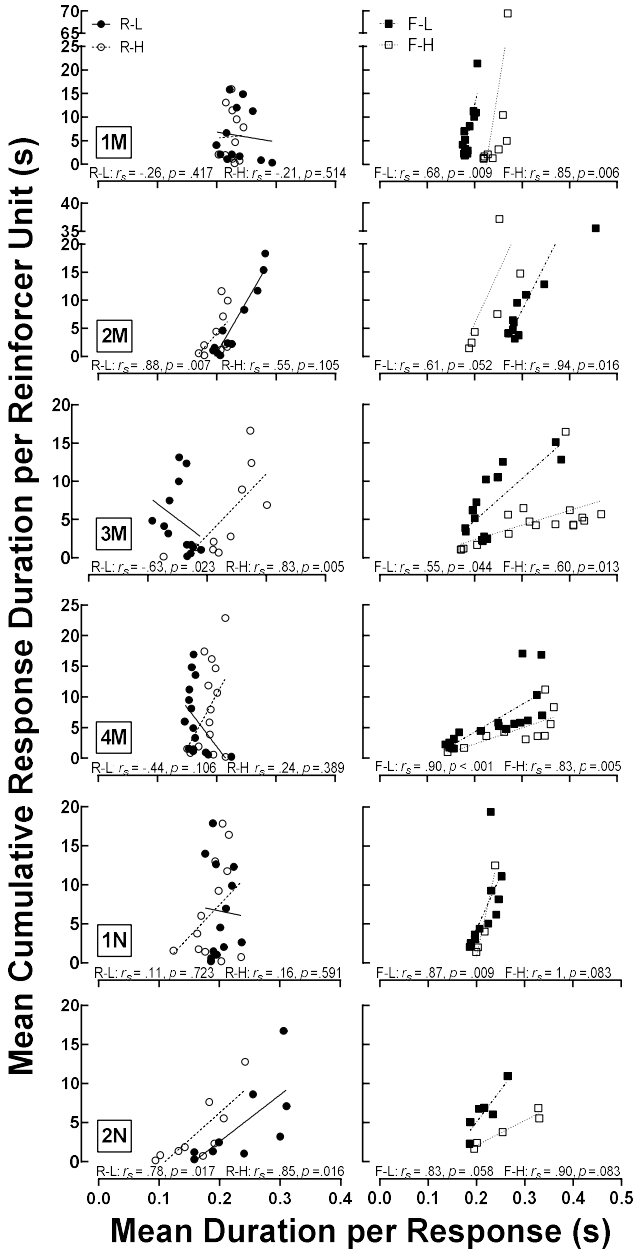

Figure 15. Correlations between mean duration per response and cumulative response duration per reinforcer unit. Mean duration per response is shown along the x-axis, and mean cumulative response duration per reinforcer unit is along the y-axis. Closed circles and solid lines show R-L progressions, open circles and dashed lines show R-H progressions, closed squares and dot-dashed lines show F-L progressions, and open squares and dotted lines show F-H progressions.

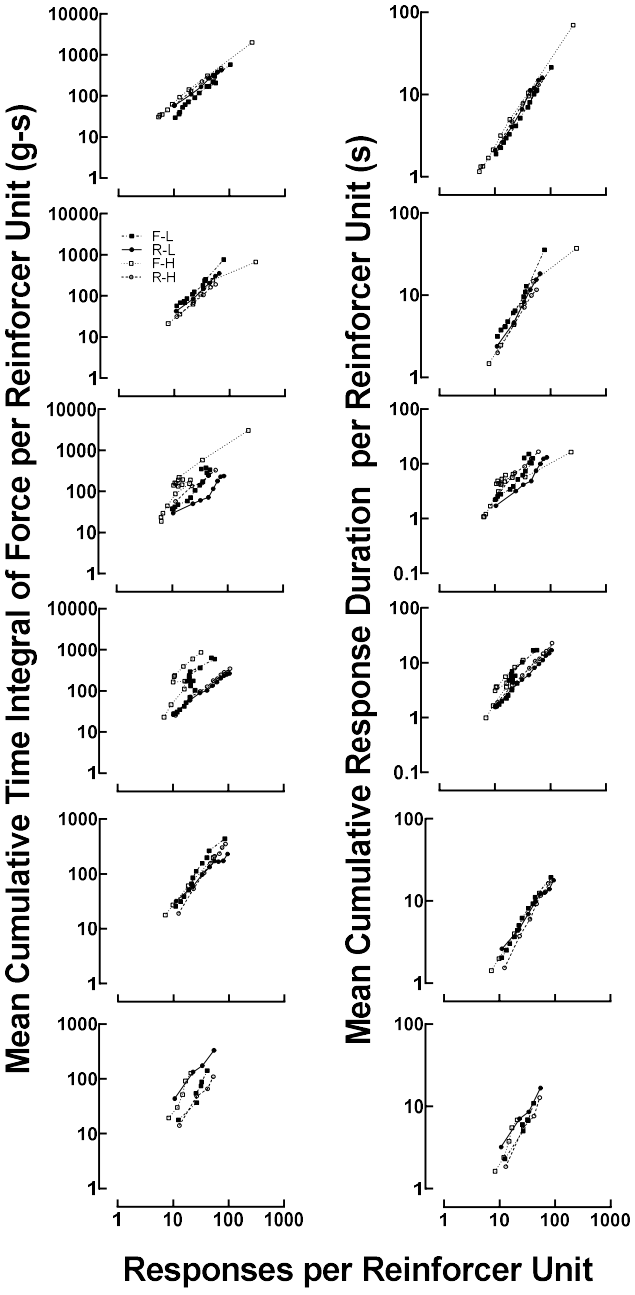

Figure 16. Mean cumulative time integral of force per reinforcer unit and mean cumulative response duration per reinforcer unit. Closed circles and solid lines show R-L progressions, open circles and dashed lines show R-H progressions, closed squares and dot-dashed lines show F-L progressions, and open squares and dotted lines show F-H progressions.

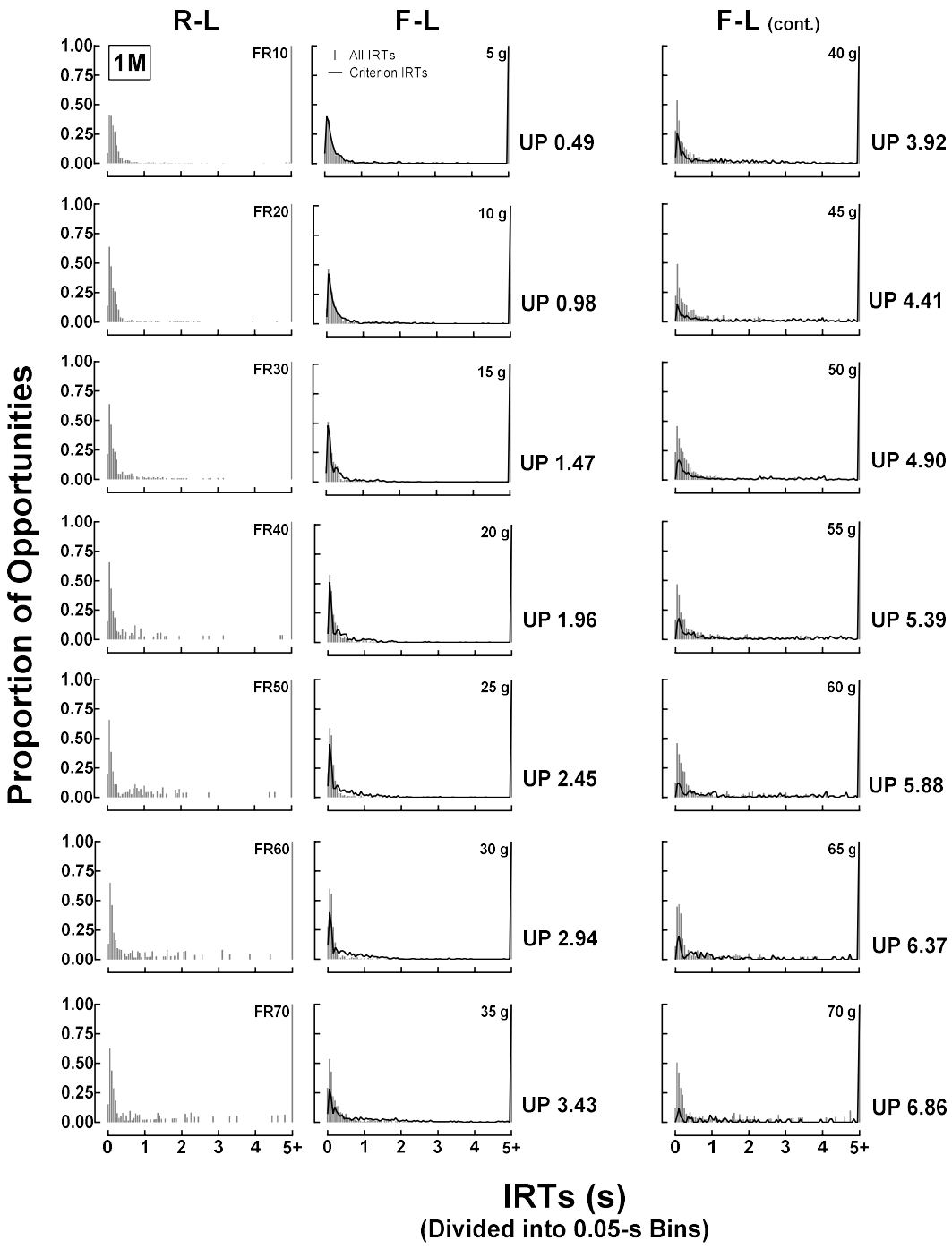

Figure 17. IRT distributions from the F-L and R-L progressions for 1M. Shown are the proportion of IRT opportunities (left y-axis) across 0.05-s bins (x-axis) for the R-L (left column) and F-L (center and right columns) progressions at each unit price (rows). Thin gray bars show all IRTs and the black data path shows criterion IRTs.

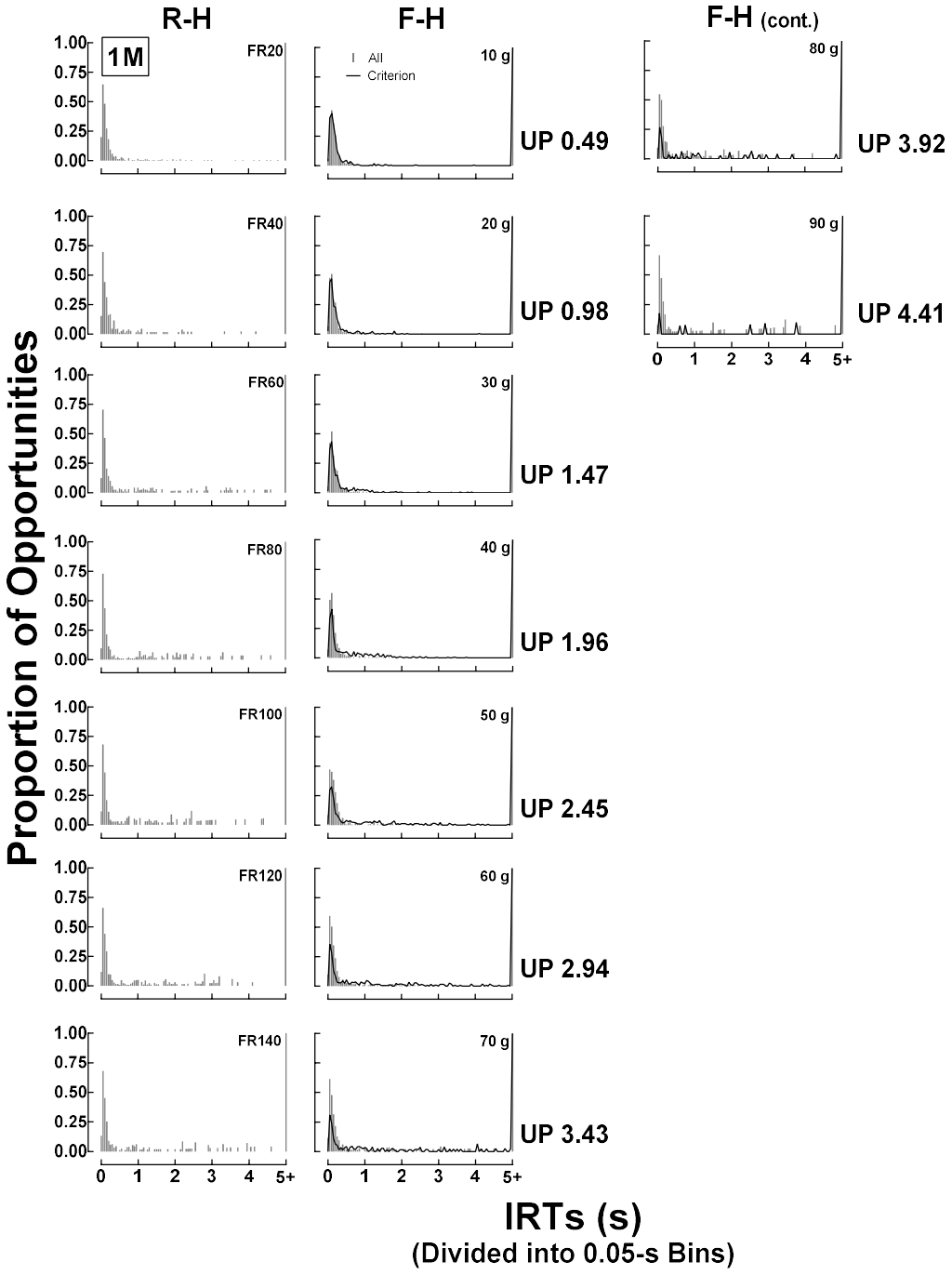

Figure 18. IRT distributions from the F-H and R-H progressions for 1M. Shown are the proportion of IRT opportunities (left y-axis) across 0.05-s bins (x-axis) for the R-H (left column) and F-H (center and right columns) progressions at each unit price (rows). Thin gray bars show all IRTs and the black data path shows criterion IRTs.

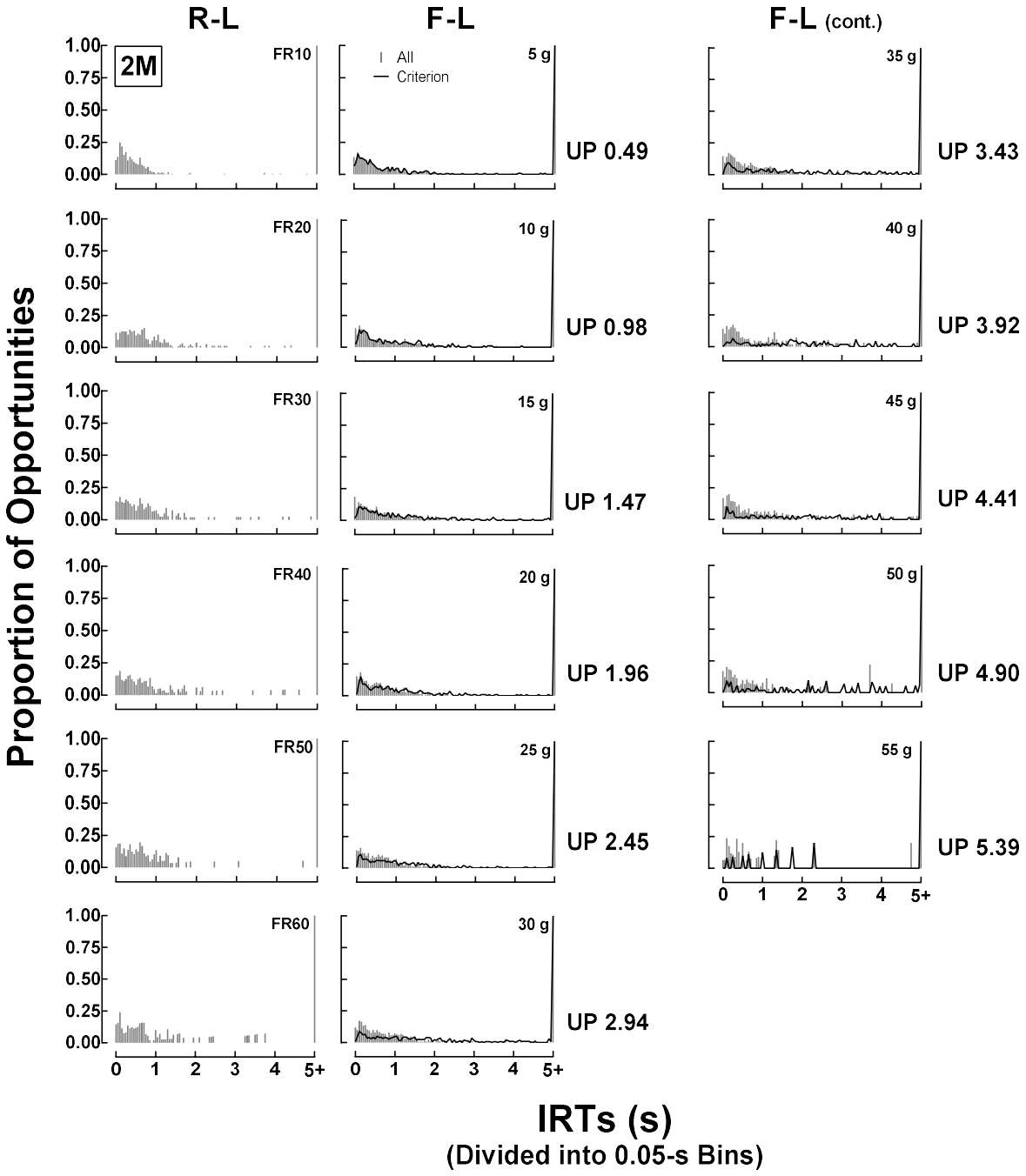

Figure 19. IRT distributions from the F-L and R-L progressions for 2M.Shown are the proportion of IRT opportunities (left y-axis) across 0.05-s bins (x-axis) for the R-L (left column) and F-L (center and right columns) progressions at each unit price (rows). Thin gray bars show all IRTs and the black data path shows criterion IRTs.

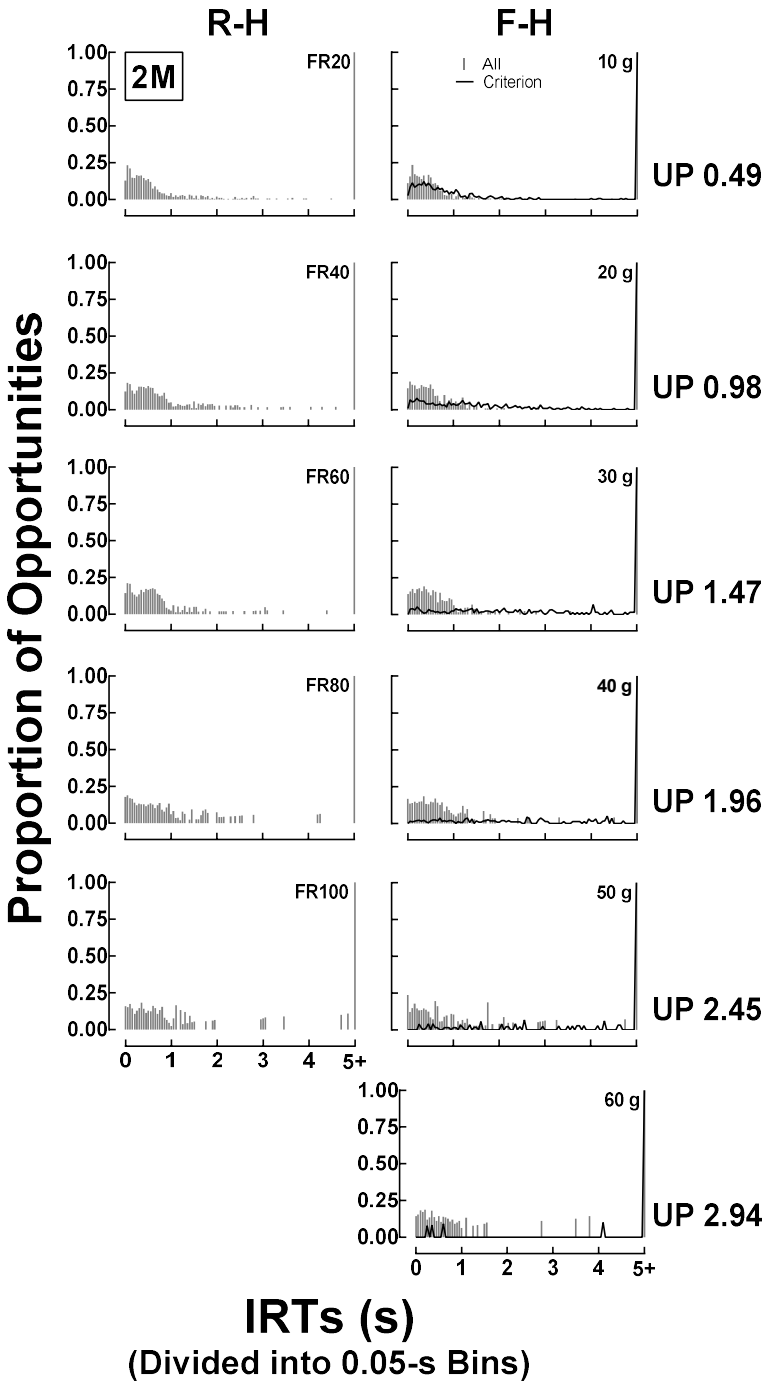

Figure 20. IRT distributions from the F-H and R-H progressions for 2M. Shown are the proportion of IRT opportunities (left y-axis) across 0.05-s bins (x-axis) for the R-H (left column) and F-H (right columns) progressions at each unit price (rows). Thin gray bars show all IRTs and the black data path shows criterion IRTs.

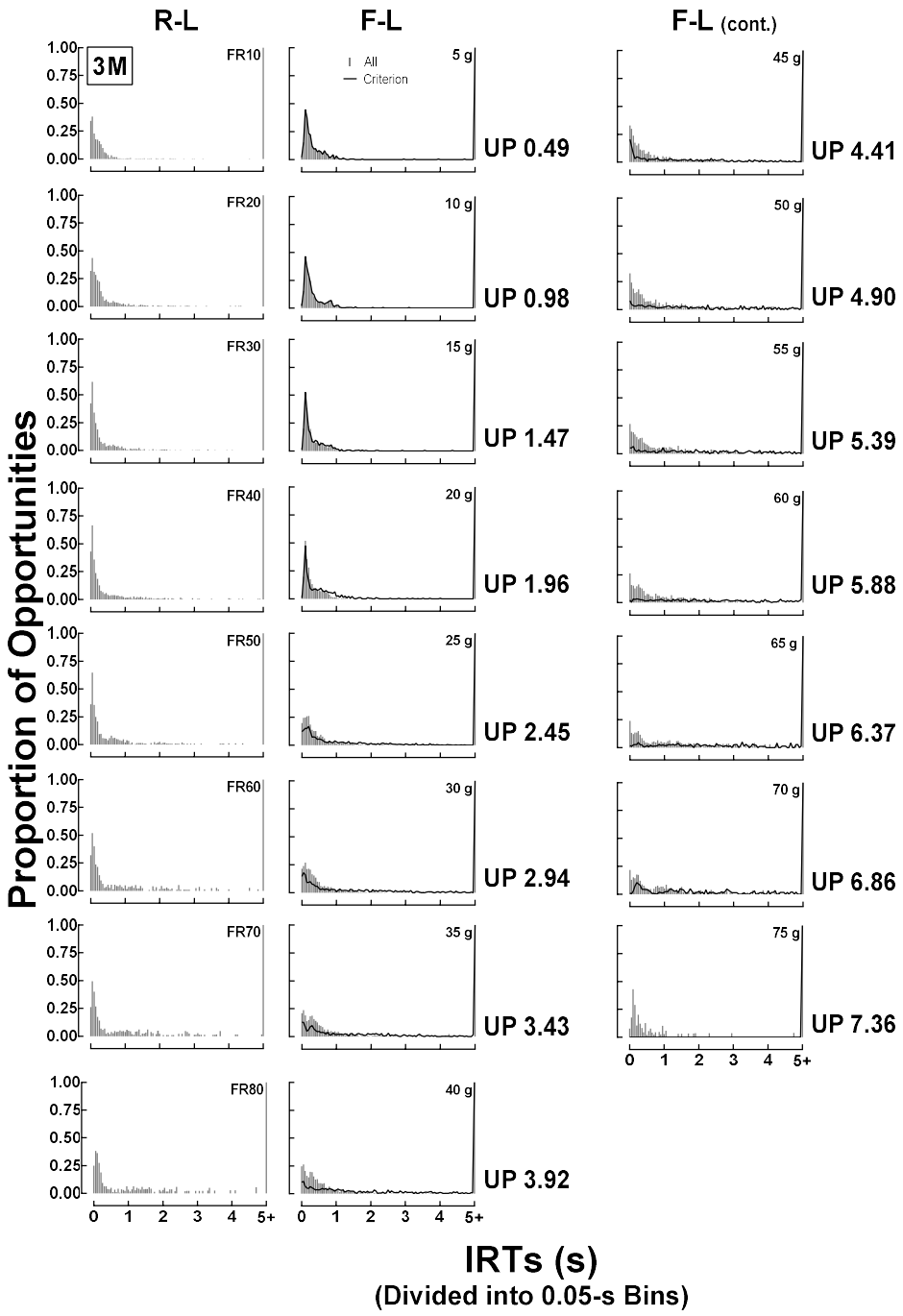

Figure 21. IRT distributions from the F-L and R-L progressions for 3M. Shown are the proportion of IRT opportunities (left y-axis) across 0.05-s bins (x-axis) for the R-L (left column) and F-L (center and right columns) progressions at each unit price (rows). Thin gray bars show all IRTs and the black data path shows criterion IRTs.

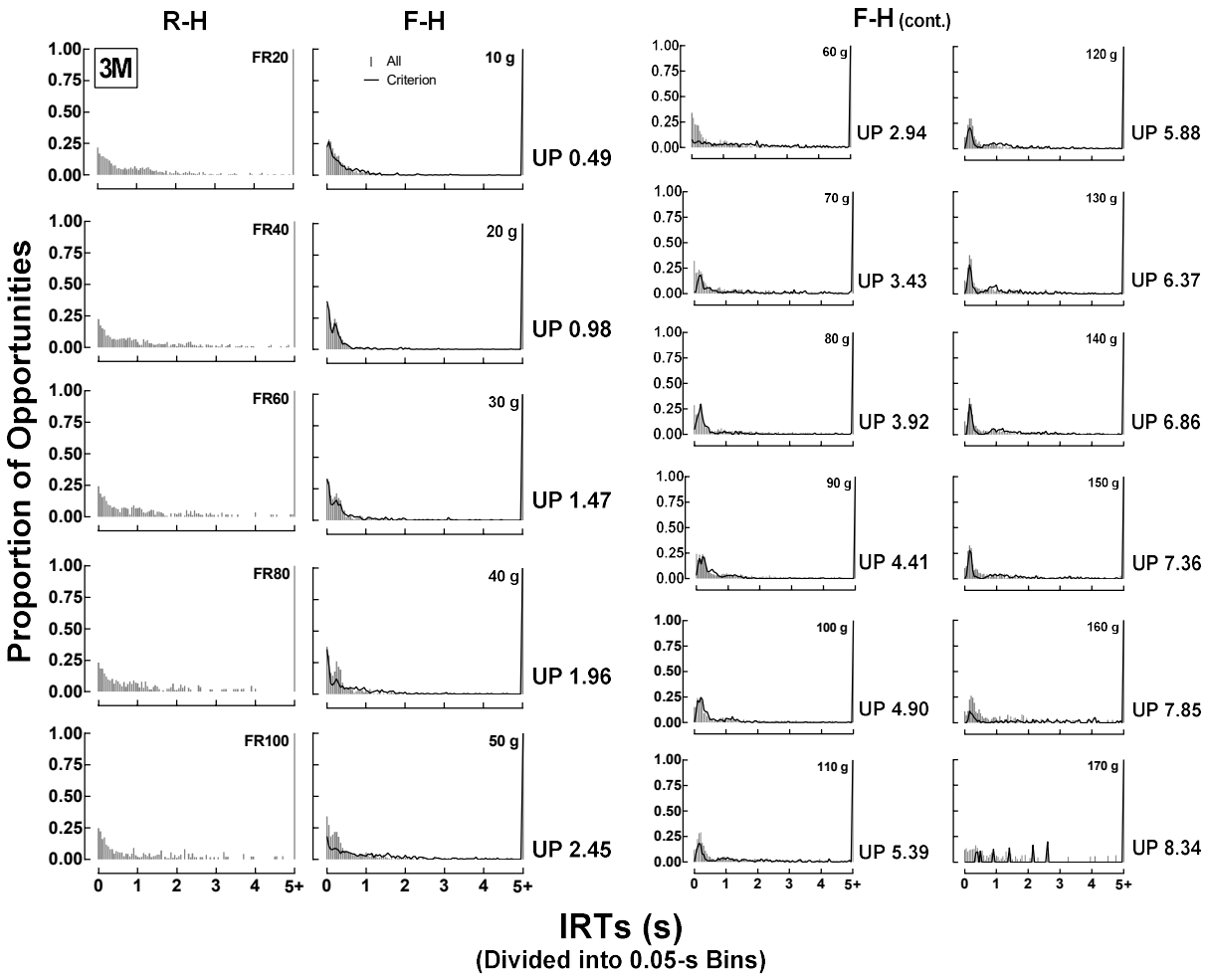

Figure 22. IRT distributions from the F-H and R-H progressions for 3M. Shown are the proportion of IRT opportunities (left y-axis) across 0.05-s bins (x-axis) for the R-H (left column) and F-H (center and right columns) progressions at each unit price (rows). Thin gray bars show all IRTs and the black data path shows criterion IRTs.

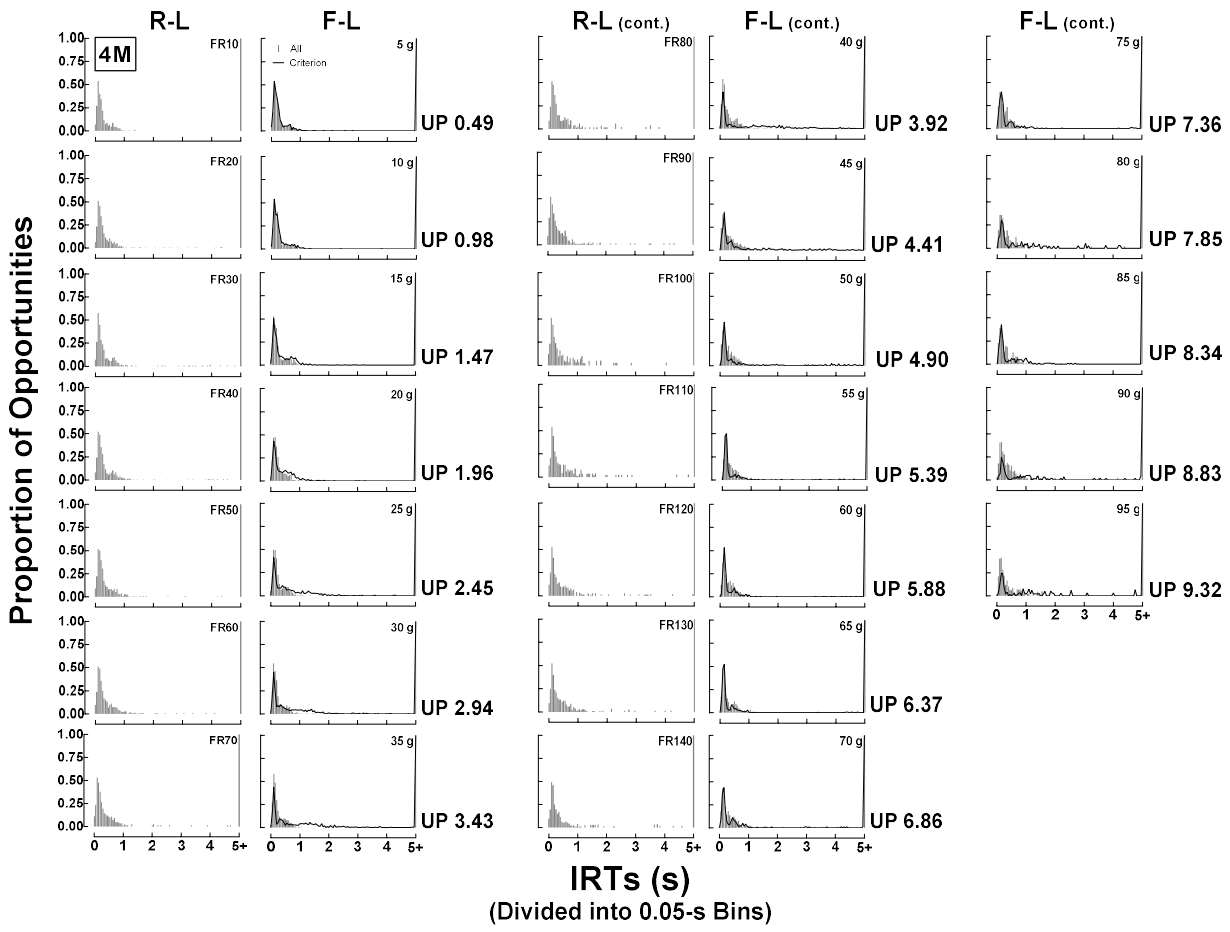

Figure 23. IRT distributions from the F-L and R-L progressions for 4M. Shown are the proportion of IRT opportunities (left y-axis) across 0.05-s bins (x-axis) for the R-L (left columns in each pair) and F-L (right columns) progressions at each unit price (rows). Thin gray bars show all IRTs and the black data path shows criterion IRTs.

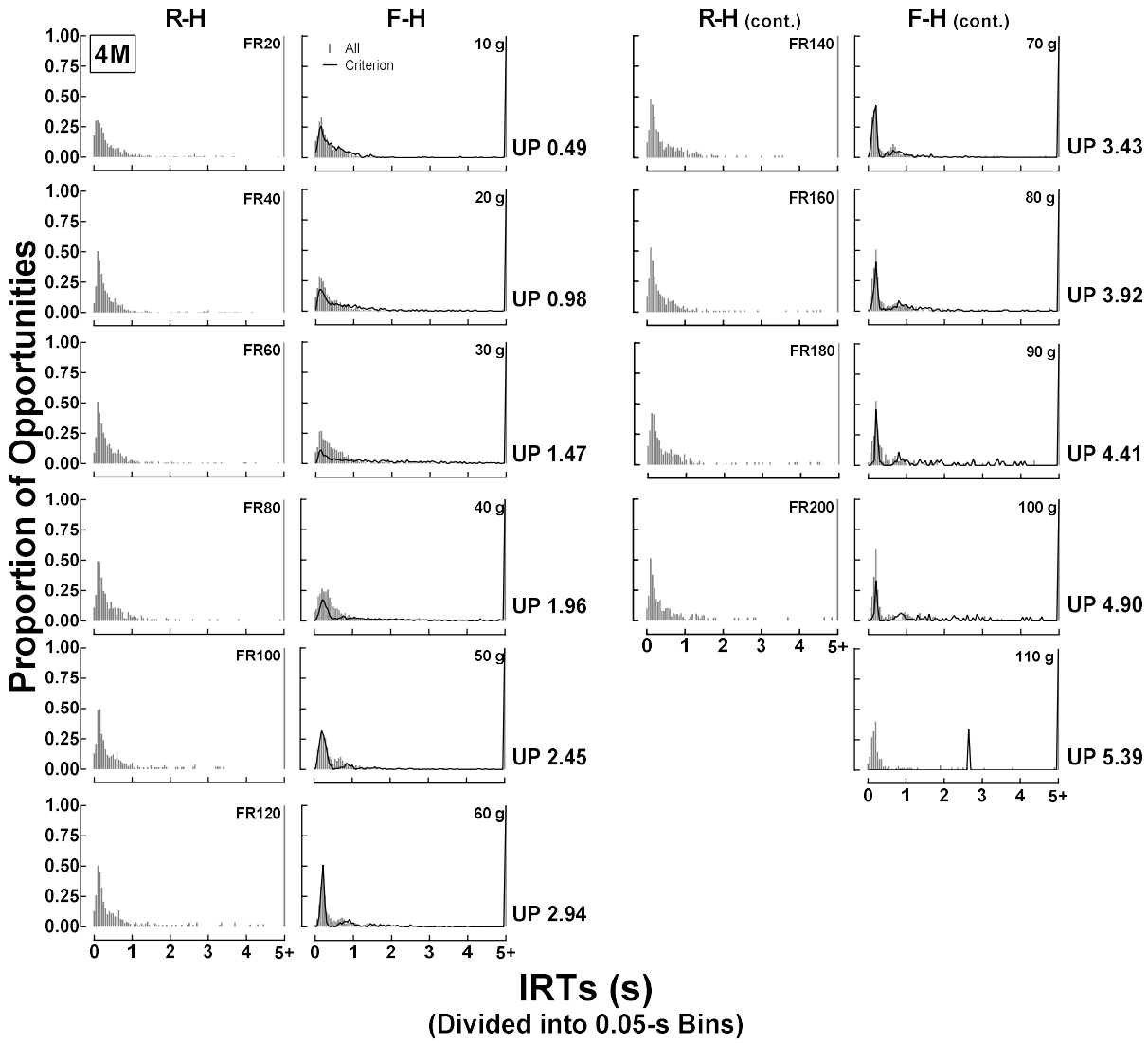

Figure 24. IRT distributions from the F-H and R-H progressions for 4M. Shown are the proportion of IRT opportunities (left y-axis) across 0.05-s bins (x-axis) for the R-H (left column in each pair) and F-H (right column in each pair) progressions at each unit price (rows). Thin gray bars show all IRTs and the black data path shows criterion IRTs.

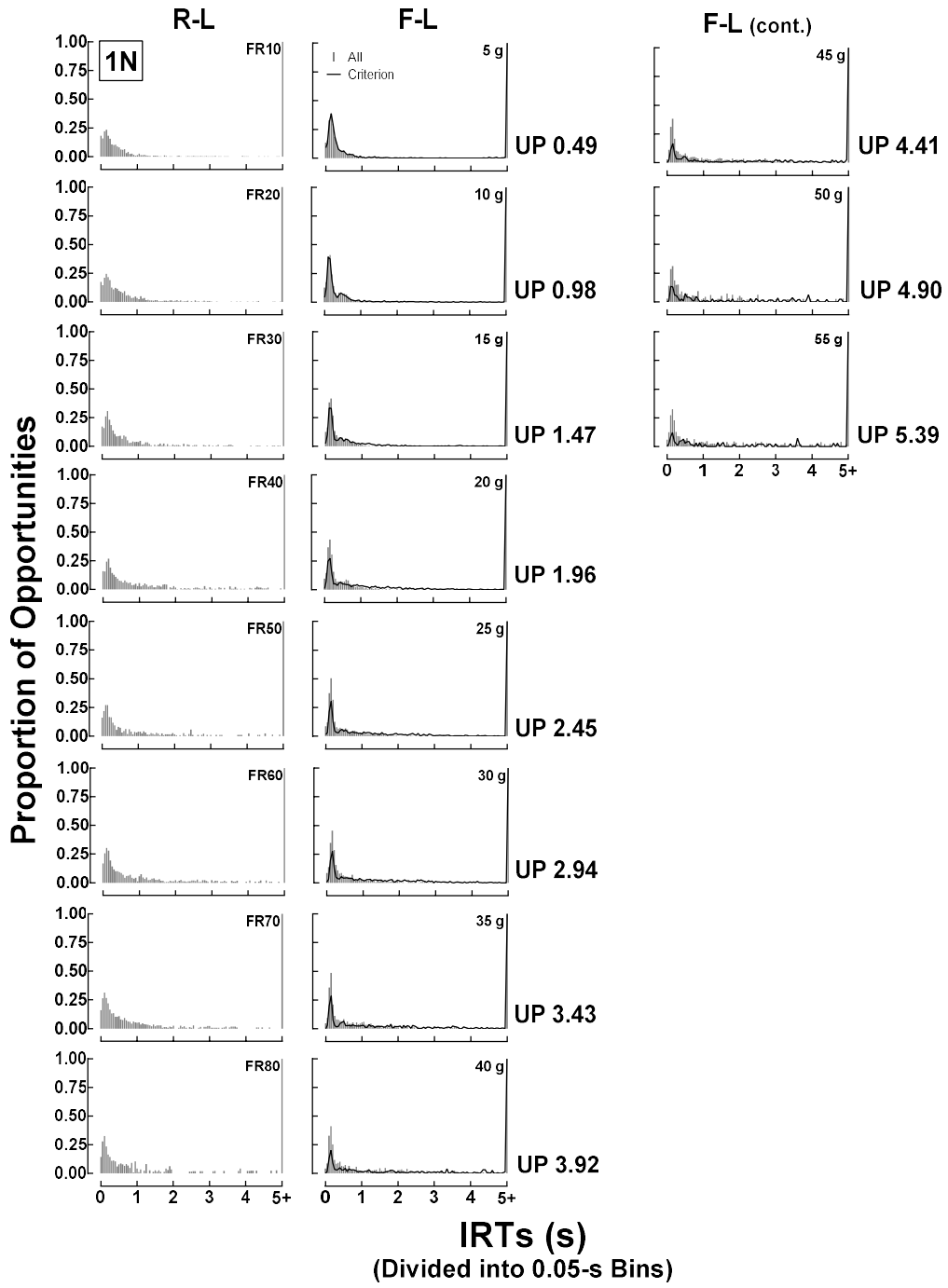

Figure 25. IRT distributions from the F-L and R-L progressions for 1N. Shown are the proportion of IRT opportunities (left y-axis) across 0.05-s bins (x-axis) for the R-L (left column) and F-L (center and right columns) progressions at each unit price (rows). Thin gray bars show all IRTs and the black data path shows criterion IRTs.

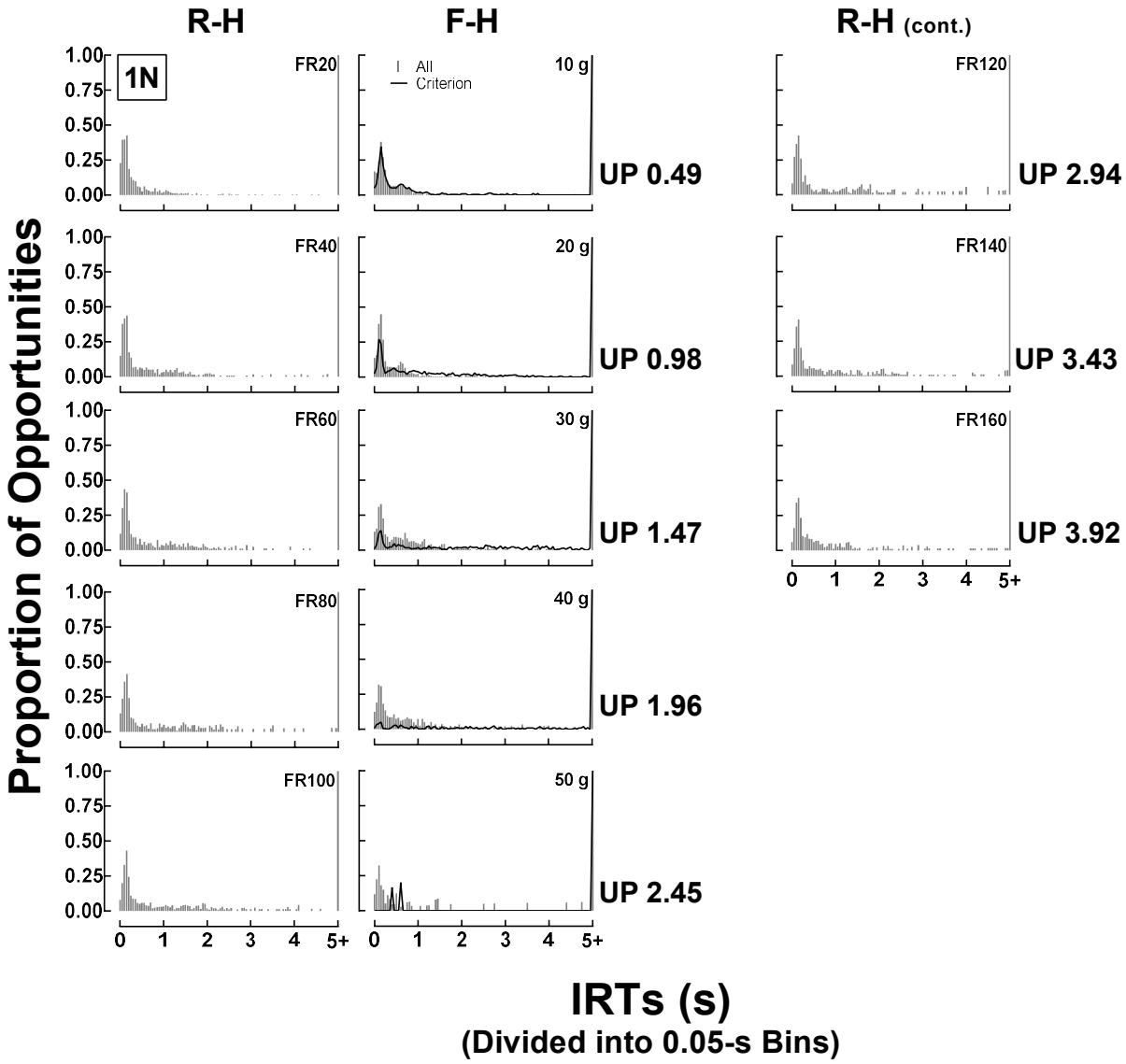

Figure 26. IRT distributions from the F-H and R-H progressions for 1N. Shown are the proportion of IRT opportunities (left y-axis) across 0.05-s bins (x-axis) for the R-H (left and right columns) and F-H (center column) progressions at each unit price (rows). Thin gray bars show all IRTs and the black data path shows criterion IRTs.

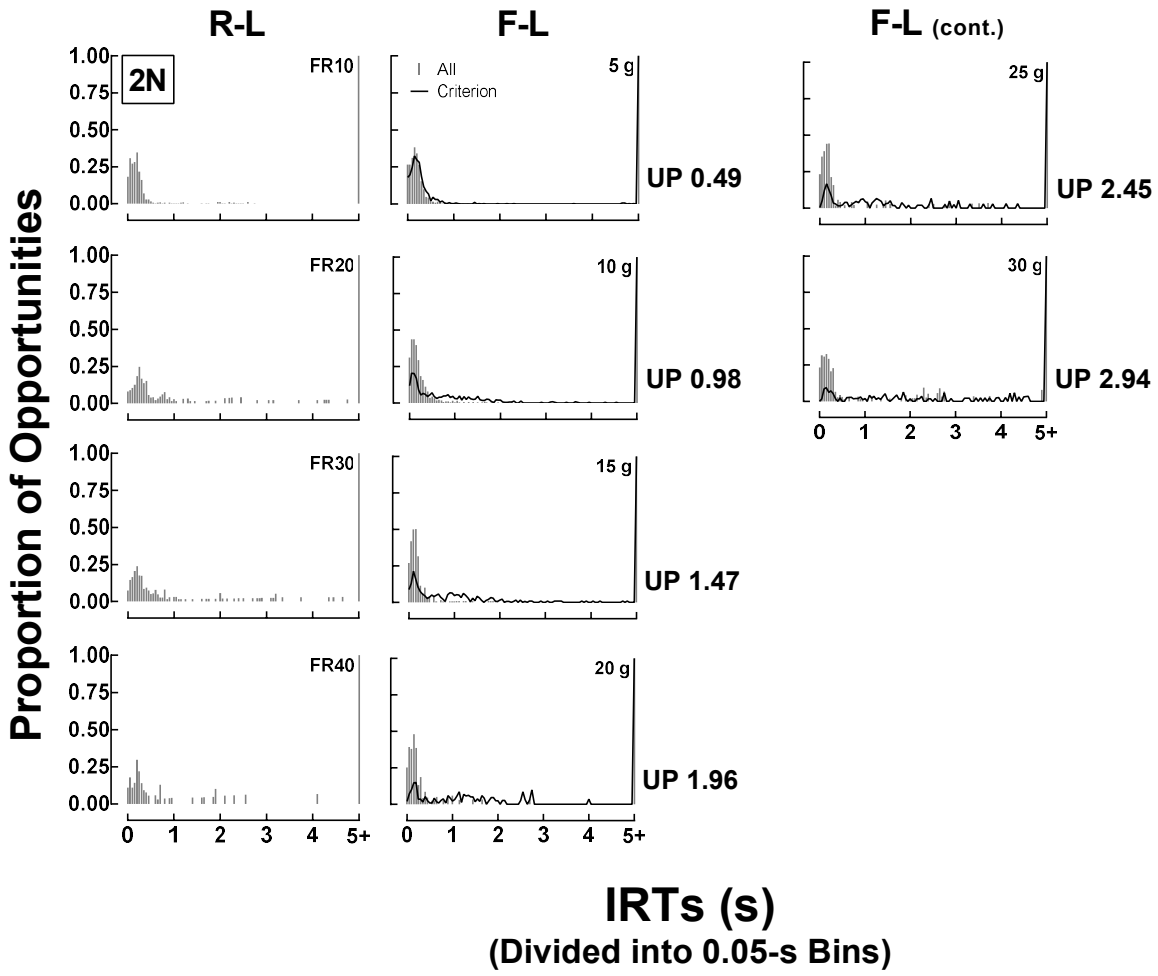

Figure 27. IRT distributions from the F-L and R-L progressions for 2N. Shown are the proportion of IRT opportunities (left y-axis) across 0.05-s bins (x-axis) for the R-L (left column) and F-L (center and right columns) progressions at each unit price (rows). Thin gray bars show all IRTs and the black data path shows criterion IRTs.

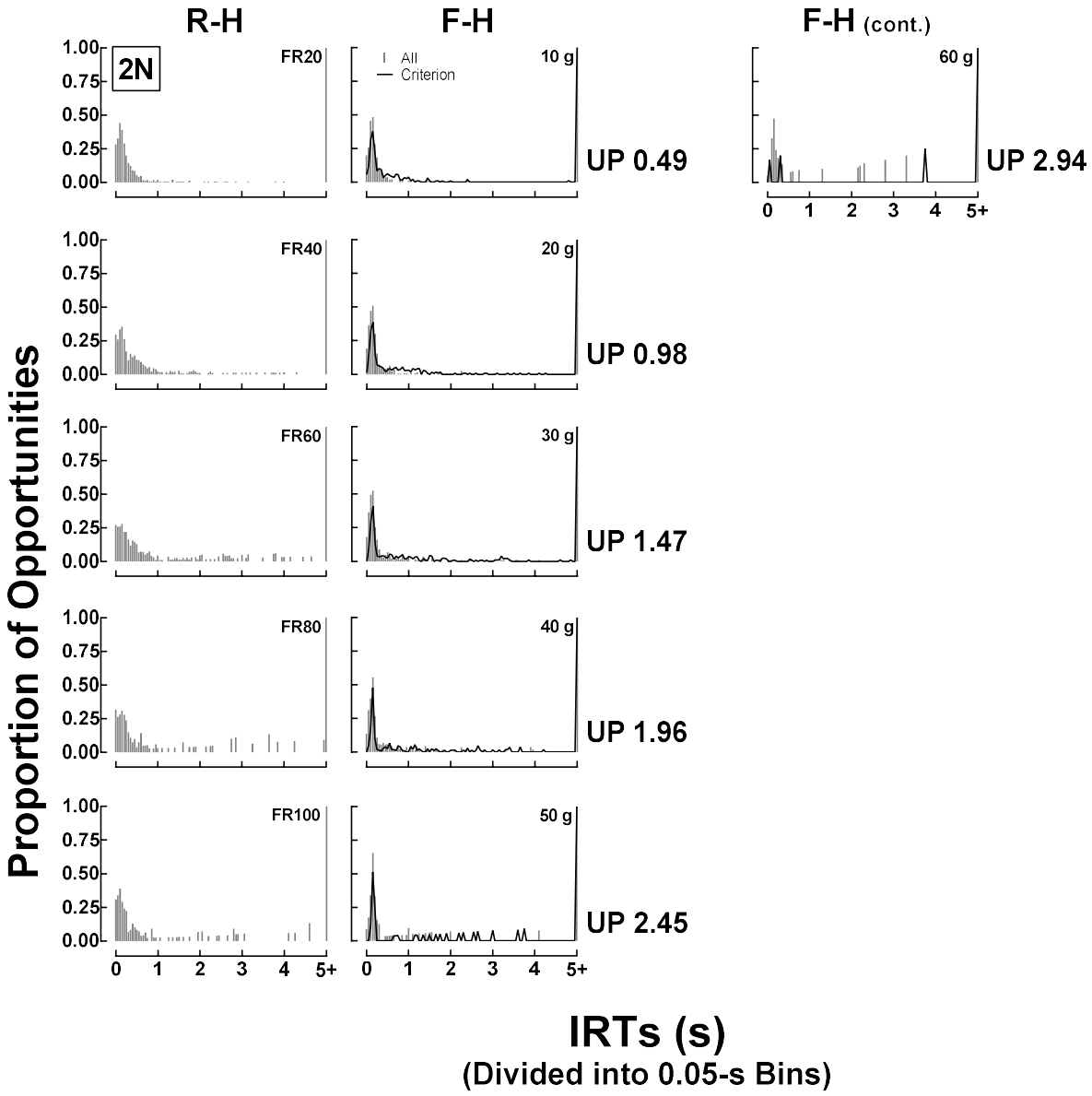

Figure 28. IRT distributions from the F-H and R-H progressions for 2N. Shown are the proportion of IRT opportunities (left y-axis) across 0.05-s bins (x-axis) for the R-H (left column) and F-H (center and right columns) progressions at each unit price (rows). Thin gray bars show all IRTs and the black data path shows criterion IRTs.

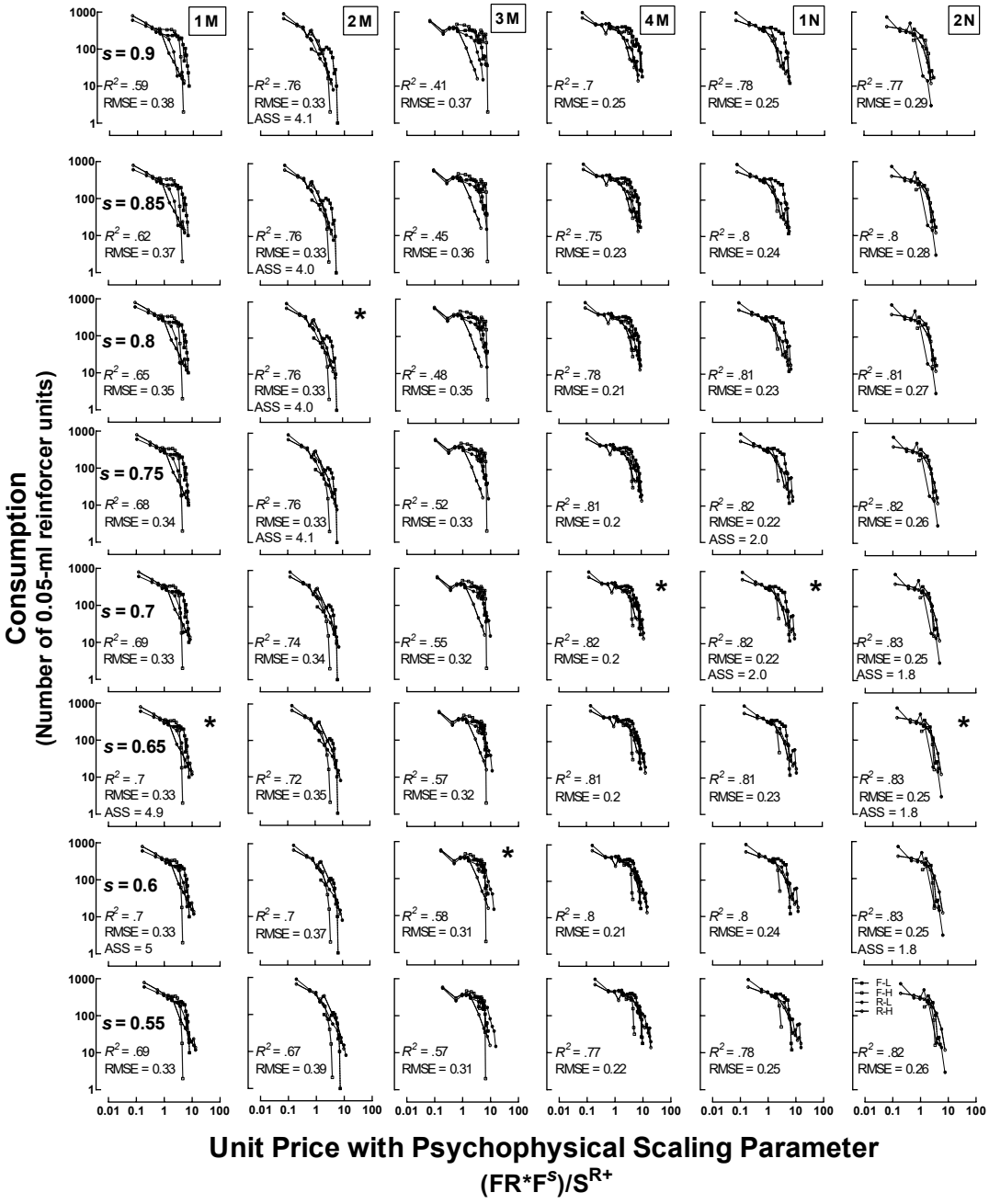

Figure 29. Consumption as a function of unit price across various psychophysical scaling parameters. Consumption is show along the y-axis for unit price with psychophysical scaling parameter transformations (x-axis) across different exponent values (*s* parameter, rows) for individual rats (columns). Asterisks show the exponent that produced the best convergence for each rat.

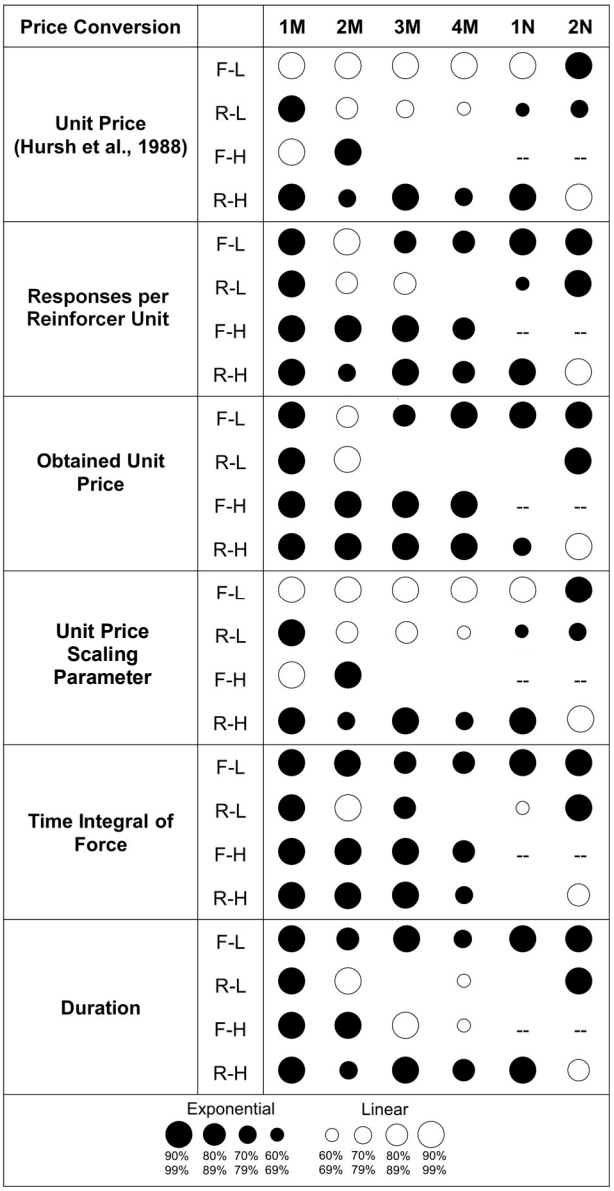

Figure 30. Model comparisons using AICc for different price modifications. Preferred model as determined by AICc comparisons is shown across rats (columns) for different price conversions and progression types (rows). Filled, black circles indicate the exponential model was preferred, and open, white circles show preference for the linear model. Circle size shows relative probability of the selected model. Comparisons that resulted in relative indifference (i.e., 50-59.9% likelihood for the more likely model) are shown by blanks, and dashed lines indicated conditions wherein too few data points were available to compare models.

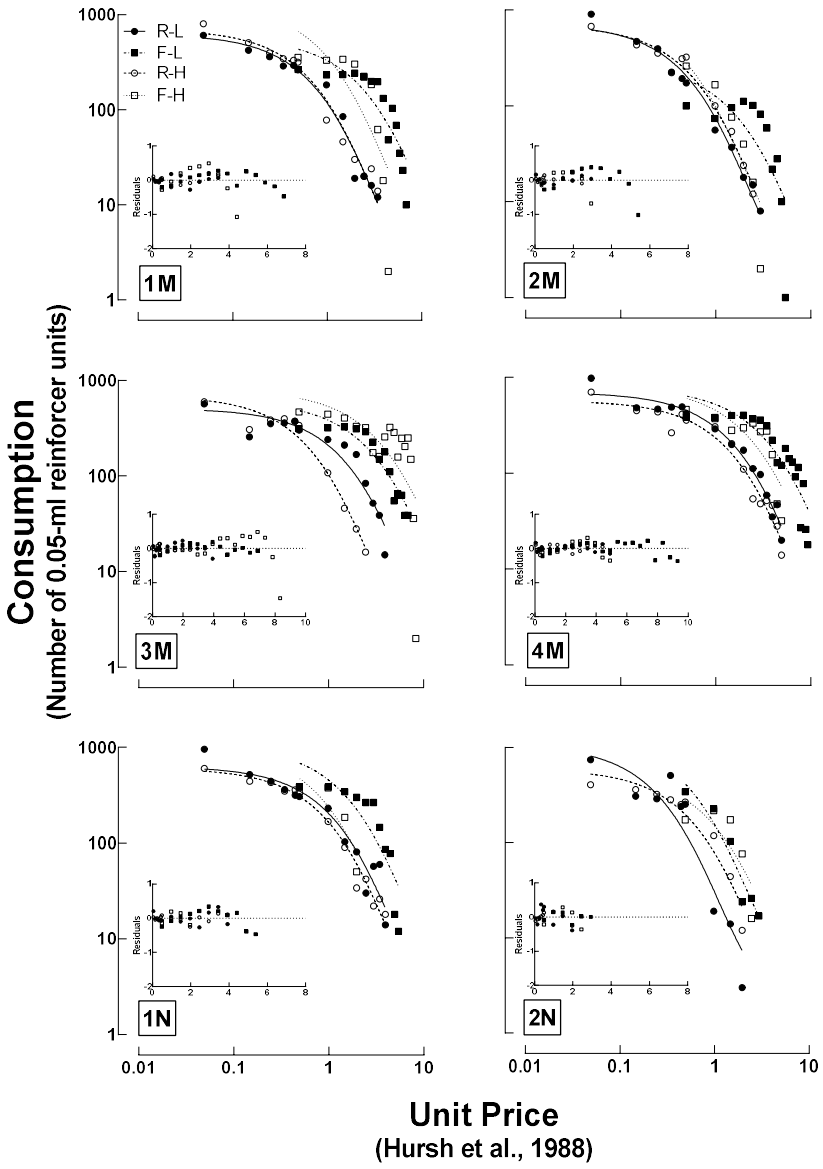

Figure 31. Exponential demand curves fit to consumption as a function of unit price across all assessed prices, excluding prices with 0 consumption. In these fits, Q_0 and α are unconstrained and a mean k value is determined for each animal by averaging range of consumption across all progressions. Closed circles and solid lines show R-L progressions, open circles and dashed lines show R-H progressions, closed squares and dot-dashed lines show F-L progressions, and open squares and dotted lines show F-H progressions. Inset panels show residuals.

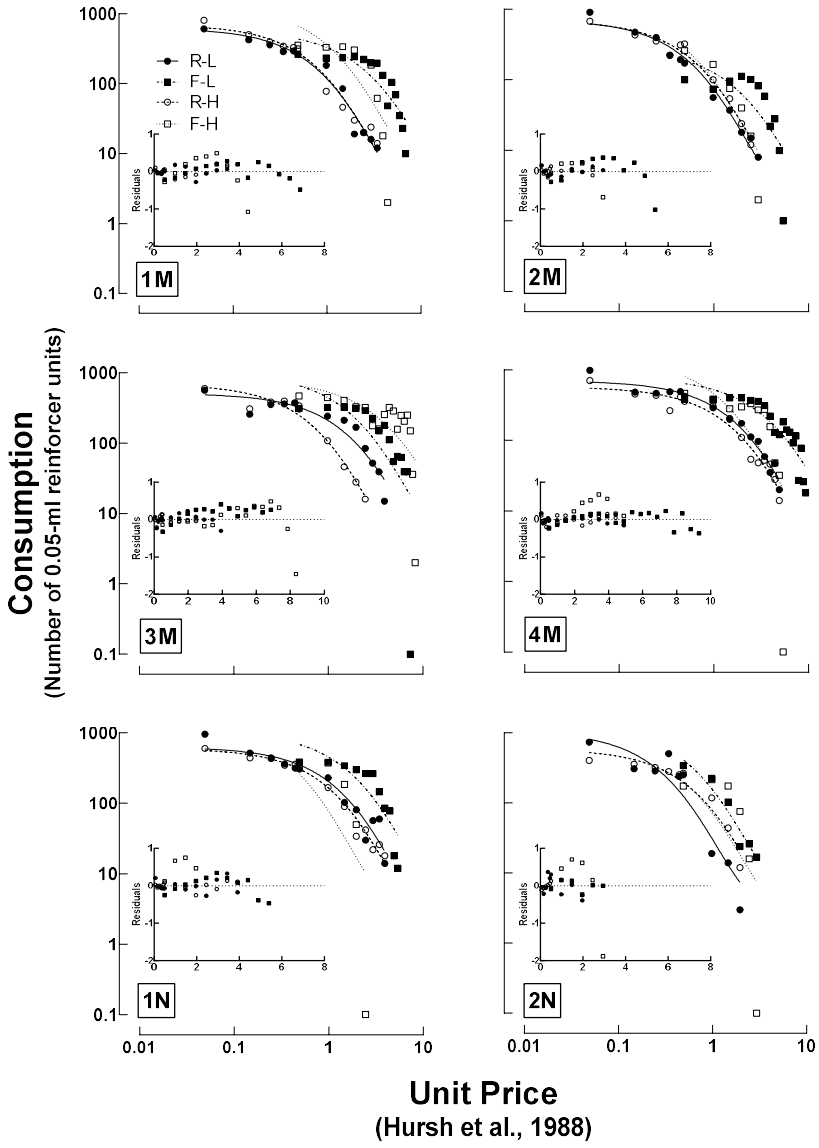

Figure 32. Exponential demand curves fit to consumption as a function of unit price across all assessed prices, including prices with 0 consumption (as 0.1). In these fits, Q_0 and α are unconstrained and a mean k value is determined for each animal by averaging range of consumption across all progressions. Closed circles and solid lines show R-L progressions, open circles and dashed lines show R-H progressions, closed squares and dot-dashed lines show F-L progressions, and open squares and dotted lines show F-H progressions. Inset panels show residuals.

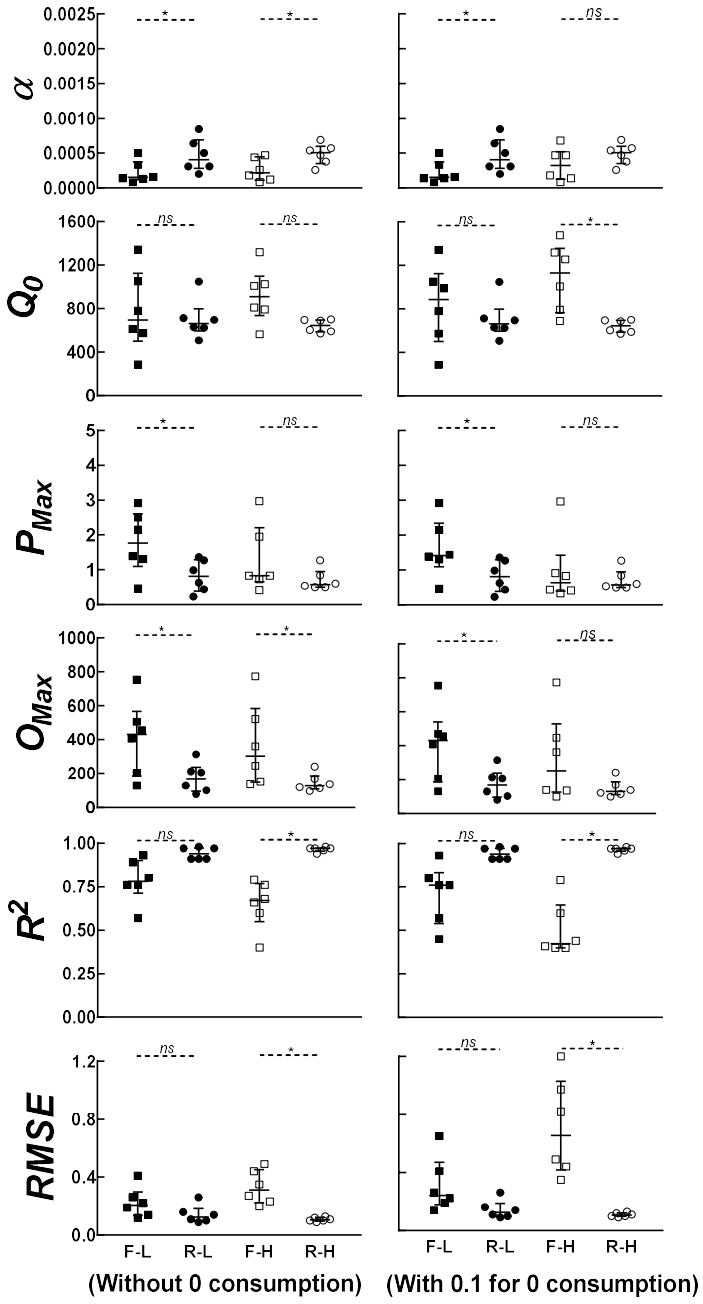

Figure 33. Parameters and goodness-of-fit measures obtained from exponential demand curves fit to consumption as a function of the Hursh et al. (1988) unit price equation. Closed circles show R-L progressions, open circles show R-H progressions, closed squares show F-L progressions, and open squares show F-H progressions. Lines and error bars show medians and IQRs.

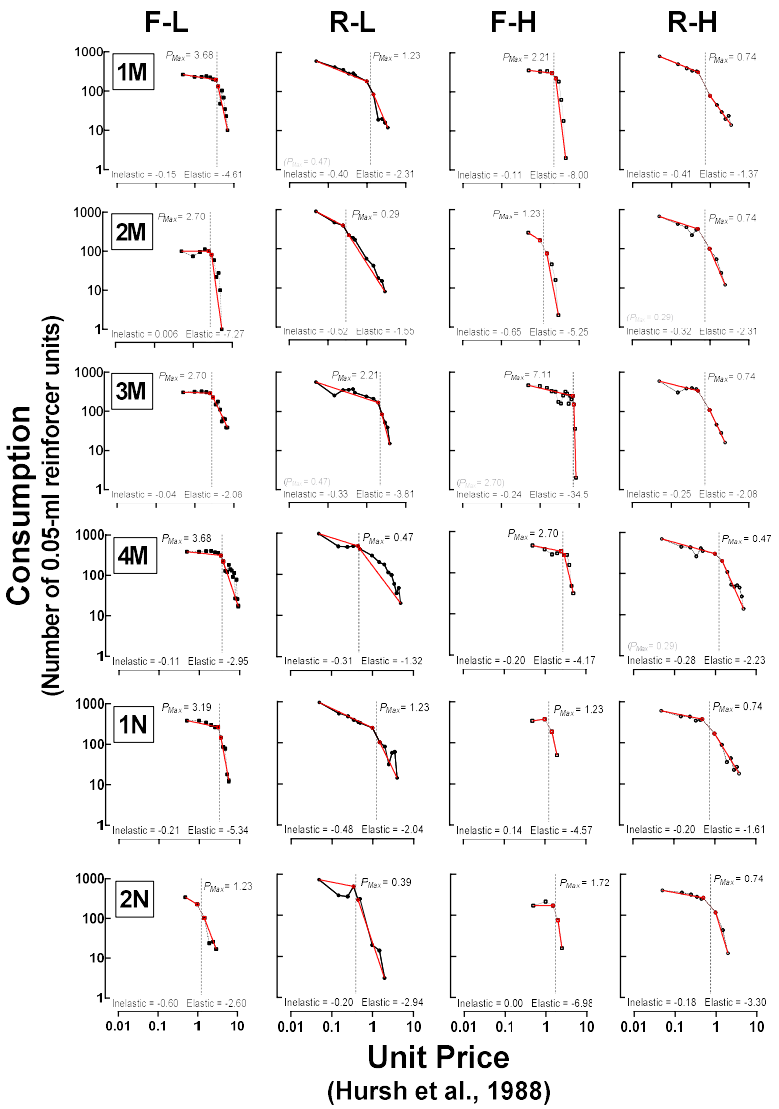

Figure 34. Local elasticity analysis for consumption as a function of unit price, sessions with 0 consumption excluded. Consumption (y-axis) is plotted as a function of unit price (x-axis) across different progressions (columns) for individual animals (rows). Solid red log-log lines show slopes of the sections identified as inelastic and elastic for each animal. The point of P_{Max} (averaged price of data successive data points with slope less than negative one) is shown by the vertical dashed line. If visual analysis identified an inconsistency that resulted in a change to P_{Max}, the first price at which the slope was less than negative one is shown in gray in the lower left corner.

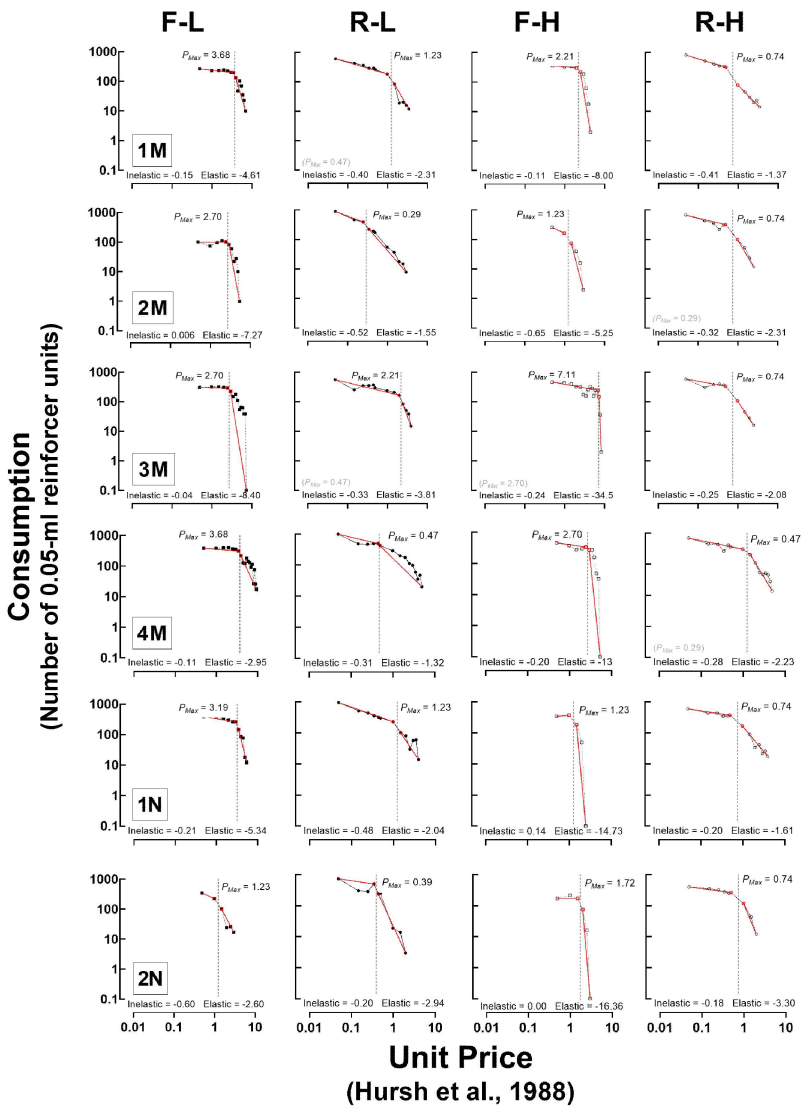

Figure 35. Local elasticity analysis for consumption as a function of unit price, sessions with 0 consumption included (as 0.1). Consumption (y-axis) is plotted as a function of unit price (x-axis) across different progressions (columns) for individual animals (rows). Solid red log-log lines show slopes of the sections identified as inelastic and elastic for each animal. The point of P_{Max} (averaged price of data successive data points with slope less than negative one) is shown by the vertical dashed line. If visual analysis identified an inconsistency that resulted in a change to P_{Max}, the first price at which the slope was less than negative one is shown in gray in the lower left corner.

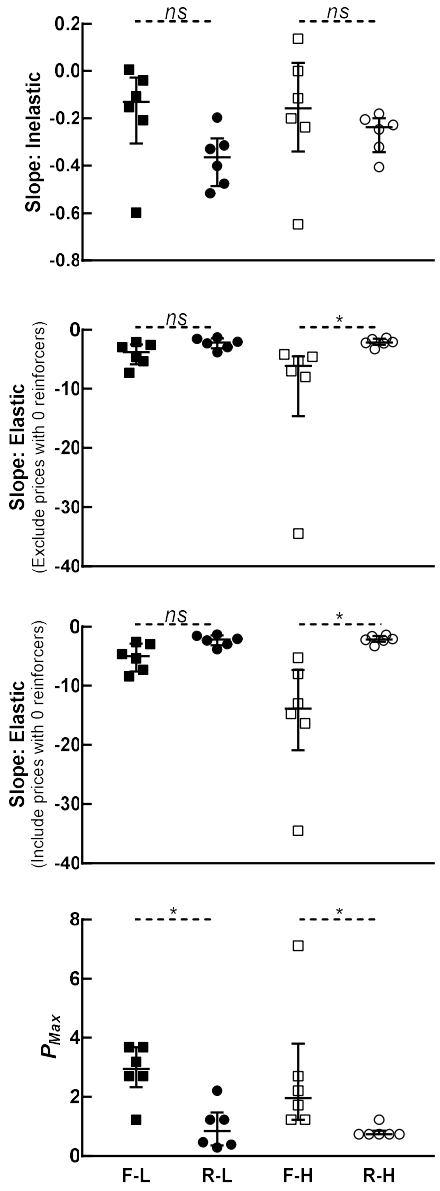

Figure 36. Slopes and P_{Max} as determined by local elasticity analyses. Shown are the points of P_{Max} (bottom panel), as well as slopes from log-log lines fit to the inelastic portion of each progression (top panel) and the elastic portion of each progression (middle panels show slopes when prices with 0 consumption were and were not included). Closed circles show R-L progressions, open circles show R-H progressions, closed squares show F-L progressions, and open squares show F-H progressions. Lines and error bars show medians and IQRs.

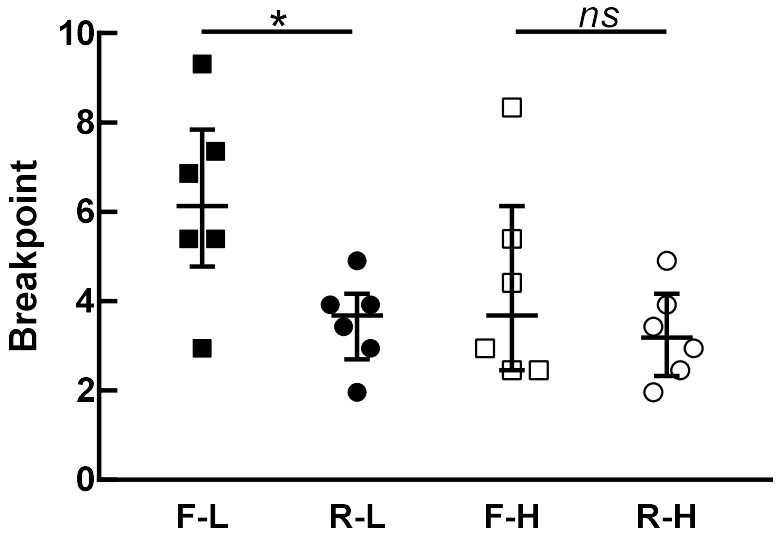

Figure 37. Breakpoint comparisons based on unit price. Shows breakpoints with medians and IQRs across progression types (x-axis); significant differences are shown by an asterisk.

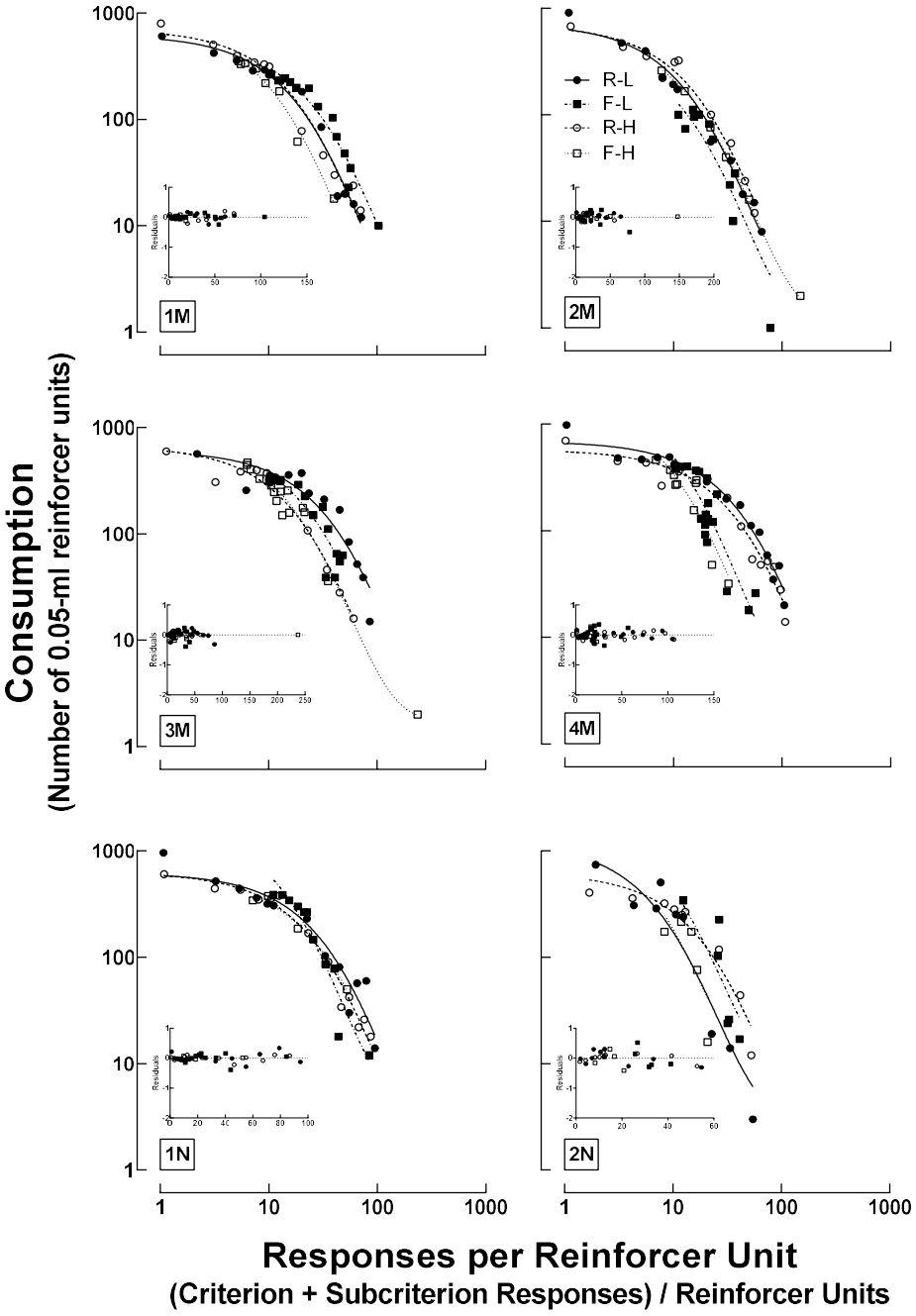

Figure 38. Exponential demand curves fit to consumption as a function of responses per reinforcer unit. Closed circles and solid lines show R-L progressions, open circles and dashed lines show R-H progressions, closed squares and dot-dashed lines show F-L progressions, and open squares and dotted lines show F-H progressions. Inset panels show residuals.

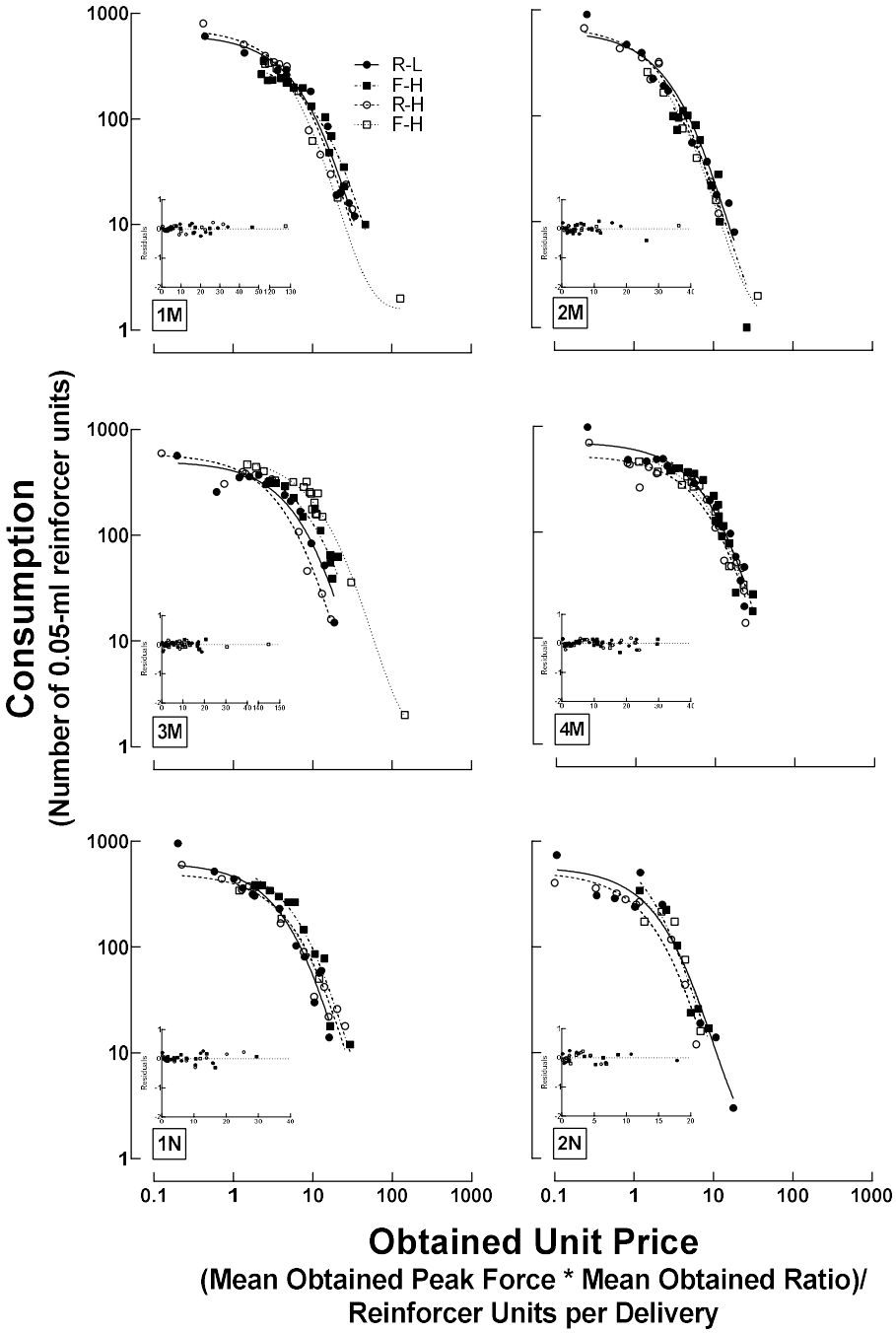

Figure 39. Exponential demand curves fit to consumption as a function of obtained unit price. Closed circles and solid lines show R-L progressions, open circles and dashed lines show R-H progressions, closed squares and dot-dashed lines show F-L progressions, and open squares and dotted lines show F-H progressions. Inset panels show residuals.

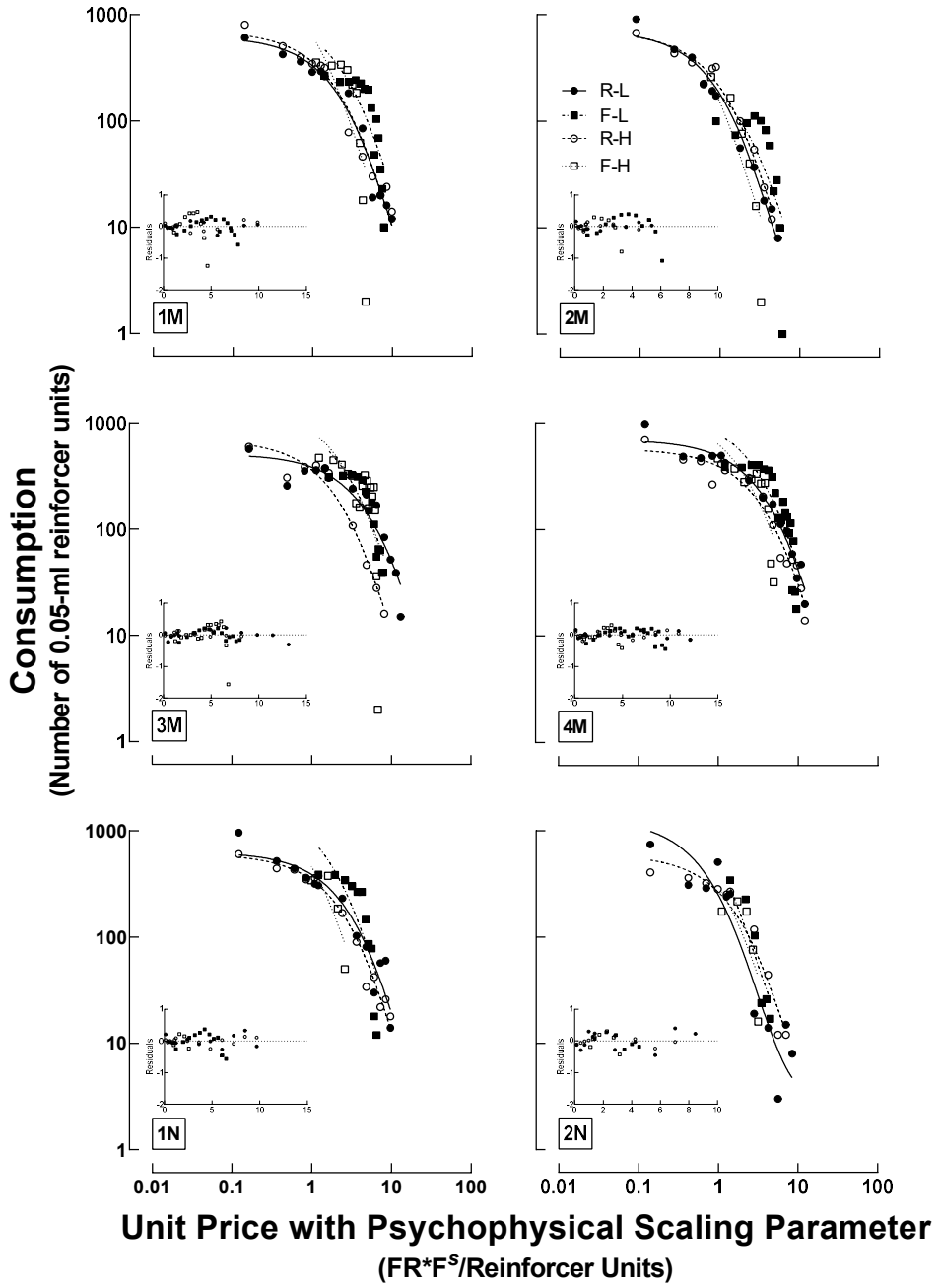

Figure 40. Exponential demand curves fit to consumption as a function of unit price adjusted with psychophysical scaling parameters. Closed circles and solid lines show R-L progressions, open circles and dashed lines show R-H progressions, closed squares and dot-dashed lines show F-L progressions, and open squares and dotted lines show F-H progressions. Inset panels show residuals.

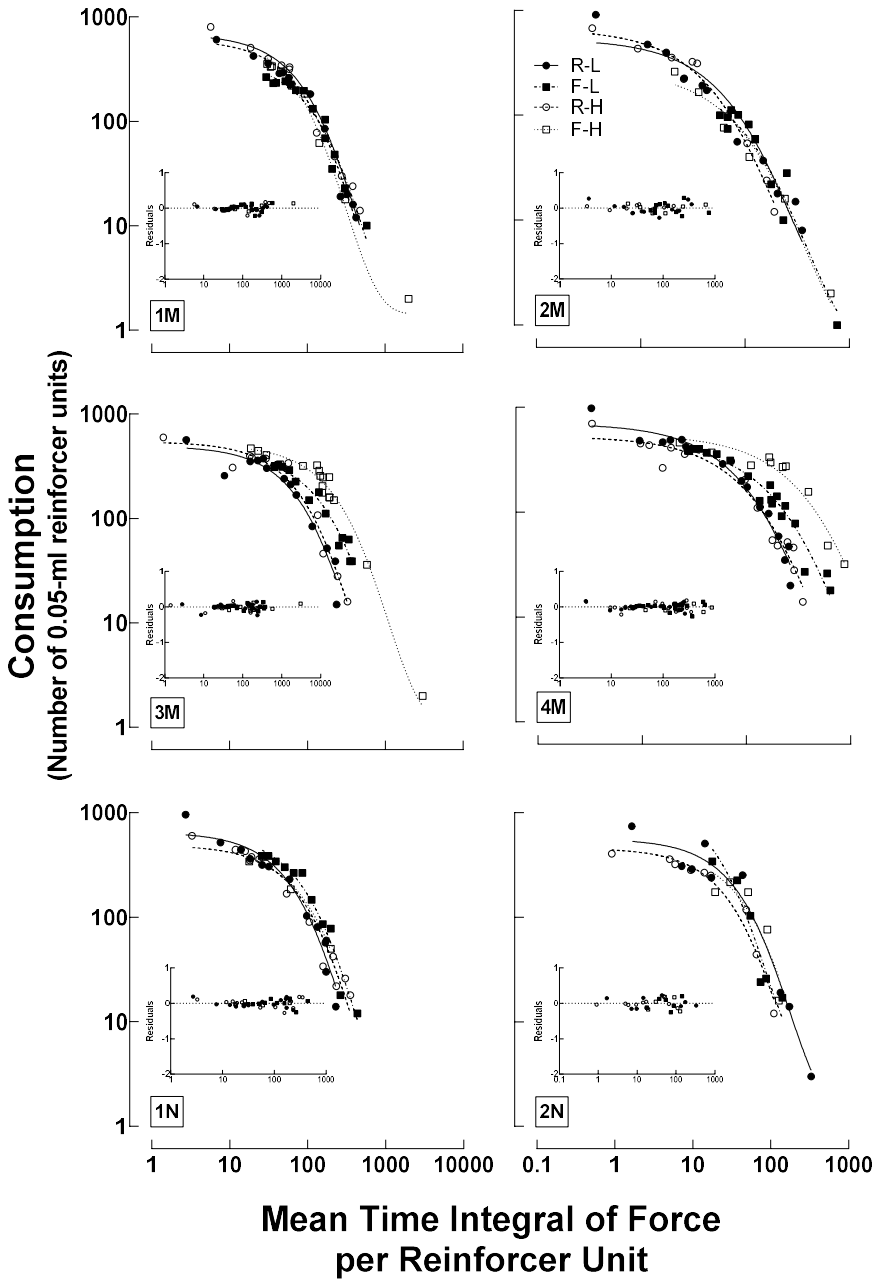

Figure 41. Exponential demand curves fit to consumption as a function of obtained time integral of force per reinforcer unit. Closed circles and solid lines show R-L progressions, open circles and dashed lines show R-H progressions, closed squares and dot-dashed lines show F-L progressions, and open squares and dotted lines show F-H progressions. Inset panels show residuals.

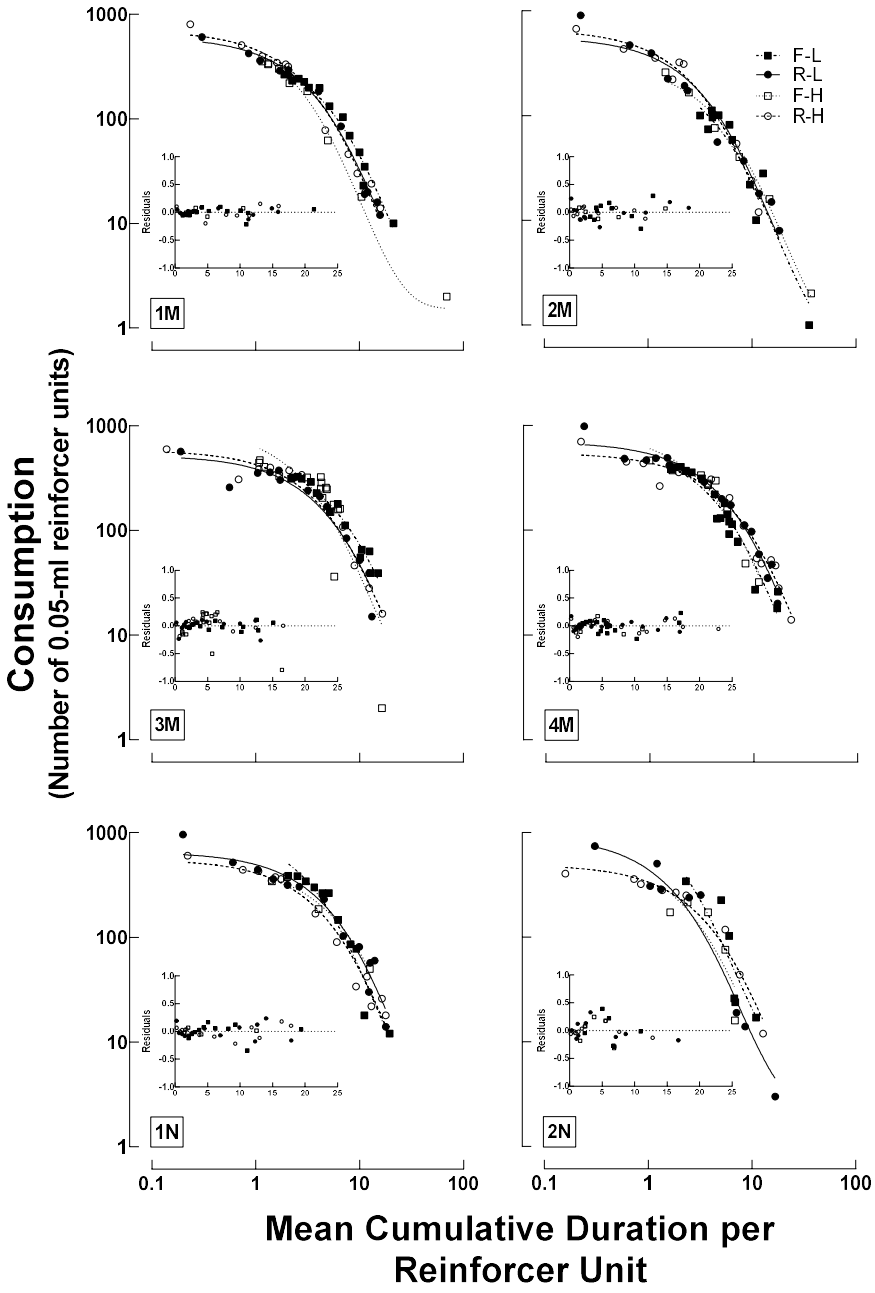

Figure 42. Exponential demand curves fit to consumption as a function of mean cumulative response duration per reinforcer unit. Closed circles and solid lines show R-L progressions, open circles and dashed lines show R-H progressions, closed squares and dot-dashed lines show F-L progressions, and open squares and dotted lines show F-H progressions. Inset panels show residuals.

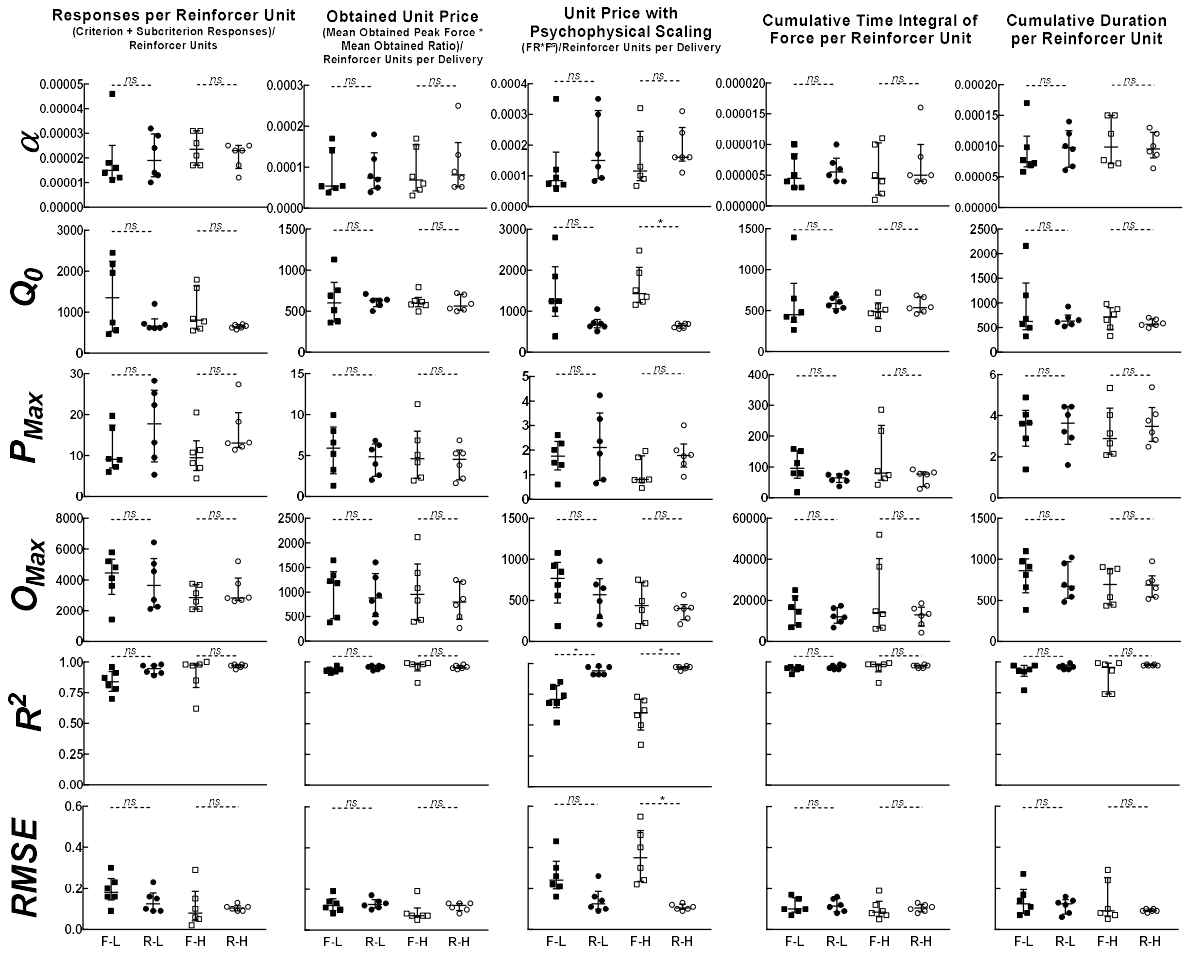

Figure 43. Derived parameters and goodness-of-fit measures for individual animals across different price conversions. Closed circles show R-L progressions, open circles show R-H progressions, closed squares show F-L progressions, and open squares show F-H progressions. Lines and error bars show medians and IQRs.

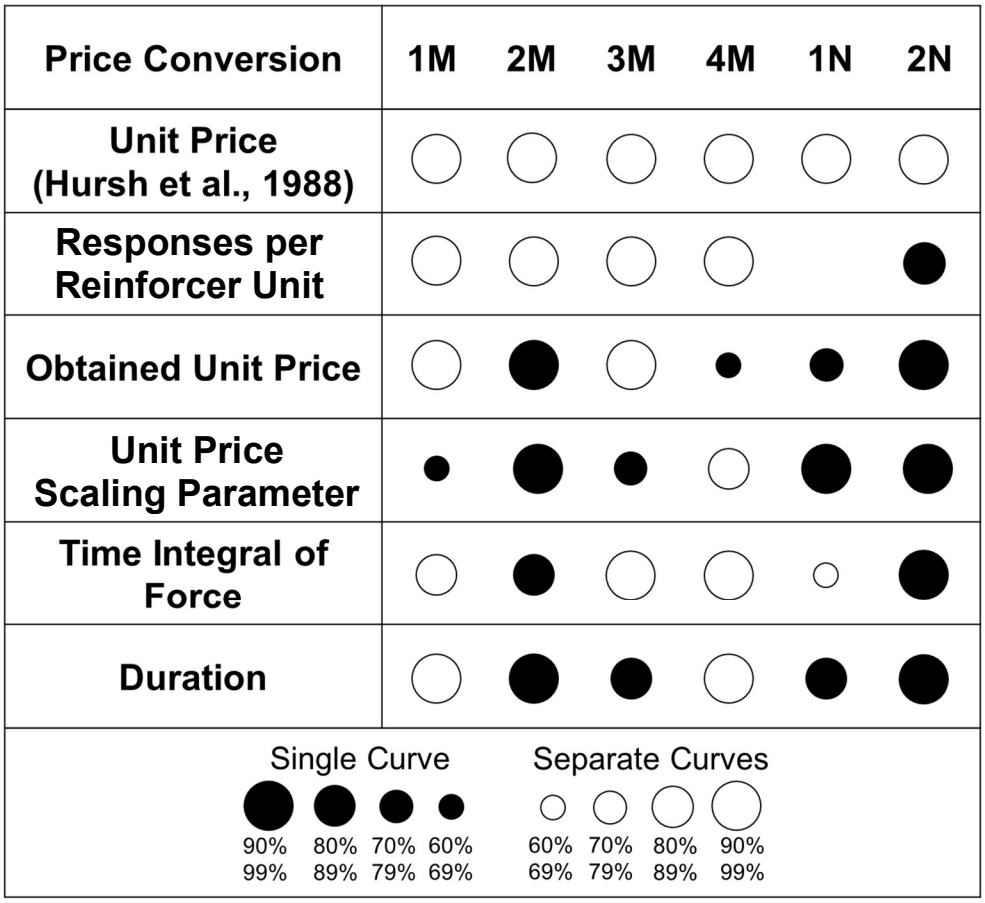

Figure 44. Results of AICc comparisons of single versus separate curves for each price conversion for each animal. Preferred model as determined by AICc comparisons is shown across rats (columns) for different price conversions (rows). Filled, black circles indicate a single curve for all progression types (F-L, R-L, F-H, and R-H) was preferred; open, white circles indicate preference for separate curves for the different progressions. Circle size shows relative probability. Comparisons that resulted in relative indifference (i.e., 50-59.9% likelihood) are shown by blanks.

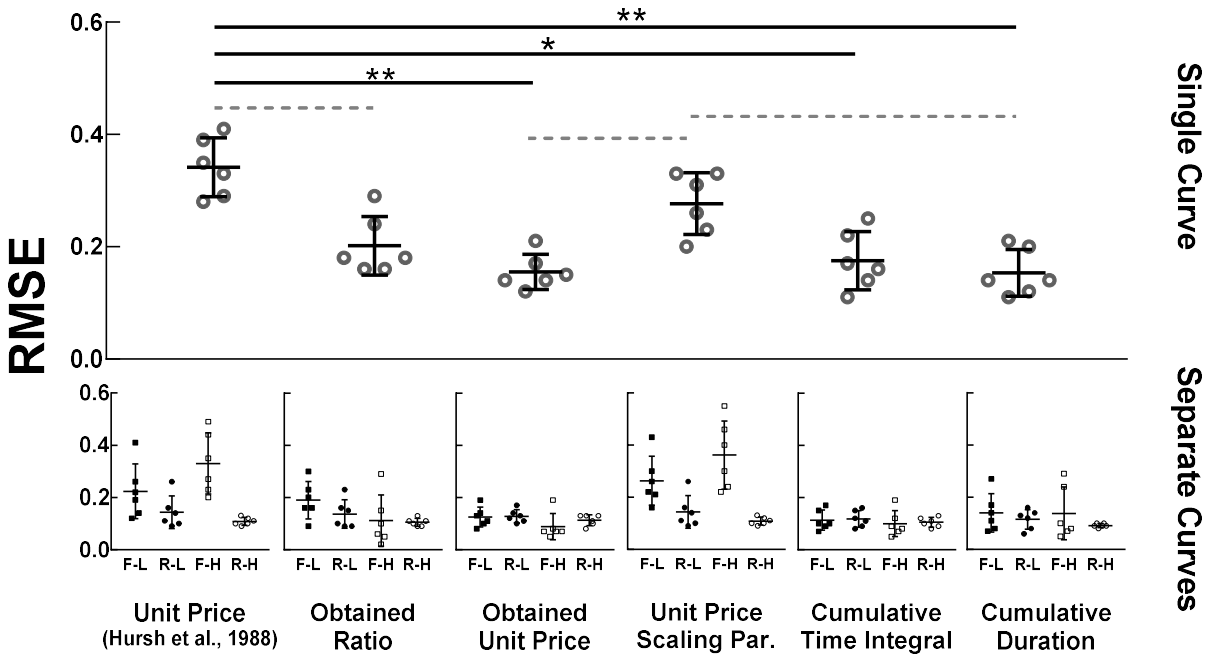

Figure 45. RMSE for a single curve and separate curves fit to each animal's progressions. Top panel shows RMSE for a single curve, with data from each animal shown by a gray open disc at each price. Significant differences prior to correction for multiple comparisons are shown by gray dashed lines, and multiple comparisons that remained significant after Dunn's corrections are shown by black solid lines. Bottom panels show RMSE for separate curves for each progression for each animal across price conditions (separate panels).

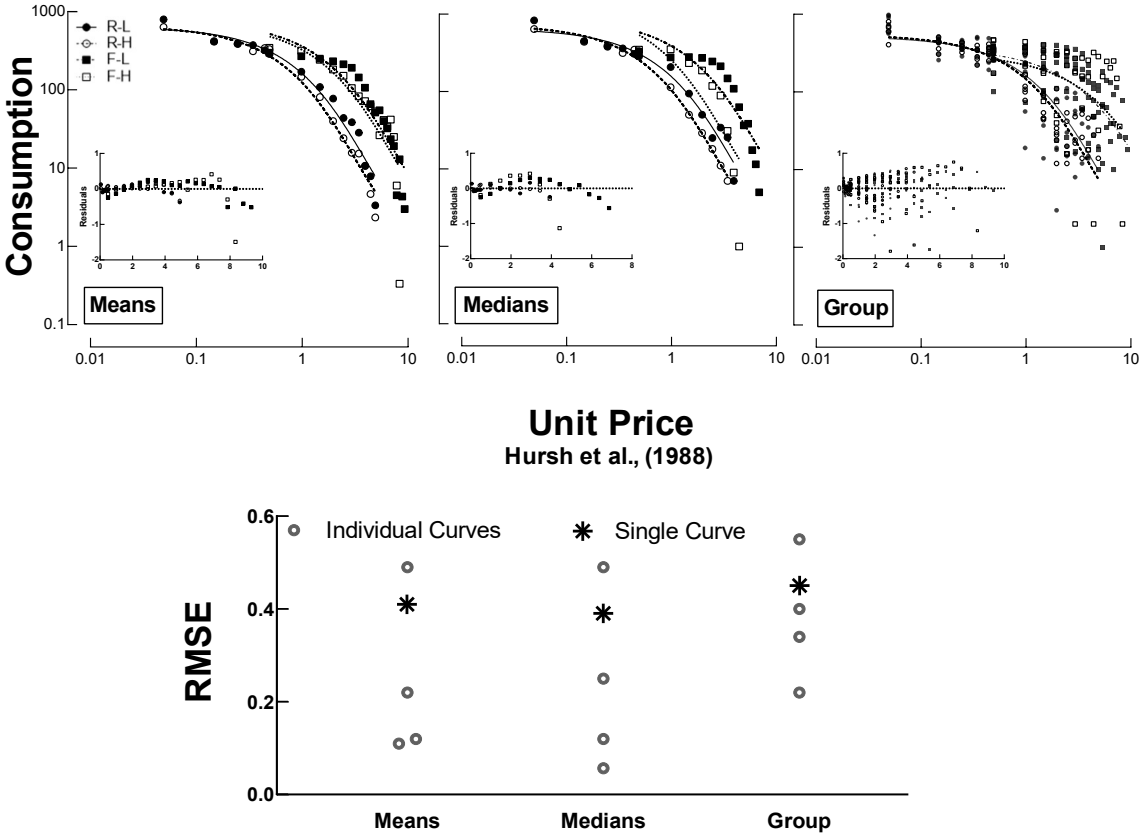

Figure 46. Exponential demand curves fit to aggregate consumption data as a function of unit price. Shown are curves fit to mean data (top left panel), median data (top middle panel), and all group data (top right panel). Inset panels show residuals. Bottom panel shows RMSE for separate curves for each progression (gray discs) and a single curve for all progressions (black stars) across different approaches to aggregating consumption.

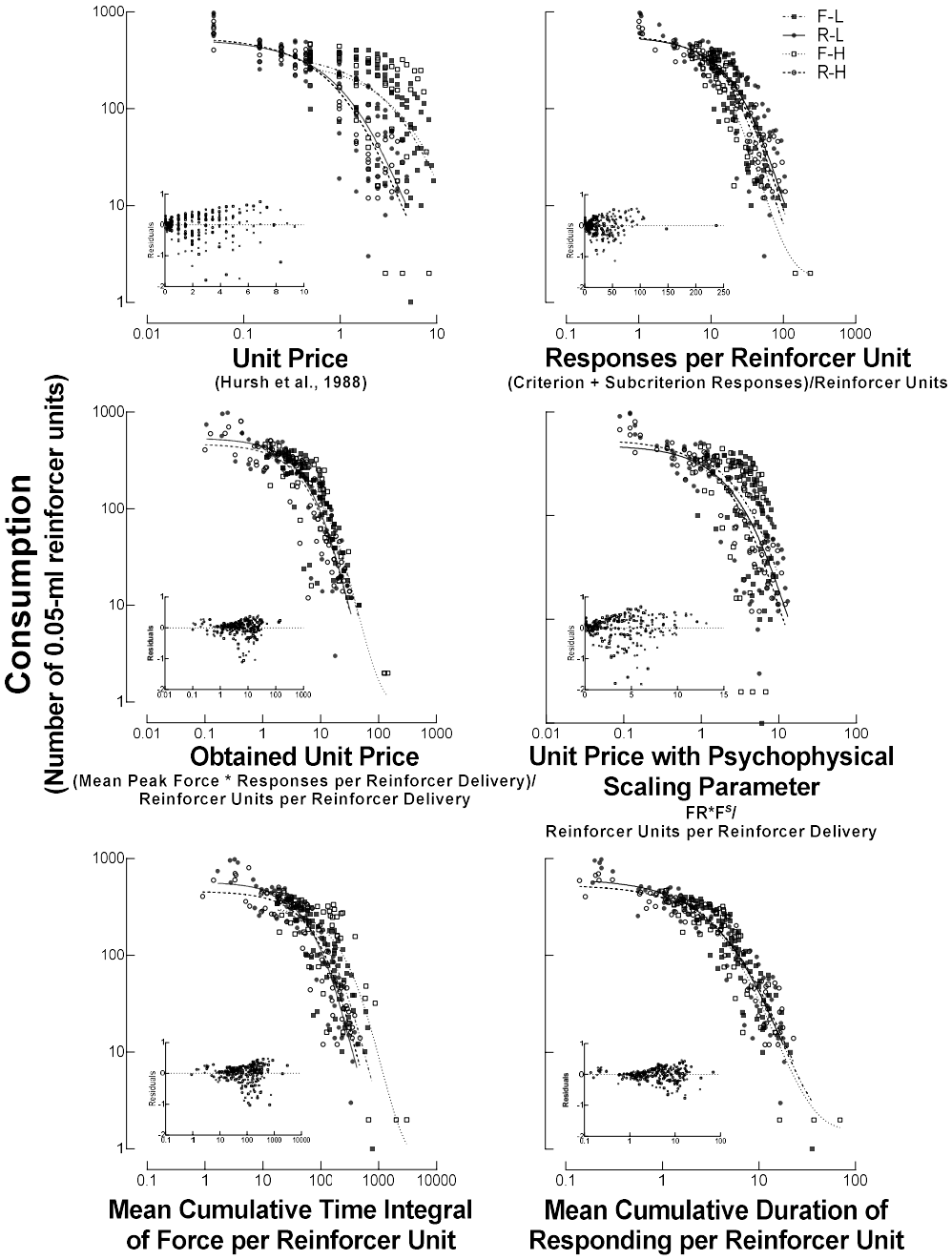

Figure 47. Exponential demand curves fit to consumption data across different price modifications. Closed circles and solid lines show R-L progressions, open circles and dashed lines show R-H progressions, closed squares and dot-dashed lines show F-L progressions, and open squares and dotted lines show F-H progressions. Inset panels show residuals.

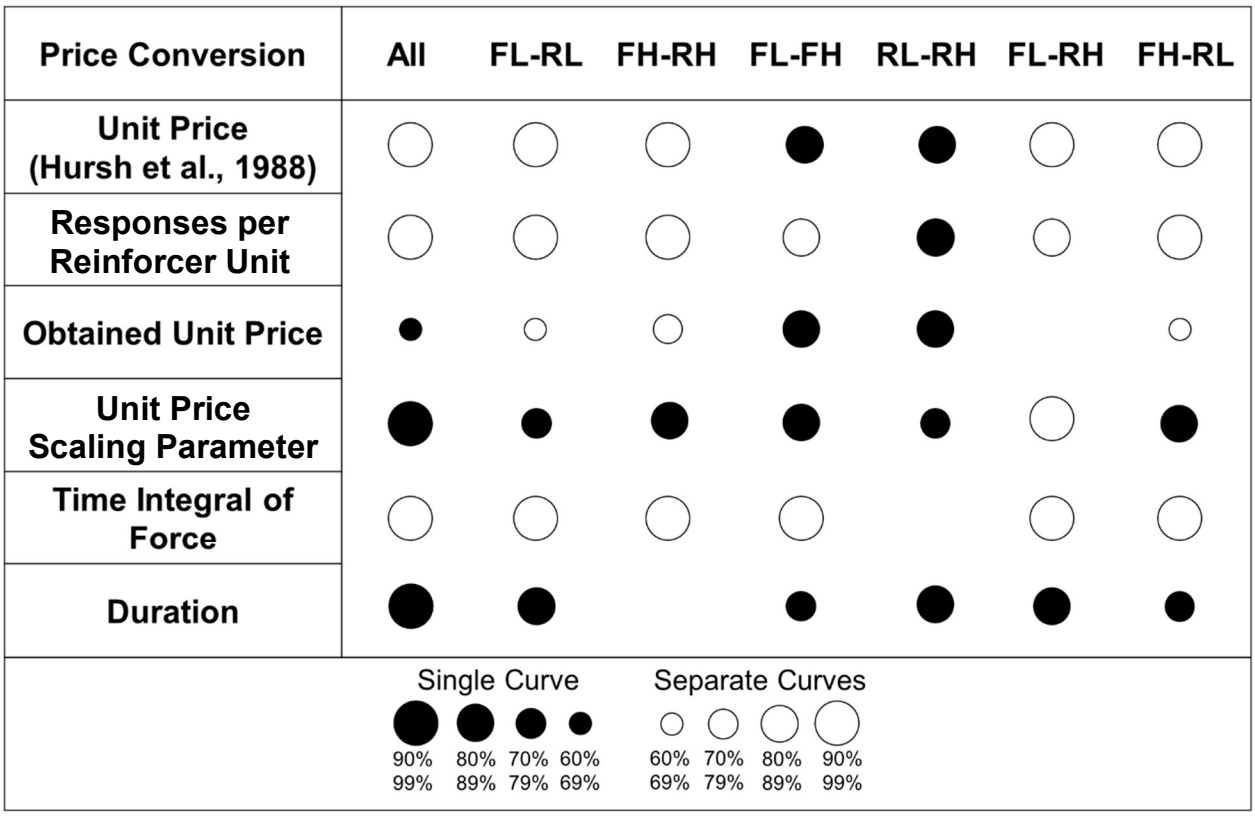

Figure 48. Results of AICc comparisons for exponential demand curves fit to group consumption data. Preferred model as determined by AICc comparisons is shown across different comparisons (columns) for different price conversions (rows). Filled, black circles indicate a single curve for the specified progressions was preferred; open, white circles indicate preference for separate curves for the progressions. Circle size shows relative probability. Comparisons that resulted in relative indifference (i.e., 50-59.9% likelihood) are shown by blanks.

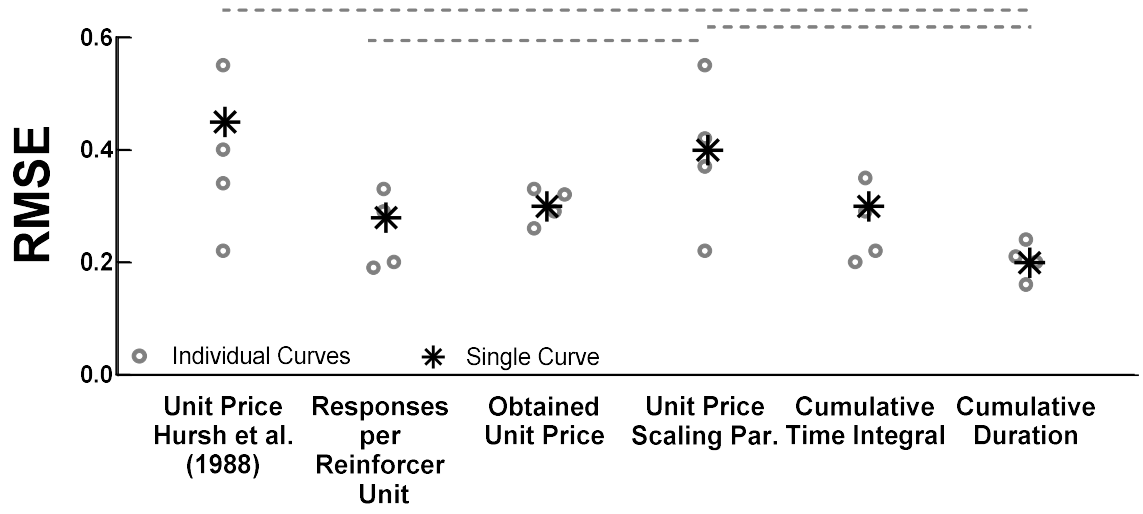

Figure 49. Group RMSE for separate versus shared expontential demand curves with different price conversions. Shown is RMSE for each progression type (gray discs; F-L, R-L, F-H, or R-H) and a single curve for all progressions (black stars). Gray dashed lines show significant post-hoc comparisons of RMSE comparing individual curves that did not remain significant after correcting for multiple comparisons.

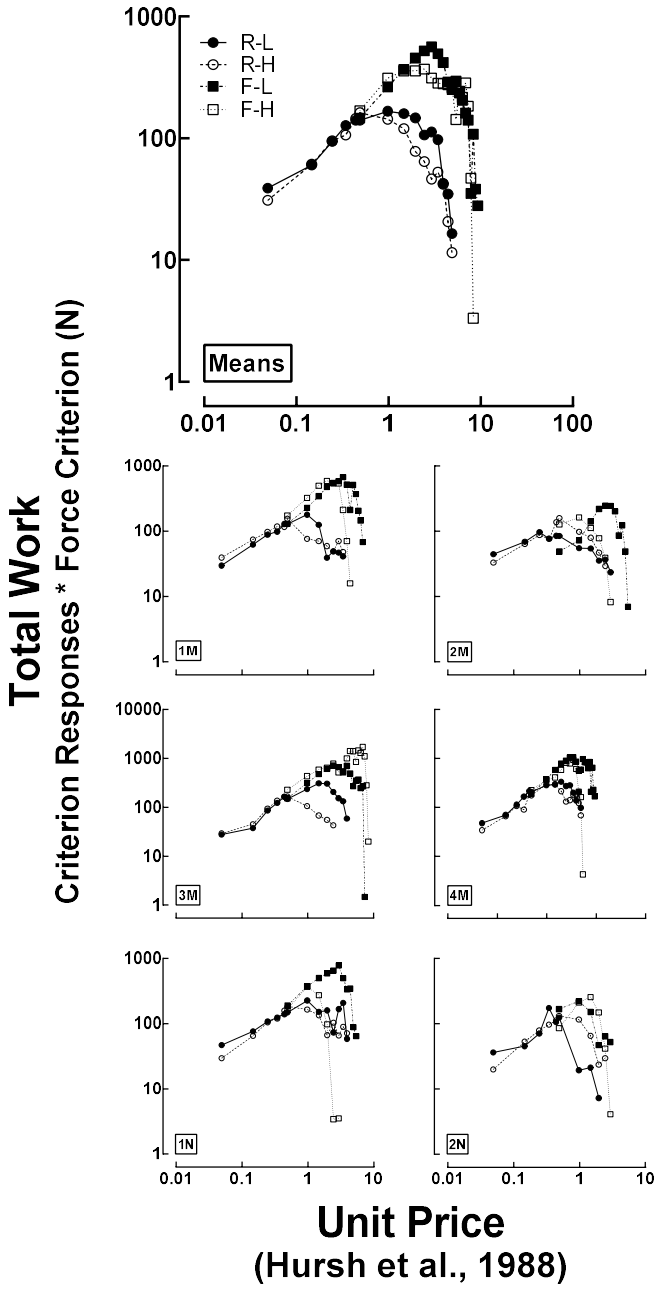

Figure 50. Total work (criterion responses * force criterion) as a function of unit price. Top panel shows means and six lower panels show data from individual rats (subject codes at lower left). Closed circles and solid lines show R-L progressions, open circles and dashed lines show R-H progressions, closed squares and dot-dashed lines show F-L progressions, and open squares and dotted lines show F-H progressions.

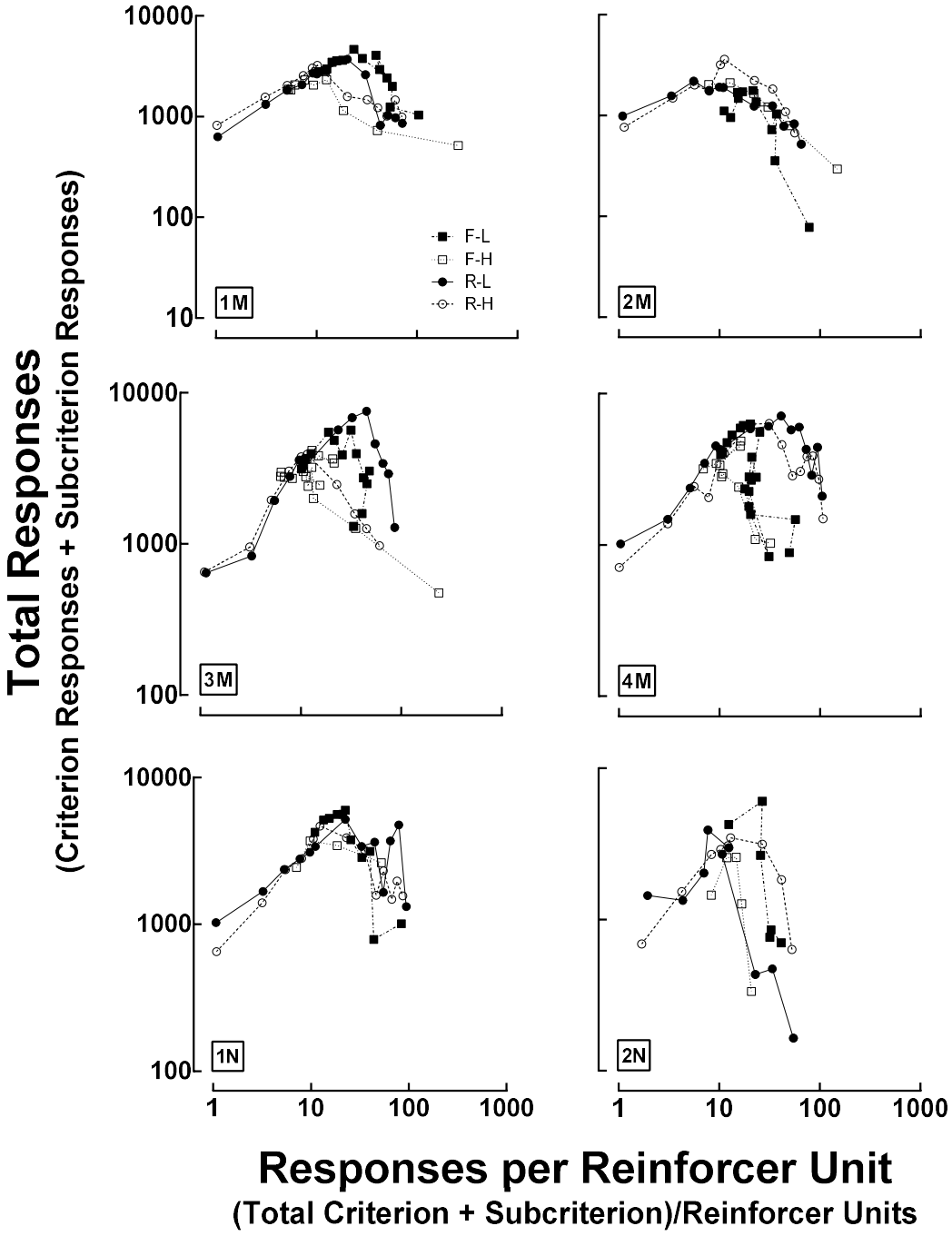

Figure 51. Work function relating total responses and responses per reinforcer unit. Closed circles and solid lines show R-L progressions, open circles and dashed lines show R-H progressions, closed squares and dot-dashed lines show F-L progressions, and open squares and dotted lines show F-H progressions.

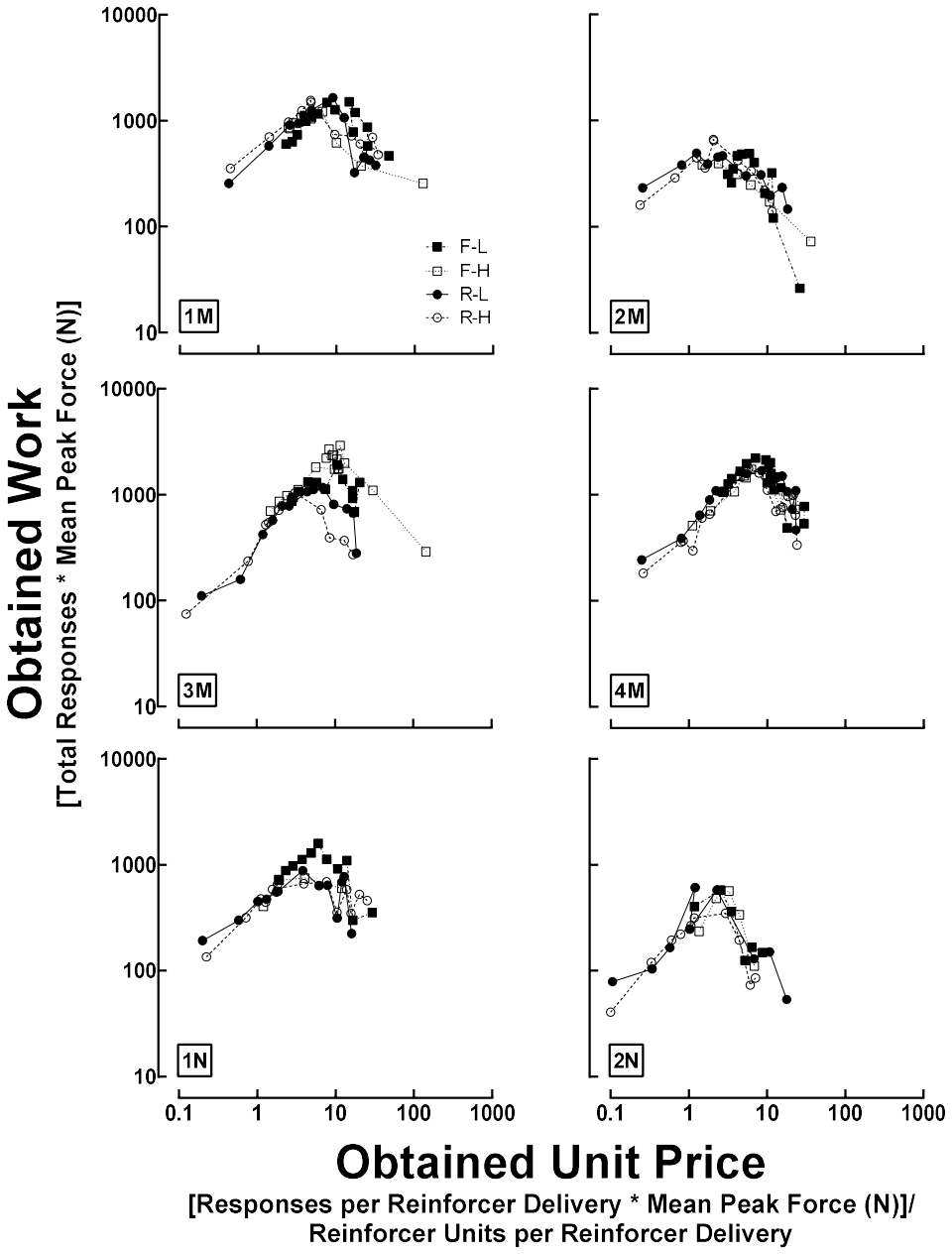

Figure 52. Work function based on obtained unit price. Obtained unit price was determined by multiplying responses per reinforcer delivery by mean peak force and then dividing by number of reinforcers. Closed circles and solid lines show R-L progressions, open circles and dashed lines show R-H progressions, closed squares and dot-dashed lines show F-L progressions, and open squares and dotted lines show F-H progressions.

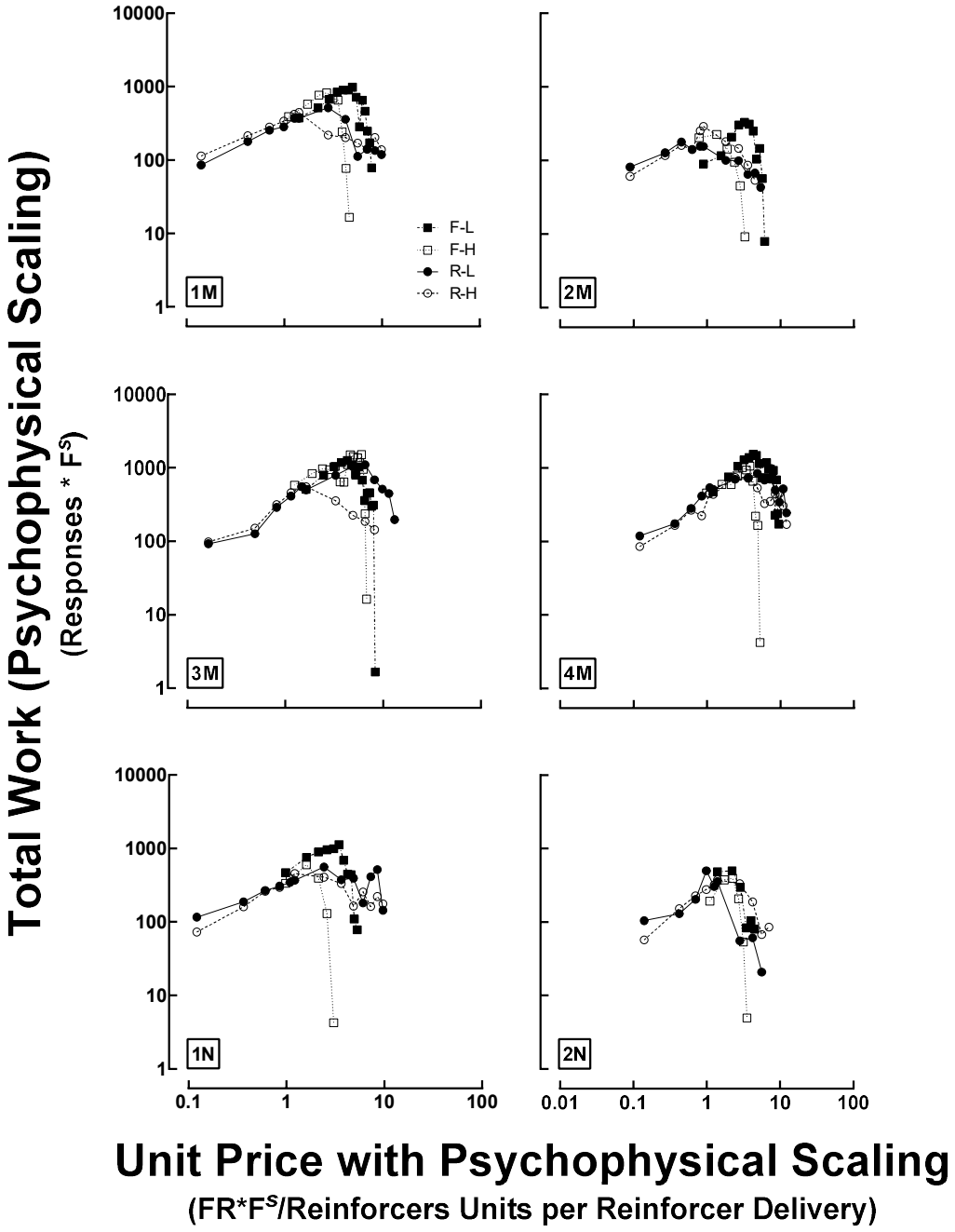

Figure 53. Work function based on psychophysical scaling adjustments of unit price. Closed circles and solid lines show R-L progressions, open circles and dashed lines show R-H progressions, closed squares and dot-dashed lines show F-L progressions, and open squares and dotted lines show F-H progressions.

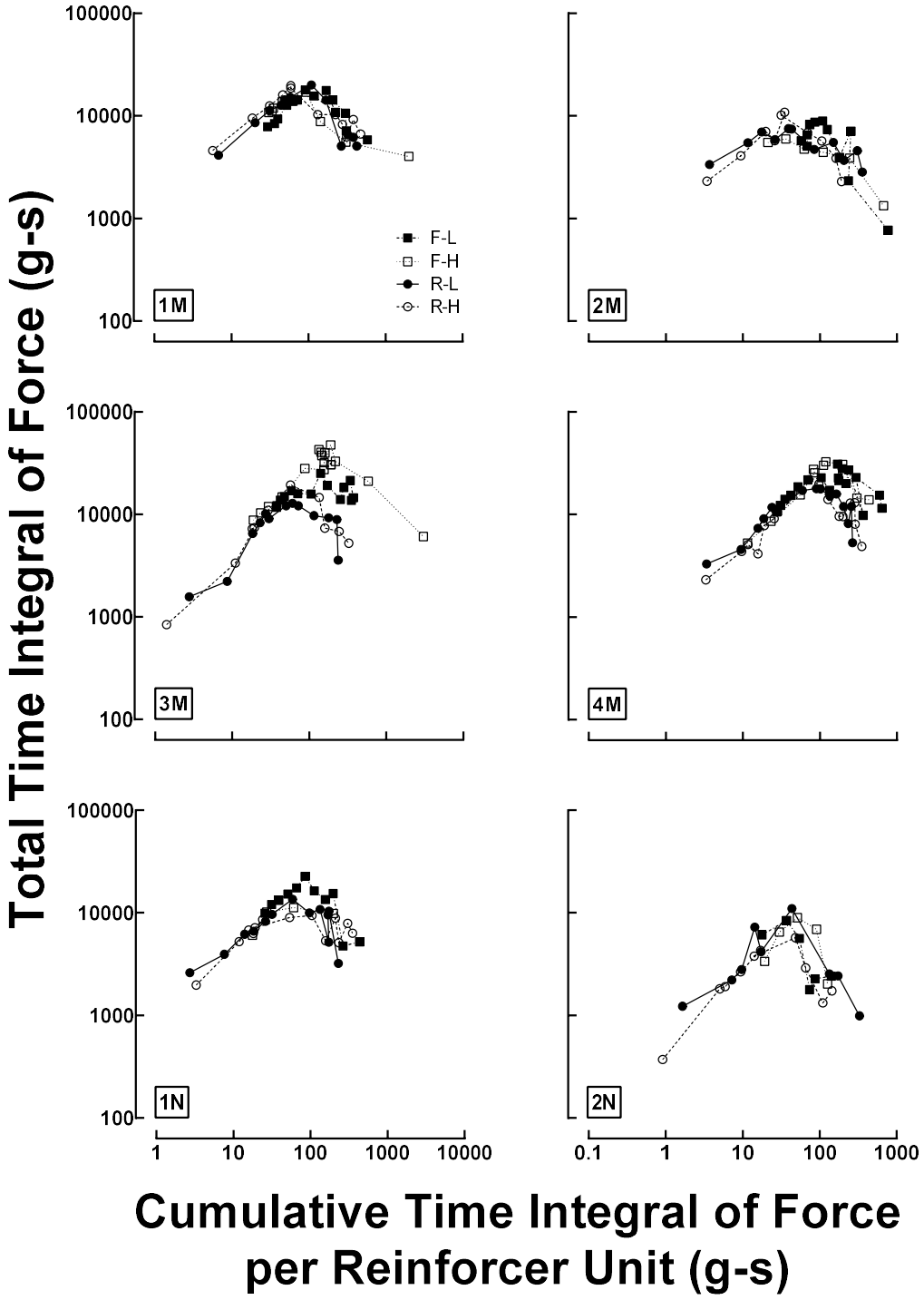

Figure 54. Work function based on time integral of force. Closed circles and solid lines show R-L progressions, open circles and dashed lines show R-H progressions, closed squares and dot-dashed lines show F-L progressions, and open squares and dotted lines show F-H progressions.

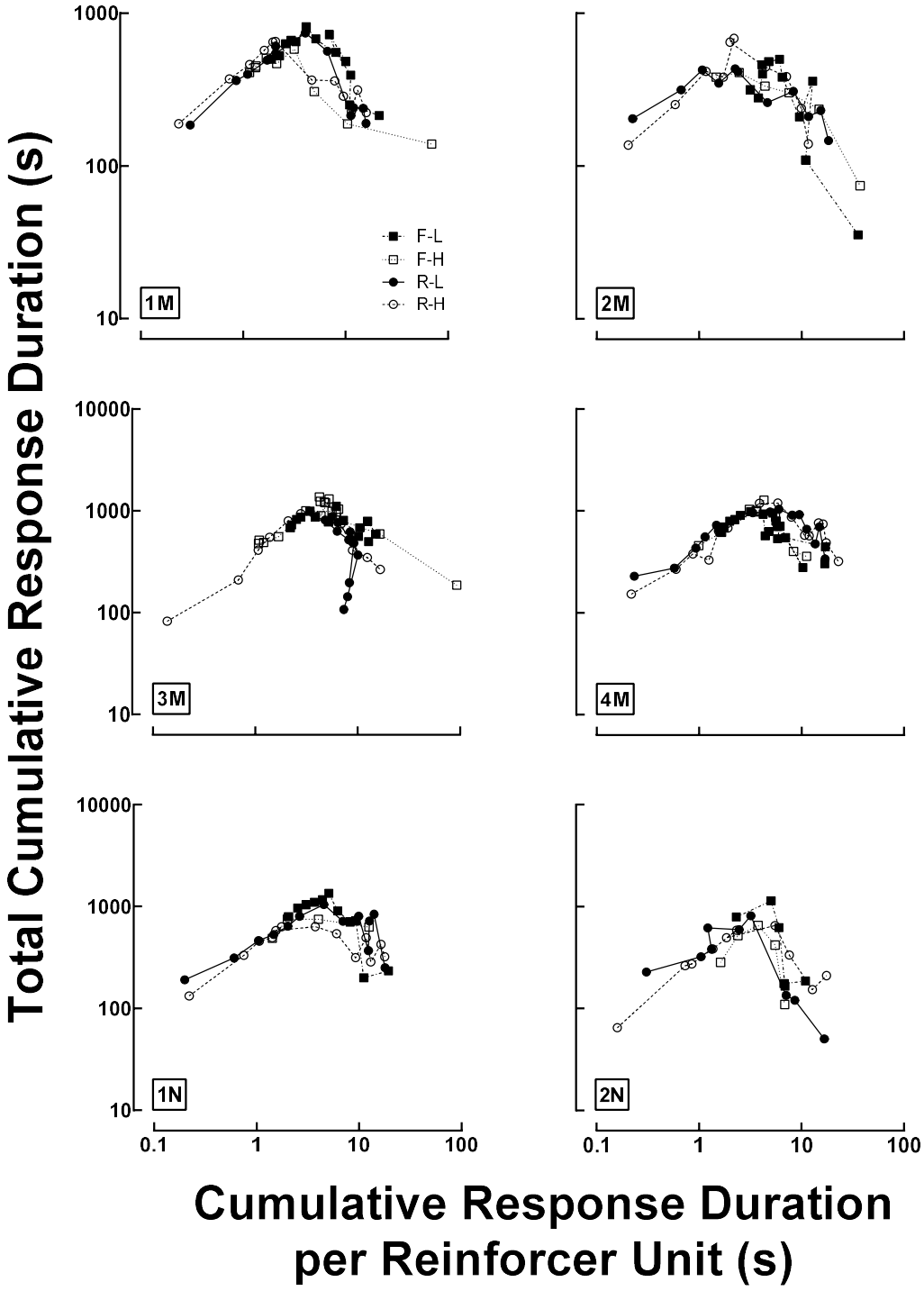

Figure 55. Work function based on cumulative duration. Closed circles and solid lines show R-L progressions, open circles and dashed lines show R-H progressions, closed squares and dot-dashed lines show F-L progressions, and open squares and dotted lines show F-H progressions.

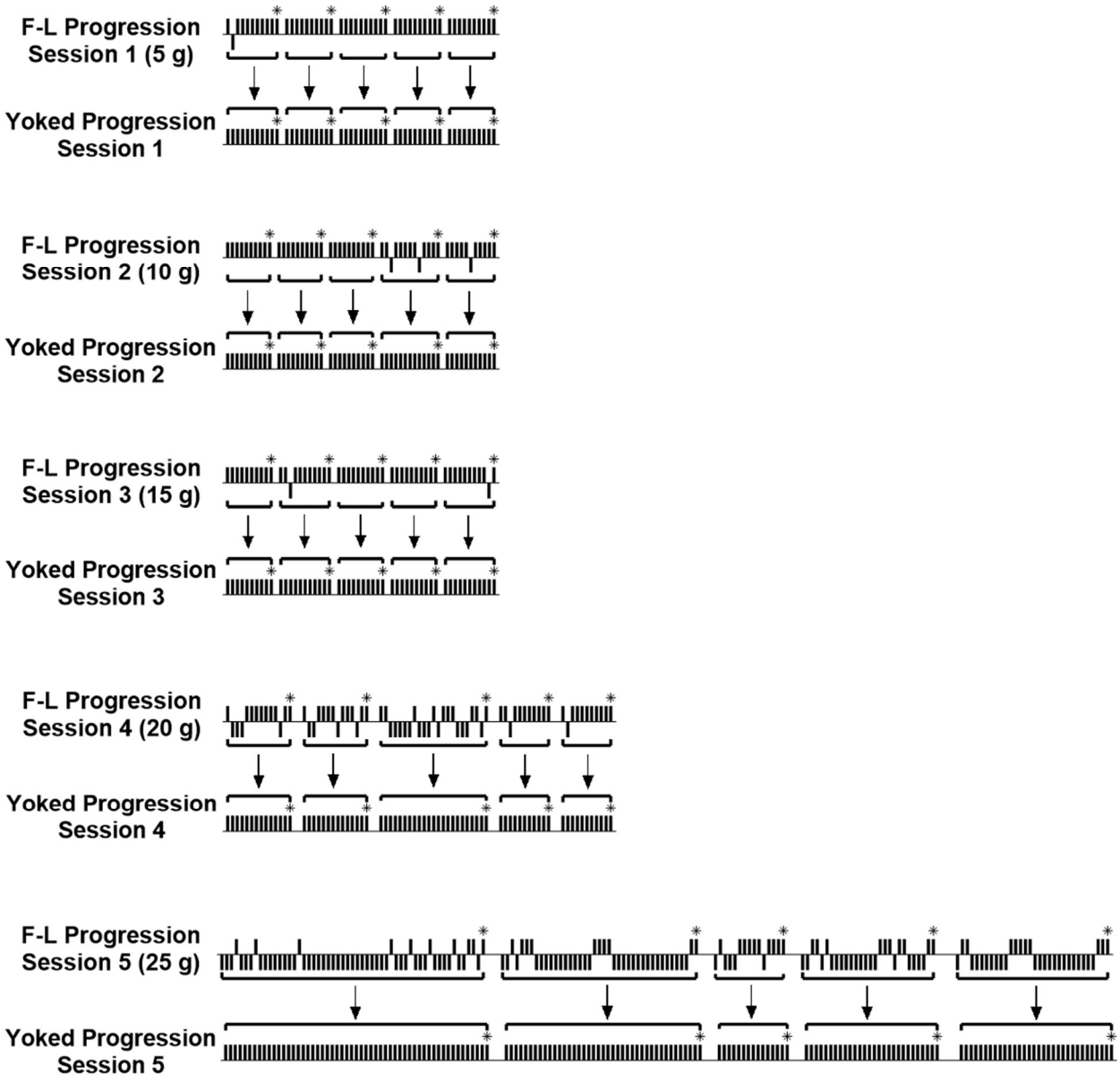

Figure 56. Schematic of yoking procedure. Total responses (criterion and subcriterion) are shown for the first five reinforcer deliveries for each of the first five sessions of the F-L progression and corresponding yoked sessions for 3M. Ticks above the horizontal line show criterion responses, and ticks below the horizontal line show subcriterion responses. In the yoked conditions, the force criterion was set to the threshold (4 g), so no subcriterion responses were recorded. Brackets show ratio runs, and asterisks show reinforcer deliveries. This yoking procedure was repeated for every reinforcer delivery across all force progression sessions.

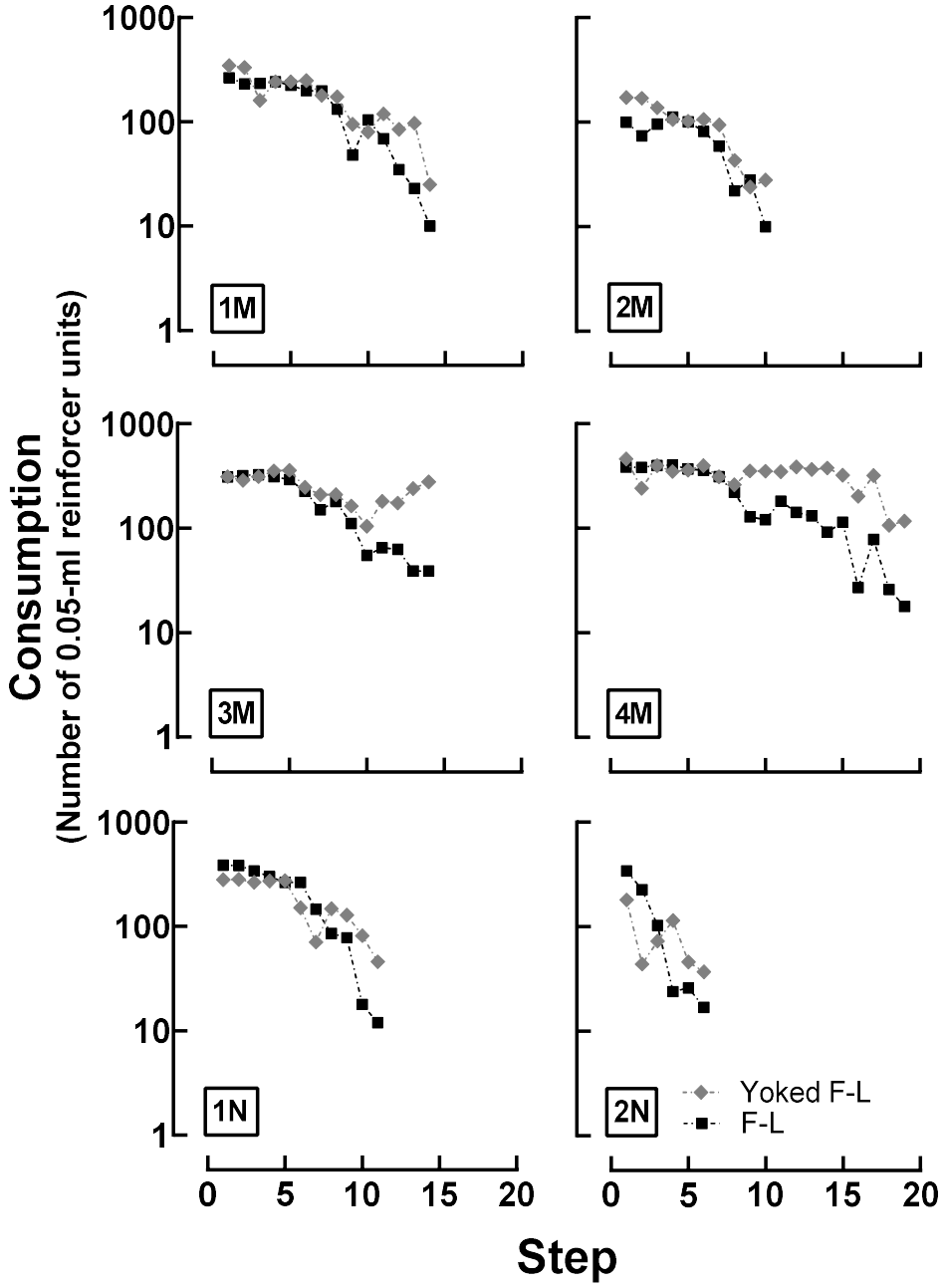

Figure 57. Demand curves yoked to F-L progression by step. Consumption (y-axis) plotted as a function of step (x-axis). Original demand curves (Experiment 1; black filled squares and dot-dashed lines) and yoked demand curves (gray filled diamonds and dot-dashed lines). Separate panels show individual animals (subject code in lower left corner).

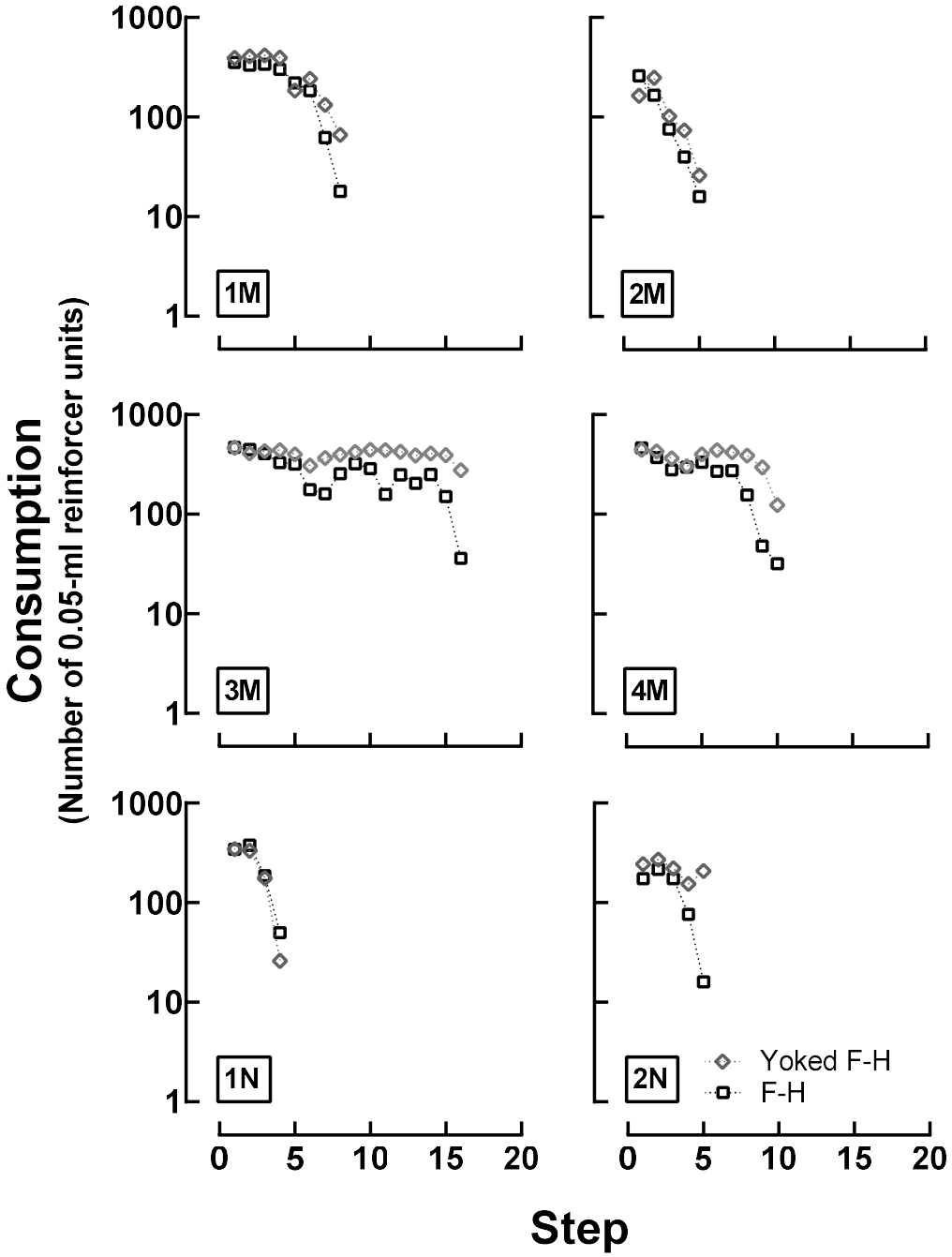

Figure 58. Demand curves yoked to F-H progression by step. Consumption (y-axis) plotted as a function of step (x-axis). Original demand curves (Experiment 1; black open squares and dotted lines) and yoked demand curves (gray open diamonds and dotted lines). Separate panels show individual animals (subject code in lower left corner).

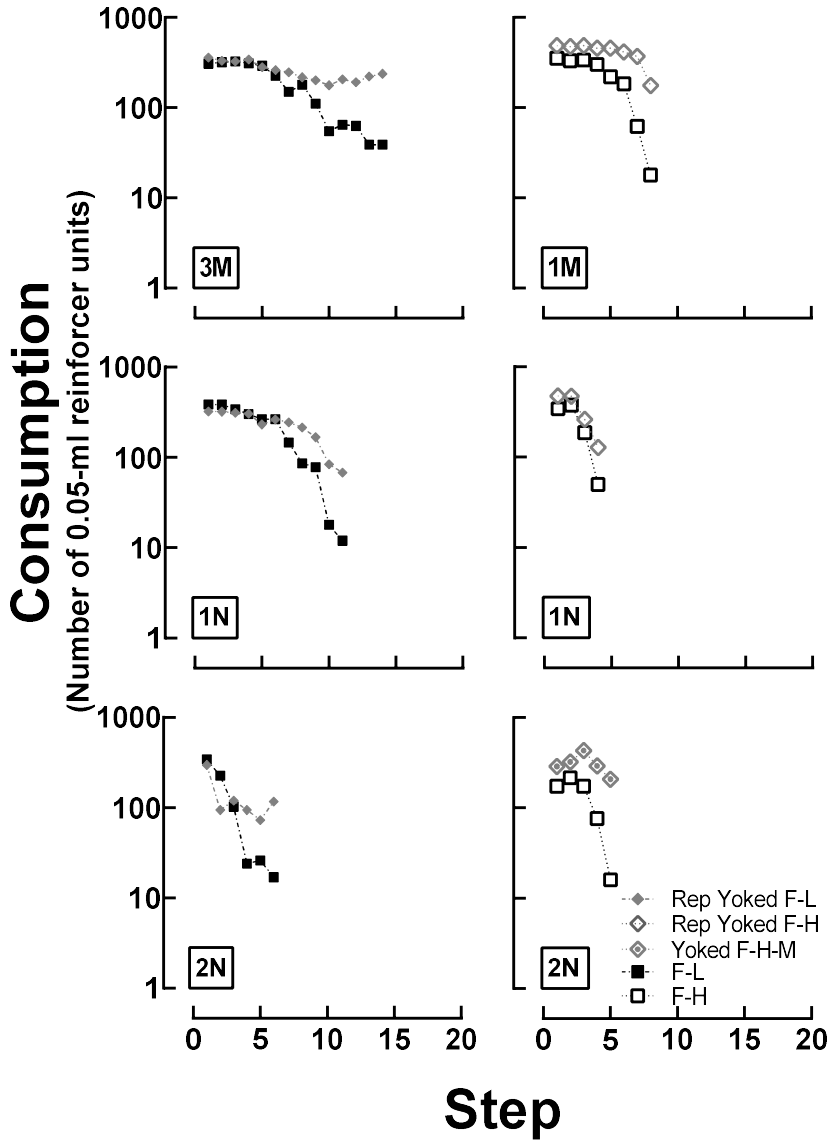

Figure 59. Replications of demand curves yoked to original F-L and F-H progressions. Consumption (y-axis) plotted as a function of step (x-axis). Replicated demand curves are shown from Experiment 1 for F-L progressions (black filled squares and dot-dashed lines) and F-H progressions (black open squares and dot-dashed lines). Yoked demand curves are shown for F-L progressions (black filled diamonds and dotted lines) and F-H progressions (gray open diamonds and dotted lines). The open gray diamonds with a dot show data from yoking to means (2N only). Separate panels show individual animals (subject code in lower left corner).

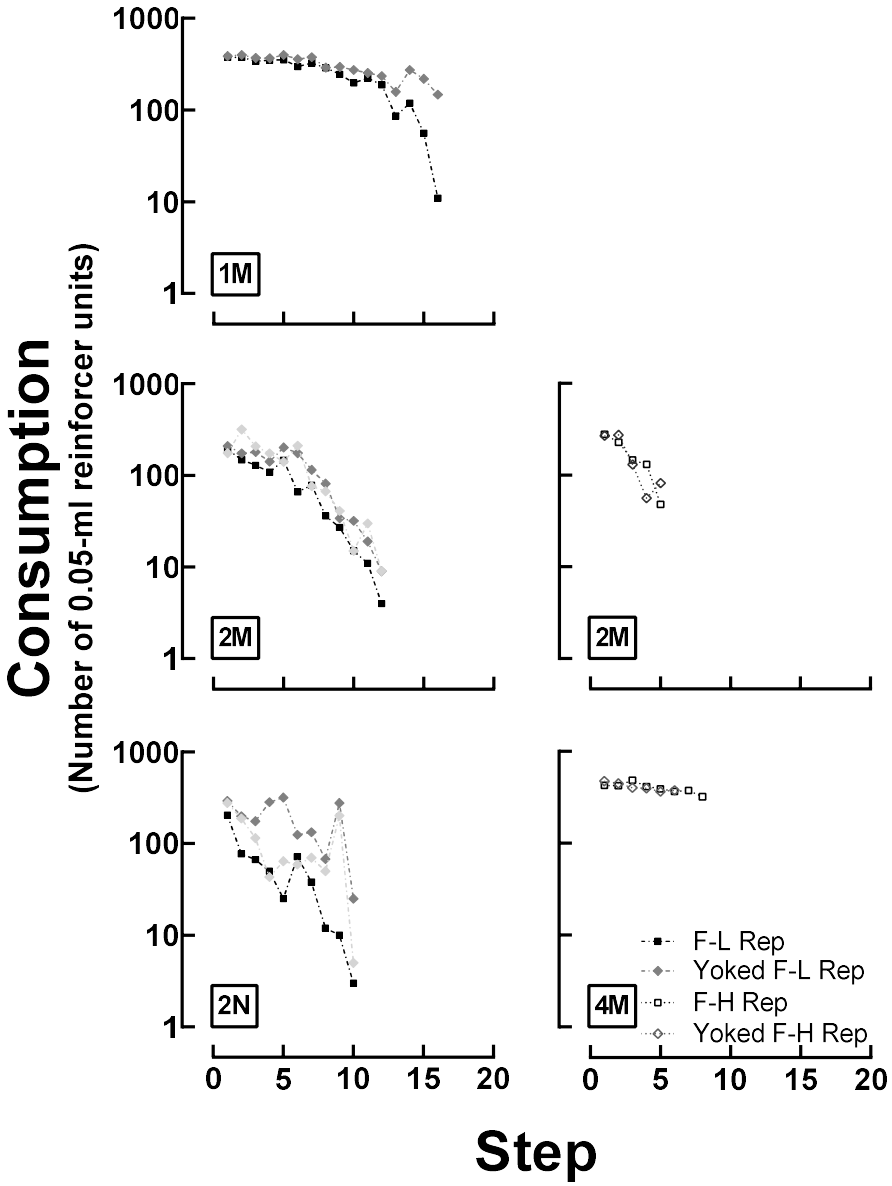

Figure 60. Demand curves yoked to replicated progressions by step. Consumption (y-axis) plotted as a function of step (x-axis). Replicated demand curves are shown from Experiment 1 for F-L progressions (black filled squares and dot-dashed lines) and F-H progressions (black open squares and dot-dashed lines). Yoked demand curves are shown for F-L progressions (gray filled diamonds and dotted lines; lighter gray shows replication) and F-H progressions (gray open diamonds and dotted lines). Panels show individual animals (subject code in lower left).

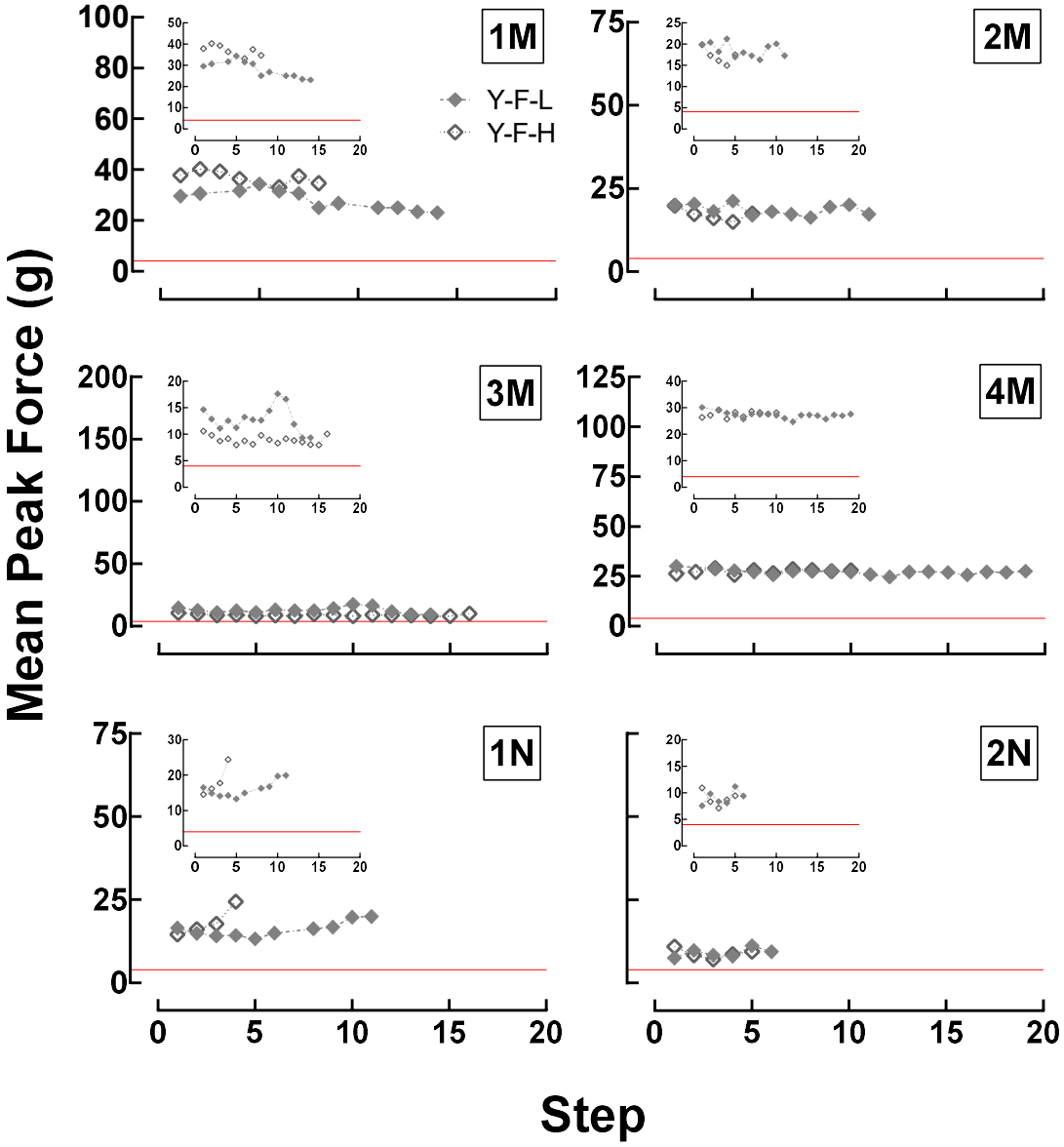

Figure 61. Mean peak force as a function of step for yoked progressions. The y-axis show mean peak force (g), and the x-axis shows step for the Yoked F-L (gray closed diamonds and dot-dashed lines) and F-H progressions (gray open diamonds and dotted lines) for each animal (separate panels). The red reference line shows the peak force criterion (4 g; same as threshold). Inset panels show the same data but with axes scaled only to the yoked progressions. The SEM was calculated for each session but was too small to be plotted with the data points.

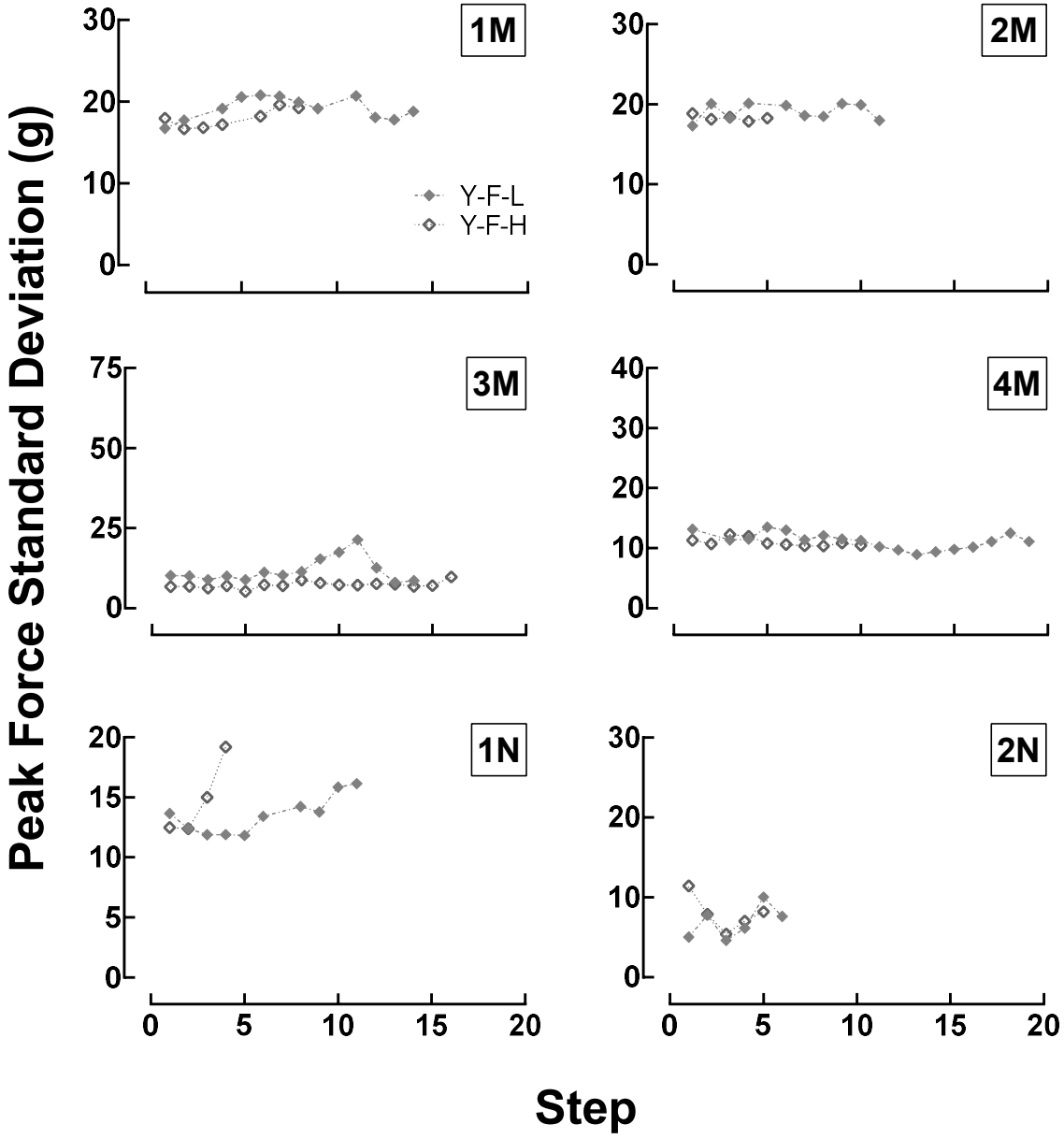

Figure 62. Peak force standard deviation by step for yoked progressions. The y-axis shows peak force standard deviation (g), and the x-axis shows step for the Yoked F-L (gray closed diamonds and dot-dashed lines) and F-H progressions (gray open diamonds and dotted lines) for each animal (separate panels).

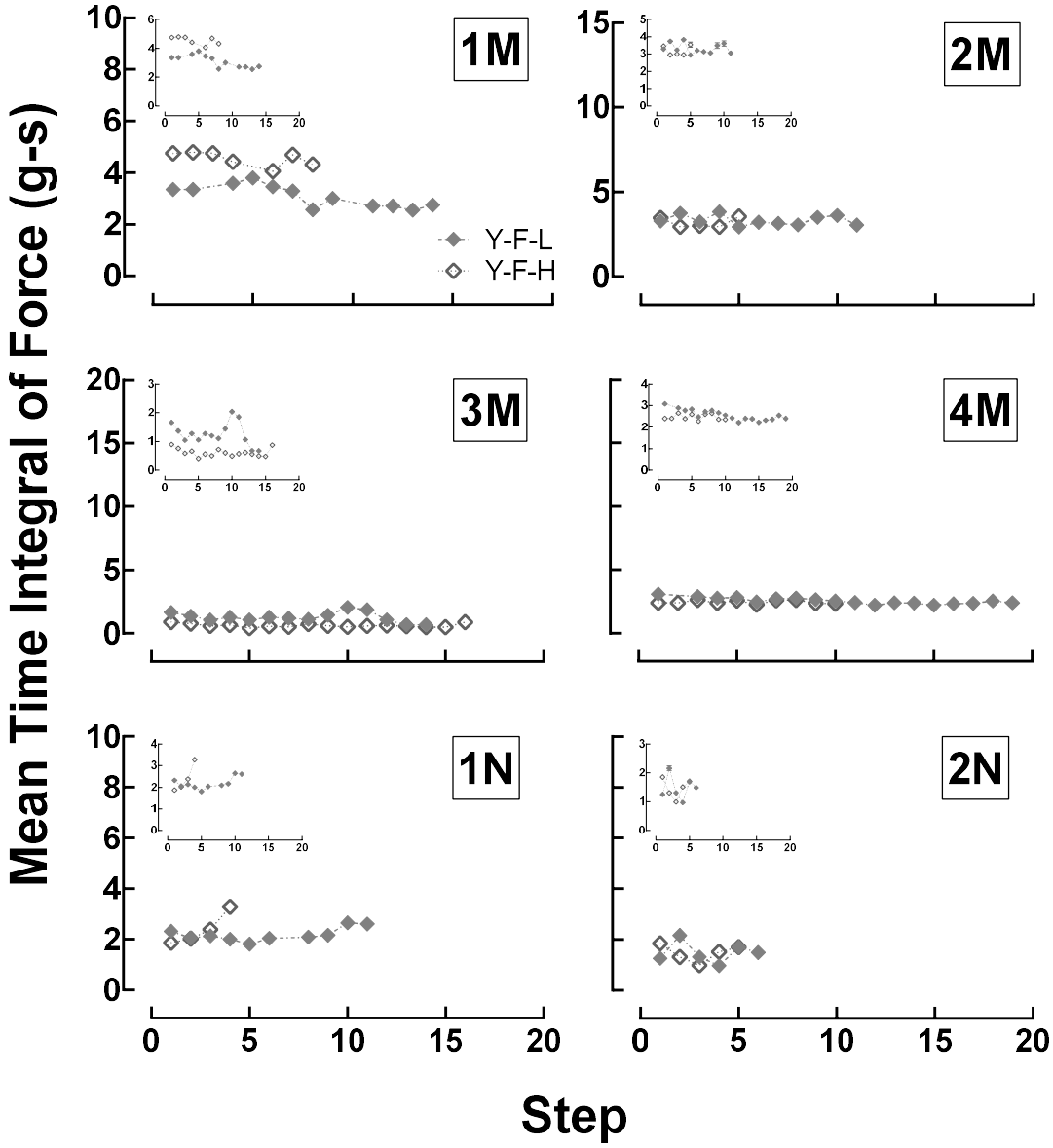

Figure 63. Time integral of force as a function of step for yoked progressions. The y-axis show mean time integral of force (gram-seconds; g-s), and the x-axis shows step for the Yoked F-L (gray closed diamonds and dot-dashed lines) and F-H progressions (gray open diamonds and dotted lines) for each animal (separate panels). Inset panels show the same data but with the y-axes scaled to just the yoked sessions. The SEM was calculated for each session and if not shown, was too small to be plotted with the data points.

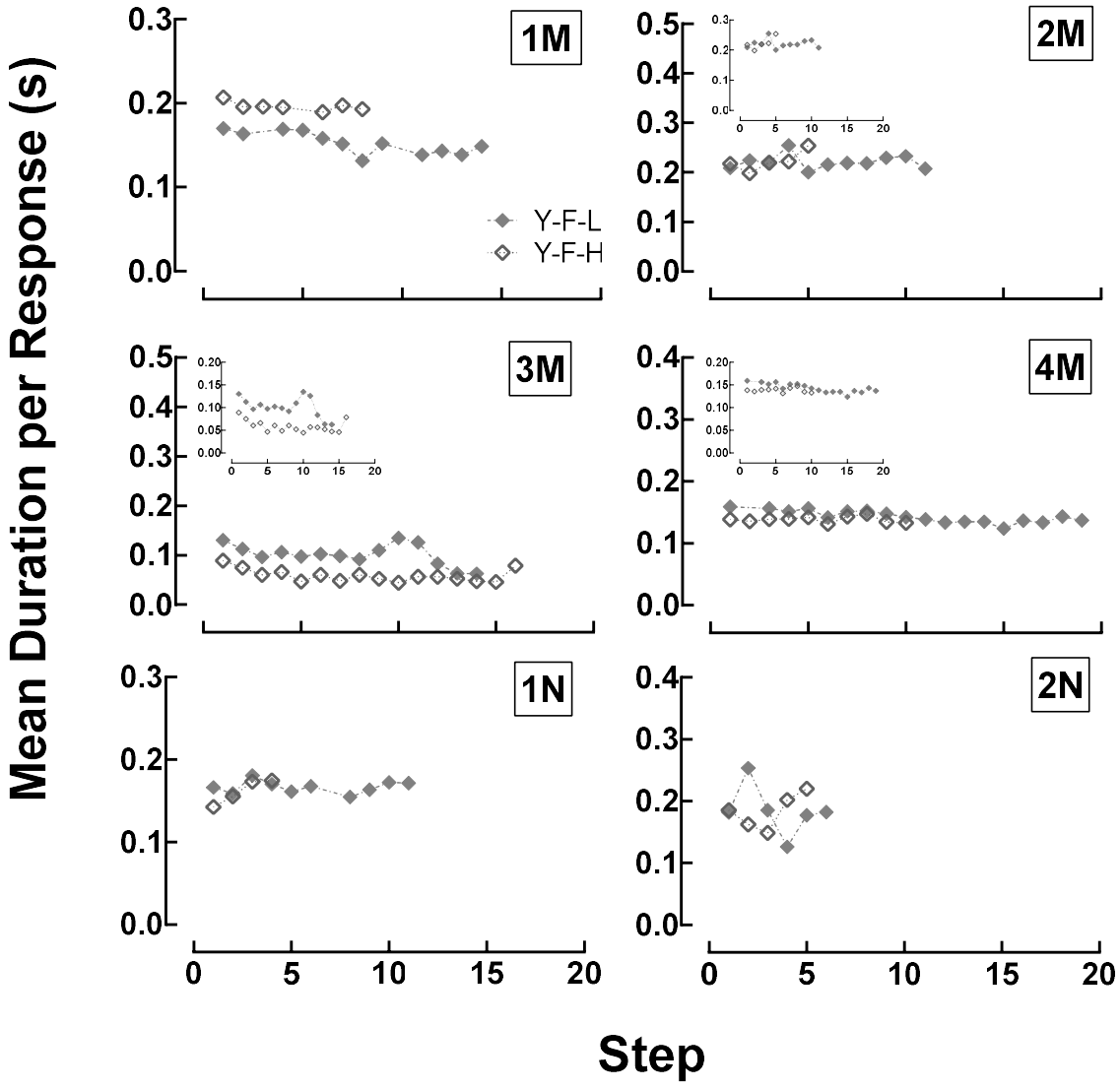

Figure 64. Mean duration per response as a function of step for yoked progressions. The y-axis show mean response duration (s), and the x-axis shows step for the Yoked F-L (gray closed diamonds and dot-dashed lines) and F-H progressions (gray open diamonds and dotted lines) for each animal (separate panels). Where shown, inset panels show the same data but with the y-axes scaled to only the yoked progressions. The SEM was calculated for each session but was too small to be plotted with the data points.

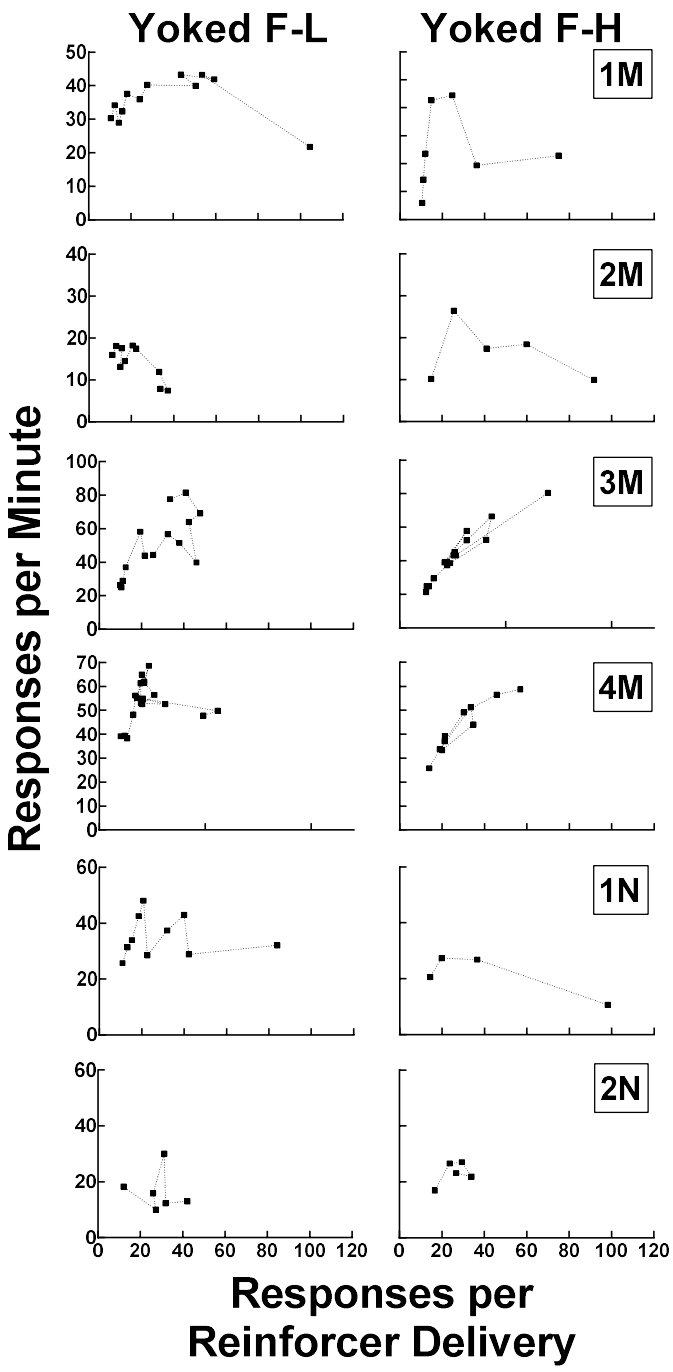

Figure 65. Response rate as a function of responses per reinforcer delivery for yoked progressions. Response rates (y-axis) plotted as a function of responses per reinforcer (i.e., obtained ratio) for the yoked F-L (left panels) and yoked F-H progressions (right panels) for individual animals (rows).

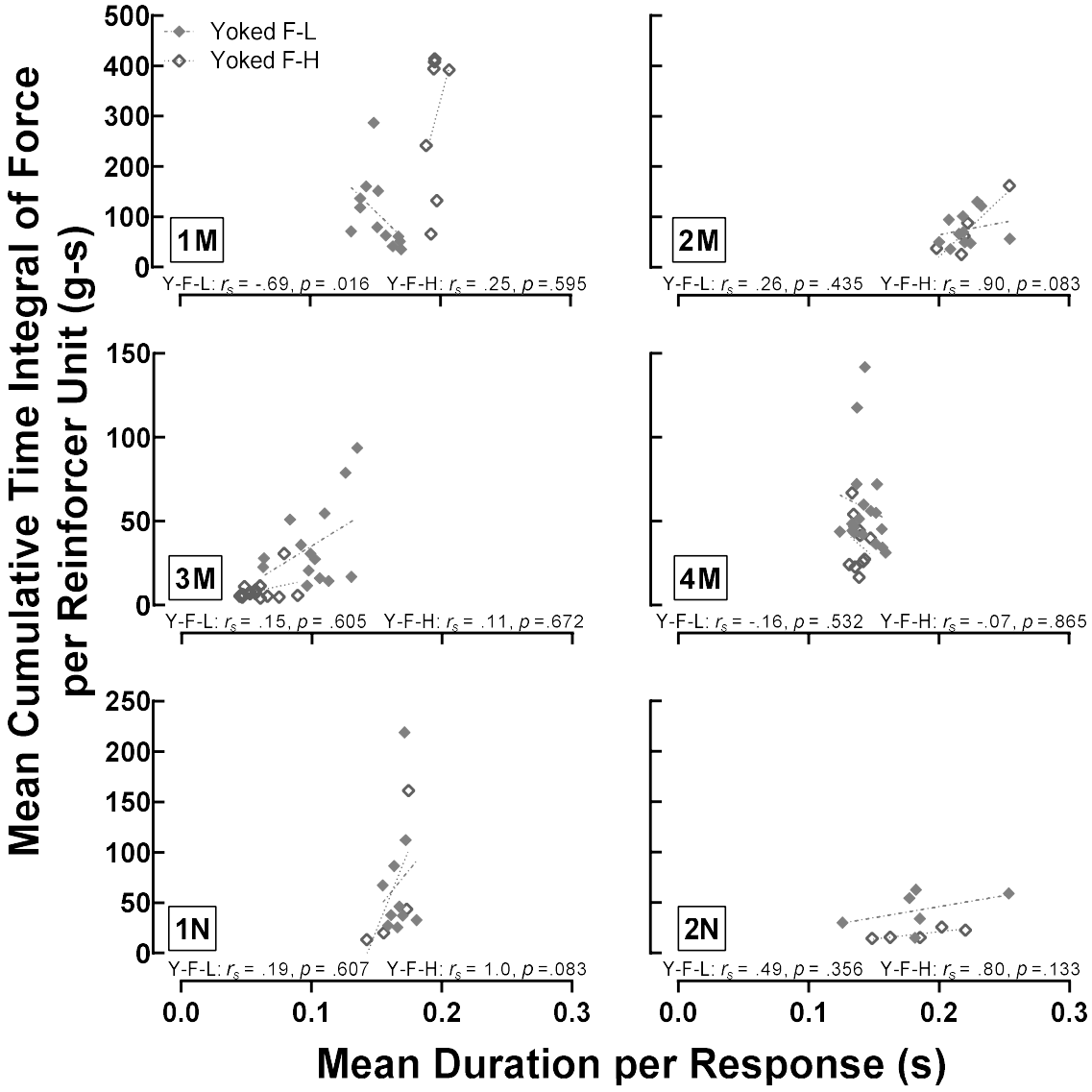

Figure 66. Correlations between mean duration per response and cumulative time integral of force per reinforcer unit for yoked progressions. Mean duration per response is shown along the x-axis, and mean cumulative time integral per reinforcer is along the y-axis. Filled gray diamonds and dot-dashed lines show data from Y-F-L progressions, and open gray diamonds dotted lines show data from Y-F-H progressions for individual animals (separate panels).

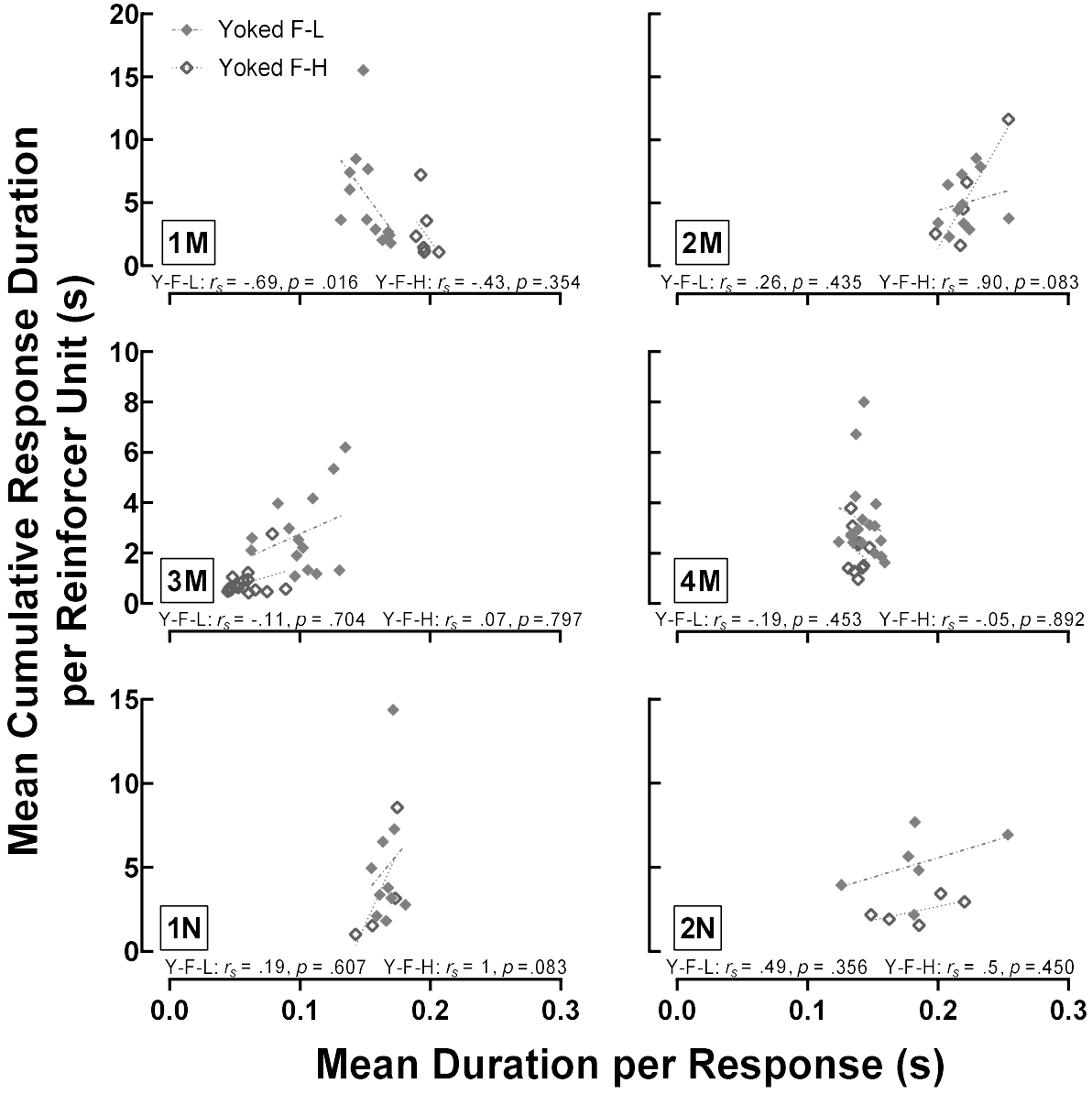

Figure 67. Correlations between mean duration per response and cumulative response duration per reinforcer unit for yoked progressions. Mean duration per response is shown along the x-axis, and cumulative response duration per reinforcer is along the y-axis. Filled gray diamonds and dot-dashed lines show data from Y-F-L progressions, and open gray diamonds dotted lines show data from Y-F-H progressions for individual animals (separate panels).

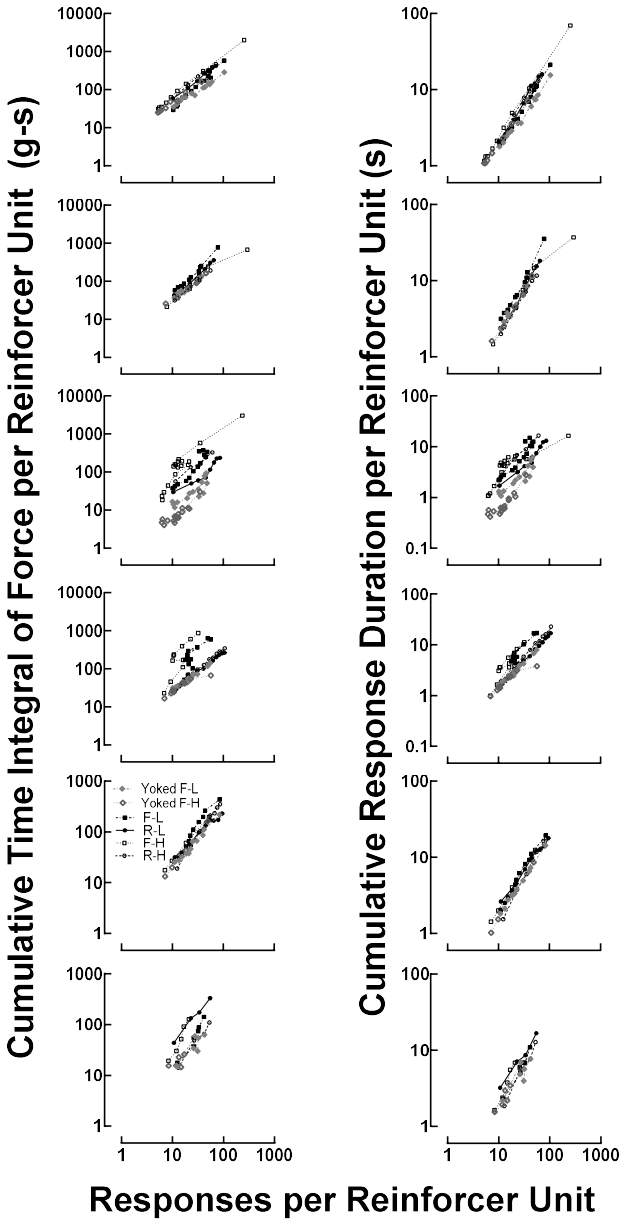

Figure 68. Mean cumulative time integral of force per reinforcer unit and mean cumulative response duration per reinforcer unit as a function of responses per reinforcer unit. From Experiment 1, data are shown for the F-L (closed back squares), F-H (open black squares), R-L (closed black circles), and R-H (open black circles) progressions, and from Experiment 2, data are shown for the Yoked F-L (closed gray diamonds) and Yoked F-H (open gray diamonds) progressions.

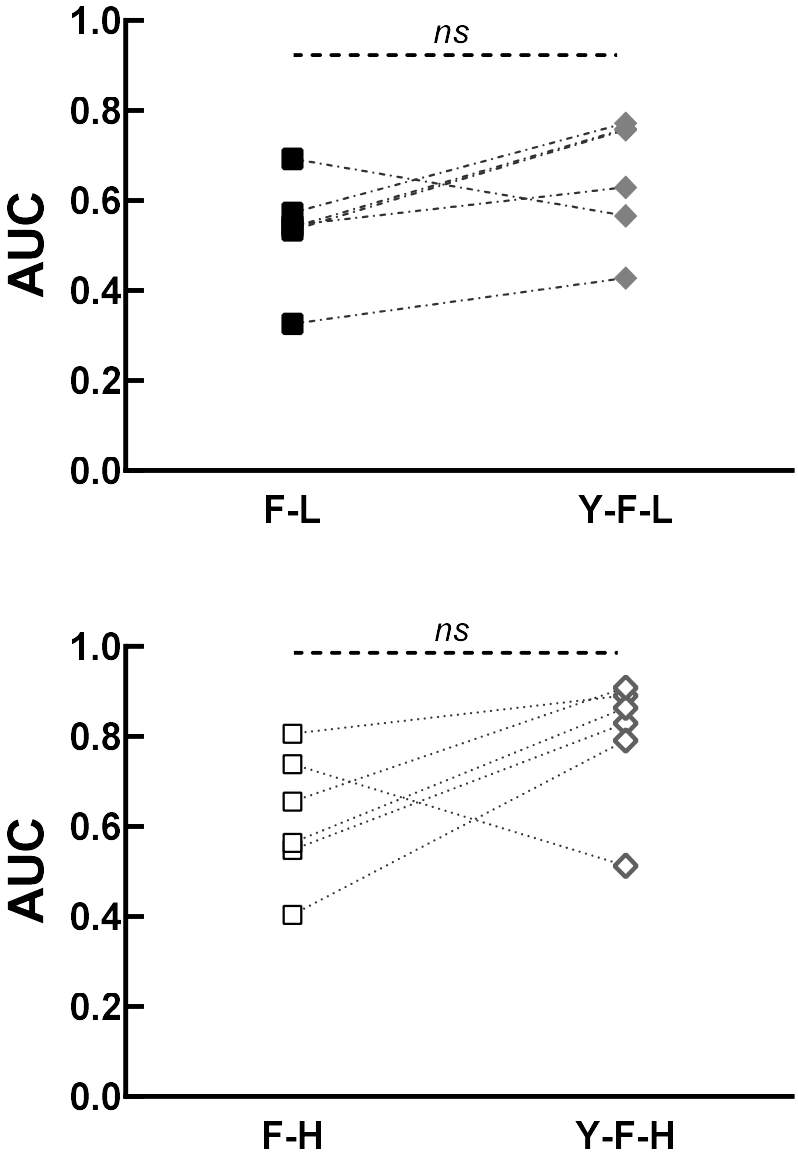

Figure 69. Area under consumption curves across force and yoked progressions. Shown are AUCs (y-axis) calculated by normalizing consumption based on consumption at the first step in that progression.

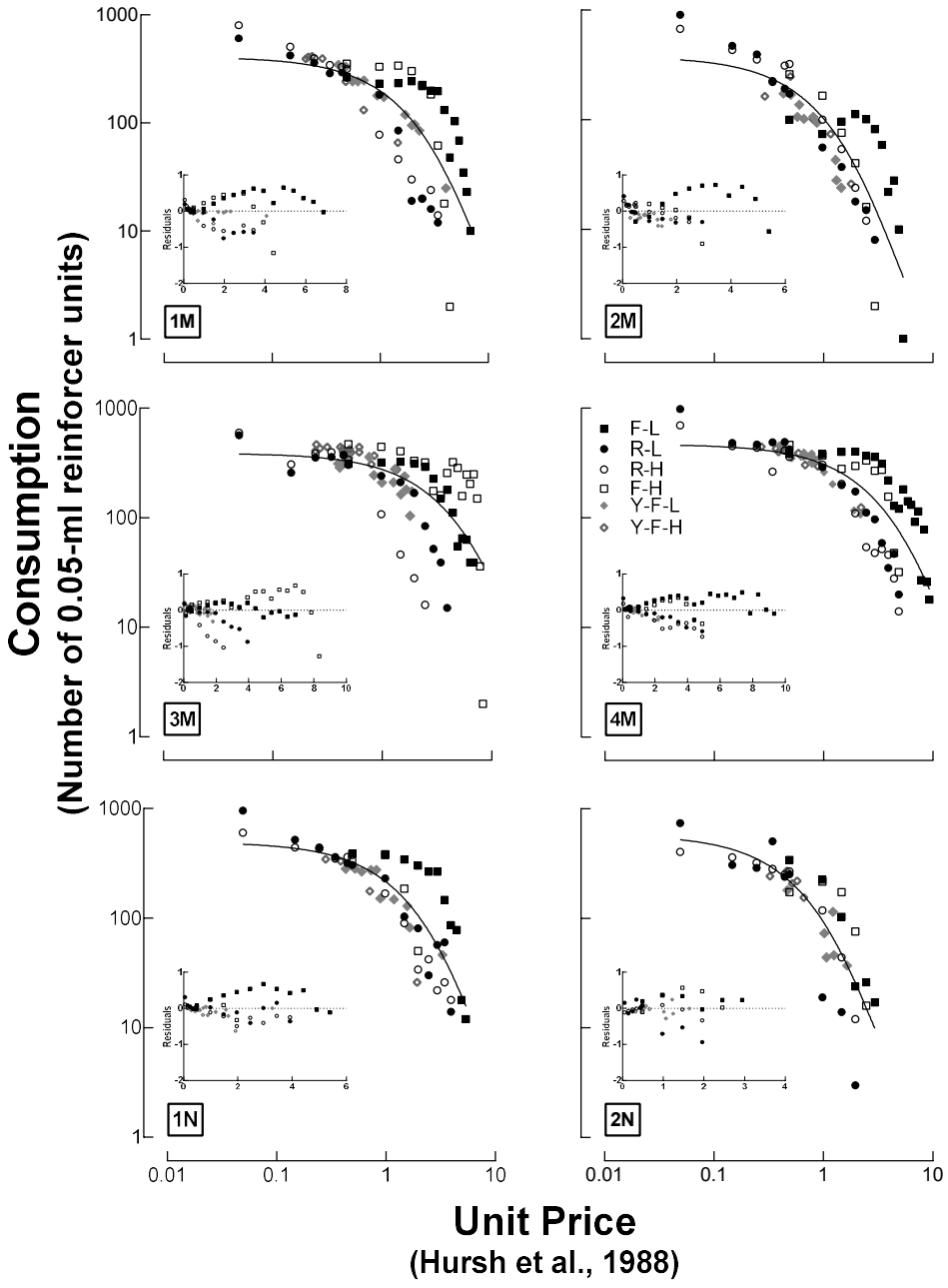

Figure 70. Single exponential demand curve fit to consumption as a function of unit price from all progressions from Experiment 1 and Experiment 2 for each animal. Closed circles show R-L progressions, open circles show R-H progressions, closed squares show F-L progressions, open squares show F-H progressions, closed gray diamond show Y-F-L progressions, and open gray diamonds show Y-F-H progressions.

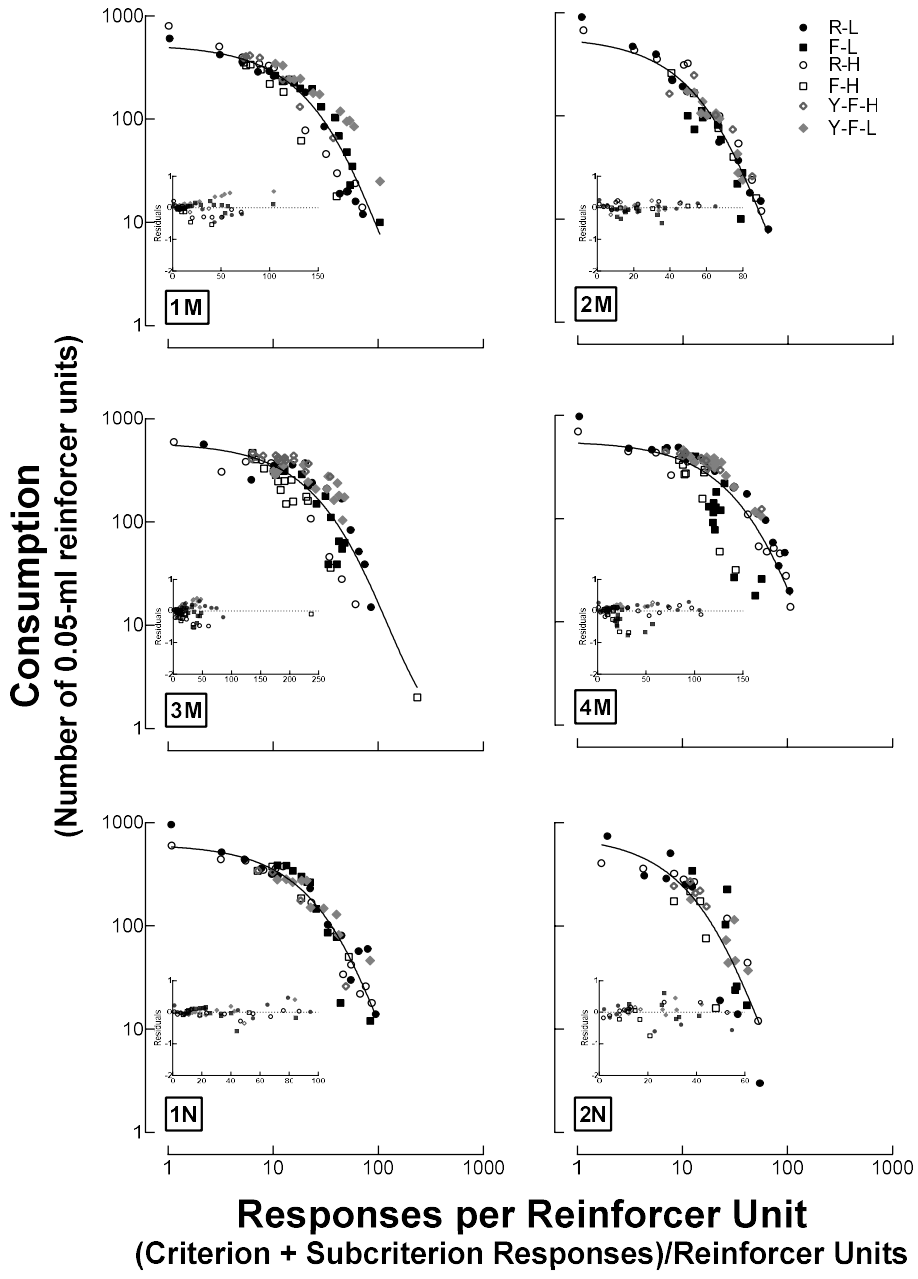

Figure 71. Single exponential demand curve fit to consumption as a function responses per reinforcer unit for all progressions from Experiment 1 and Experiment 2 for each animal. Closed circles show R-L progressions, open circles show R-H progressions, closed squares show F-L progressions, open squares show F-H progressions, closed gray diamond show Y-F-L progressions, and open gray diamonds show Y-F-H progressions.

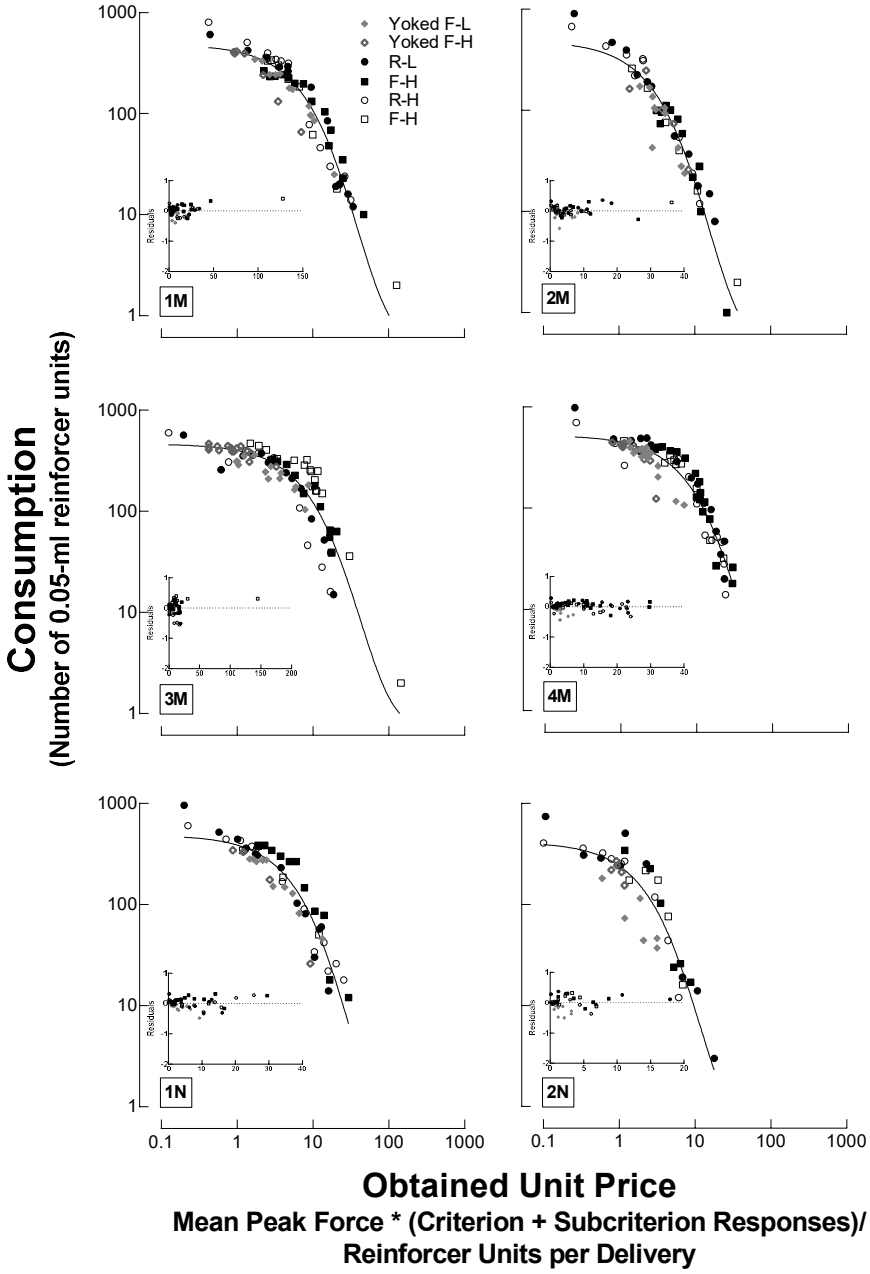

Figure 72. Single exponential demand curve fit to consumption as a function of obtained unit price from all progressions for each animal from Experiment 1 and Experiment 2. Closed circles show R-L progressions, open circles show R-H progressions, closed squares show F-L progressions, open squares show F-H progressions, closed gray diamond show Y-F-L progressions, and open gray diamonds show Y-F-H progressions.

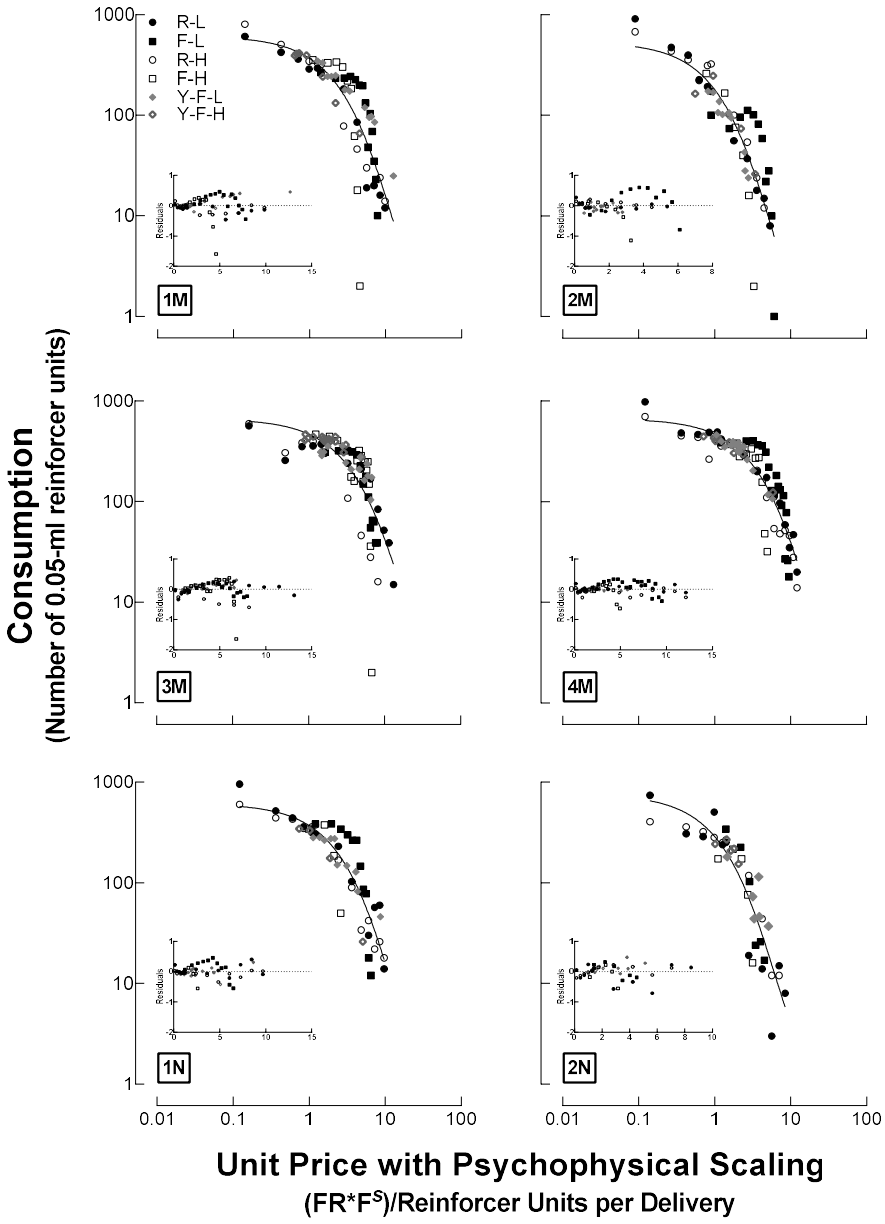

Figure 73. Single exponential demand curve fit to consumption as a function of unit price with psychophysical scaling parameter adjustments for all progressions for each animal from Experiment 1 and Experiment 2. Closed circles show R-L progressions, open circles show R-H progressions, closed squares show F-L progressions, open squares show F-H progressions, closed gray diamond show Y-F-L progressions, and open gray diamonds show Y-F-H progressions.

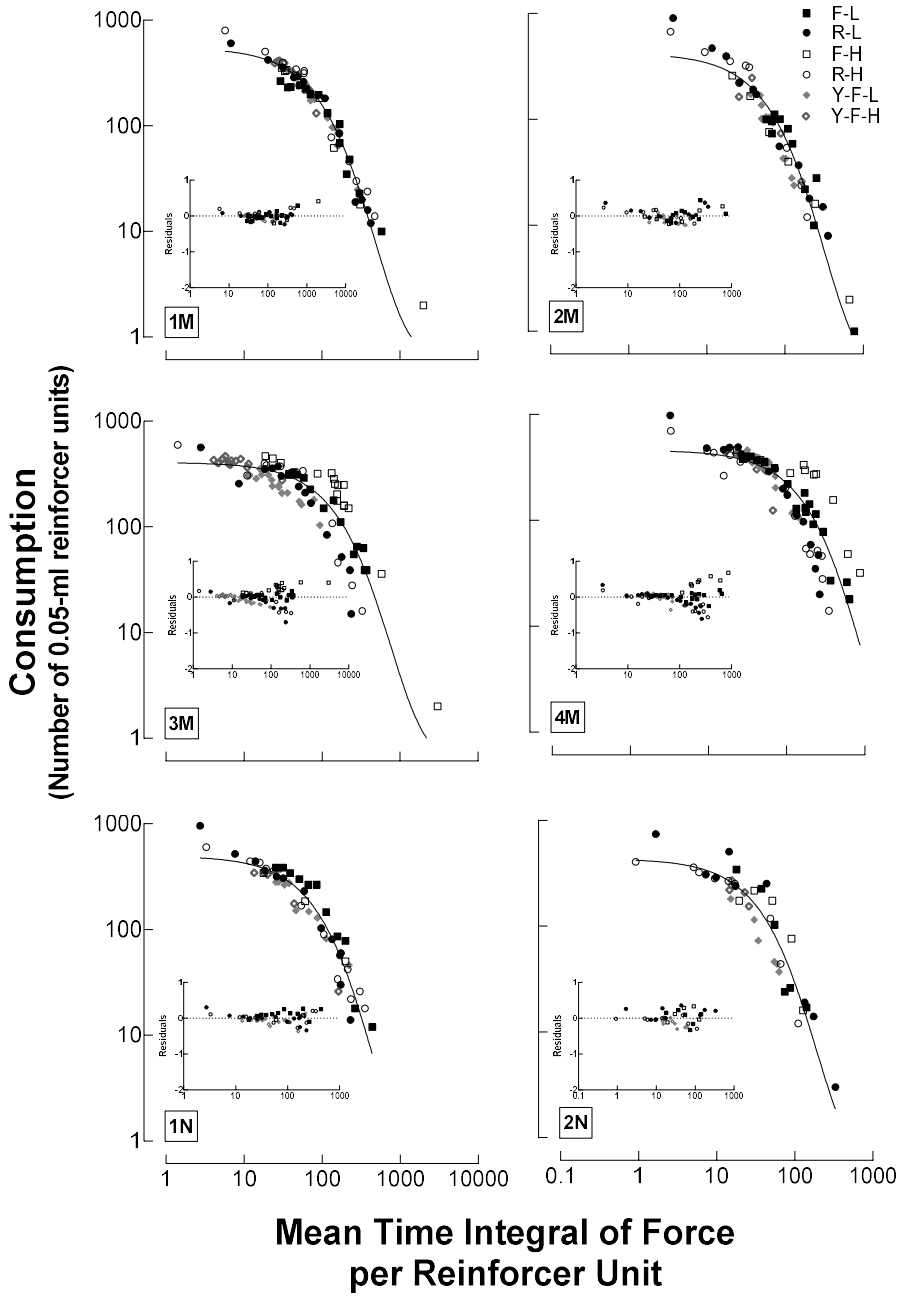

Figure 74. Single exponential demand curve fit to consumption as a function of cumulative time integral of force per reinforcer unit from all progressions for each animal from Experiment 1 and Experiment 2. Closed circles show R-L progressions, open circles show R-H progressions, closed squares show F-L progressions, open squares show F-H progressions, closed gray diamond show Y-F-L progressions, and open gray diamonds show Y-F-H progressions.

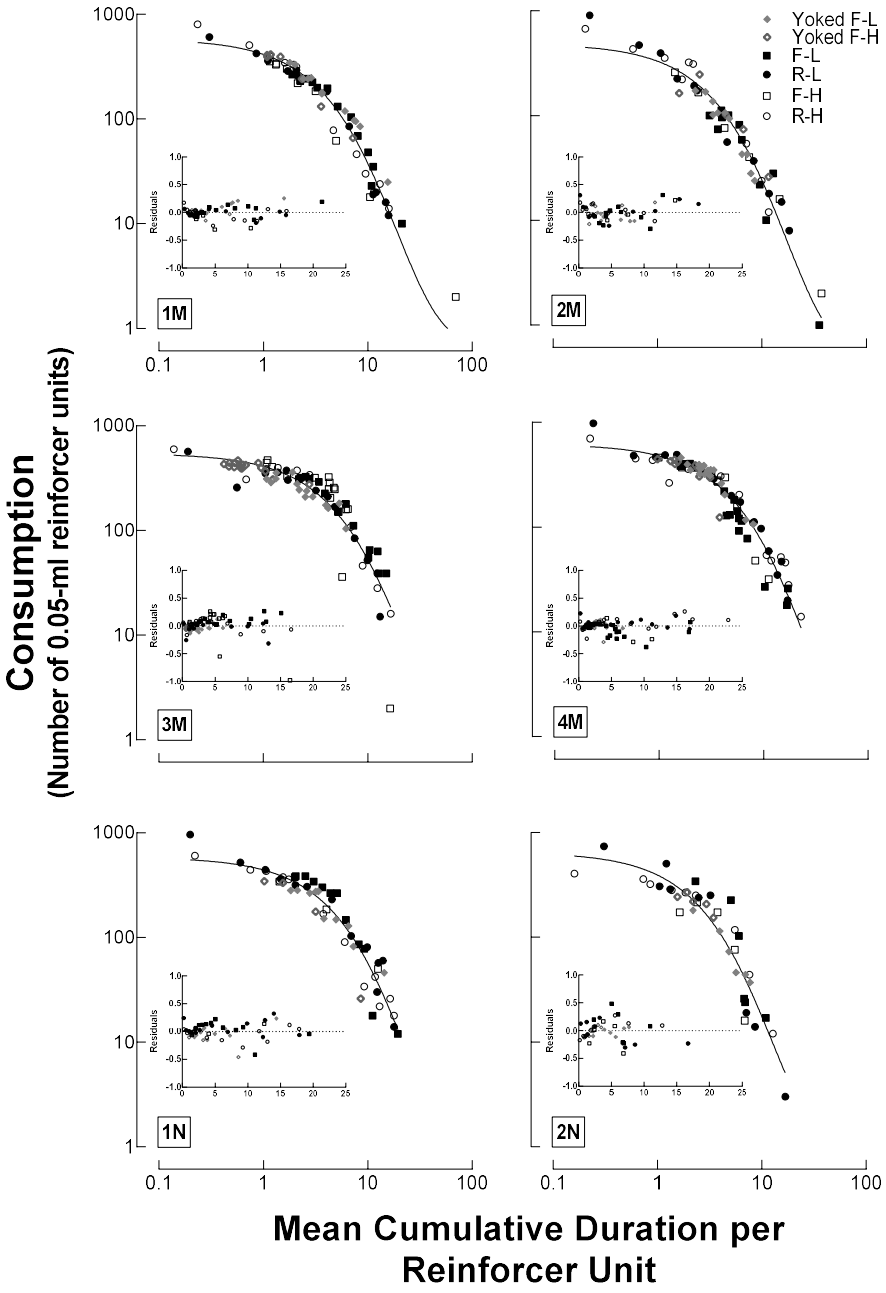

Figure 75. Single exponential demand curve fit to consumption as a function of cumulative response duration per reinforcerunit from all progressions for each animal from Experiment 1 and Experiment 2. Closed circles show R-L progressions, open circles show R-H progressions, closed squares show F-L progressions, open squares show F-H progressions, closed gray diamond show Y-F-L progressions, and open gray diamonds show Y-F-H progressions.

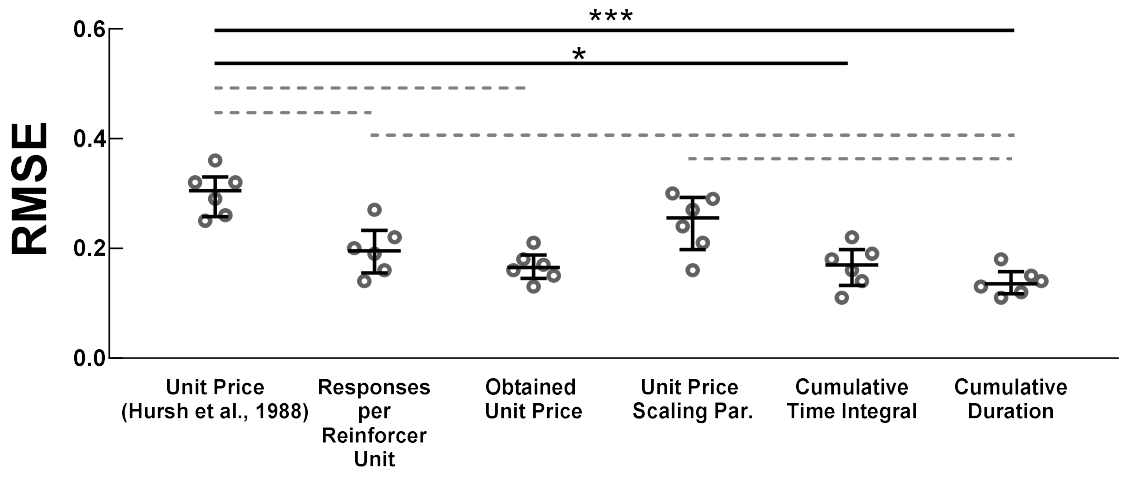

Figure 76. RMSE for a single exponential curve fit to each animal's data across all progressions for different price conversions. Data are included from Experiment 1 and Experiment 2. Gray open circles show each animal's RMSE for a single curve fit to data from all progressions. Lines and error bars show medians and IQRs. Gray dashed lines show significant differences prior to correction and black lines show differences that remained significant after Dunn's corrections for multiple comparisons.

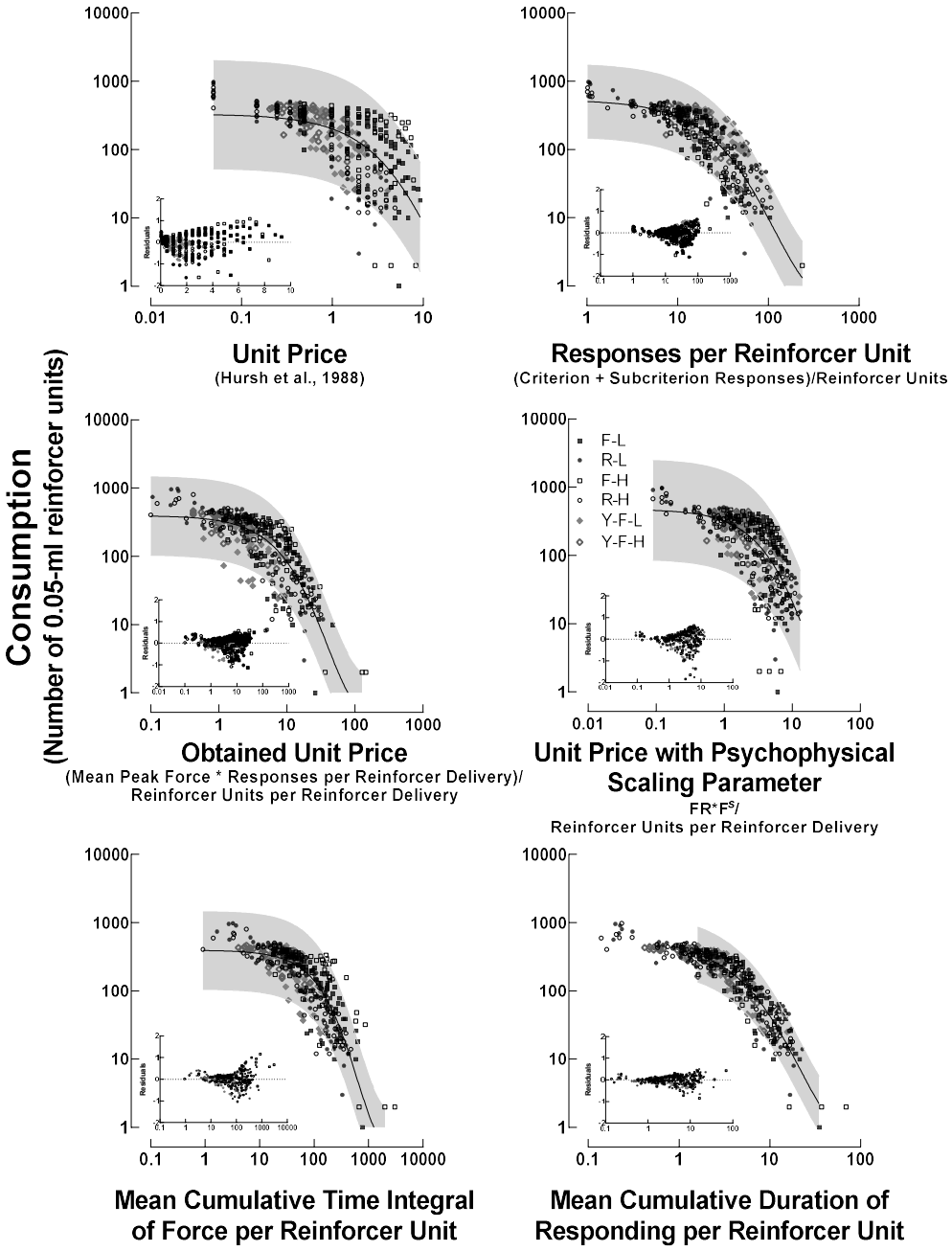

Figure 77. Exponential curves fit to group Experiment 1 and Experiment 2 data across price modifications. Closed circles show R-L progressions, open circles show R-H progressions, closed squares show F-L progressions, open squares show F-H progressions, gray closed diamonds show Y-F-L progressions, and open gray diamonds show Y-F-H progressions. The gray shaded regions show 95% prediction bands. Inset panels show residuals.

Figure 78. Error from a single exponential curve fit to all rats' data from all Experiment 1 and Experiment 2 progressions for each price modification. Shown is the RMSE for a single curve for all progression types (black stars). The y-axis shows RMSE for the respective price modifications (x-axis).

Appendices Appendix A

A. Alternative Approaches to Analyzing Demand Data

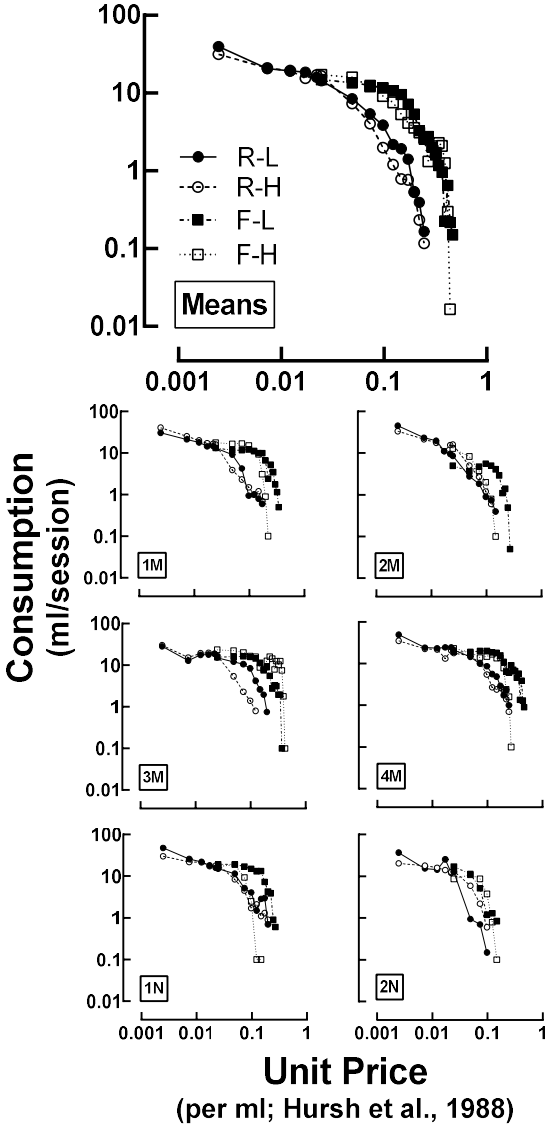

Figure A1. Consumption (ml) as a function of unit price (per ml) across demand assays. Top panel shows means, and six lower panels show data from individual rats (subject codes at lower left). Closed circles and solid lines show R-L progressions, open circles and dashed lines show R-H progressions, closed squares and dot-dashed lines show F-L progressions, and open squares and dotted lines show F-H progressions.

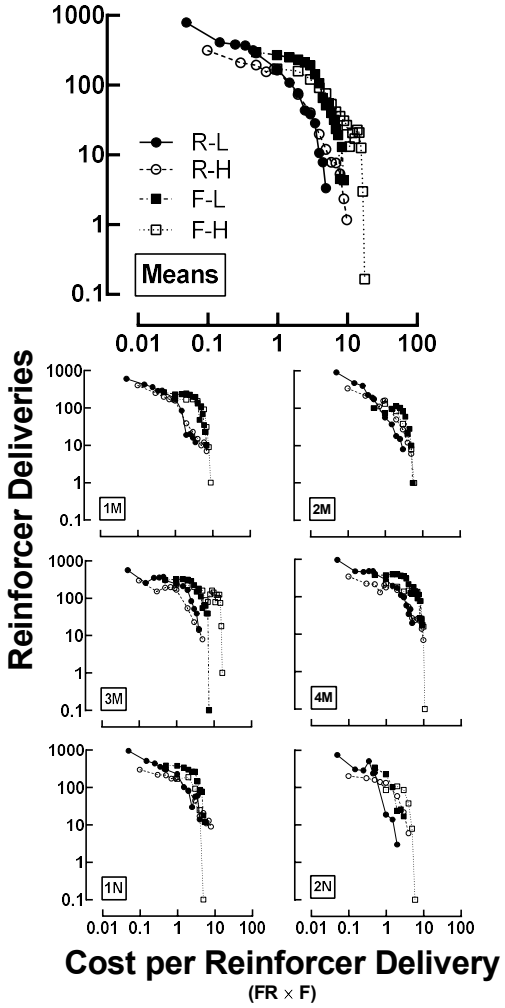

Figure A2. Reinforcer deliveries as a function of cost per reinforcer delivery (FR x Force criterion) across demand assays. Top panel shows means, and six lower panels show data from individual rats (subject codes at lower left). Closed circles and solid lines show R-L progressions, open circles and dashed lines show R-H progressions, closed squares and dot-dashed lines show F-L progressions, and open squares and dotted lines show F-H progressions. Note that cost per reinforcer delivery is greater in the higher magnitude conditions because based on the equated unit price, a greater volume of reinforcer is received for each ratio completion. Additionally, the quantity of milk for each reinforcer delivery in the low reinforcer magnitude condition was half that in the higher reinforcer magnitude condition.

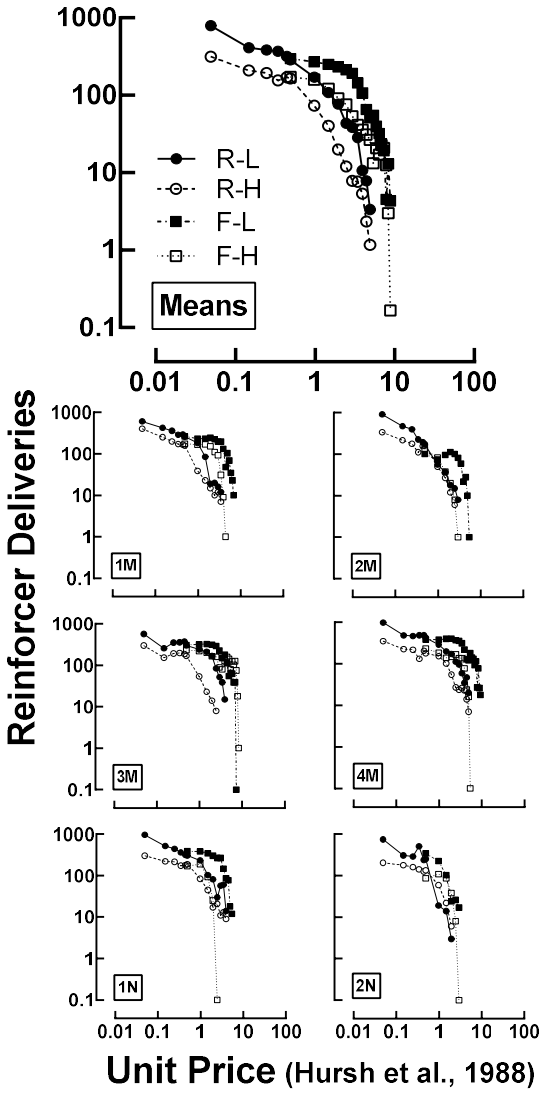

Figure A3. Reinforcer deliveries as a function of unit price across demand assays. Top panel shows means, and six lower panels show data from individual rats (subject codes at lower left). Closed circles and solid lines show R-L progressions, open circles and dashed lines show R-H progressions, closed squares and dot-dashed lines show F-L progressions, and open squares and dotted lines show F-H progressions. Note that the quantity of milk for each reinforcer delivery in the low reinforcer magnitude condition was half that in the higher reinforcer magnitude condition.

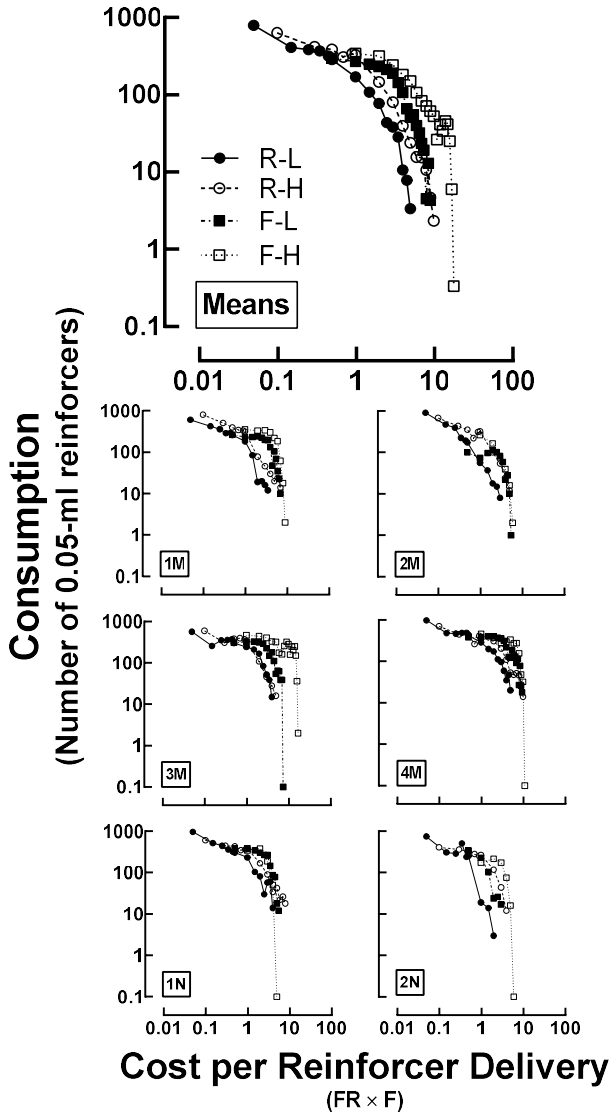

Figure A4. Consumption as a function of cost per reinforcer delivery (FR x Force criterion) across demand assays. Top panel shows means, and six lower panels show data from individual rats (subject codes at lower left). Closed circles and solid lines show R-L progressions, open circles and dashed lines show R-H progressions, closed squares and dot-dashed lines show F-L progressions, and open squares and dotted lines show F-H progressions. Note that cost per reinforcer delivery is greater in the higher magnitude conditions because based on the equated unit price, a greater volume of reinforcer is received for each ratio completion.

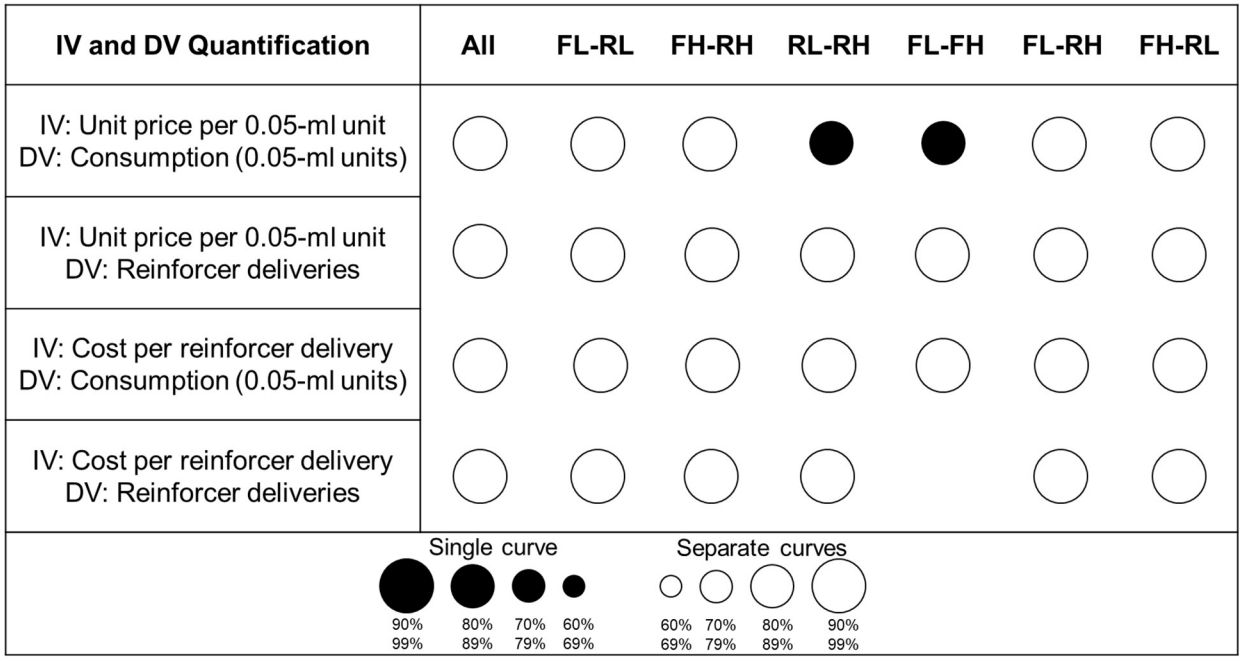

Figure A5. Comparisons using AICc of group data across different approaches to quantifying cost and benefit. Preferred model as determined by AICc comparisons is shown across different comparisons for different price conversions (rows). Filled, black circles indicate a single curve for the specified progressions was preferred; open, white circles indicate preference for separate curves for the progressions. Circle size shows relative probability. Comparisons that resulted in relative indifference (i.e., 50-59.9% likelihood) are shown by blanks.

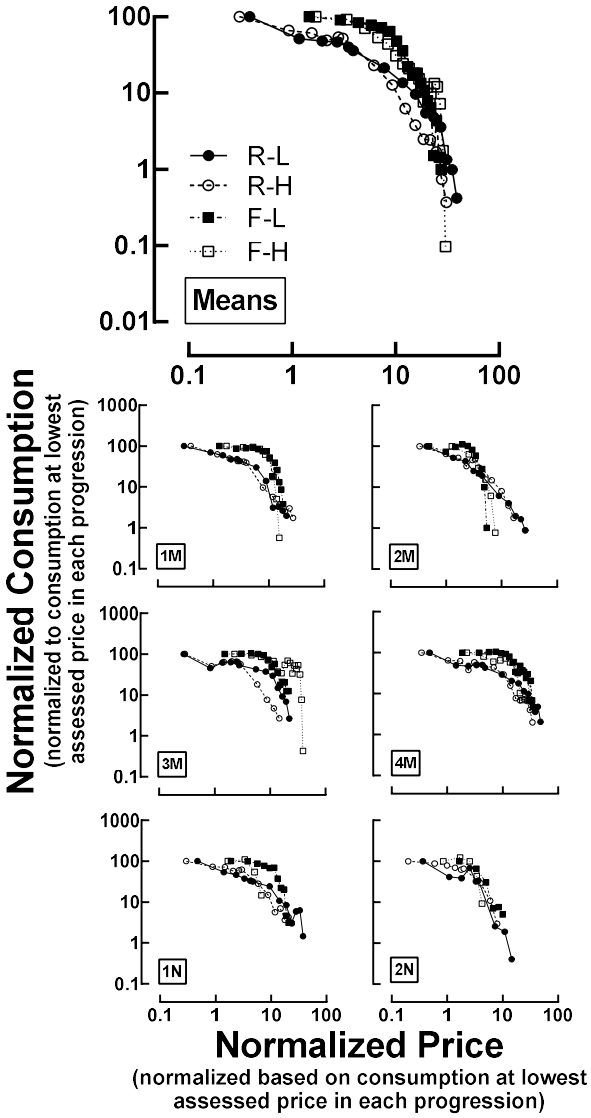

Figure A6. Normalized consumption as a function of normalized price, with consumption and price normalized based on consumption at first assessed price within each progression. Top panel shows means, and six lower panels show data from individual rats (subject codes at lower left). Closed circles and solid lines show R-L progressions, open circles and dashed lines show R-H progressions, closed squares and dot-dashed lines show F-L progressions, and open squares and dotted lines show F-H progressions.

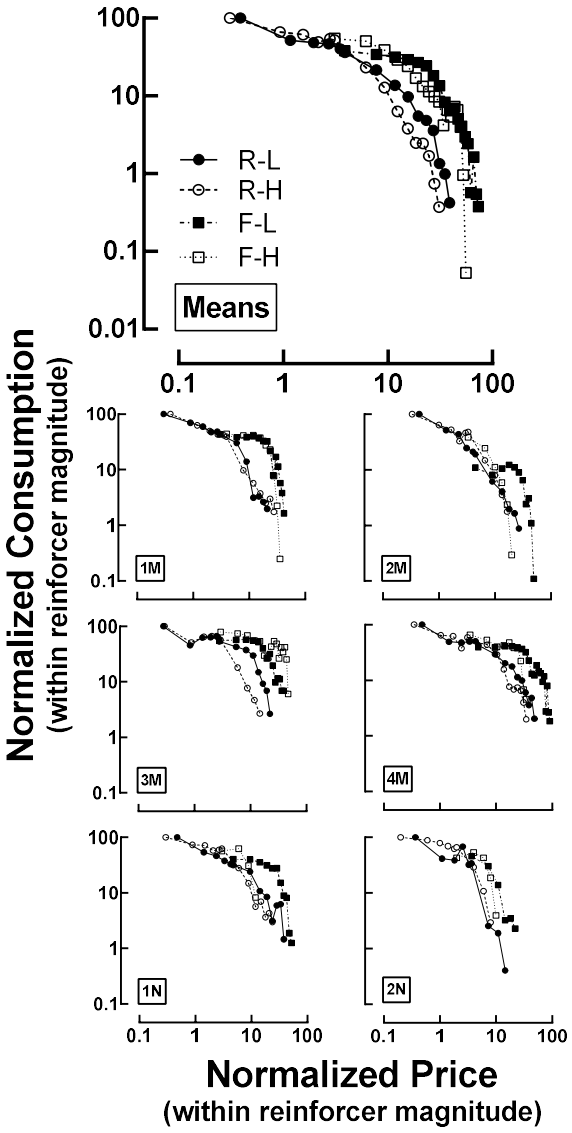

Figure A7. Normalized consumption as a function of normalized price, with consumption and price normalized based on consumption at first assessed price within each reinforcer magnitude (i.e., consumption at UP 0.05 in the R-L or R-H progression). Top panel shows means, and six lower panels show data from individual rats (subject codes at lower left). Closed circles and solid lines show R-L progressions, open circles and dashed lines show R-H progressions, closed squares and dot-dashed lines show F-L progressions, and open squares and dotted lines show F-H progressions.

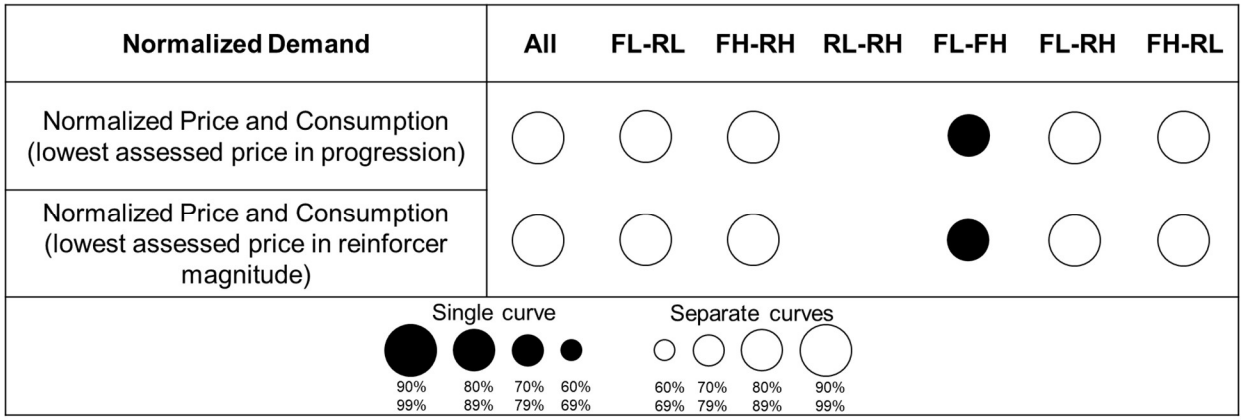

Figure A8. Comparisons using AICc of group data across different normalization approaches. Preferred model as determined by AICc comparisons is shown across different comparisons for different price conversions (rows). Filled, black circles indicate a single curve for the specified progressions was preferred; open, white circles indicate preference for separate curves for the progressions. Circle size shows relative probability. Comparisons that resulted in relative indifference (i.e., 50-59.9% likelihood) are shown by blanks.

Appendix B

B. Additional Analyses

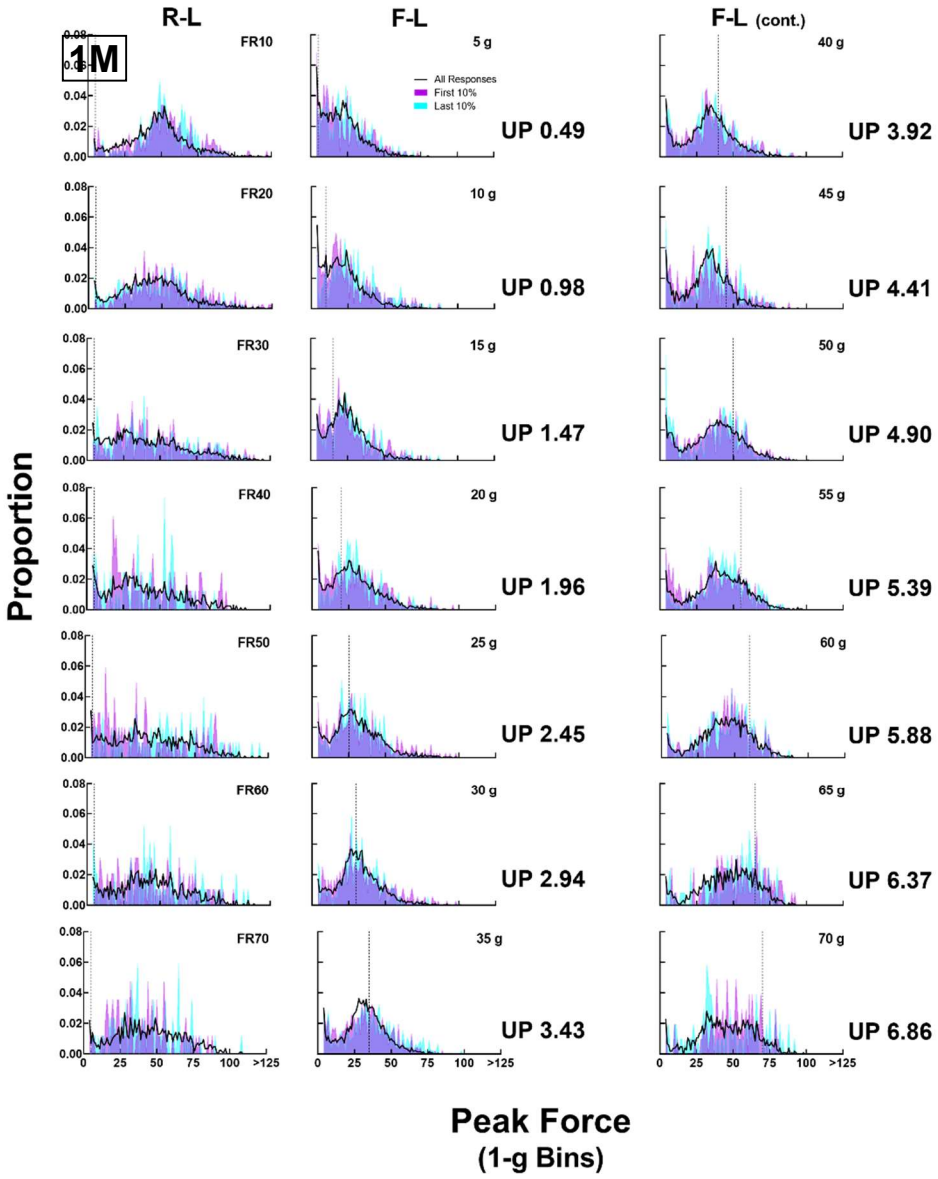

Figure B1. Peak force distributions from the R-L and F-L progressions for 1M. The proportion of responses (y-axis) in 1-g force bins (x-axis) is shown for all responses (black data path), first 10% of responses (magenta shaded region) and last 10% of responses (cyan shaded region) in each session. Horizontal dashed lines show the force criterion. Matched unit prices are shown by rows for the R-L (left column) and F-L (middle column; continued in right column).

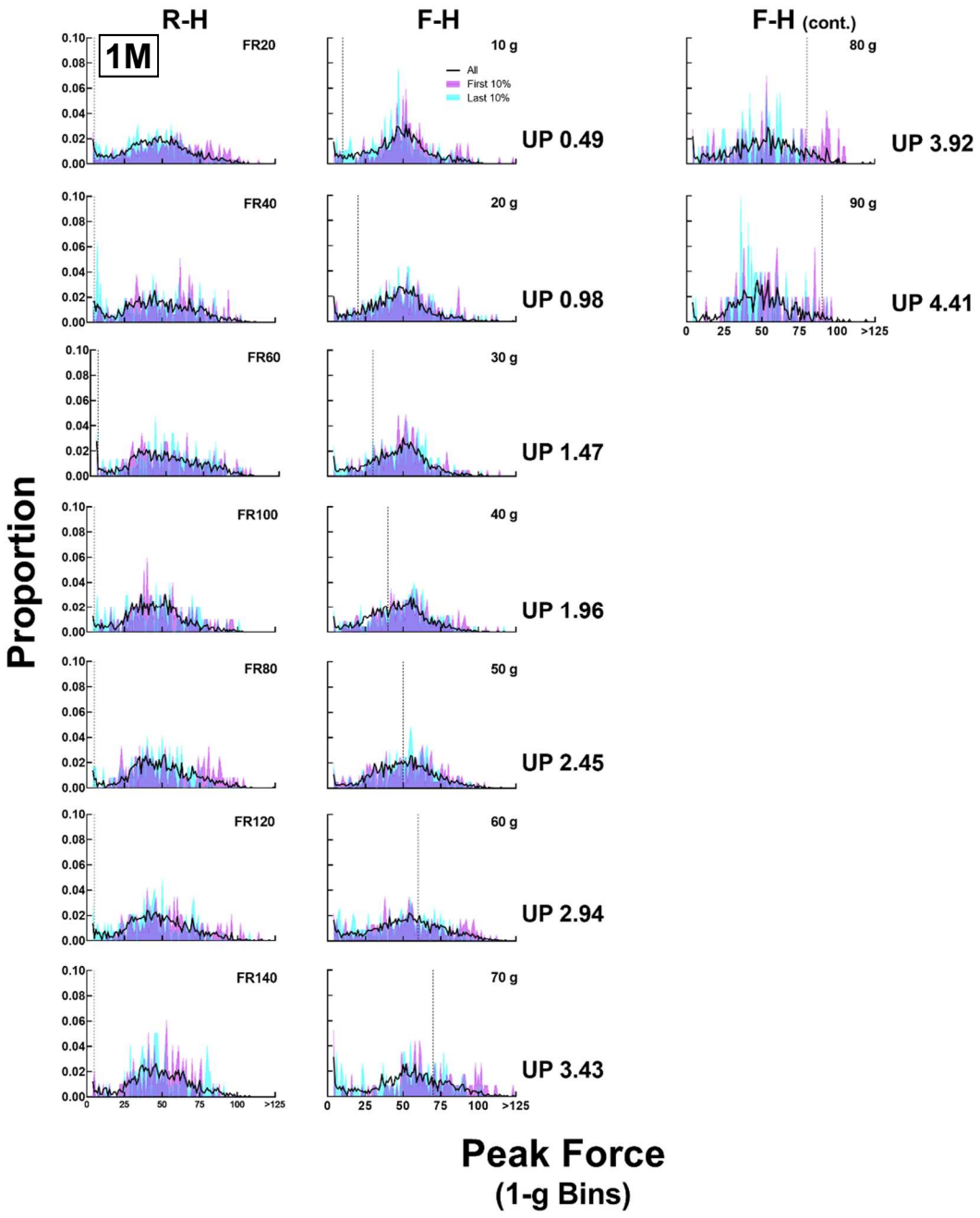

Figure B2. Peak force distributions from the R-H and F-H progressions for 1M. The proportion of responses (y-axis) in 1-g force bins (x-axis) is shown for all responses (black data path), first 10% of responses (magenta shaded region) and last 10% of responses (cyan shaded region) in each session. Horizontal dashed lines show the force criterion. Matched unit prices are shown by rows for the R-H (left column) and F-H (middle column; continued in right column).

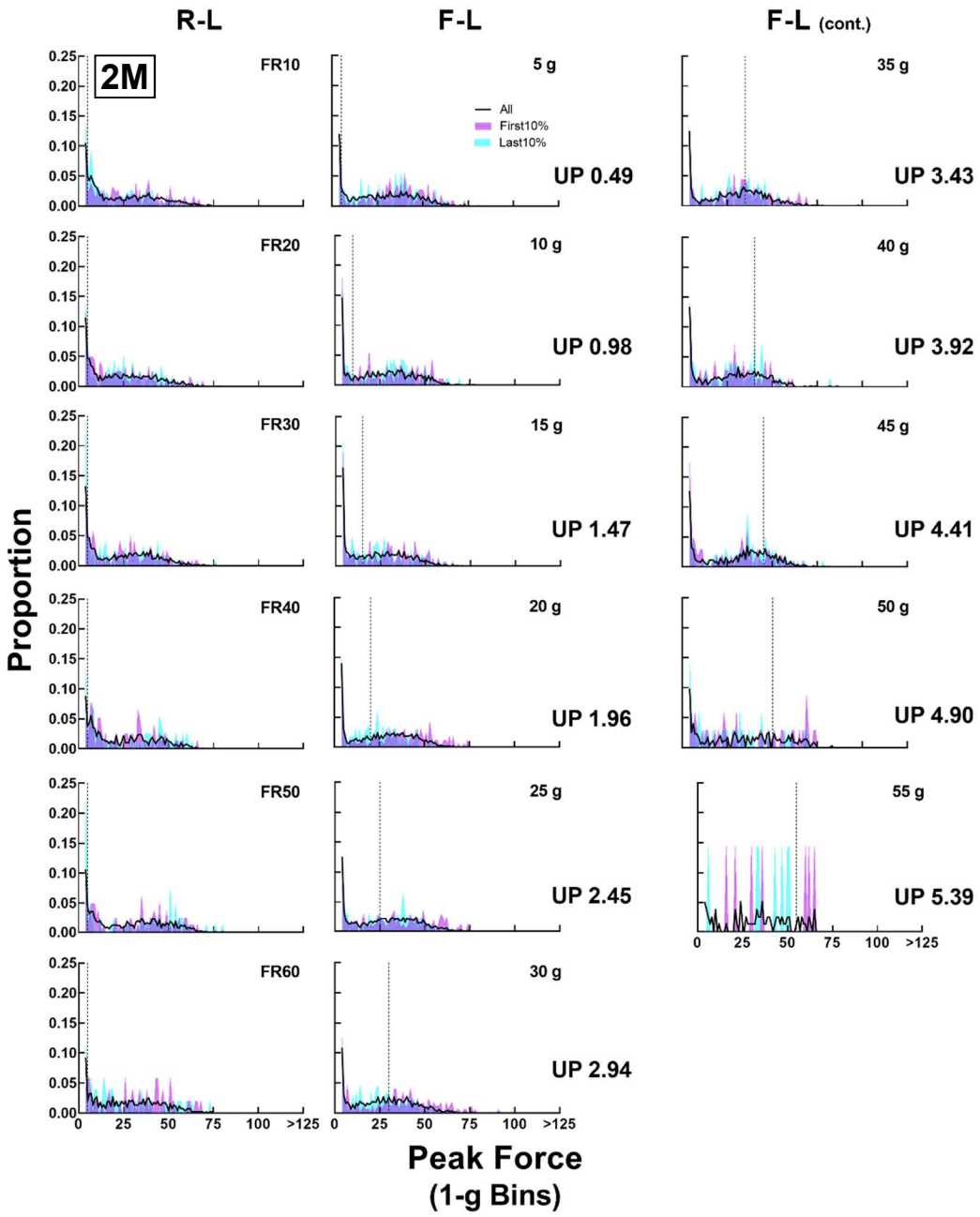

Figure B3. Peak force distributions from the R-L and F-L progressions for 2M. The proportion of responses (y-axis) in 1-g force bins (x-axis) is shown for all responses (black data path), first 10% of responses (magenta shaded region) and last 10% of responses (cyan shaded region) in each session. Horizontal dashed lines show the force criterion. Matched unit prices are shown by rows for the R-L (left column) and F-L (middle column; continued in right column).

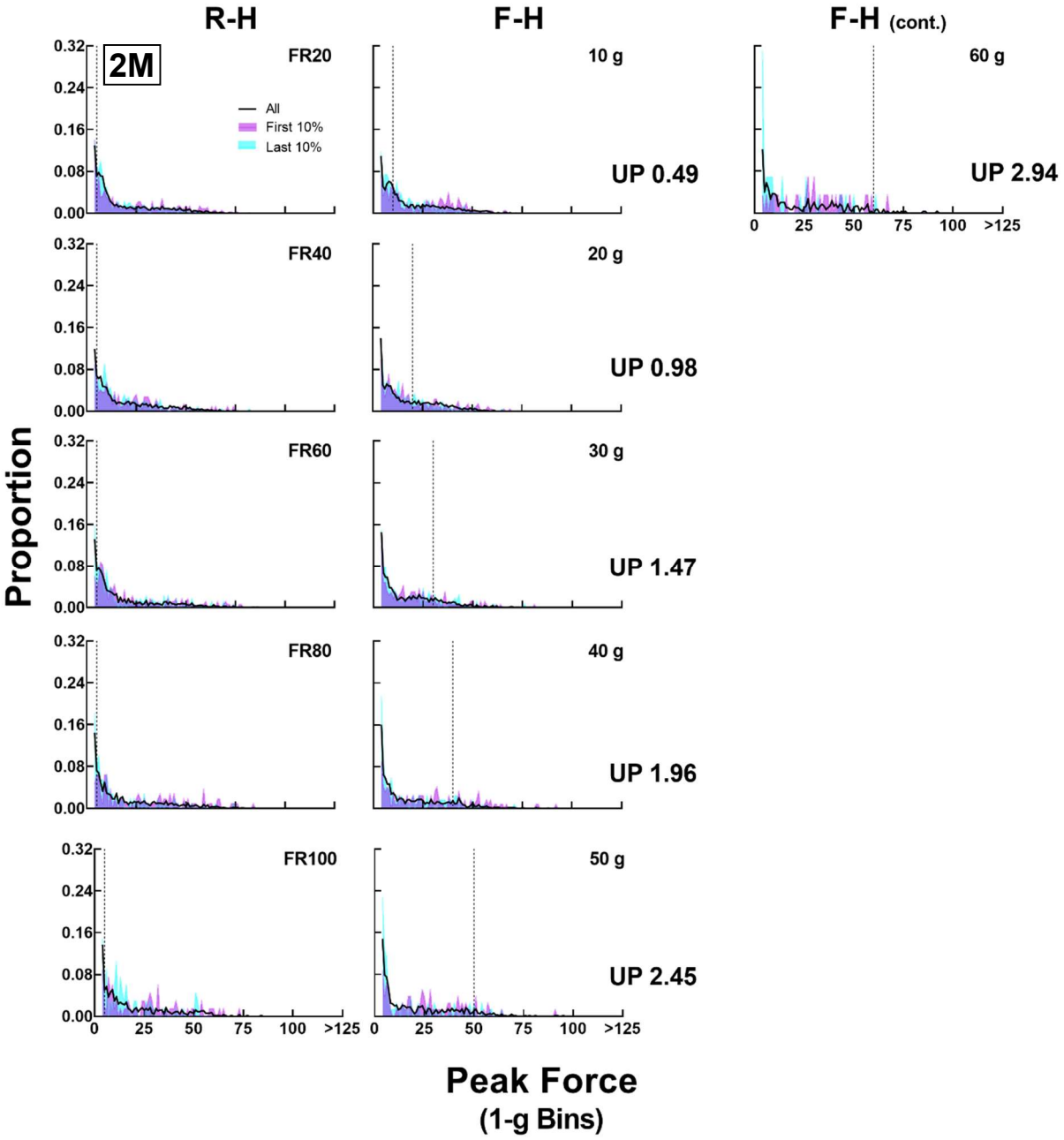

Figure B4. Peak force distributions from the R-H and F-H progressions for 2M. The proportion of responses (y-axis) in 1-g force bins (x-axis) is shown for all responses (black data path), first 10% of responses (magenta shaded region) and last 10% of responses (cyan shaded region) in each session. Horizontal dashed lines show the force criterion. Matched unit prices are shown by rows for the R-H (left column) and F-H (middle column; continued in right column).

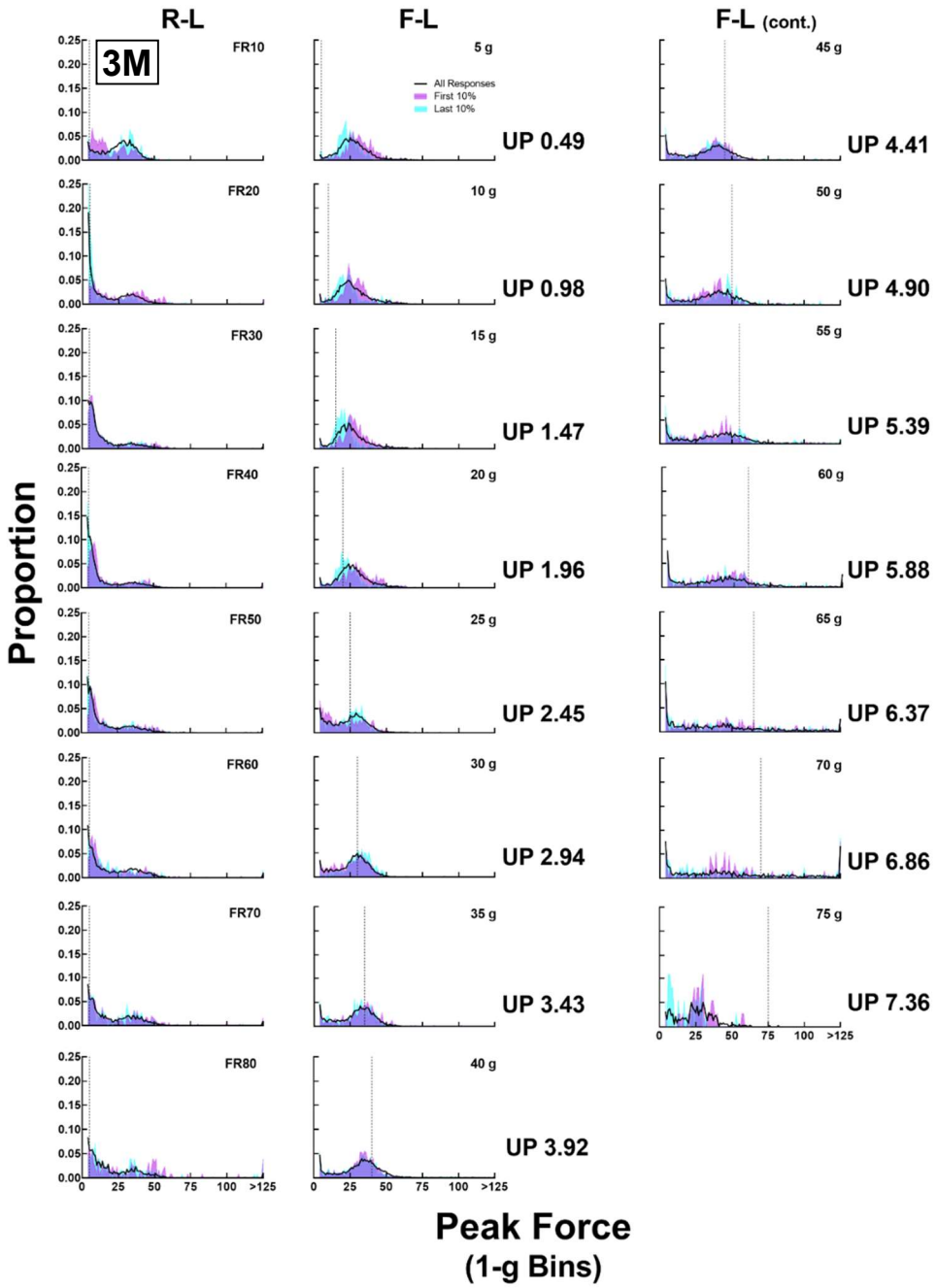

Figure B5. Peak force distributions from the R-L and F-L progressions for 3M. The proportion of responses (y-axis) in 1-g force bins (x-axis) is shown for all responses (black data path), first 10% of responses (magenta shaded region) and last 10% of responses (cyan shaded region) in each session. Horizontal dashed lines show the force criterion. Matched unit prices are shown by rows for the R-L (left column) and F-L (middle column; continued in right column).

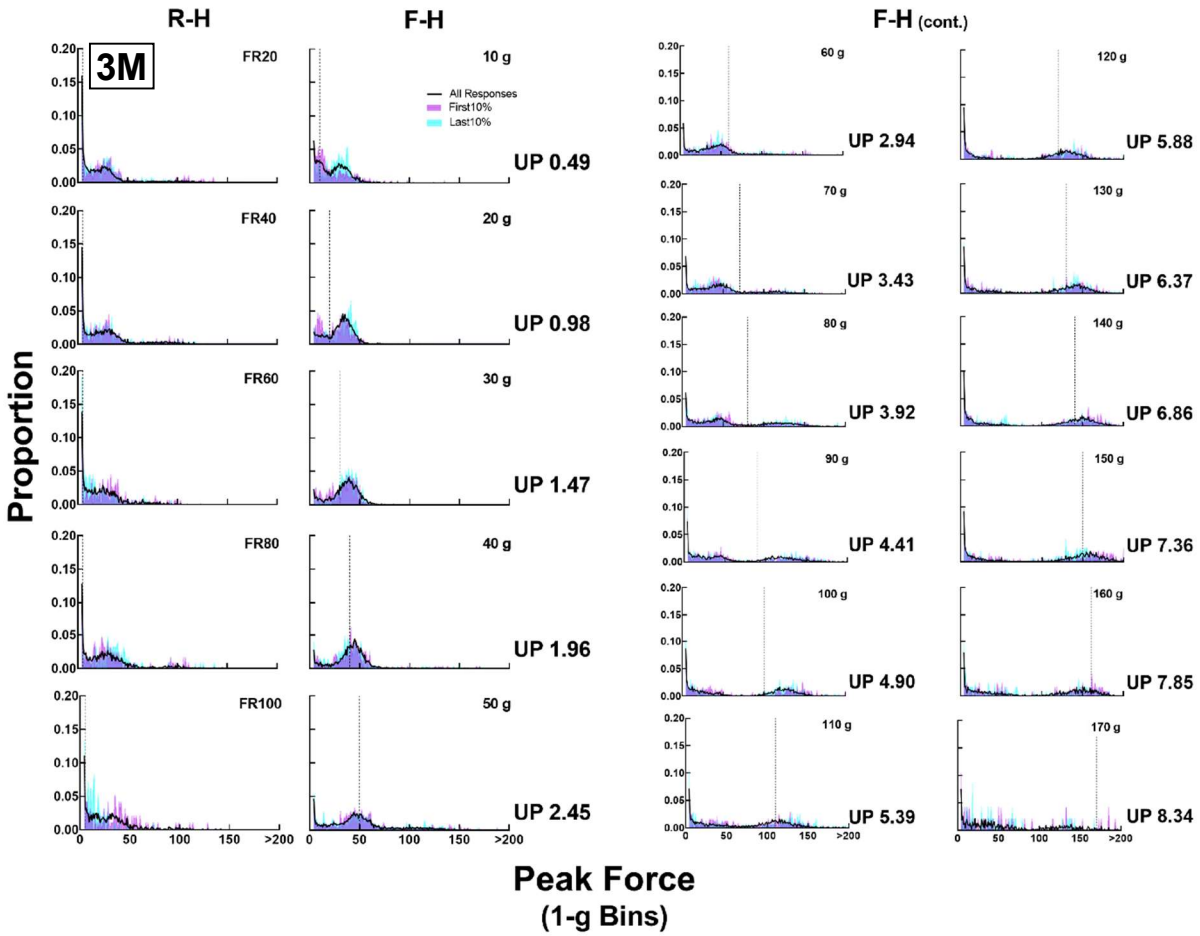

Figure B6. Peak force distributions from the R-H and F-H progressions for 3M. The proportion of responses (y-axis) in 1-g force bins (x-axis) is shown for all responses (black data path), first 10% of responses (magenta shaded region) and last 10% of responses (cyan shaded region) in each session. Horizontal dashed lines show the force criterion. Matched unit prices are shown by rows for the R-H (left column) and F-H (middle column; continued in right column).

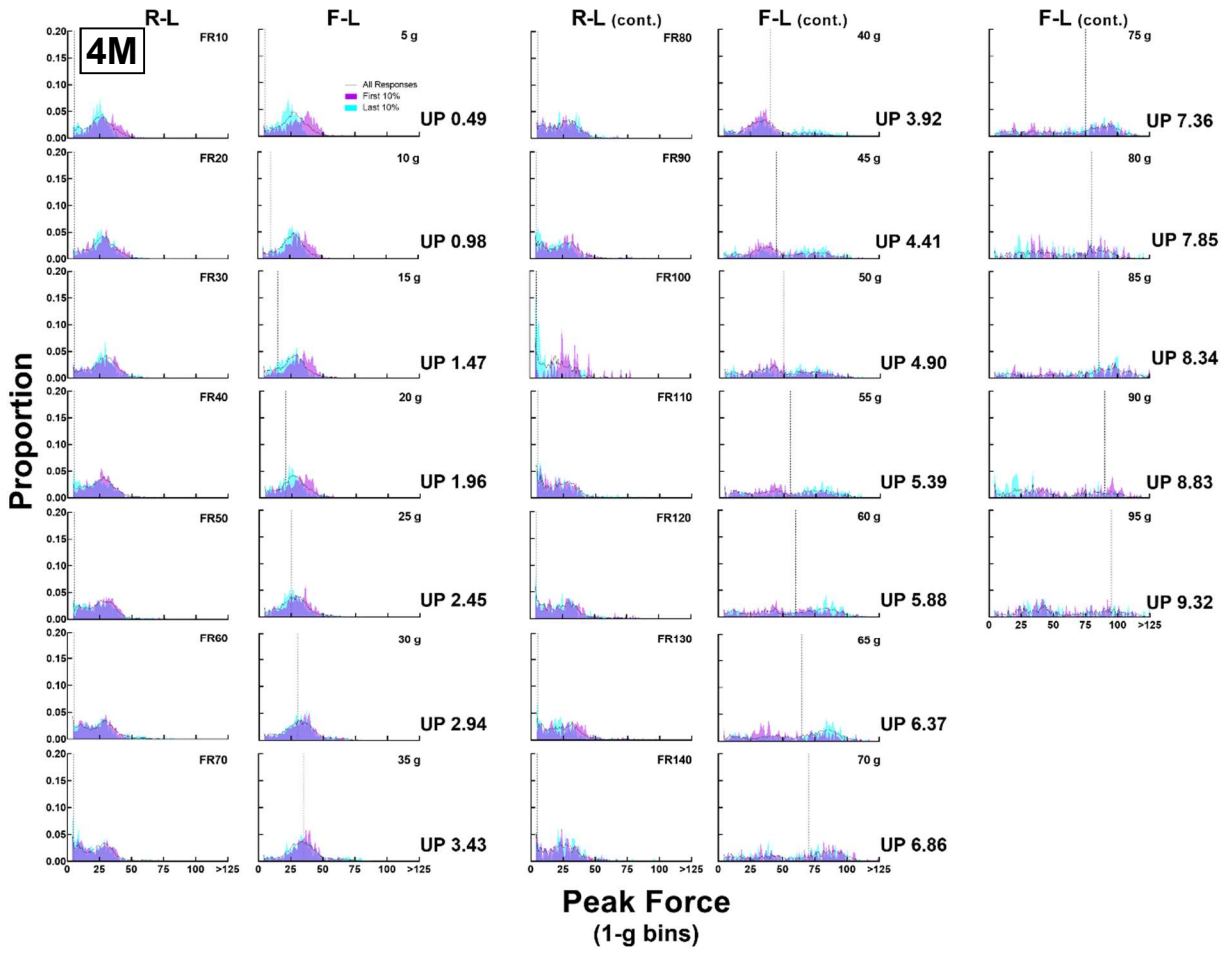

Figure B7. Peak force distributions from the R-L and F-L progressions for 4M. The proportion of responses (y-axis) in 1-g force bins (x-axis) is shown for all responses (black data path), first 10% of responses (magenta shaded region) and last 10% of responses (cyan shaded region) in each session. Horizontal dashed lines show the force criterion. Matched unit prices are shown by rows for the R-L (left column) and F-L (middle column; continued in right column).

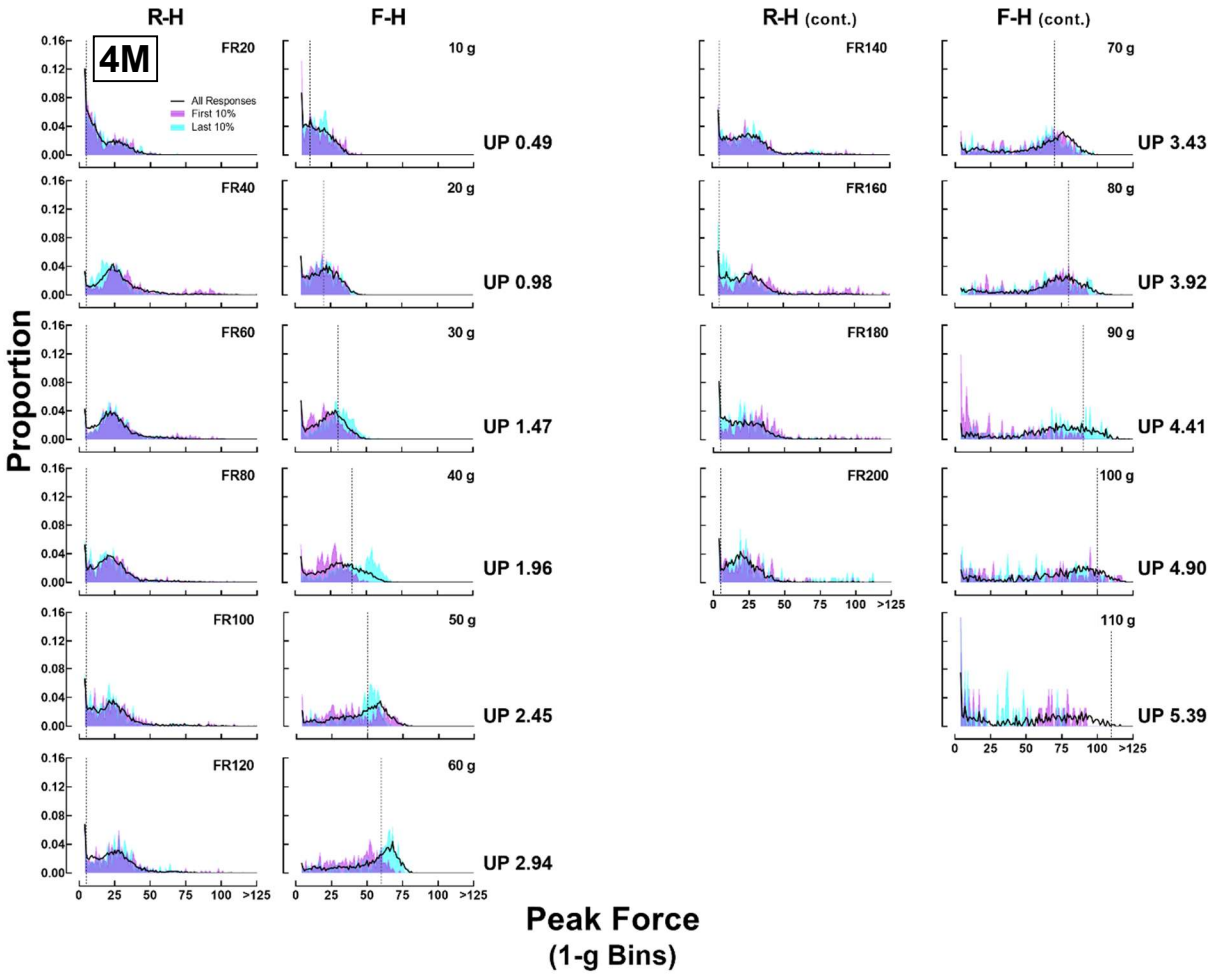

Figure B8. Peak force distributions from the R-H and F-H progressions for 4M. The proportion of responses (y-axis) in 1-g force bins (x-axis) is shown for all responses (black data path), first 10% of responses (magenta shaded region) and last 10% of responses (cyan shaded region) in each session. Horizontal dashed lines show the force criterion. Matched unit prices are shown by rows for the R-H (left column) and F-H (middle column; continued in right column).

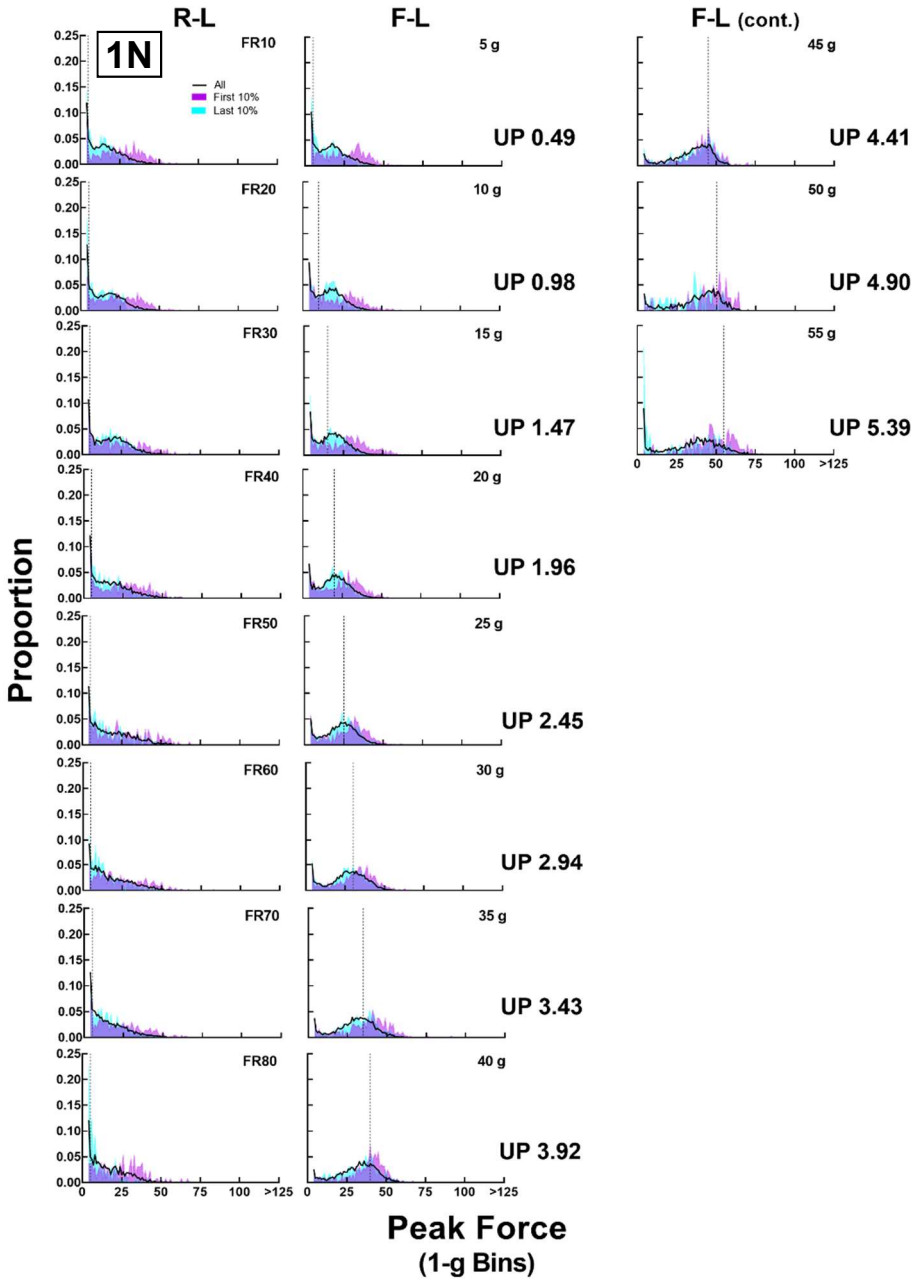

Figure B9. Peak force distributions from the R-L and F-L progressions for 1N. The proportion of responses (y-axis) in 1-g force bins (x-axis) is shown for all responses (black data path), first 10% of responses (magenta shaded region) and last 10% of responses (cyan shaded region) in each session. Horizontal dashed lines show the force criterion. Matched unit prices are shown by rows for the R-L (left column) and F-L (middle column; continued in right column).

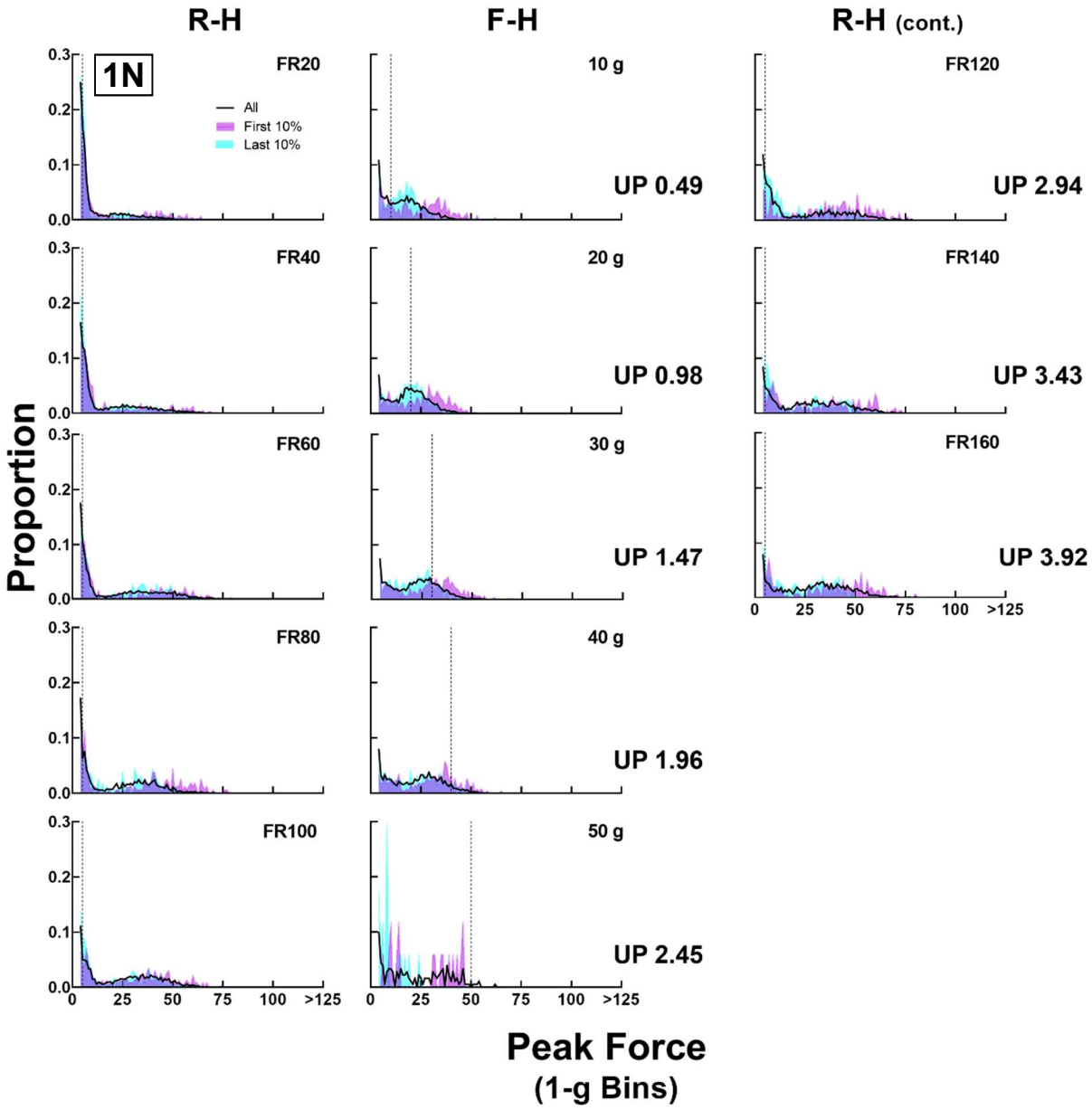

Figure B10. Peak force distributions from the R-H and F-H progressions for 1N. The proportion of responses (y-axis) in 1-g force bins (x-axis) is shown for all responses (black data path), first 10% of responses (magenta shaded region) and last 10% of responses (cyan shaded region) in each session. Horizontal dashed lines show the force criterion. Matched unit prices are shown by rows for the R-H (left column) and F-H (middle column; continued in right column).

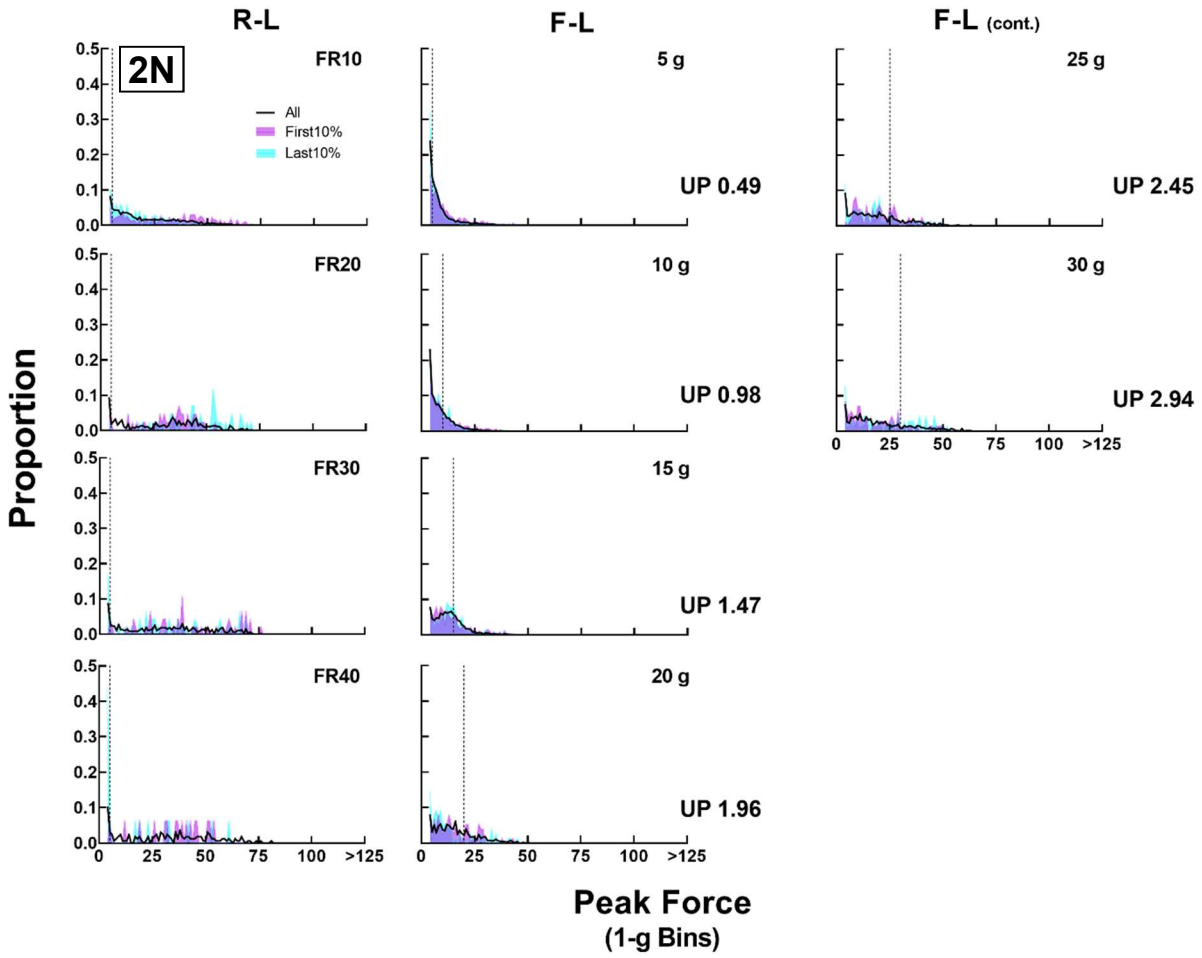

Figure B11. Peak force distributions from the R-L and F-L progressions for 2N. The proportion of responses (y-axis) in 1-g force bins (x-axis) is shown for all responses (black data path), first 10% of responses (magenta shaded region) and last 10% of responses (cyan shaded region) in each session. Horizontal dashed lines show the force criterion. Matched unit prices are shown by rows for the R-L (left column) and F-L (middle column; continued in right column).

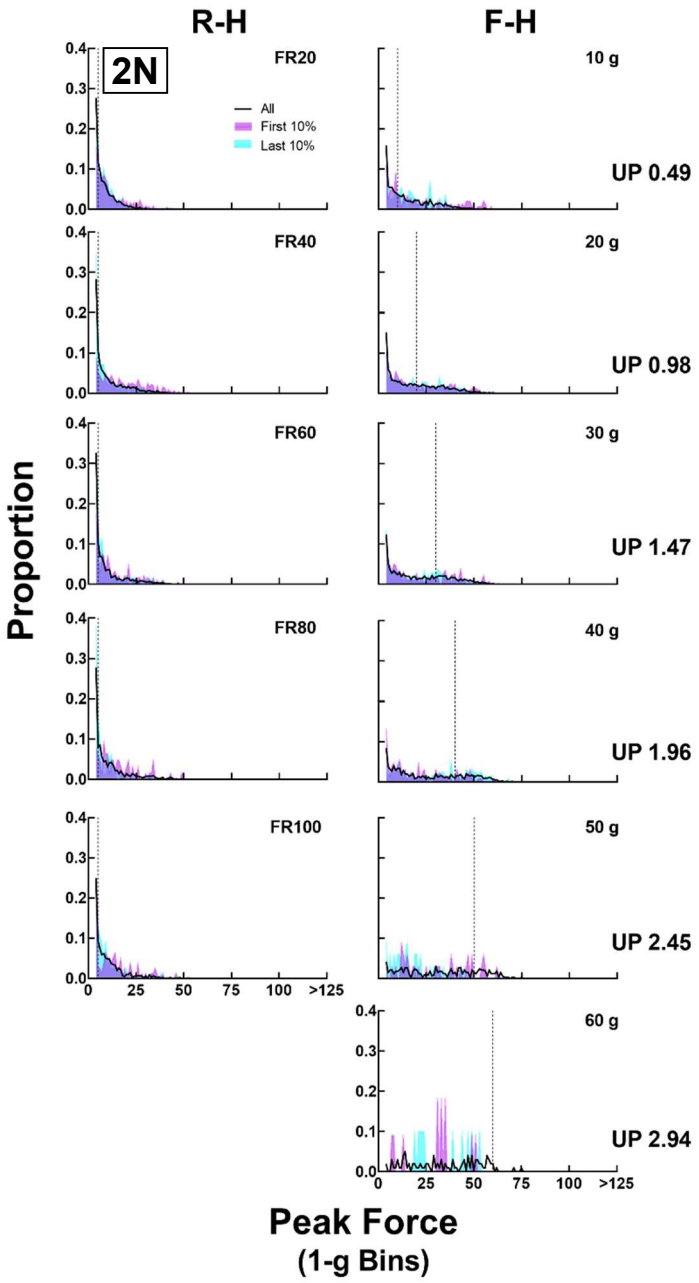

Figure B12. Peak force distributions from the R-H and F-H progressions for 2N. The proportion of responses (y-axis) in 1-g force bins (x-axis) is shown for all responses (black data path), first 10% of responses (magenta shaded region) and last 10% of responses (cyan shaded region) in each session. Horizontal dashed lines show the force criterion. Matched unit prices are shown by rows for the R-H (left column) and F-H (middle column; continued in right column).

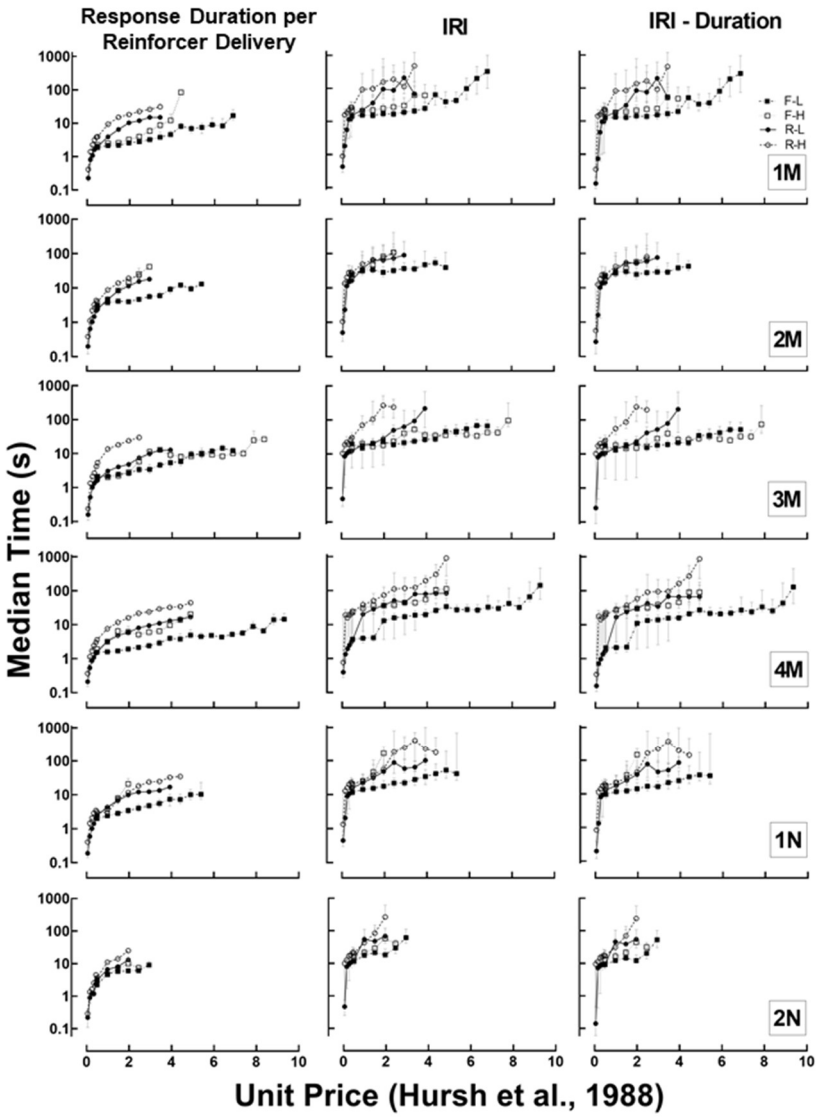

Figure B13. Cumulative response duration per reinforcer delivery, interreinforcement intervals, and difference. First column shows cumulative response duration per reinforcer; second column shows interreinforcement interval (IRI), and last column shows the difference. Median time (s) is plotted along the y-axis as a function of unit price along the x-axis for individual animals in rows. Closed circles and solid lines show R-L progressions, open circles and dashed lines show R-H progressions, closed squares and dot-dashed lines show F-L progressions, and open squares and dotted lines show F-H progressions. Error bars show IQRs.

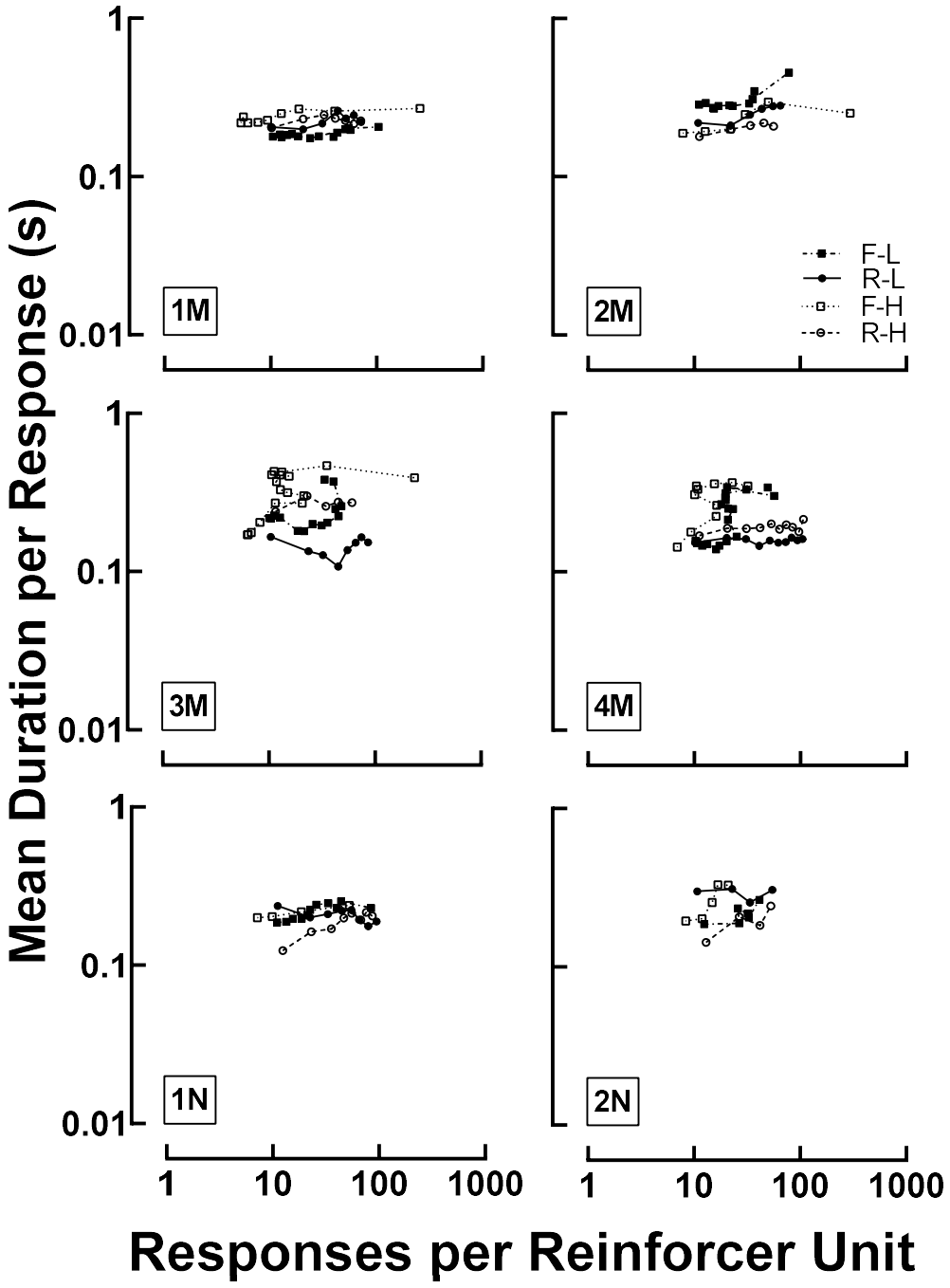

Figure B14. Mean duration per response as a function of responses per reinforcer unit. Closed circles and solid lines show R-L progressions, open circles and dashed lines show R-H progressions, closed squares and dot-dashed lines show F-L progressions, and open squares and dotted lines show F-H progressions.

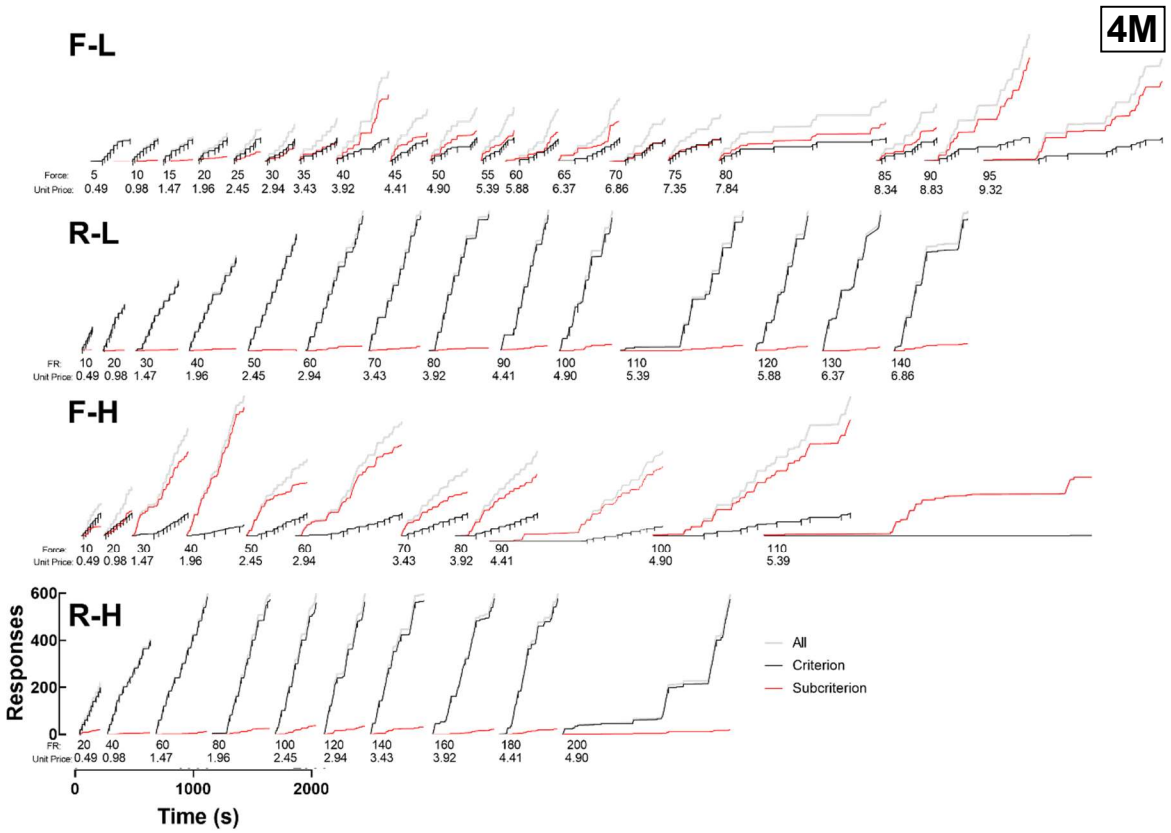

Figure B15. Detailed cumulative record for 4M. Shown are the first 10 reinforcer deliveries or first 600 responses for every price point for the F-L, R-L, F-H, and R-H progressions by rows. Cumulative responses (y-axis) are shown as a function of time in 2-hr session (x-axis). Light gray data paths show all responses, black data paths show criterion responses, and red data paths show subcriterion responses. Black ticks along the criterion data path show reinforcer deliveries.

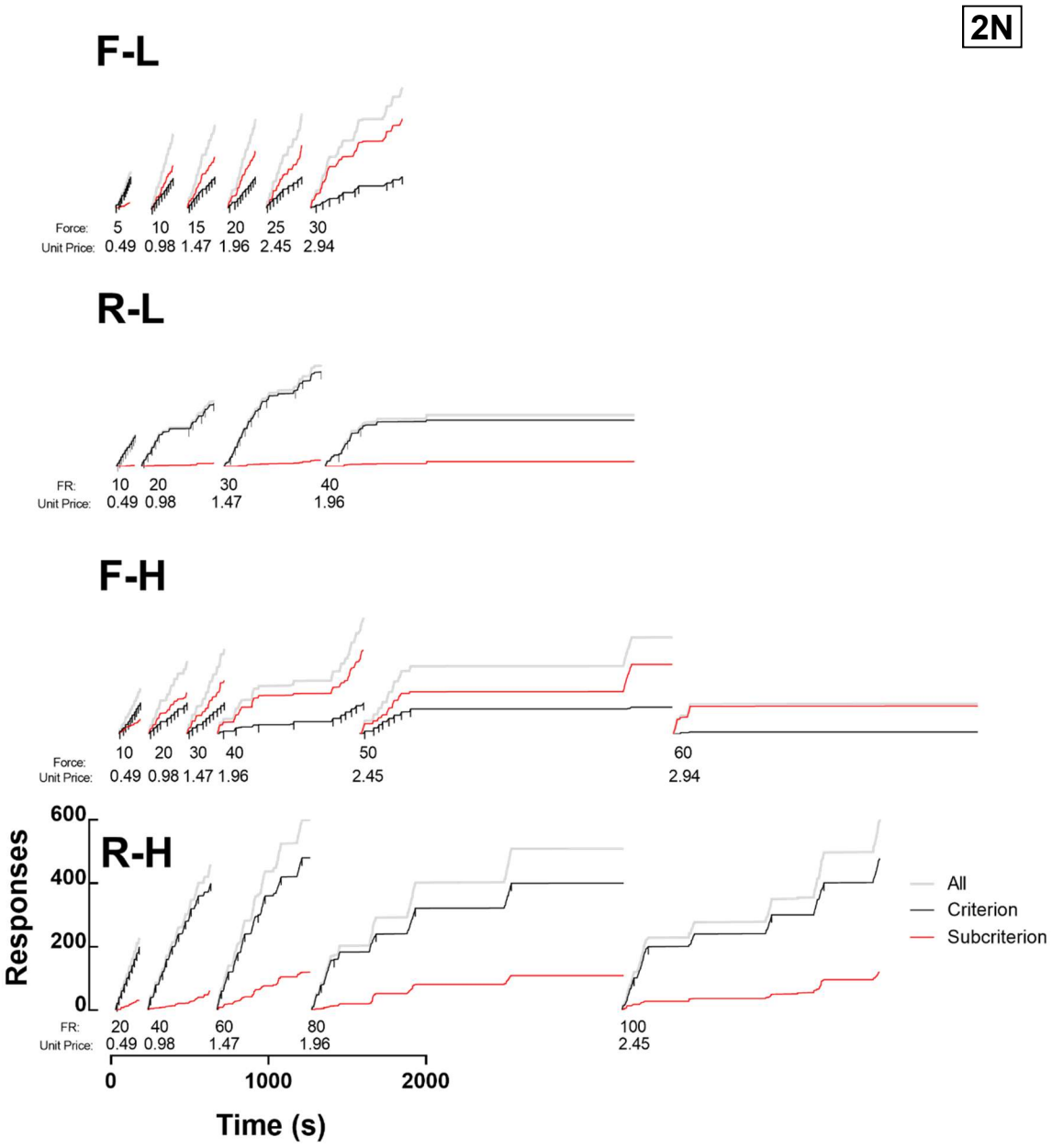

Figure B16. Detailed cumulative record for 2N. Shown are the first 10 reinforcer deliveries or first 600 responses for every price point for the F-L, R-L, F-H, and R-H progressions by rows. Cumulative responses (y-axis) are shown as a function of time in 2-hr session (x-axis). Light gray data paths show all responses, black data paths show criterion responses, and red data paths show subcriterion responses. Black ticks along the criterion data path show reinforcer deliveries.

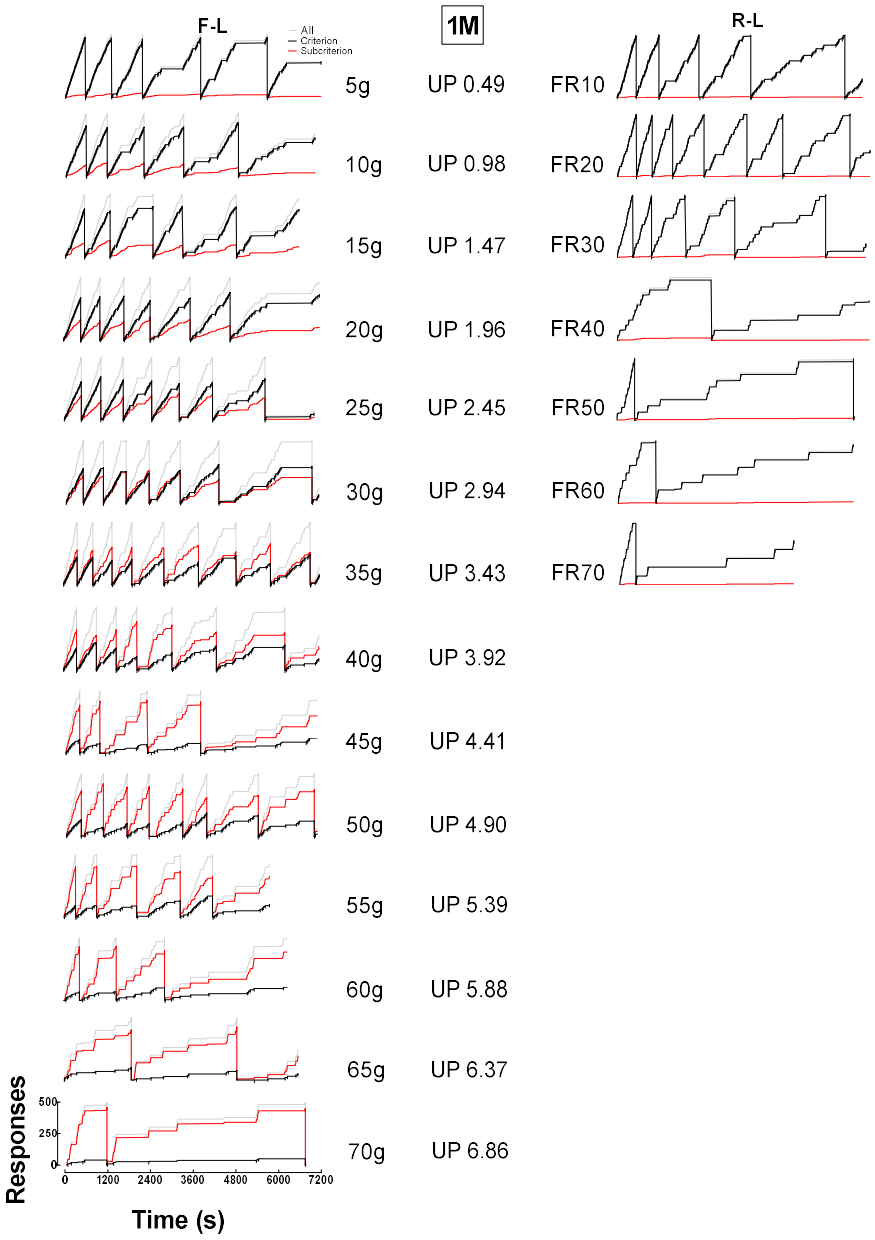

Figure B17. Cumulative records for the F-L and R-L progressions for 1M. Cumulative responses (y-axis) are shown as a function of time in 2-hr session (x-axis). Light gray data paths show all responses, black data paths show criterion responses, and red data paths show subcriterion responses. Black ticks along the criterion data path show reinforcer deliveries. Matched unit prices are shown across rows with the F-L progression in the left column and R-L progression on the right.

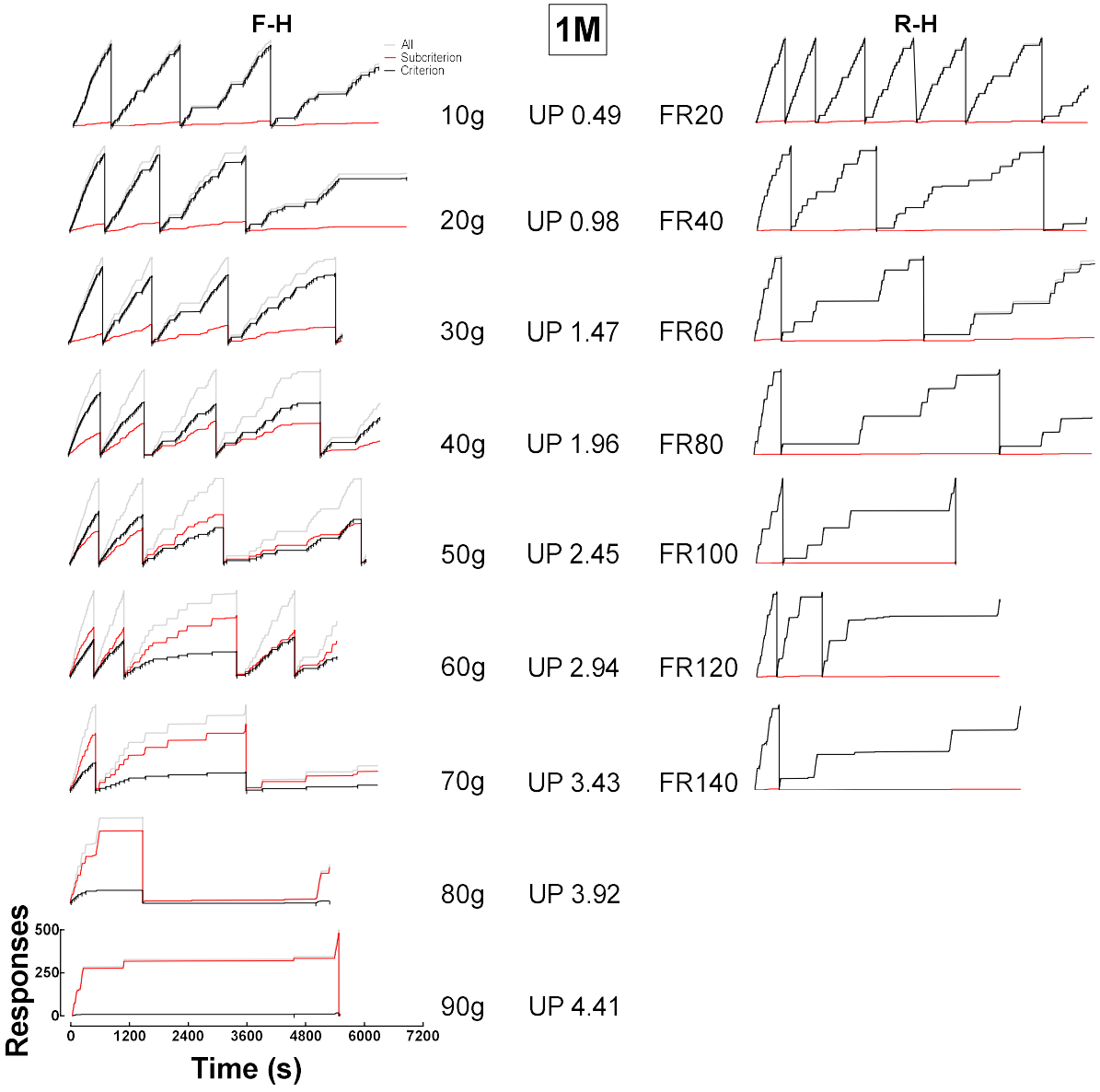

Figure B18.Cumulative records for the F-H and R-H progressions for 1M. Cumulative responses (y-axis) are shown as a function of time in each 2-hr session (x-axis). Light gray data paths show all responses, black data paths show criterion responses, and red data paths show subcriterion responses. Black ticks along the criterion data path show reinforcer deliveries. Matched unit prices are shown across rows with the F-H progression in the left column and R-H progression on the right.

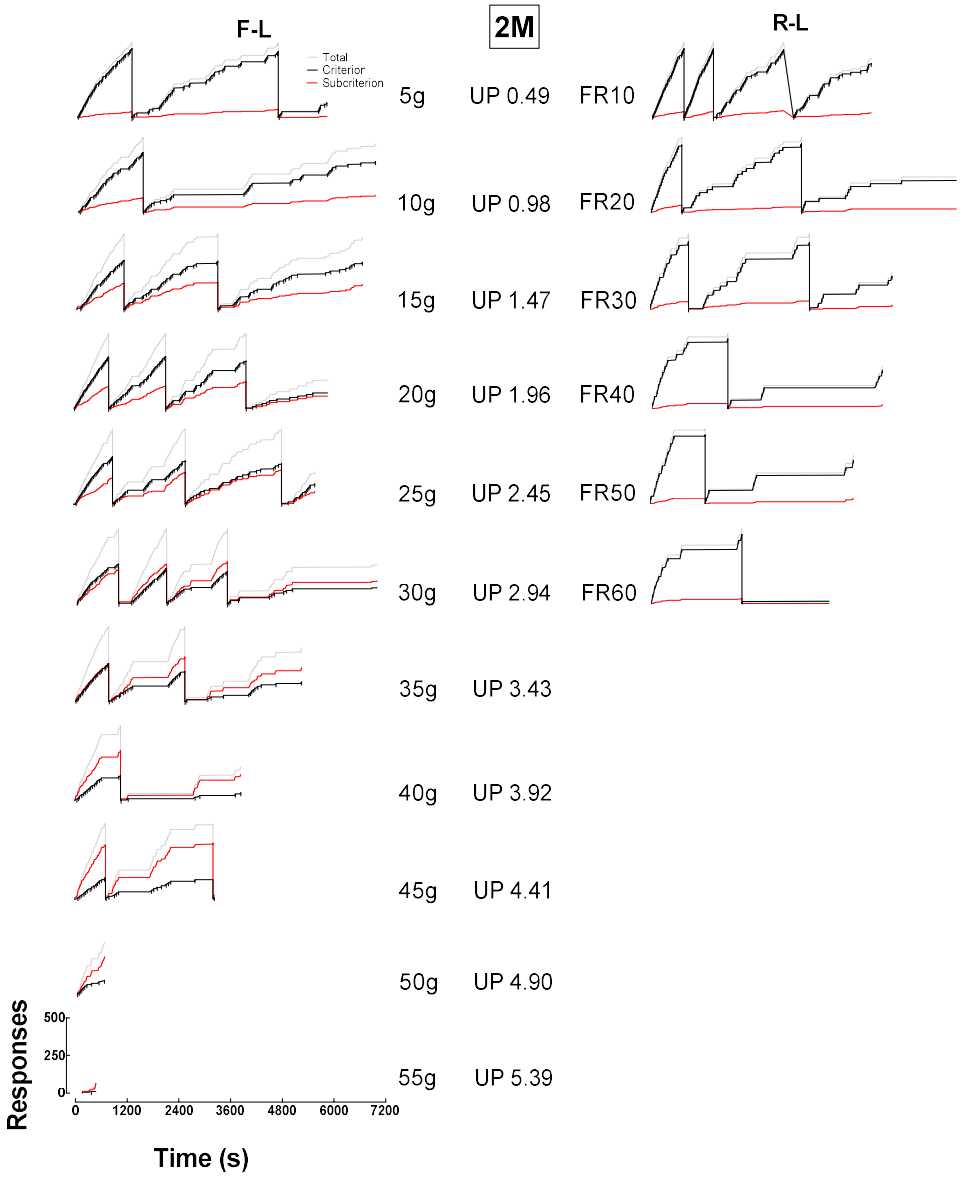

Figure B19. Cumulative records for the F-L and R-L progressions for 2M. Cumulative responses (y-axis) are shown as a function of time in 2-hr session (x-axis). Light gray data paths show all responses, black data paths show criterion responses, and red data paths show subcriterion responses. Black ticks along the criterion data path show reinforcer deliveries. Matched unit prices are shown across rows with F-L progression on the left and R-L progression on the right.

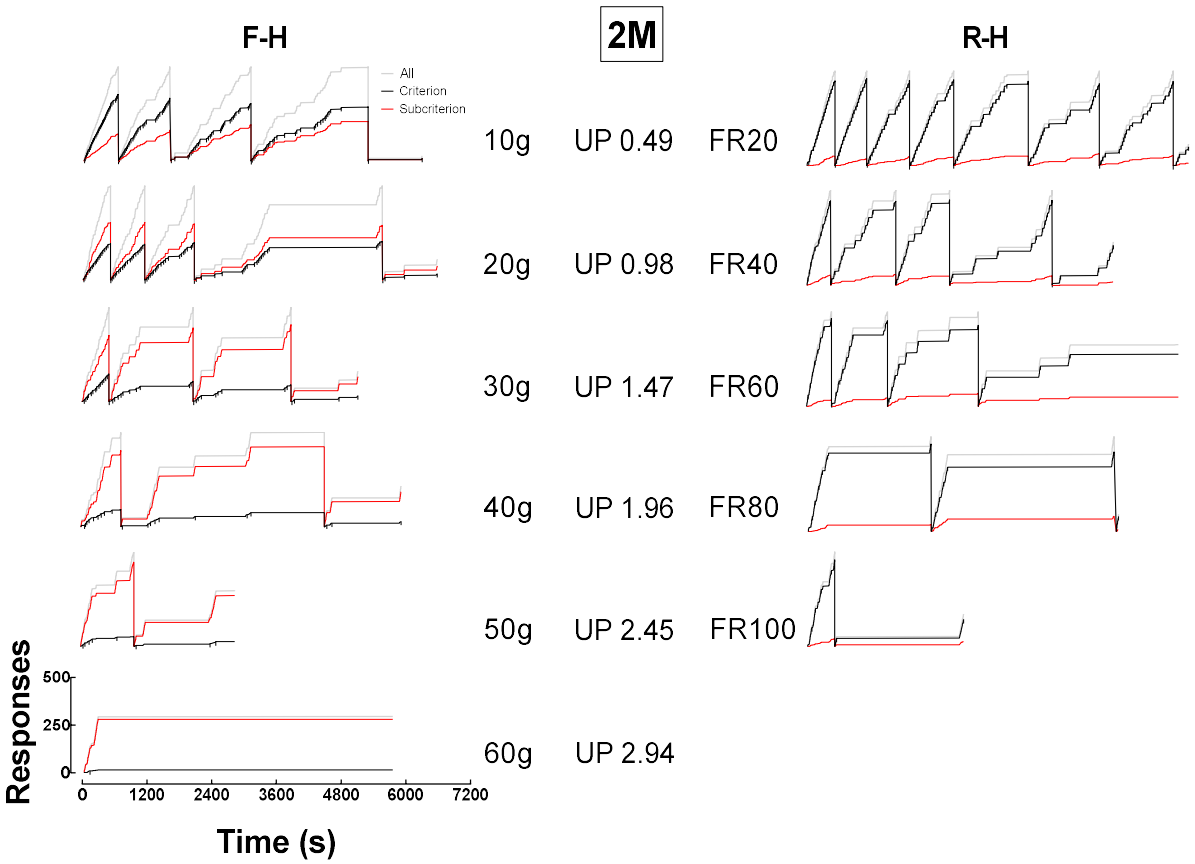

Figure B20.Cumulative records for the F-H and R-H progressions for 2M. Cumulative responses (y-axis) are shown as a function of time in 2-hr session (x-axis). Light gray data paths show all responses, black data paths show criterion responses, and red data paths show subcriterion responses. Black ticks along the criterion data path show reinforcer deliveries. Matched unit prices are shown across rows with the F-H progression in the left column and R-H progression on the right.

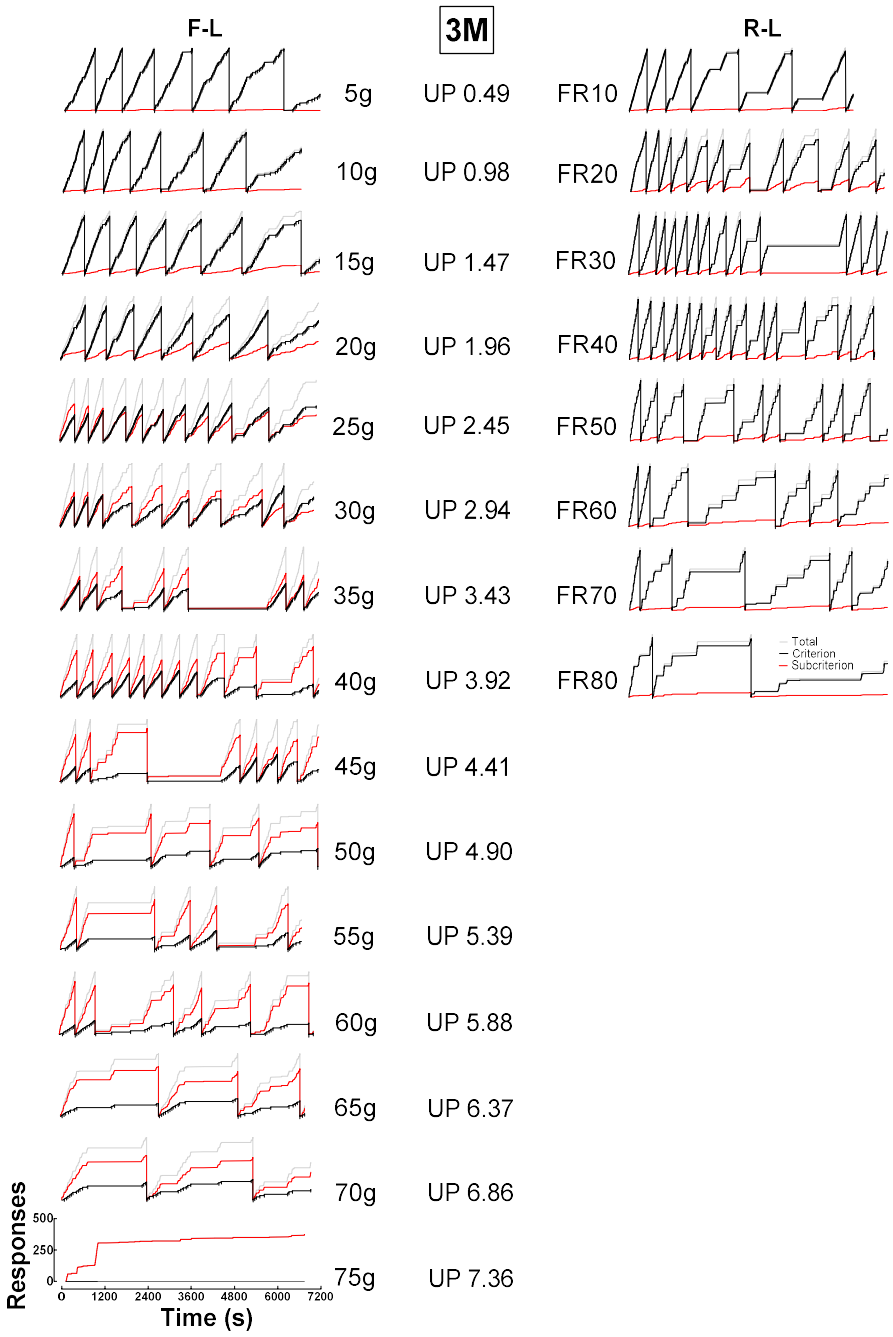

Figure B21. Cumulative records for the F-L and R-L progressions for 3M. Cumulative responses (y-axis) are shown as a function of time in 2-hr session (x-axis). Light gray data paths show all responses, black data paths show criterion responses, and red data paths show subcriterion responses. Black ticks along the criterion data path show reinforcer deliveries. Matched unit prices are shown across rows with F-L progression on the left and R-L progression on the right.

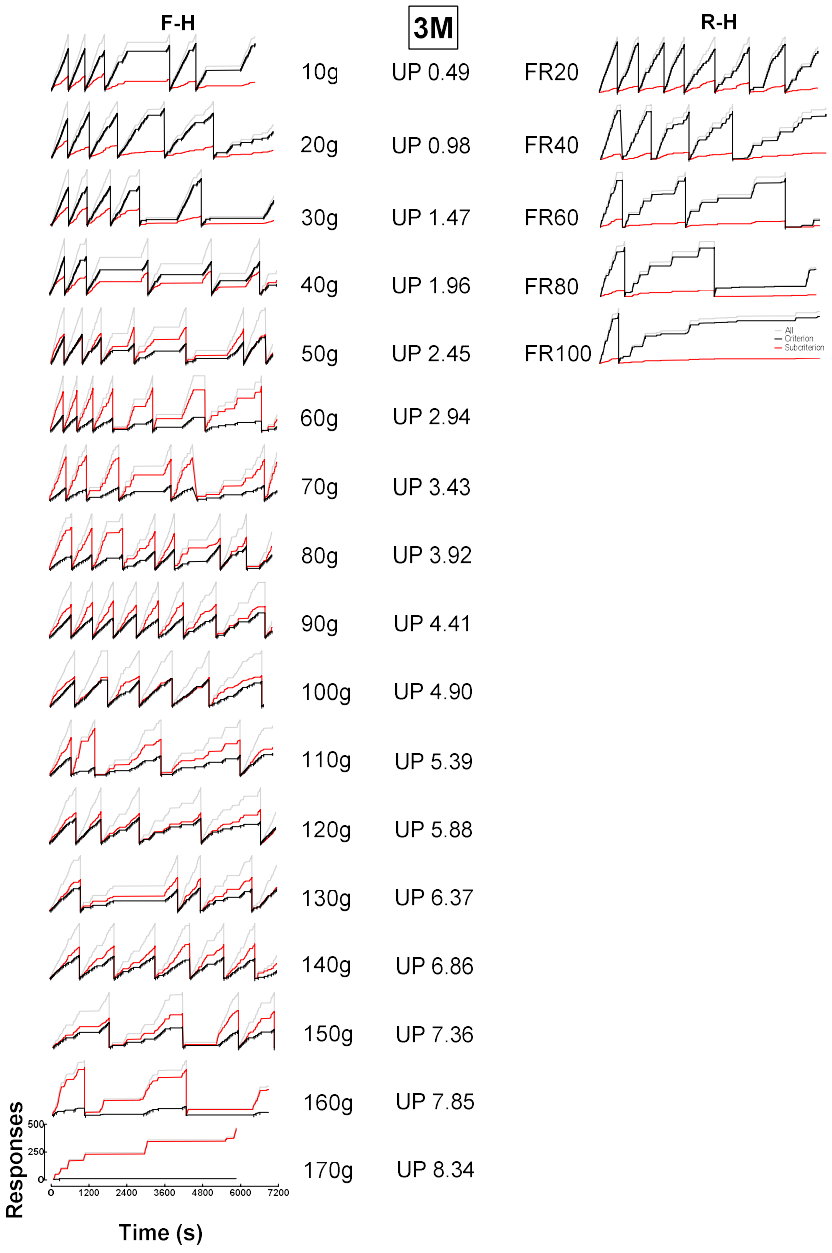

Figure B22. Cumulative records for the F-H and R-H progressions for 3M. Cumulative responses (y-axis) are shown as a function of time in 2-hr session (x-axis). Light gray data paths show all responses, black data paths show criterion responses, and red data paths show subcriterion responses. Black ticks along the criterion data path show reinforcer deliveries. Matched unit prices are shown across rows with the F-H progression in the left column and R-H progression on the right.

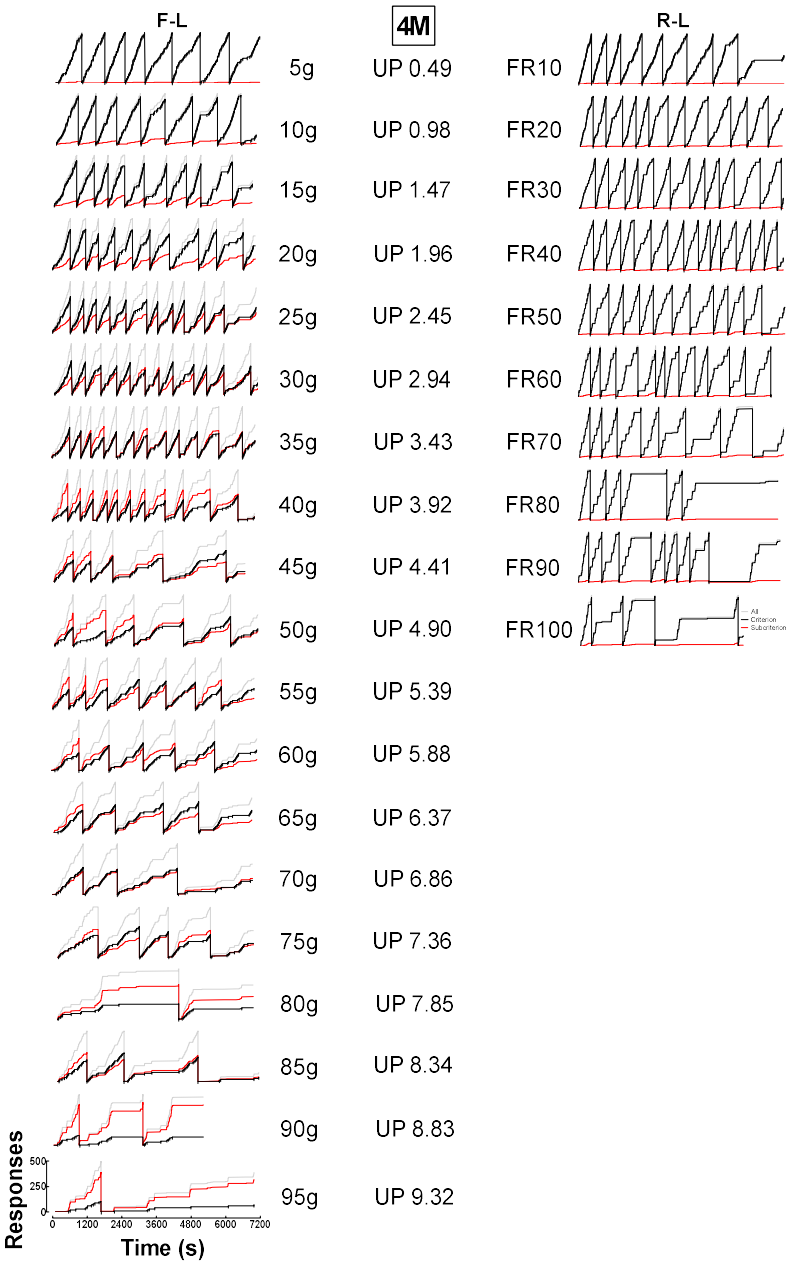

Figure B23. Cumulative records for the F-L and R-L progressions for 4M. Cumulative responses (y-axis) are shown as a function of time in 2-hr session (x-axis). Light gray data paths show all responses, black data paths show criterion responses, and red data paths show subcriterion responses. Black ticks along the criterion data path show reinforcer deliveries. Matched unit prices are shown across rows with the F-L progression in the left column and R-L progression on the right.

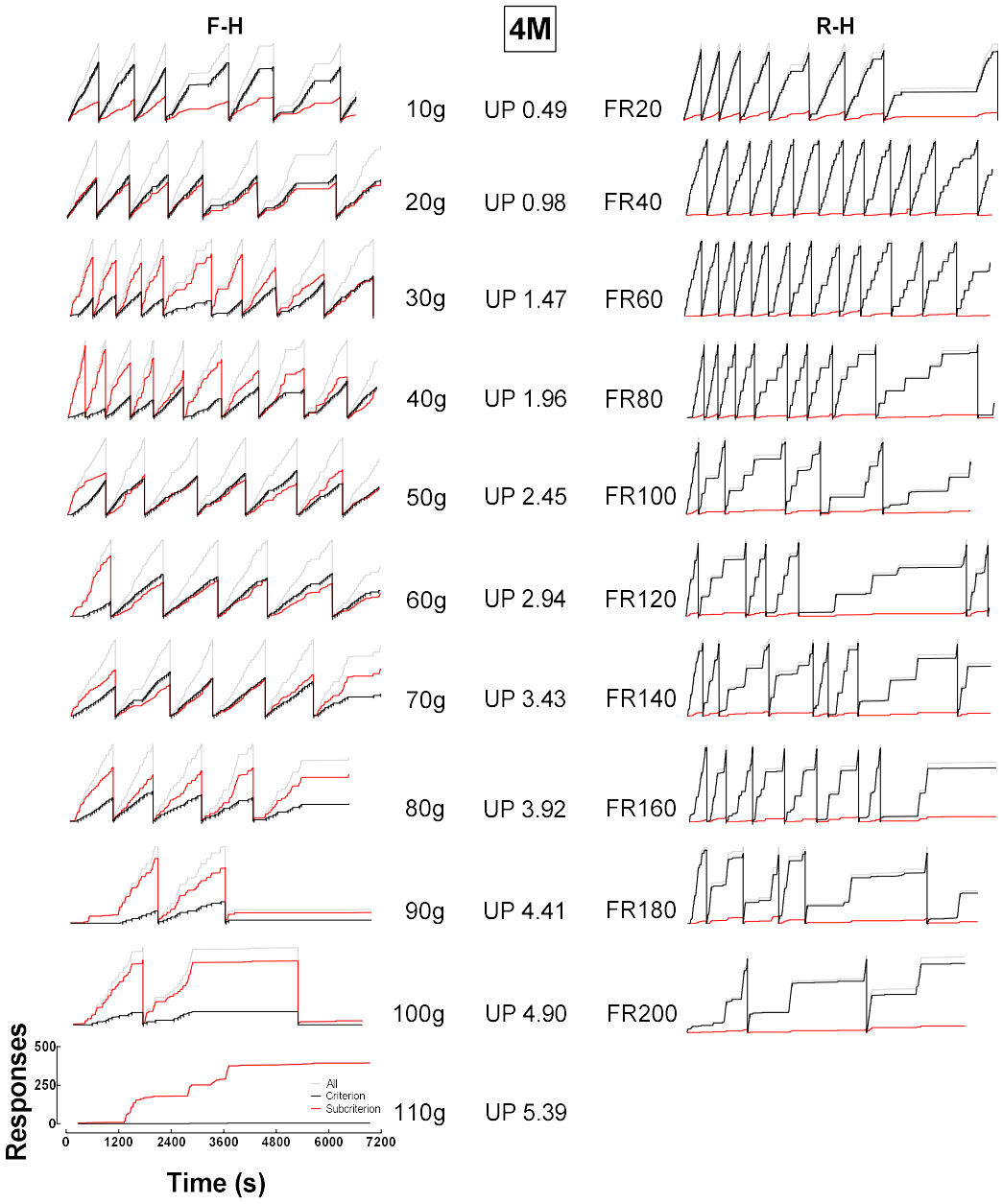

Figure B24. Cumulative records for the F-H and R-H progressions for 4M. Cumulative responses (y-axis) are shown as a function of time in 2-hr session (x-axis). Light gray data paths show all responses, black data paths show criterion responses, and red data paths show subcriterion responses. Black ticks along the criterion data path show reinforcer deliveries. Matched unit prices are shown across rows with the F-H progression in the left column and R-H progression on the right.

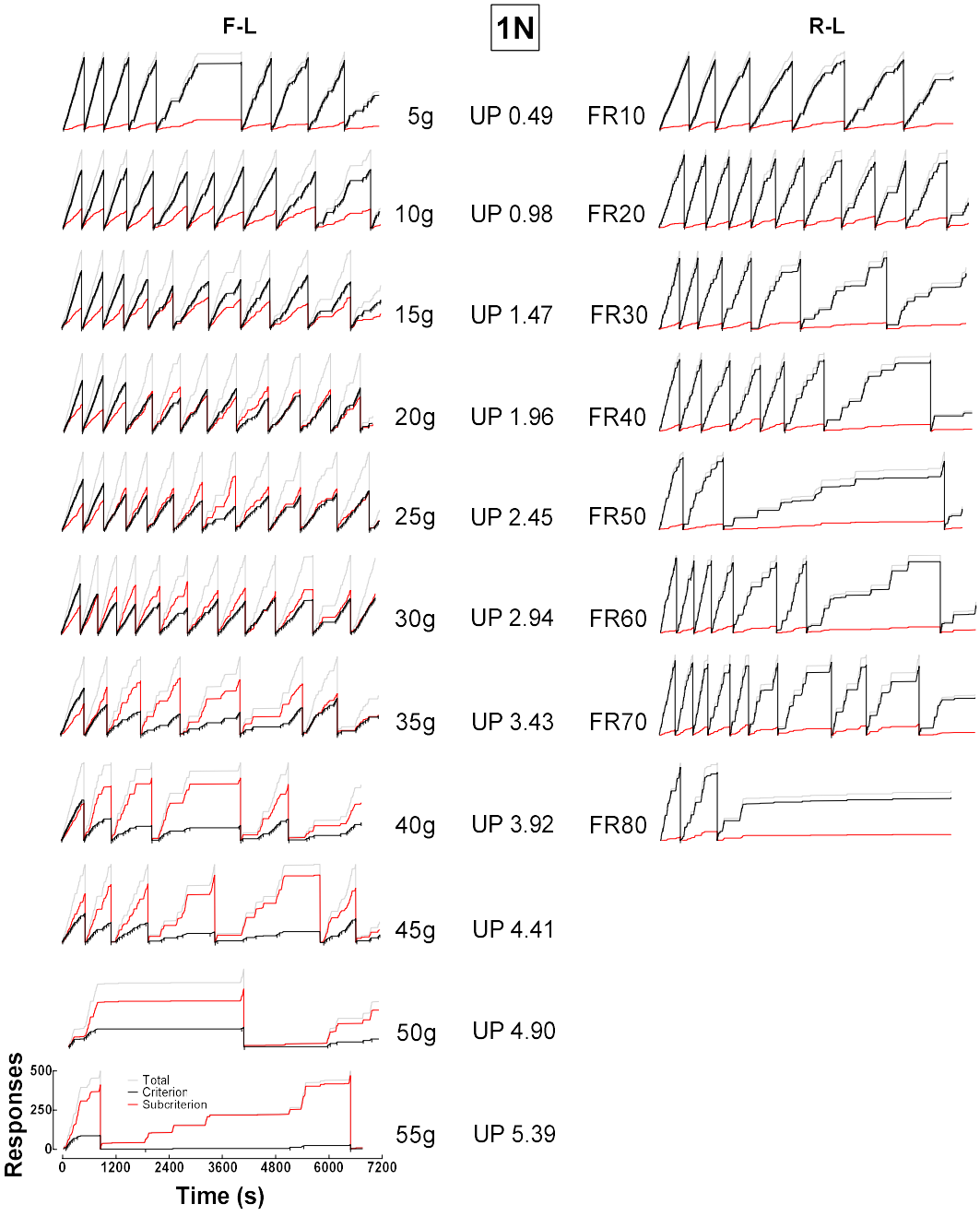

Figure B25. Cumulative records for the F-L and R-L progressions for 1N. Cumulative responses (y-axis) are shown as a function of time in 2-hr session (x-axis). Light gray data paths show all responses, black data paths show criterion responses, and red data paths show subcriterion responses. Black ticks along the criterion data path show reinforcer deliveries. Matched unit prices are shown across rows with F-L progression on the left and R-L progression on the right.

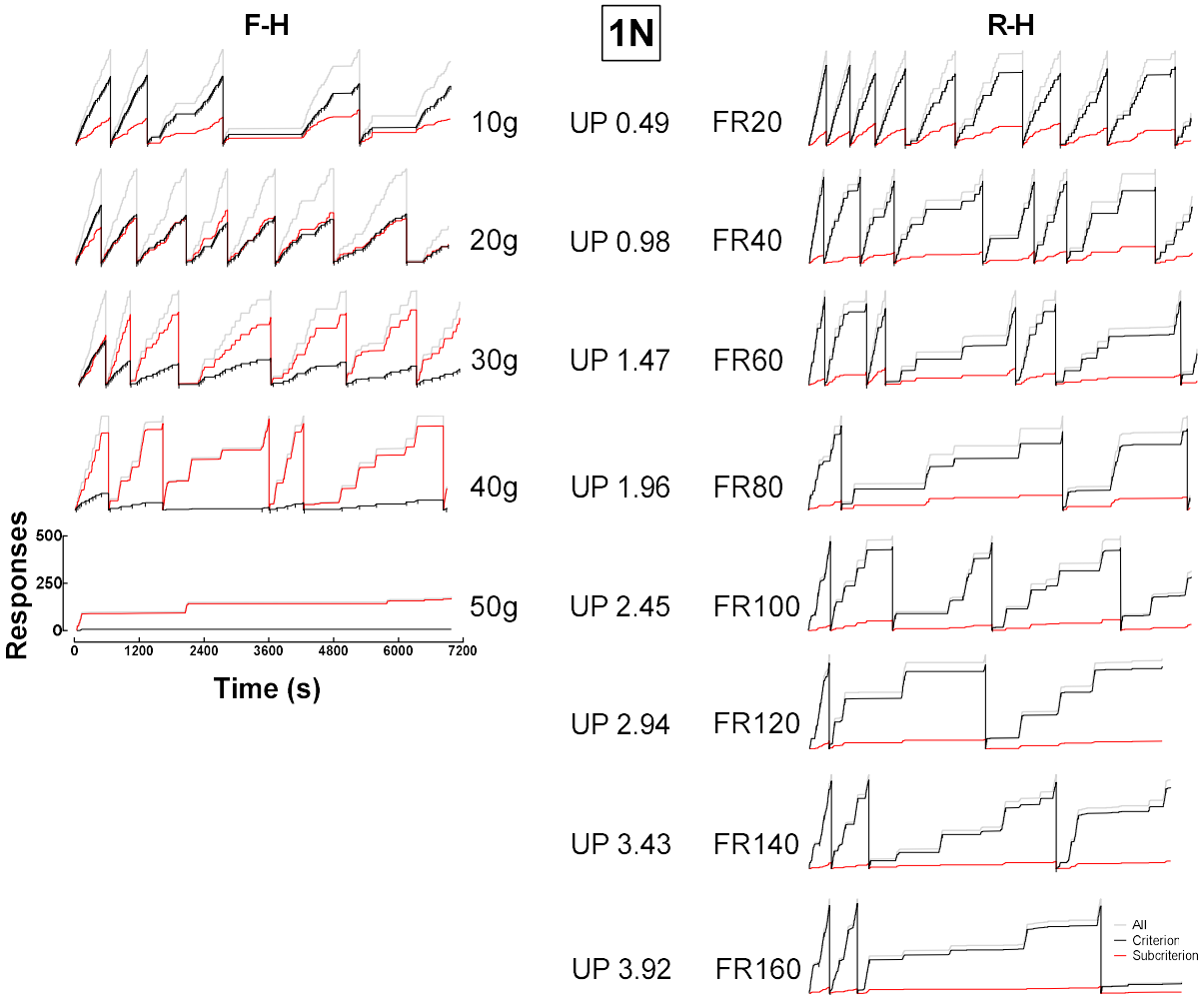

Figure B26. Cumulative records for the F-H and R-H progressions for 1N. Cumulative responses (y-axis) are shown as a function of time in 2-hr session (x-axis). Light gray data paths show all responses, black data paths show criterion responses, and red data paths show subcriterion responses. Black ticks along the criterion data path show reinforcer deliveries. Matched unit prices are shown across rows with the F-H progression in the left column and R-H progression on the right.

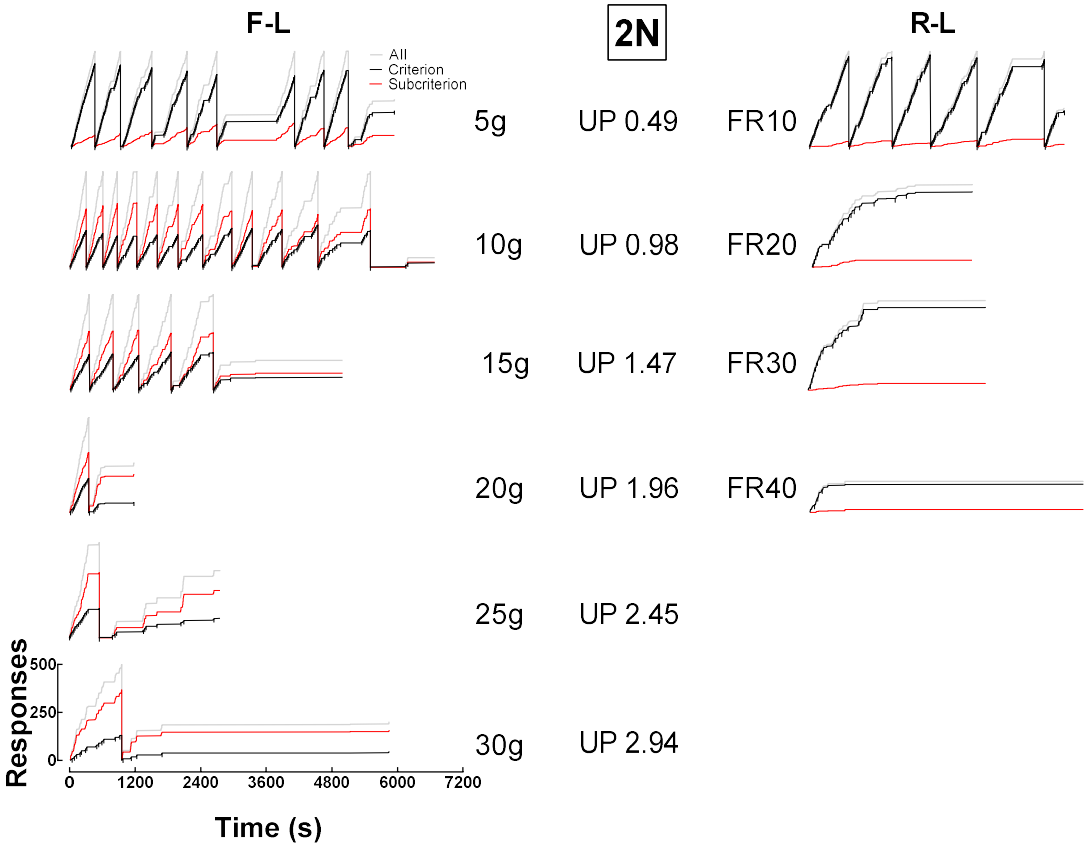

Figure B27. Cumulative records for the F-L and R-L progressions for 2N. Cumulative responses (y-axis) are shown as a function of time in 2-hr session (x-axis). Light gray data paths show all responses, black data paths show criterion responses, and red data paths show subcriterion responses. Black ticks along the criterion data path show reinforcer deliveries. Matched unit prices are shown across rows with the F-L progression in the left column and R-L progression on the right.

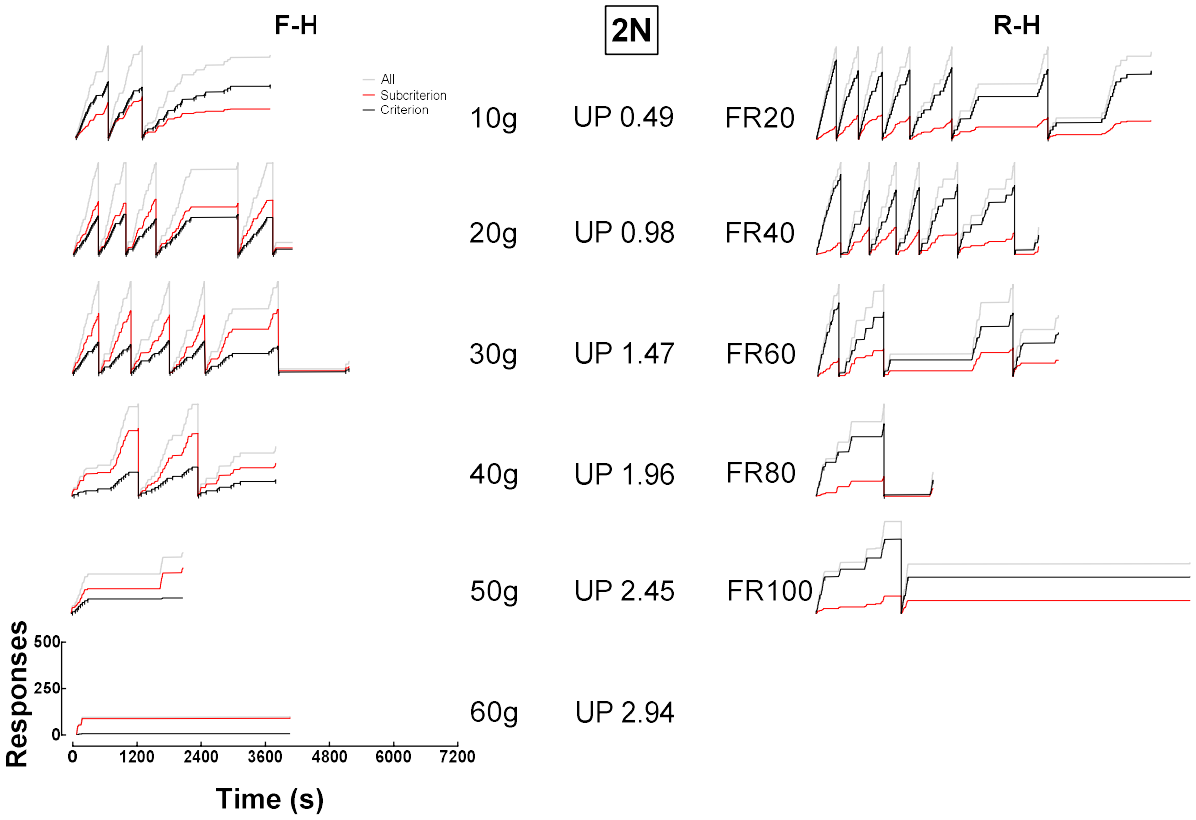

Figure B28. Cumulative records for the F-H and R-H progressions for 2N. Cumulative responses (y-axis) are shown as a function of time in 2-hr session (x-axis). Light gray data paths show all responses, black data paths show criterion responses, and red data paths show subcriterion responses. Black ticks along the criterion data path show reinforcer deliveries. Matched unit prices are shown across rows with the F-H progression in the left column and R-H progression on the right.

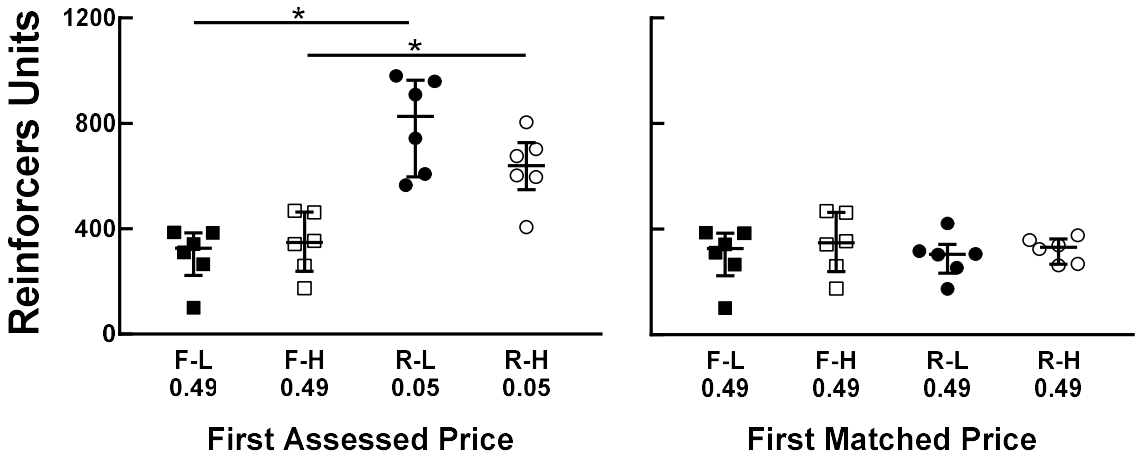

Figure B29. Reinforcer units earned at first assessed unit price and first matched unit price. Closed circles show R-L progressions, open circles show R-H progressions, closed squares show F-L progressions, and open squares show F-H progressions. Lines and error bars show medians and IQRs. Significant differences are shown by asterisks.

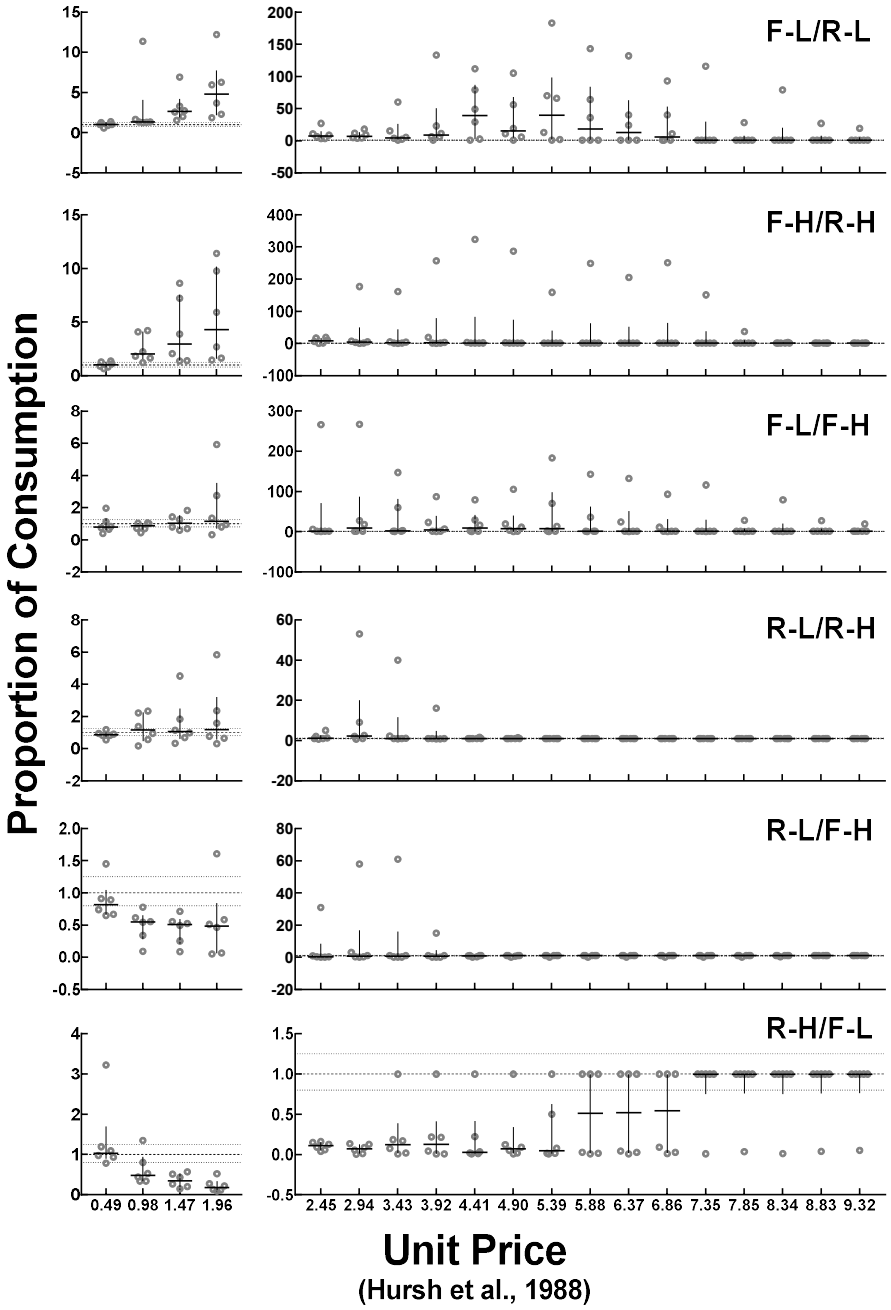

Figure B30. Consumption as a proportion of consumption in a comparison condition across unit prices. Shown are consumption proportions (y-axis; conditions shown as dividend/divisor in top right of each panel) across different unit prices (x-axis). Gray open circles show proportions for individual animals, and lines show medians and error bars show IQRs. A zone of equivalence (based on confidence intervals) is shown between 0.8-1.25 (dotted lines)

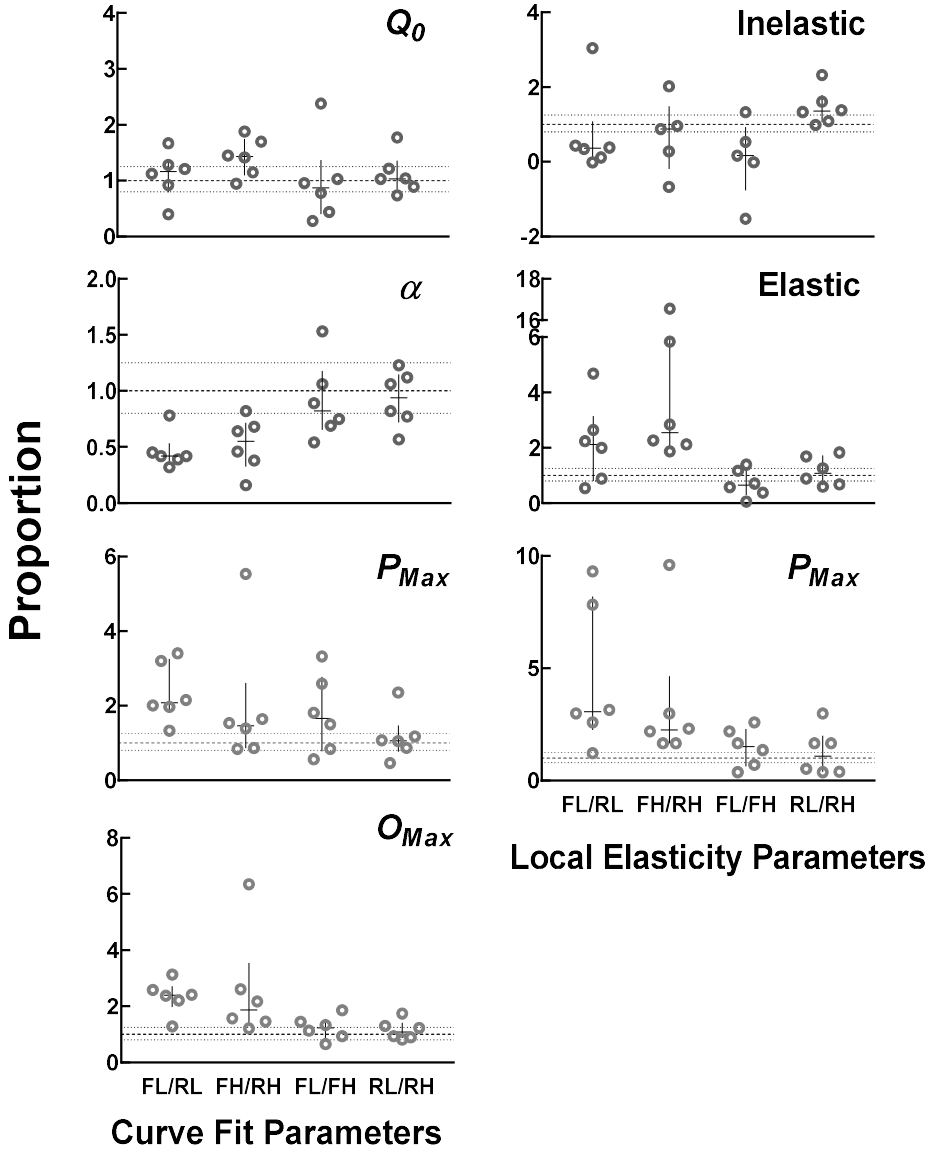

Figure B31. Proportions for fitted parameters obtained from consumption as a function of unit price. Shown are data obtained from analyses when price points with 0 consumption were excluded. The y-axis shows proportion measures calculated by dividing each animal's parameter in one progression by its parameters in another (x-axis). Lines show medians and error bars show IQRs. A zone of equivalence (based on confidence intervals) is shown between 0.8-1.25 (dotted lines).

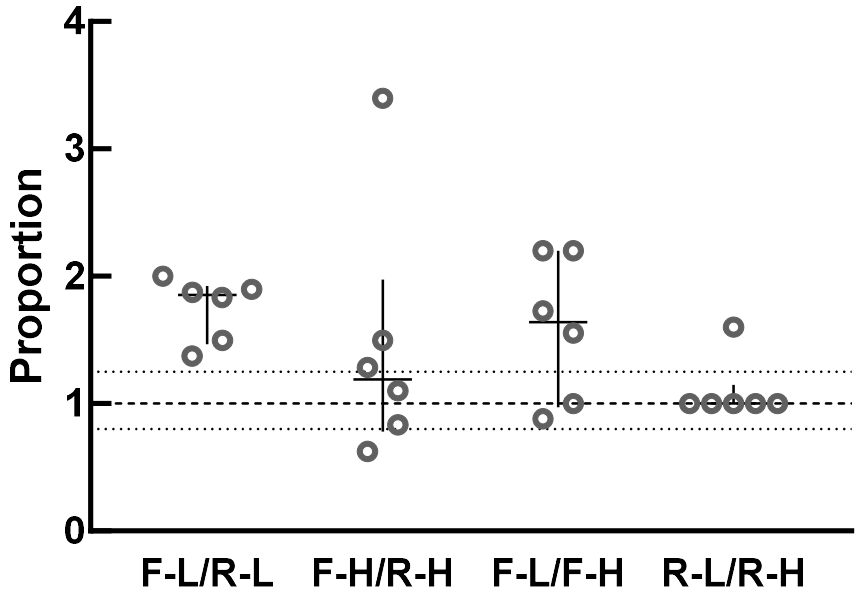

Figure B32. Breakpoint comparisons based on unit price. Shows a proportion measure (y-axis) calculated by dividing one progression by another (x-axis). Lines show medians and error bars show IQRs. A zone of equivalence is shown by the dotted lines at 0.8-1.25 (dotted lines).

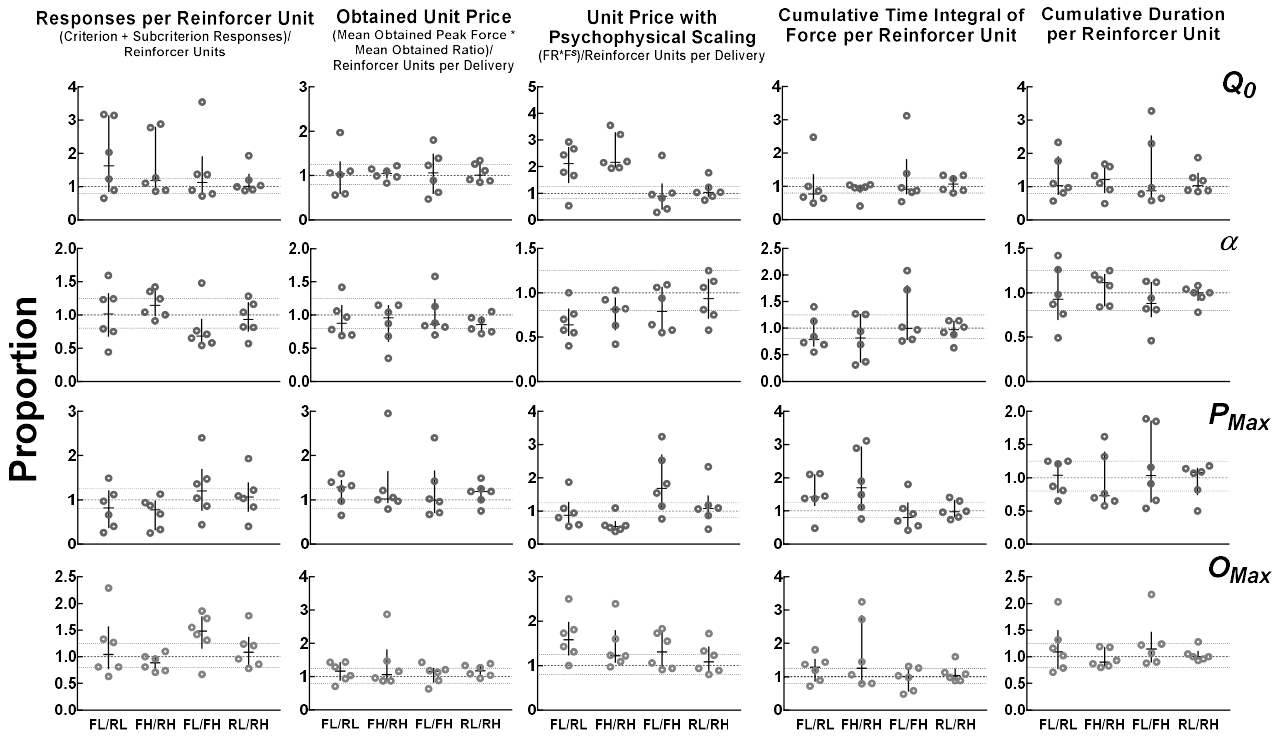

Figure B33. Proportions comparing derived parameters across different price conversions. Closed circles show R-L progressions, open circles show R-H progressions, closed squares show F-L progressions, and open squares show F-H progressions. Shown are proportion measures (y-axis) calculated by dividing each animal's parameter in one progression by its parameters in another (x-axis). Lines show medians and error bars show IQRs. A zone of equivalence (based on confidence intervals) is shown between 0.8-1.25 (dotted lines).

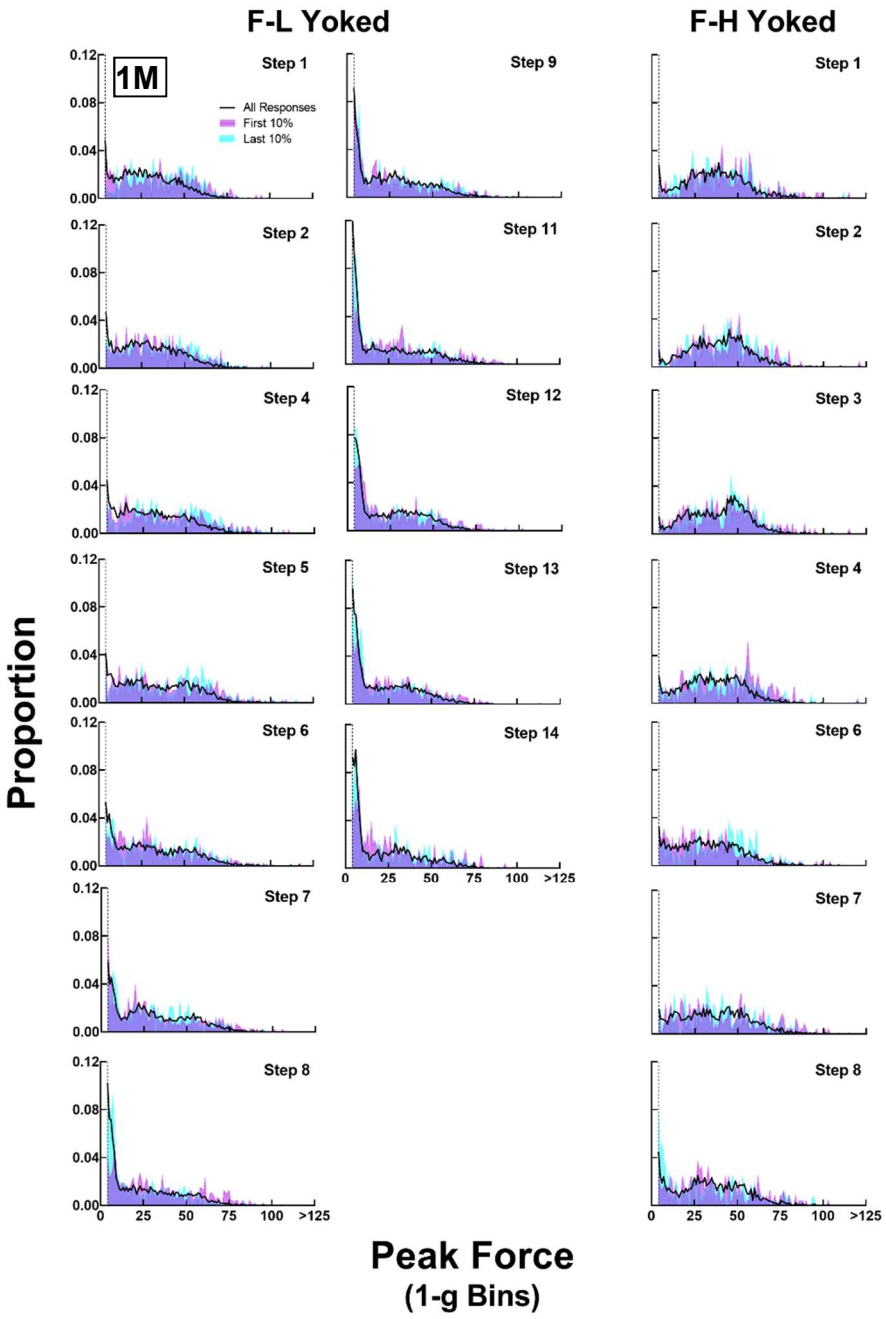

Figure B34. Peak force distributions for yoked progressions for 1M. The proportion of responses (y-axis) in 1-g force bins (x-axis) is shown for all responses (black data path), the first 10% of responses (magenta shaded region) and last 10% of responses (cyan shaded region) in each session for the Yoked F-L (left columns) and Yoked F-H (right column) progressions.

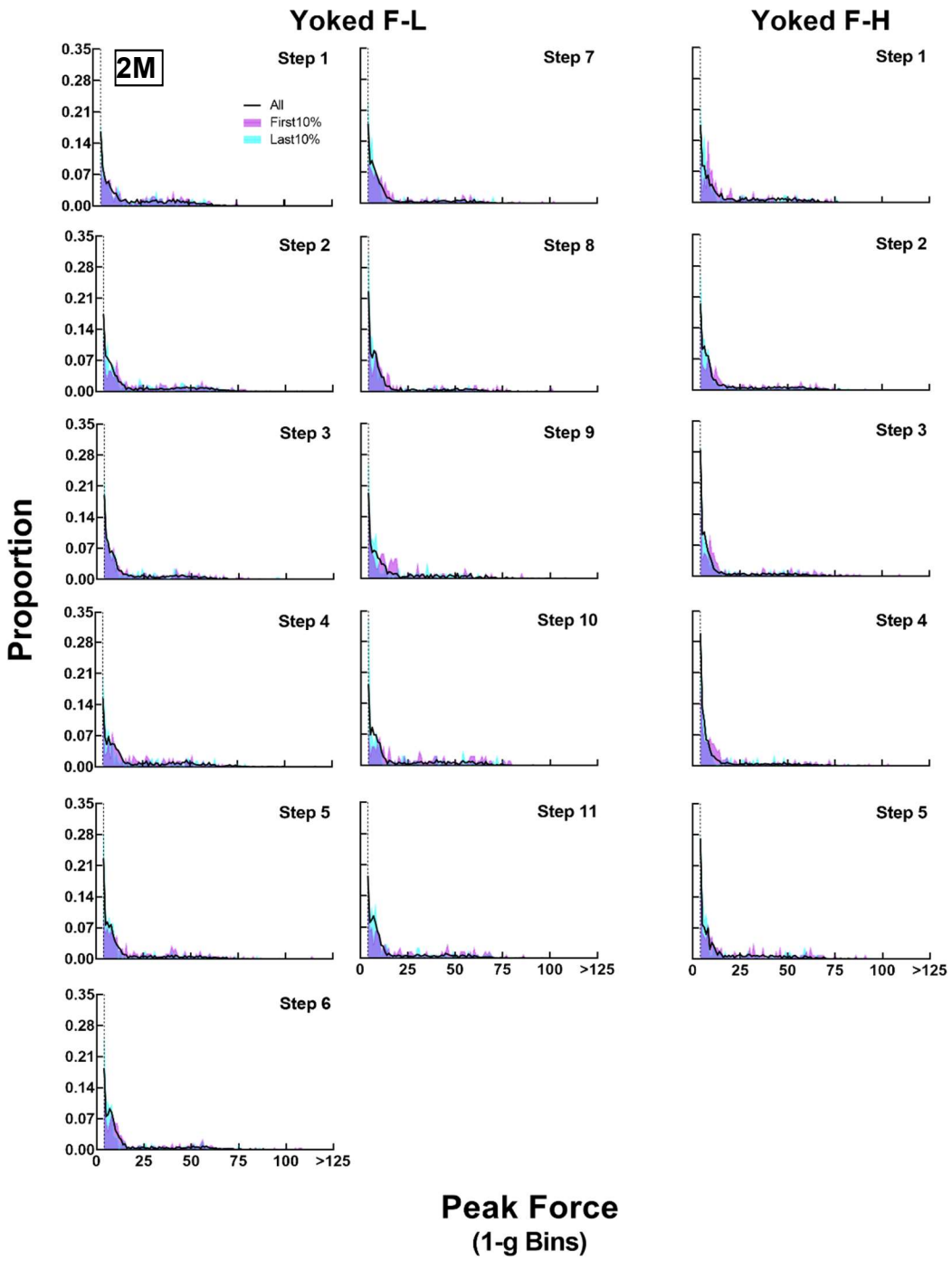

Figure B35. Peak force distributions for yoked progressions for 2M. The proportion of responses (y-axis) in 1-g force bins (x-axis) is shown for all responses (black data path), the first 10% of responses (magenta shaded region) and last 10% of responses (cyan shaded region) in each session for the Yoked F-L (left columns) and Yoked F-H (right column) progressions.

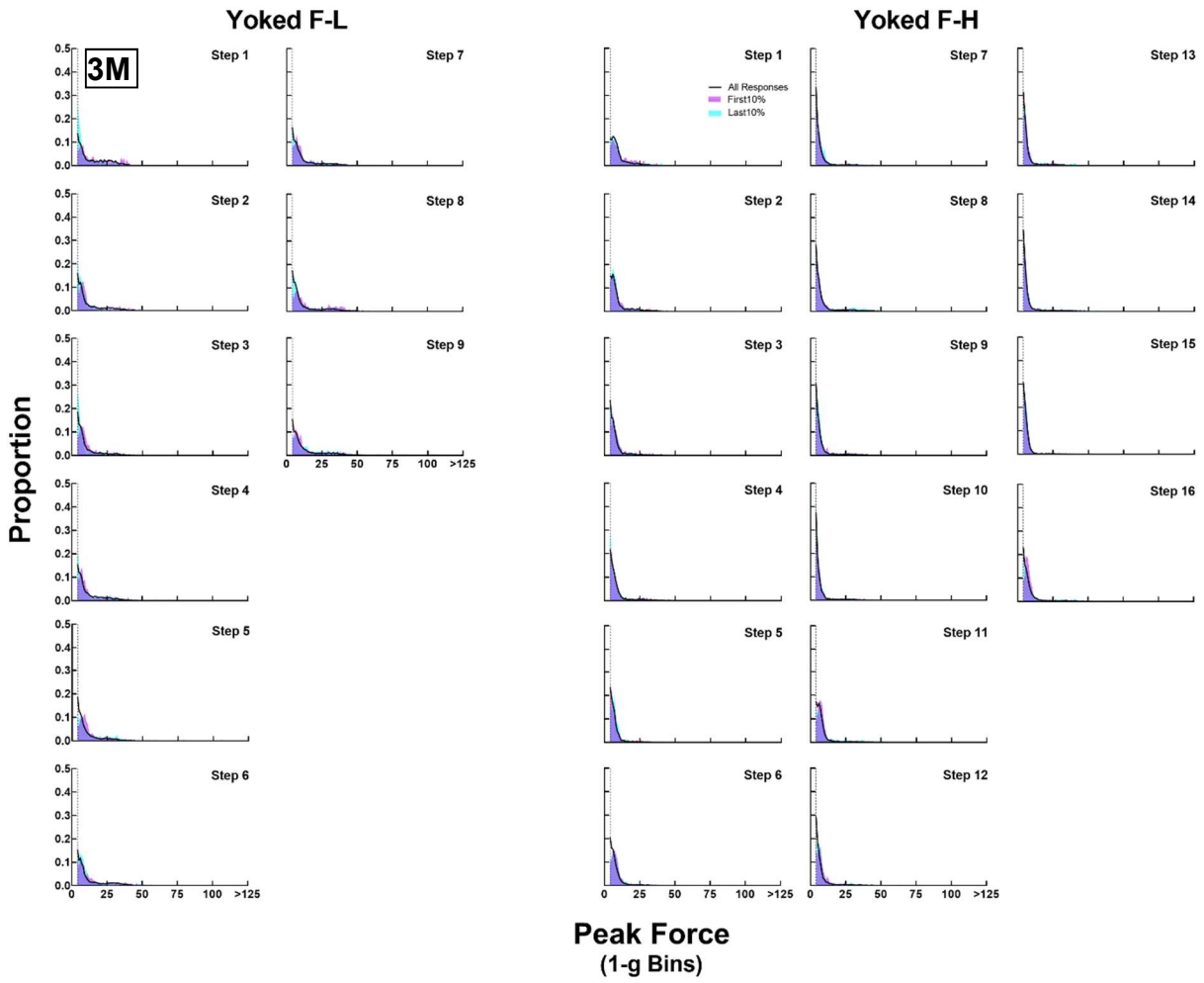

Figure B36. Peak force distributions for yoked progressions for 3M. The proportion of responses (y-axis) in 1-g force bins (x-axis) is shown for all responses (black data path), the first 10% of responses (magenta shaded region) and last 10% of responses (cyan shaded region) in each session for the Yoked F-L (left columns) and Yoked F-H (right columns) progressions.

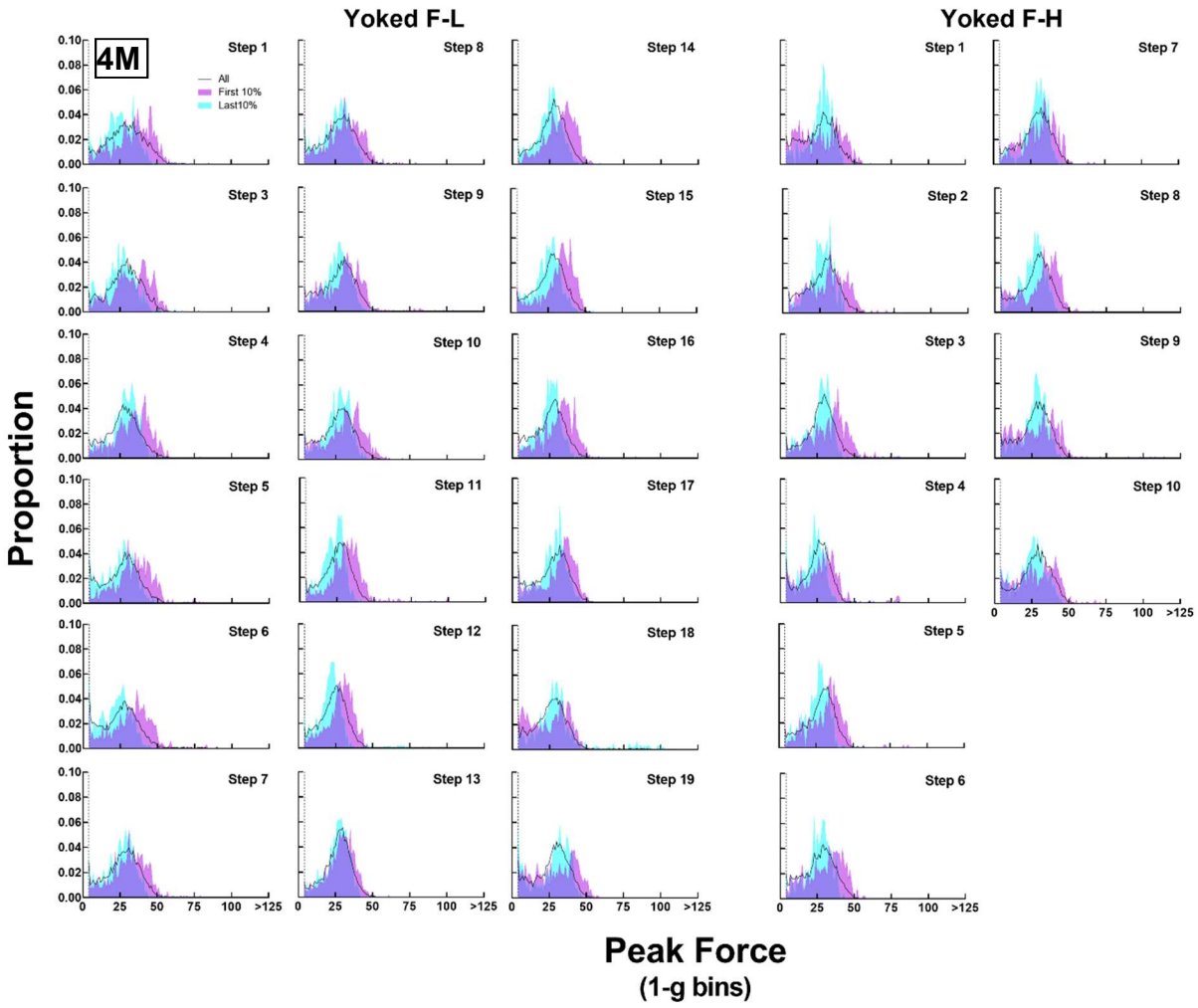

Figure B37. Peak force distributions for yoked progressions for 4M. The proportion of responses (y-axis) in 1-g force bins (x-axis) is shown for all responses (black data path), the first 10% of responses (magenta shaded region) and last 10% of responses (cyan shaded region) in each session for the Yoked F-L (left columns) and Yoked F-H (right columns) progressions.

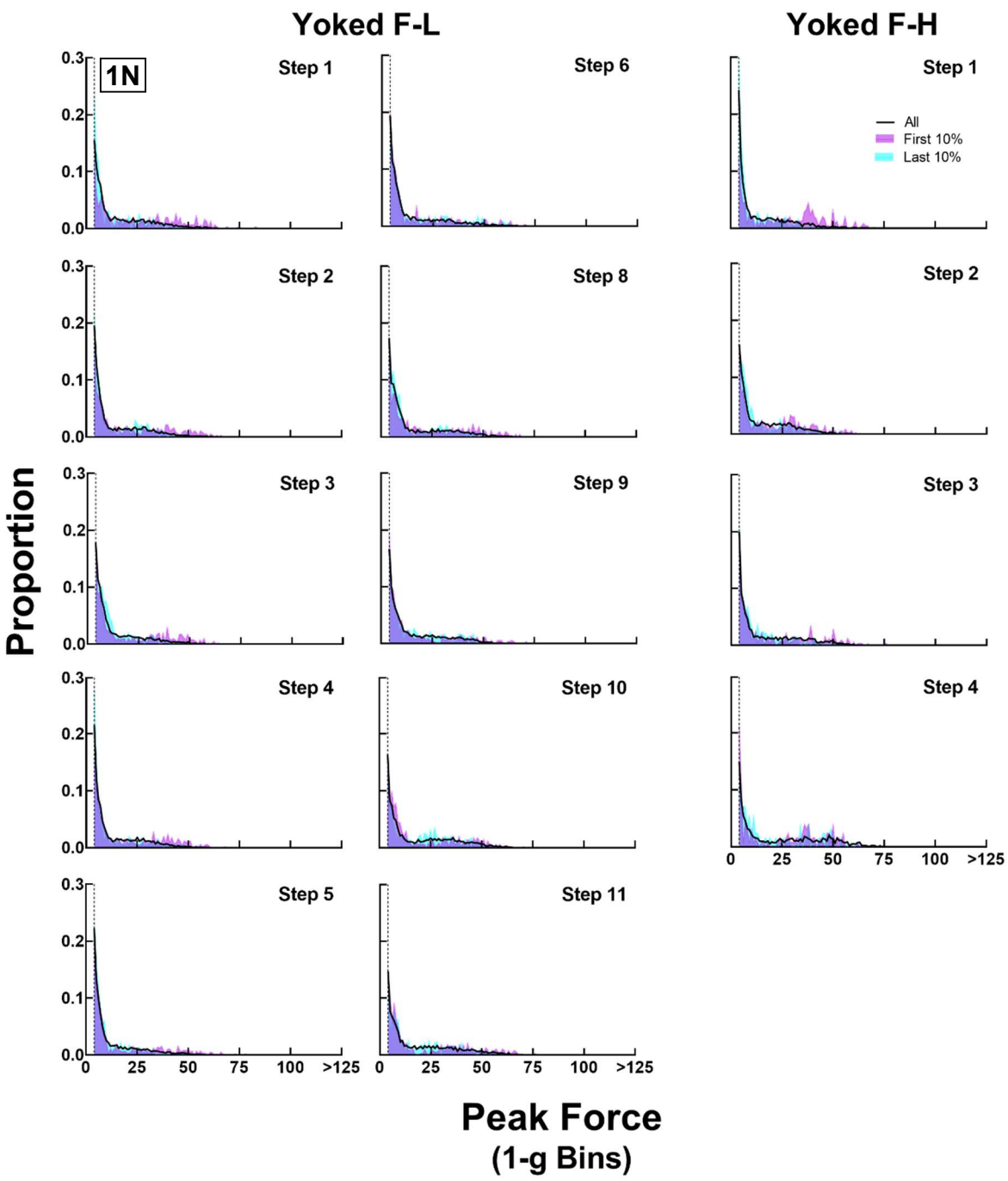

Figure B38. Peak force distributions for yoked progressions for 1N. The proportion of responses (y-axis) in 1-g force bins (x-axis) is shown for all responses (black data path), the first 10% of responses (magenta shaded region) and last 10% of responses (cyan shaded region) in each session for the Yoked F-L (left columns) and Yoked F-H (right column) progressions.

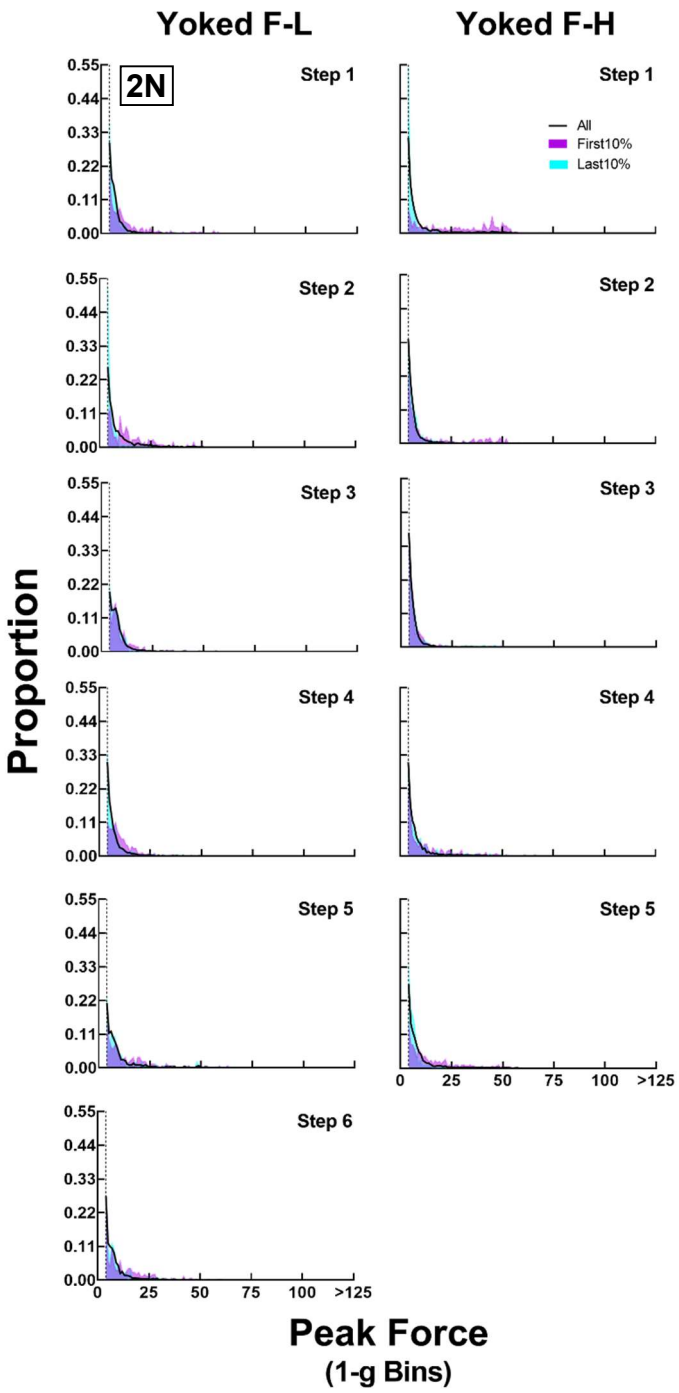

Figure B39. Peak force distributions for yoked progressions for 2N. The proportion of responses (y-axis) in 1-g force bins (x-axis) is shown for all responses (black data path), the first 10% of responses (magenta shaded region) and last 10% of responses (cyan shaded region) in each session for the Yoked F-L (left column) and Yoked F-H (right column) progressions.

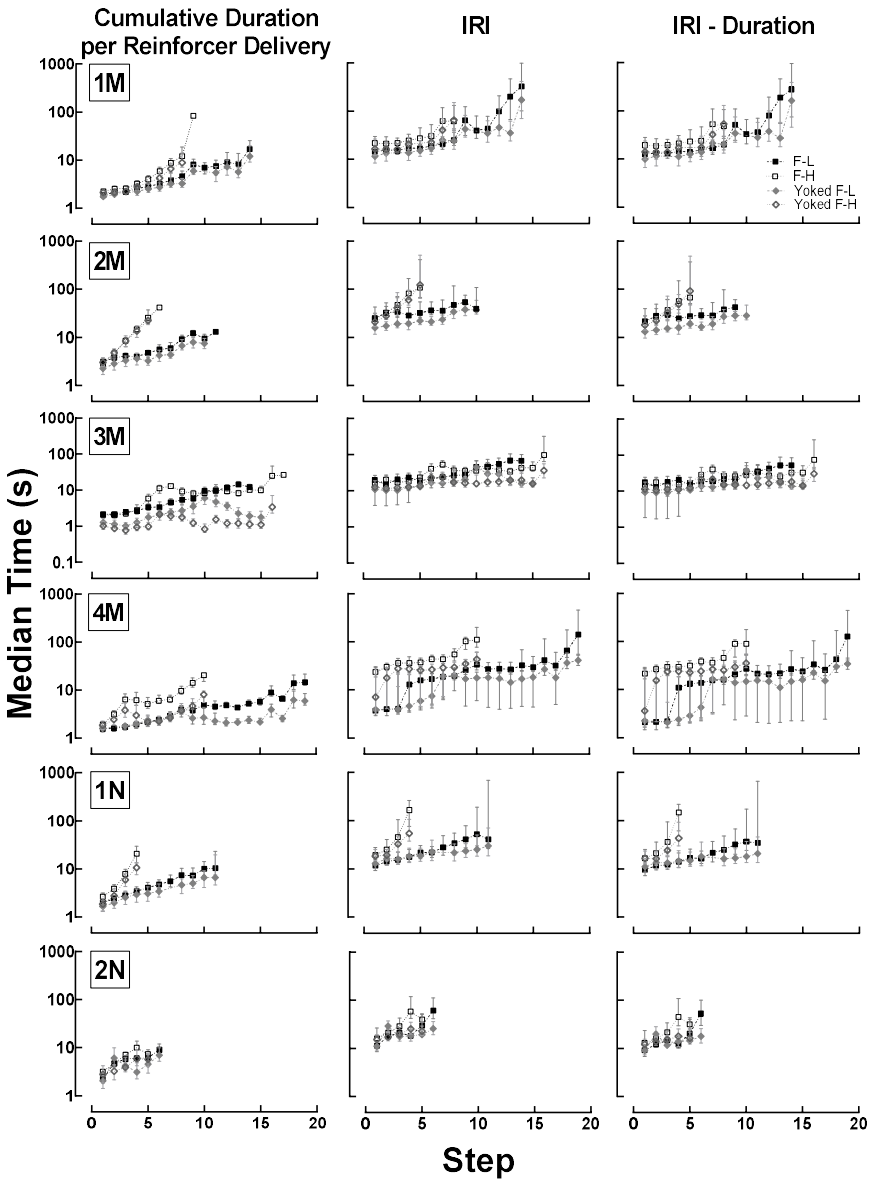

Figure B40. Cumulative response duration per reinforcer delivery and interreinforcement intervals. The first column shows cumulative response duration per reinforcer delivery; the second column shows interreinforcement interval (IRI); and the last column shows the difference. Median time (s) is along the y-axis and step is along the x-axis for individual animals in rows. Shown are data from the Experiment 1 F-L (black closed squares) and F-H (black open squares) progressions and the Experiment 2 Yoked F-L (gray closed squares) and Yoked F-H (gray open squares) progressions. Error bars show IQRs.

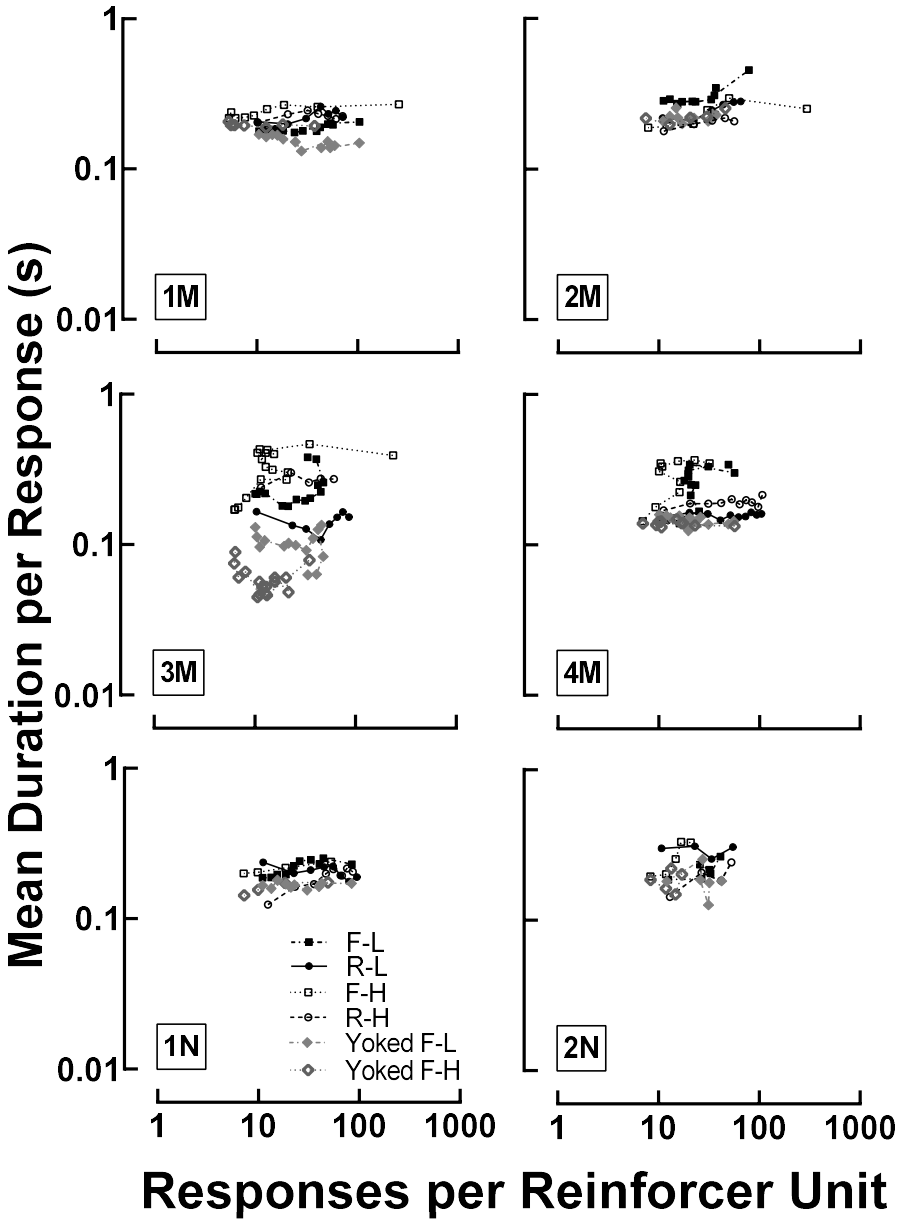

Figure B41. Duration per response as a function of responses per reinforcer. From Experiment 1, data are shown for the F-L (closed back squares), F-H (open black squares), R-L (closed black circles), and R-H (open black circles) progressions, and from Experiment 2, data are shown for the Yoked F-L (closed gray diamonds) and Yoked F-H (open gray diamonds) progressions.

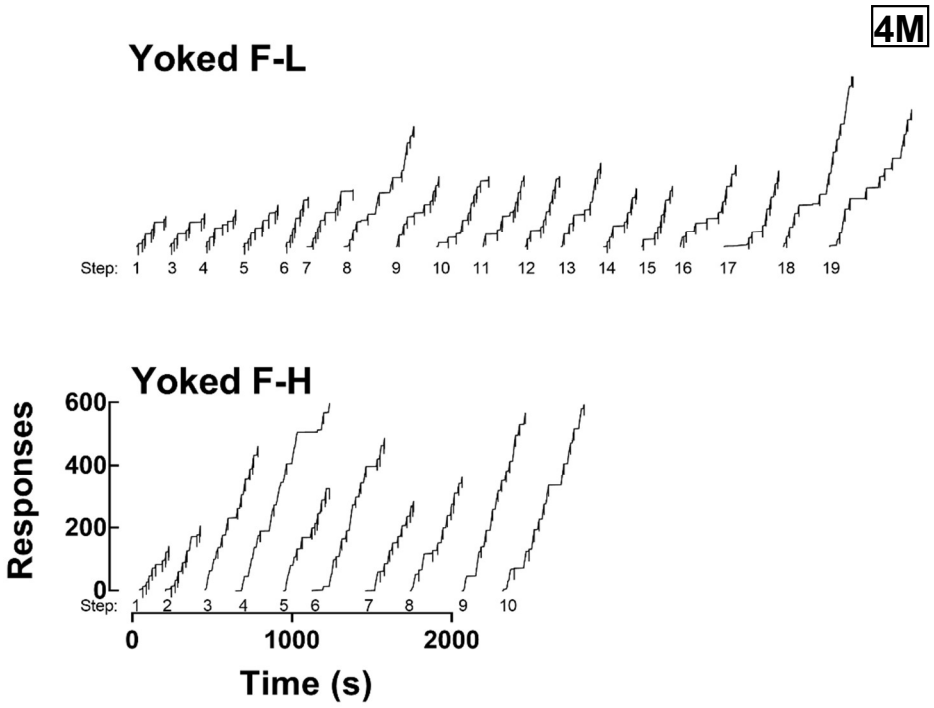

Figure B42. Detailed cumulative record for yoked progressions for 4M. Shown are the first 10 reinforcer deliveries or first 600 responses for every step for the Yoked F-L and Yoked F-H progressions in rows. Cumulative responses (y-axis) are shown as a function of time (x-axis). Black data paths show all responses, and black ticks show reinforcer deliveries.

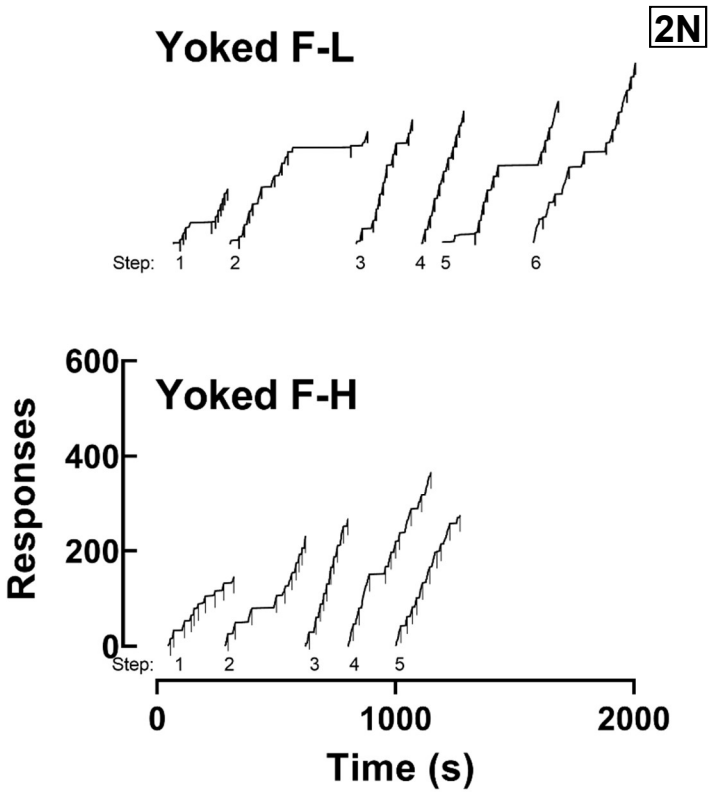

Figure B43. Detailed cumulative record for yoked progressions for 2N. Shown are the first 10 reinforcer deliveries or first 600 responses for every step for the Yoked F-L and Yoked F-H progressions in rows. Cumulative responses (y-axis) are shown as a function of time (x-axis). Black data paths show all responses, and black ticks show reinforcer deliveries.

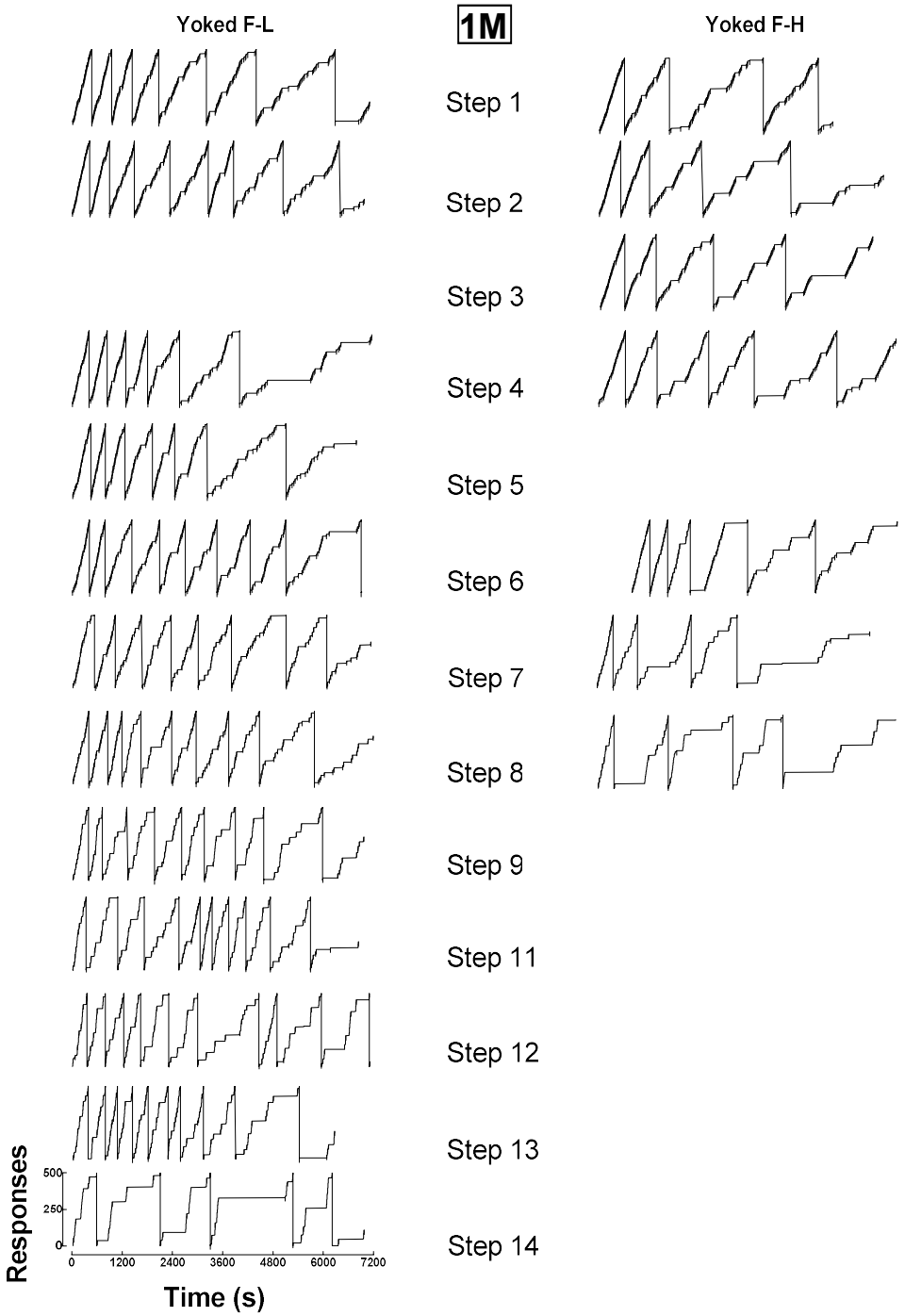

Figure B44. Cumulative record for yoked progressions for 1M. Cumulative responses (y-axis) are shown as a function of time in 2-hr sessions (x-axis). Black data paths show all responses, and black ticks show reinforcer deliveries for Yoked F-L (left column) and Yoked F-H (right column) progressions.

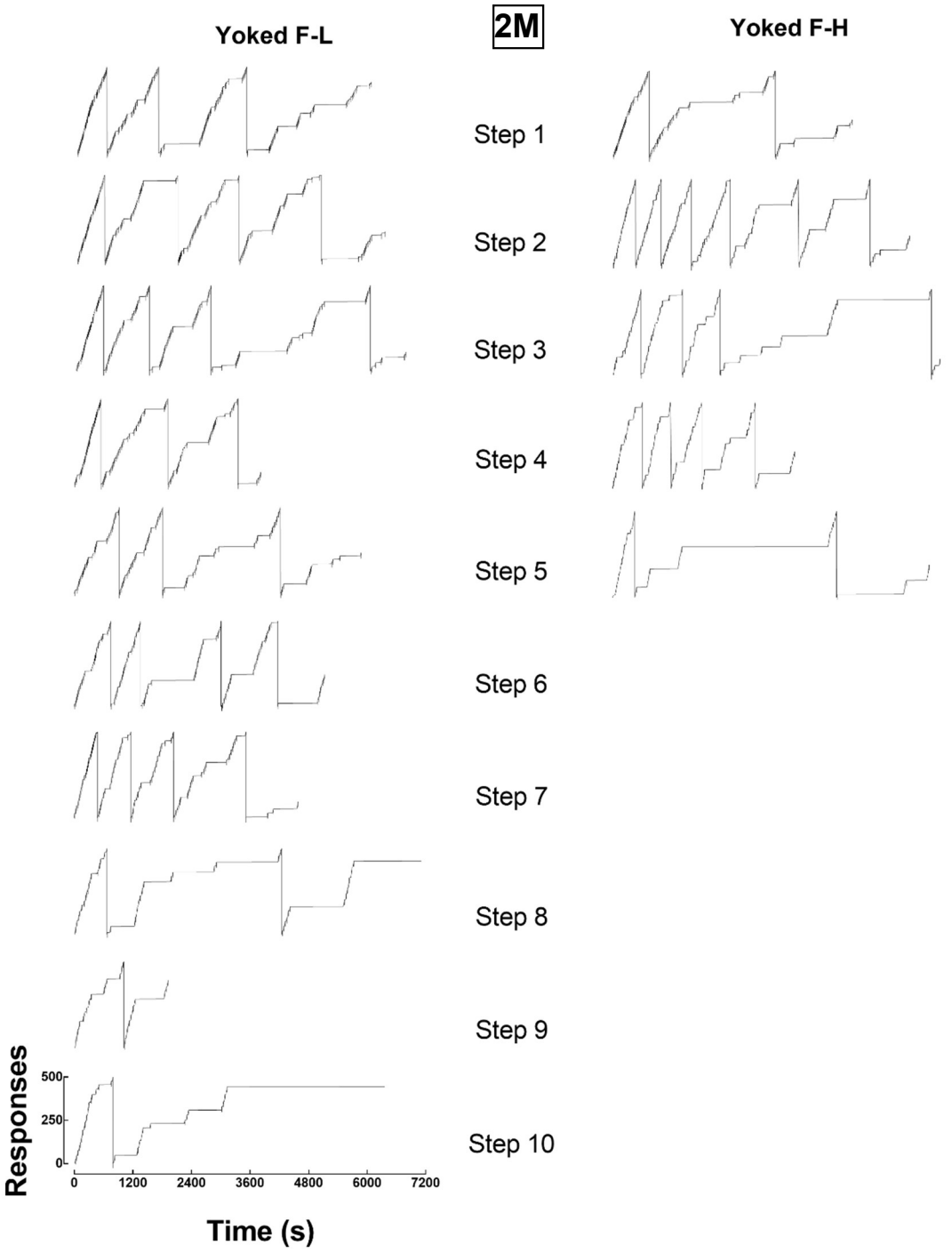

Figure B45. Cumulative record for yoked progressions for 2M. Cumulative responses (y-axis) are shown as a function of time in 2-hr sessions (x-axis). Black data paths show all responses, and black ticks show reinforcer deliveries for Yoked F-L (left column) and Yoked F-H (right column) progressions.

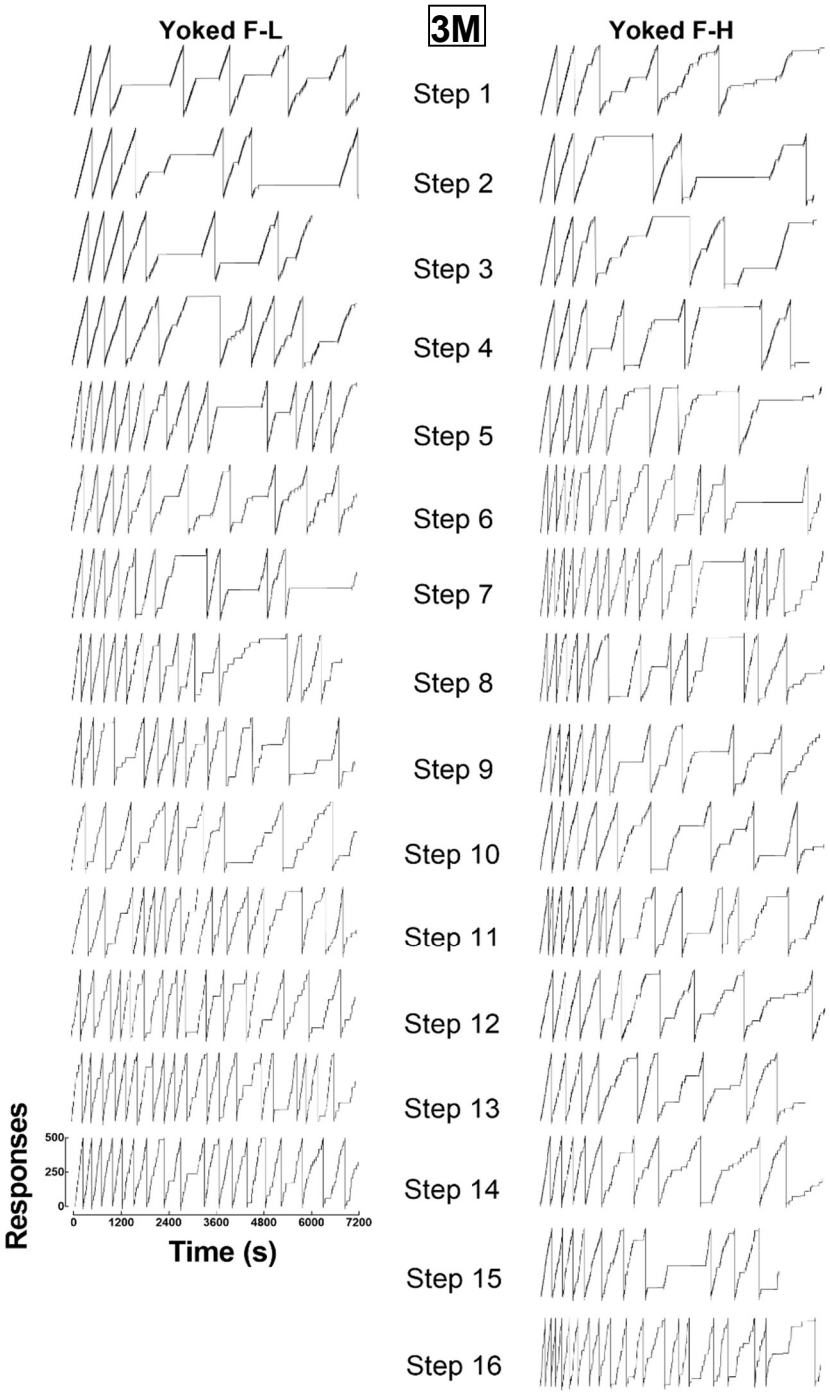

Figure B46. Cumulative record for yoked progressions for 3M. Cumulative responses (y-axis) are shown as a function of time in 2-hr sessions (x-axis). Black data paths show all responses, and black ticks show reinforcer deliveries for Yoked F-L (left column) and Yoked F-H (right column) progressions.

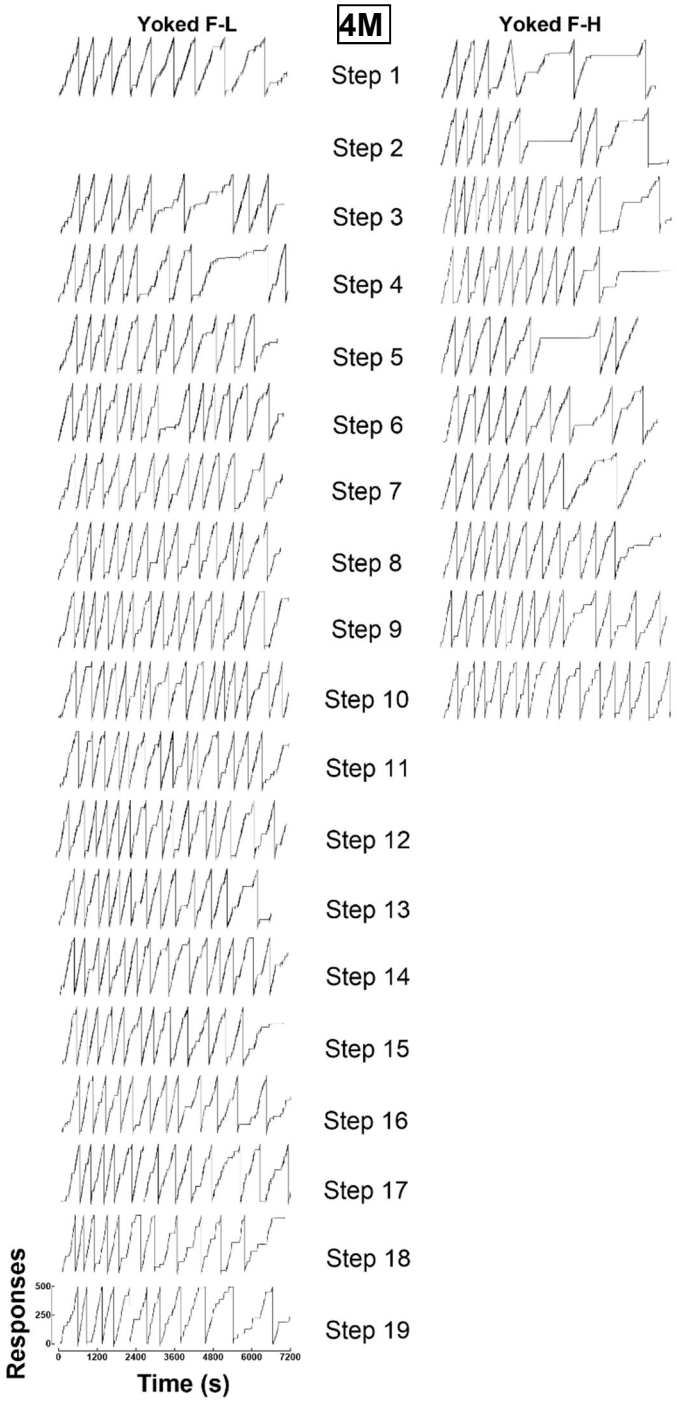

Figure B47. Cumulative record for yoked progressions for 4M. Cumulative responses (y-axis) are shown as a function of time in 2-hr sessions (x-axis). Black data paths show all responses, and black ticks show reinforcer deliveries for Yoked F-L (left column) and Yoked F-H (right column) progressions.

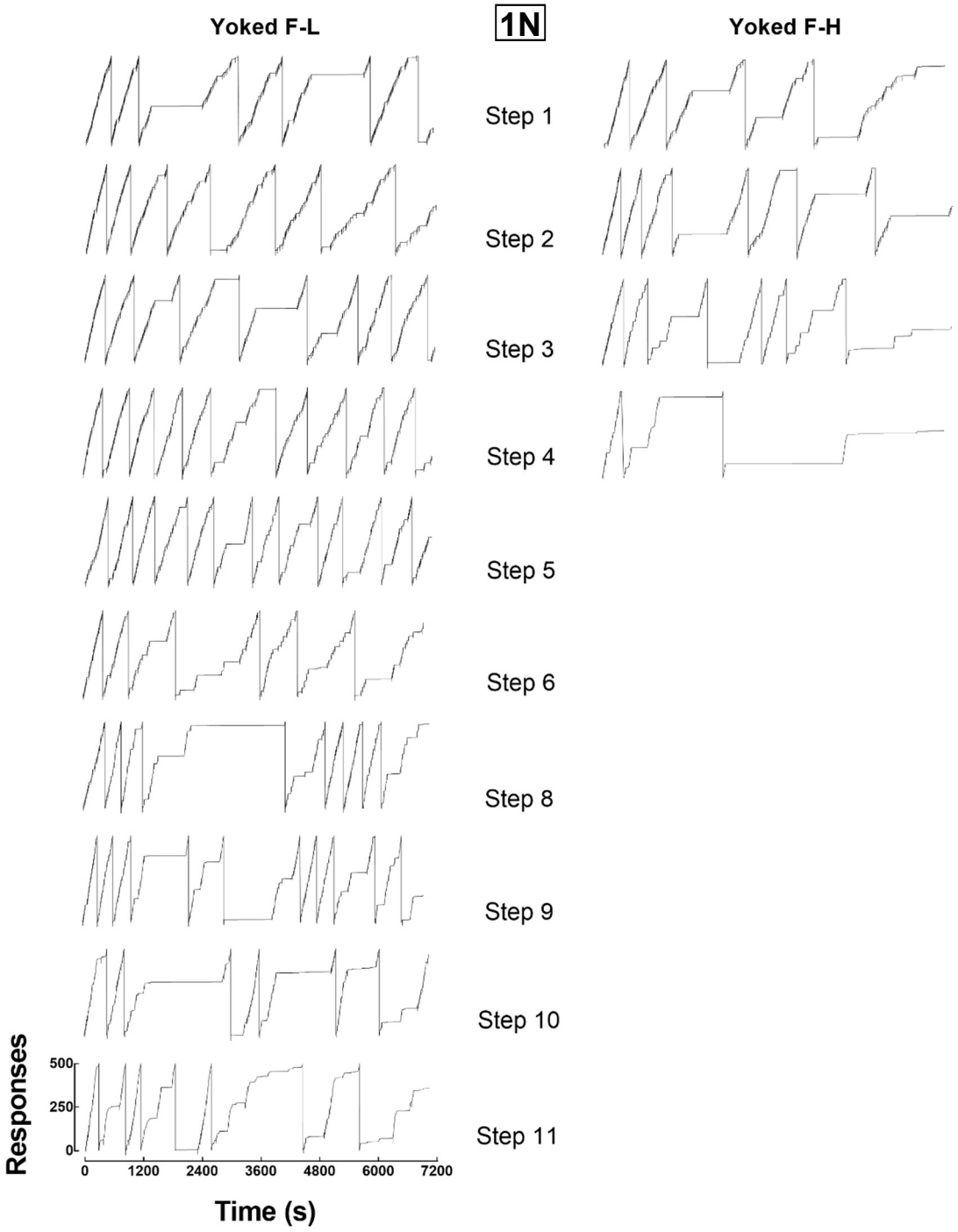

Figure B48. Cumulative record for yoked progressions for 1N. Cumulative responses (y-axis) are shown as a function of time in 2-hr sessions (x-axis). Black data paths show all responses, and black ticks show reinforcer deliveries for Yoked F-L (left column) and Yoked F-H (right column) progressions.

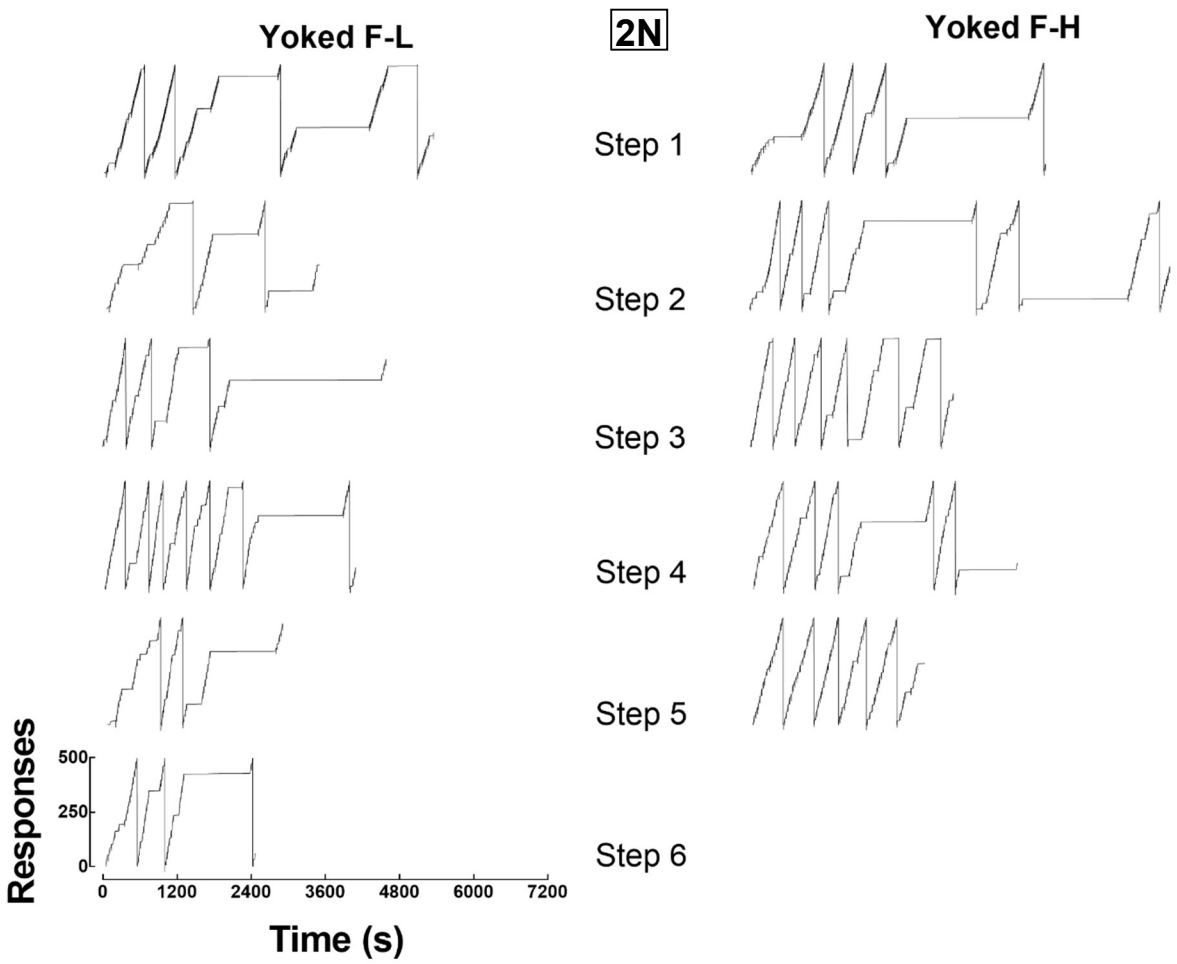

Figure B49. Cumulative record for yoked progressions for 2N. Cumulative responses (y-axis) are shown as a function of time in 2-hr sessions (x-axis). Black data paths show all responses, and black ticks show reinforcer deliveries for Yoked F-L (left column) and Yoked F-H (right column) progressions.

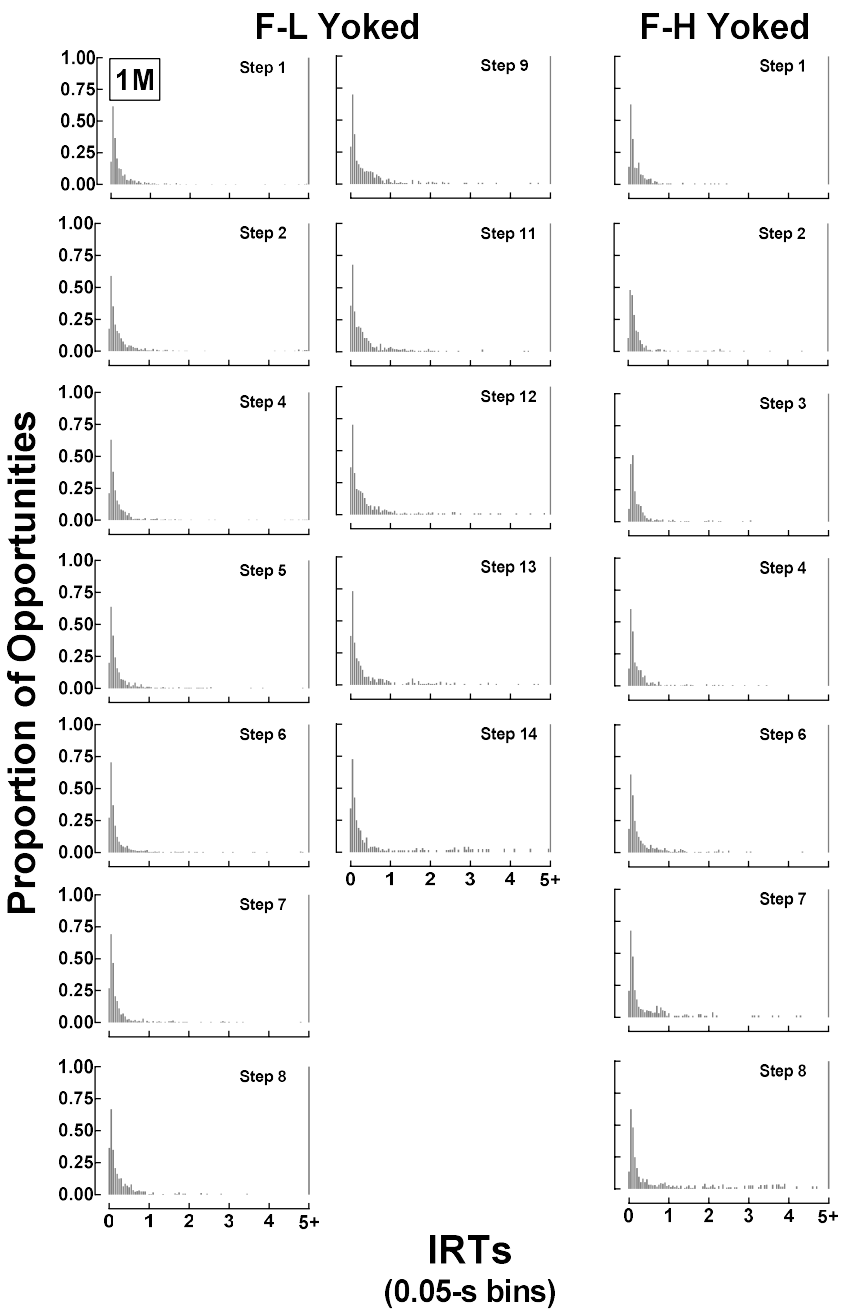

Figure B50. IRT distributions for 1M yoked progressions. Shown are the proportion of IRT opportunities (left y-axis) across 0.05-s bins (x-axis) for the Y-F-L (left columns) and Y-F-H (right column) progressions at each unit price (rows). Thin gray bars show all IRTs and the black data path shows criterion IRTs.

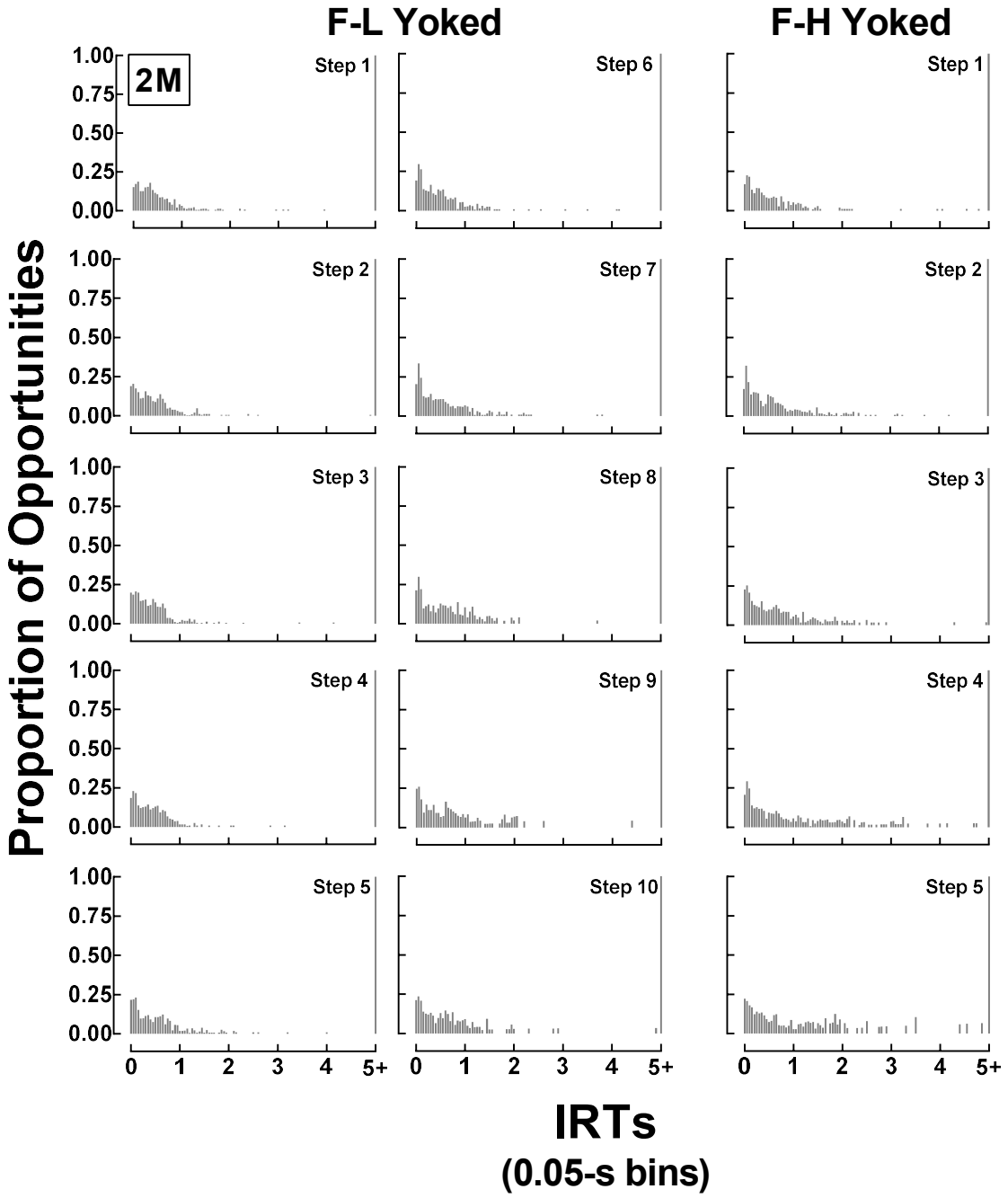

Figure B51. IRT distributions for 2M yoked progressions. Shown are the proportion of IRT opportunities (left y-axis) across 0.05-s bins (x-axis) for the Y-F-L (left columns) and Y-F-H (right column) progressions at each unit price (rows). Thin gray bars show all IRTs and the black data path shows criterion IRTs.

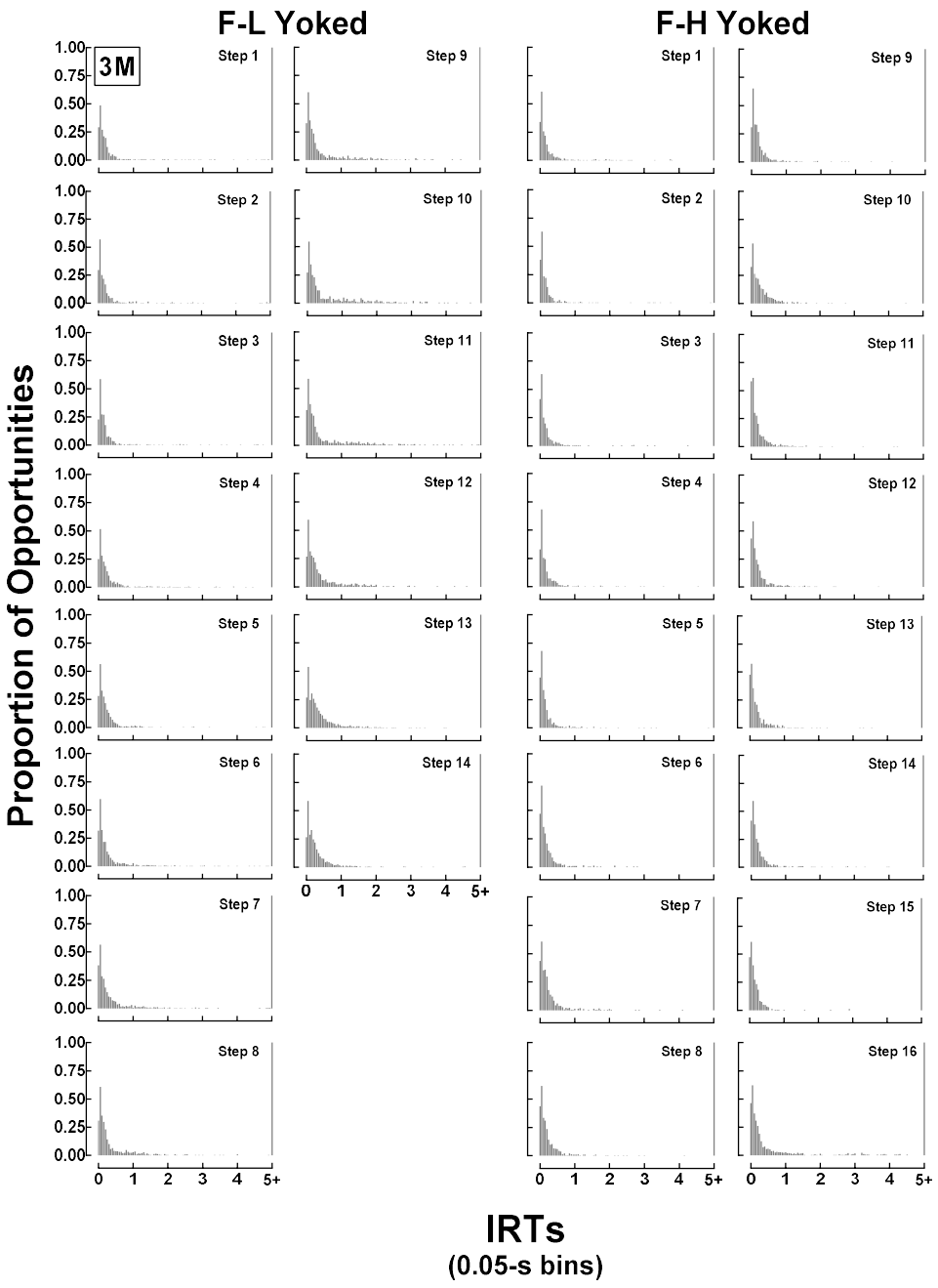

Figure B52. IRT distributions for 3M yoked progressions. Shown are the proportion of IRT opportunities (left y-axis) across 0.05-s bins (x-axis) for the Y-F-L (left columns) and Y-F-H (right column) progressions at each unit price (rows). Thin gray bars show all IRTs and the black data path shows criterion IRTs.

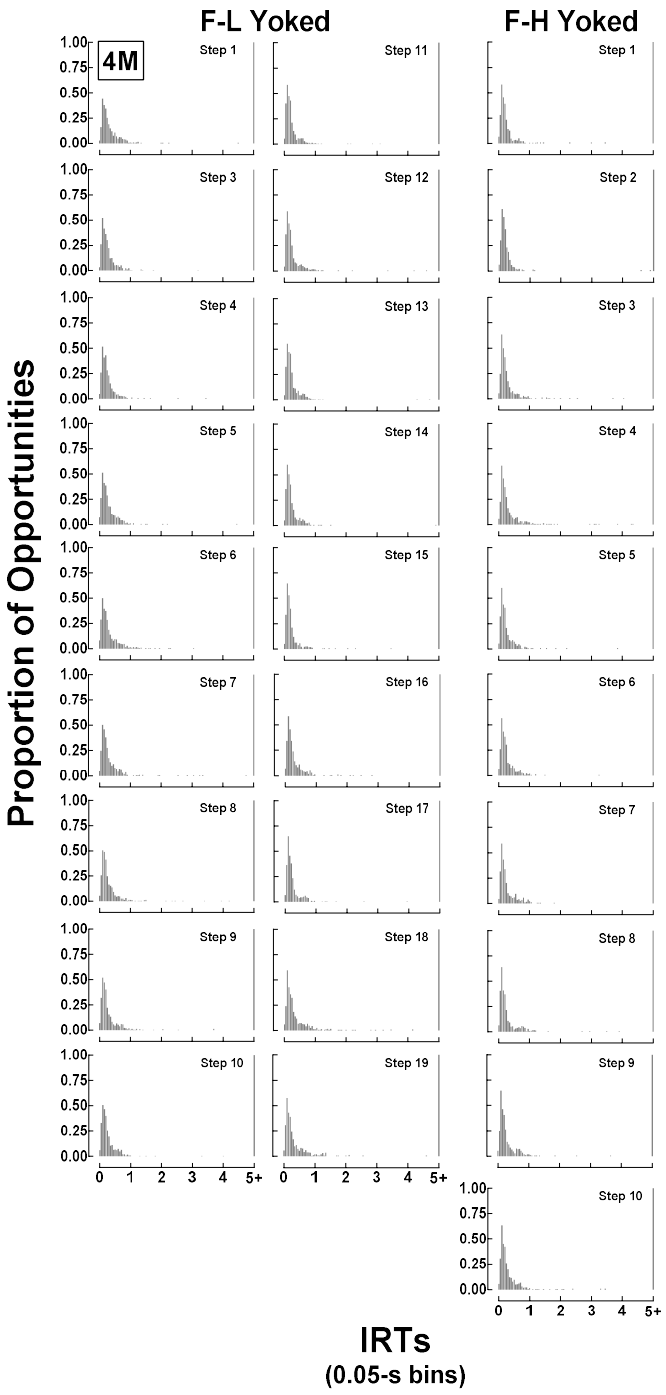

Figure B53. IRT distributions for 4M yoked progressions. Shown are the proportion of IRT opportunities (left y-axis) across 0.05-s bins (x-axis) for the Y-F-L (left columns) and Y-F-H (right column) progressions at each unit price (rows). Thin gray bars show all IRTs and the black data path shows criterion IRTs.

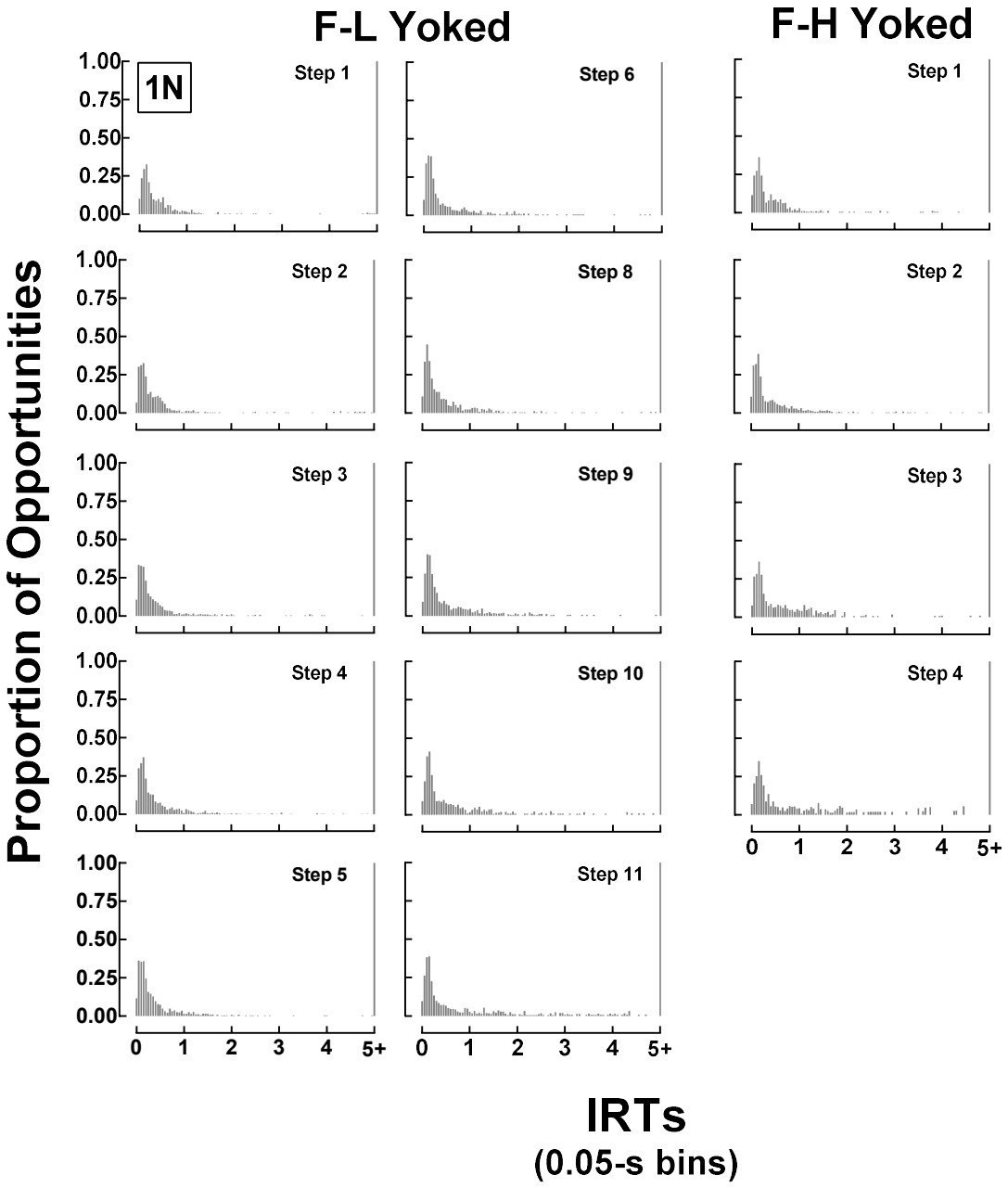

Figure B54.IRT distributions for 1N yoked progressions. Shown are the proportion of IRT opportunities (left y-axis) across 0.05-s bins (x-axis) for the Y-F-L (left columns) and Y-F-H (right column) progressions at each unit price (rows). Thin gray bars show all IRTs and the black data path shows criterion IRTs.

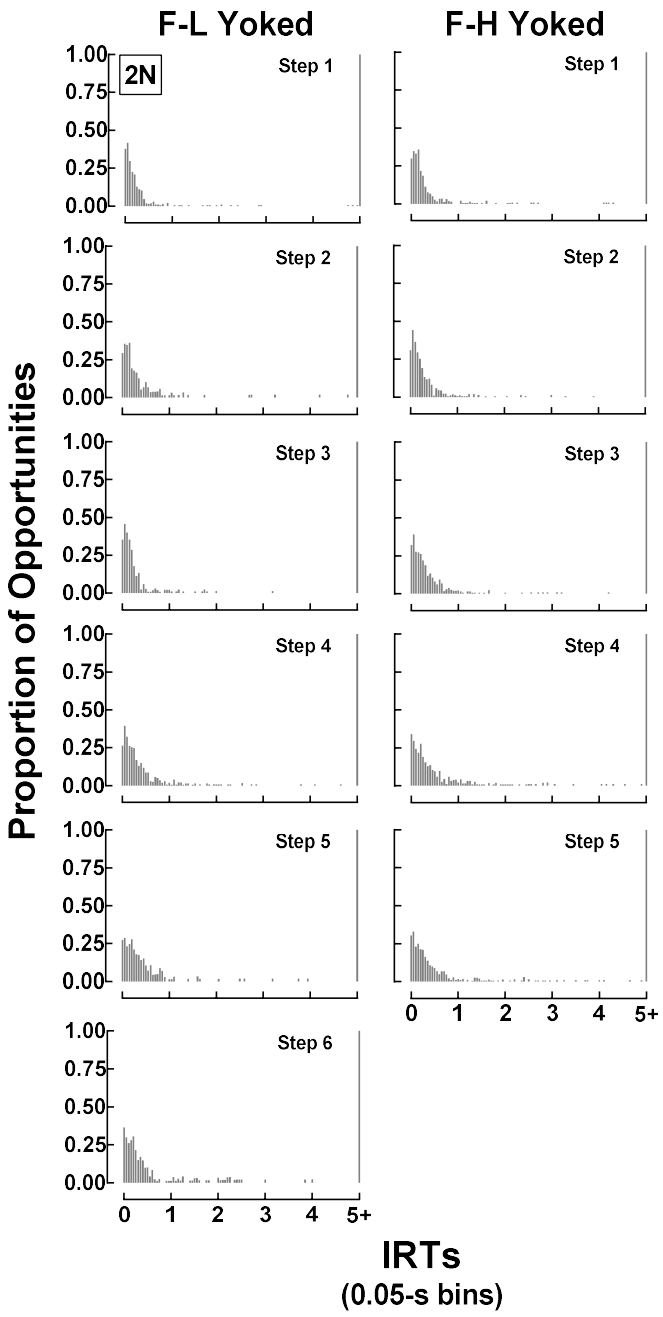

Figure B55.IRT distributions for 2N yoked progressions. Shown are the proportion of IRT opportunities (left y-axis) across 0.05-s bins (x-axis) for the Y-F-L (left columns) and Y-F-H (right column) progressions at each unit price (rows). Thin gray bars show all IRTs and the black data path shows criterion IRTs.

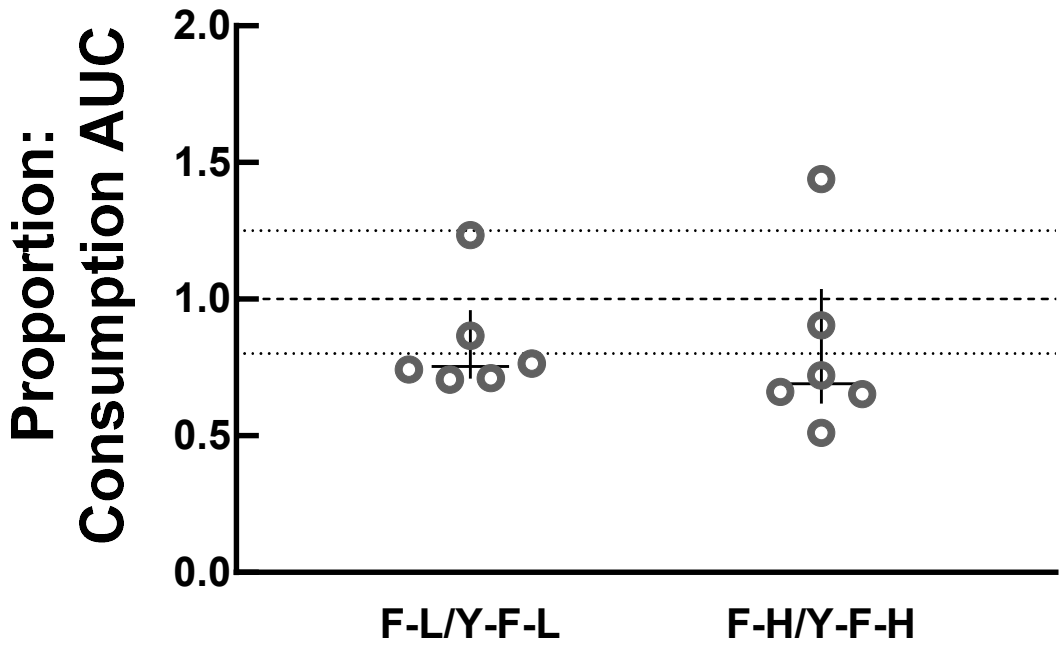

Figure B56. Proportions comparing force and yoked progression AUCs. Shown are proportion measures (y-axis) calculated by dividing the AUC from one progression by another (x-axis). Lines show medians and error bars show IQRs. A zone of equivalence (for confidence intervals) is shown between 0.8-1.25 (dotted lines).

Appendix C

C. Inconsistent Experiment 2 Consumption Data

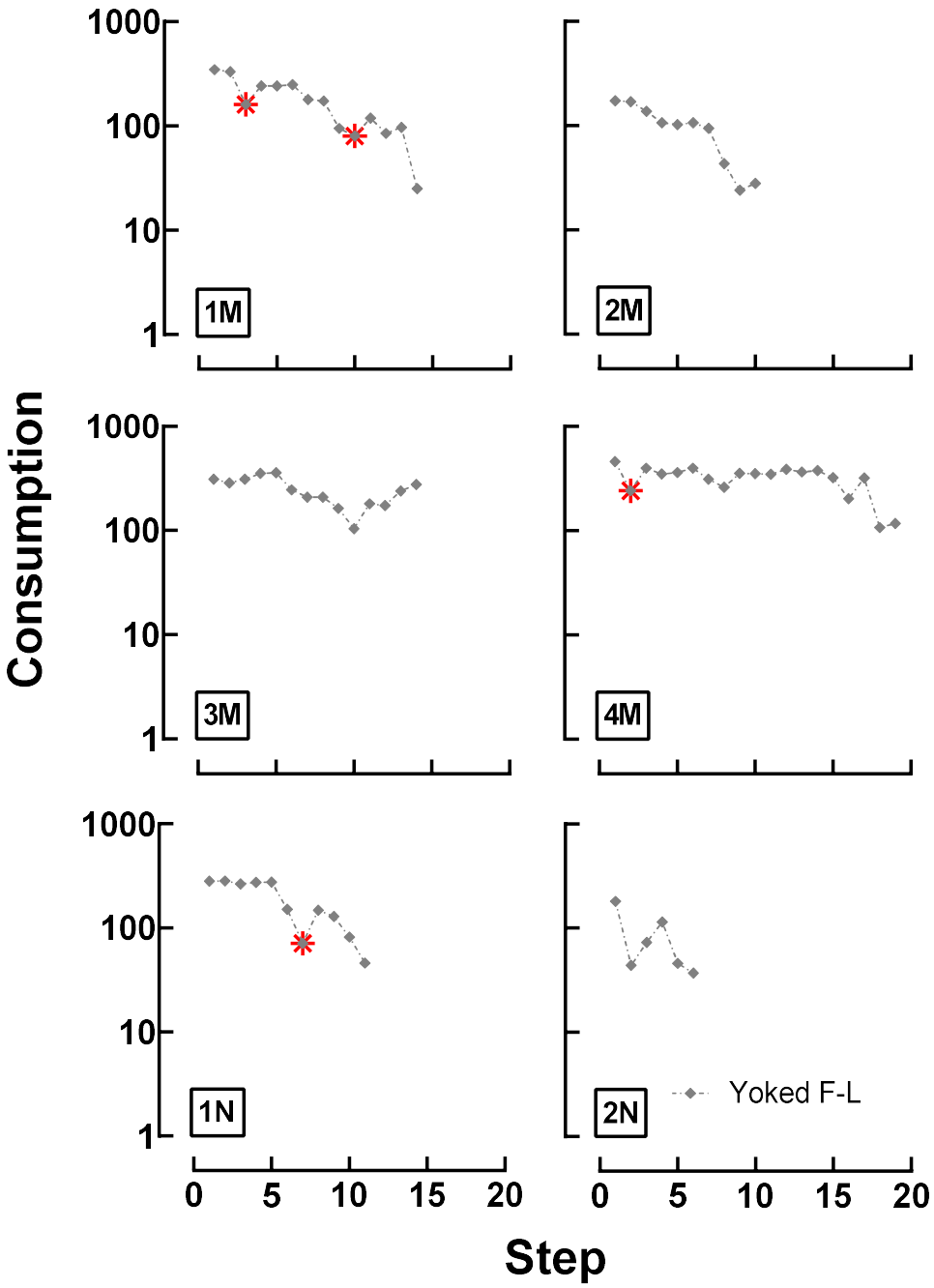

Figure C1. Inconsistent consumption from the Y-F-L condition. Red stars denote inconsistent consumption data that corresponded to dates when K changed cages.

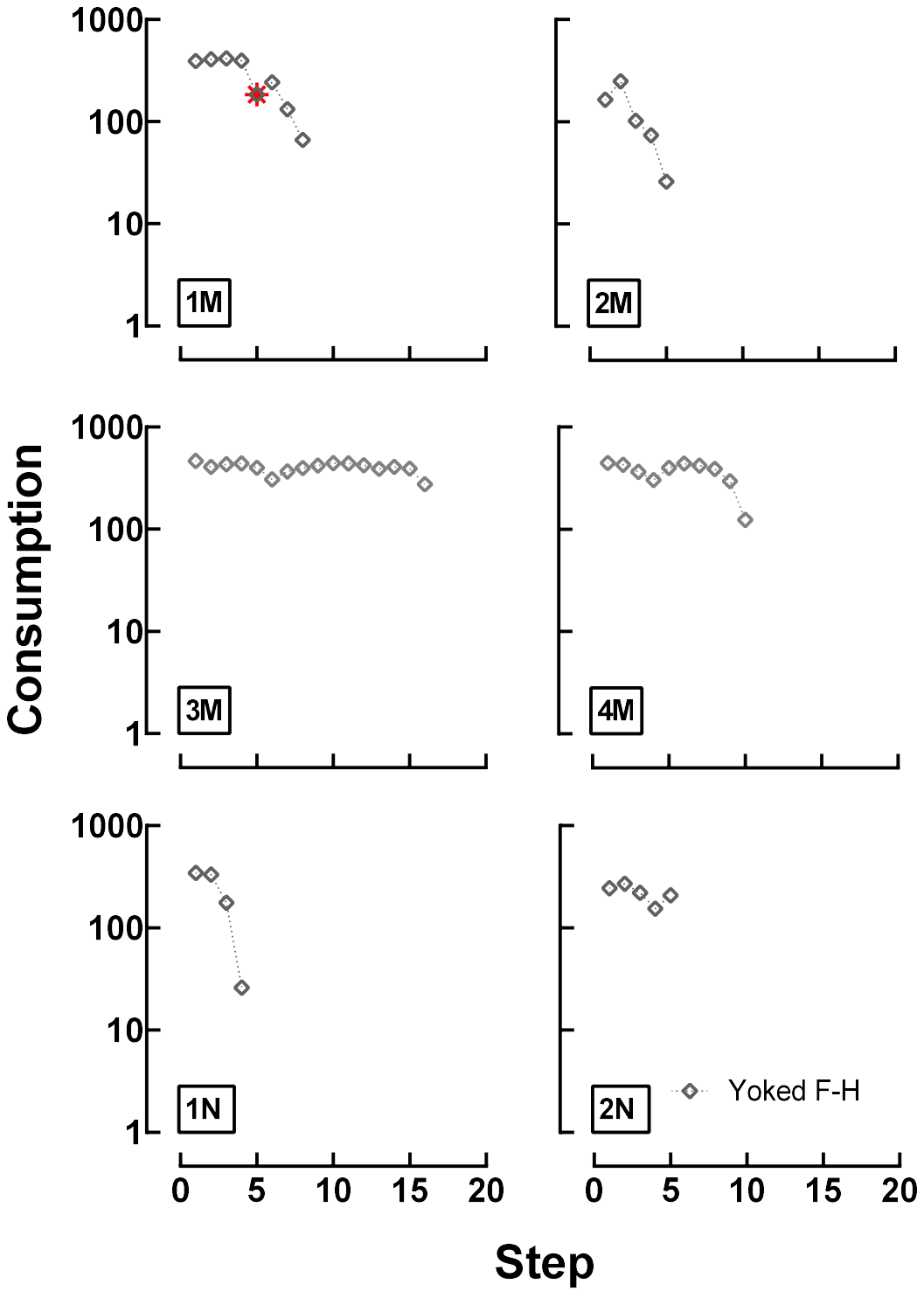

Figure C2. Inconsistent consumption from the Y-F-H condition. Red stars denotes inconsistent consumption datum that corresponded to date when K changed cages.

Appendix D

D. Inconsistent Experiment 2 Response Rate Data

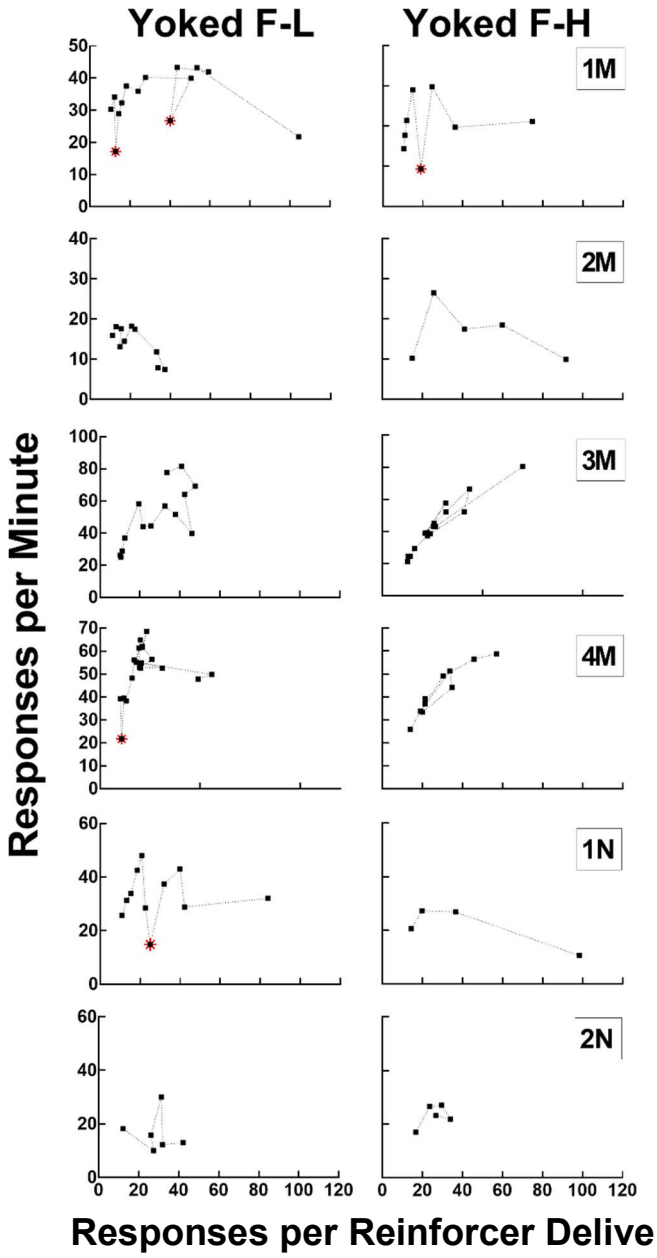

Figure D1. Inconsistent response rate data. Rates (y-axis) plotted as a function of responses per reinforcer delivery (i.e., obtained ratio) for the yoked F-L (left panels) and yoked F-H progressions (right panels) for individual animals (rows). Red stars denote inconsistent rate data that correspond to dates when K changed cages.

Appendix E

E. Email from ACU Facility Manager Describing Food Found after Cage Changes

[redacted]
to [redacted]

12:11 PM (0 minutes ago)

Hi [redacted],

I am truly sorry to hear this. K[redacted] never admitted to placing food in the bottom of the cages when asked. Just so you are aware K[redacted] no longer works for the ACU. We did see one cage with food in the bottom when she was still working in the room and we were checking in on her after she serviced the room, but she denied doing this also. Let me know if you need anything else from Dr. [redacted] and I to help you with your dissertation.

Thanks,
A[redacted]
Facility Manager
University of Kansas
Animal Care Unit
[redacted]
[redacted] Office
[redacted] Cell
Research and compassion go hand in hand.

From: Lemley, Shea Michelle
Sent: Thursday, April 26, 2018 11:50 AM
To: [redacted]
Cc: [redacted]
Subject: Feeding and Cage Change Issues for Dissertation

...

Hi A[redacted],

I'm working on my dissertation, and I believe several of my data points were impacted by K[redacted]'s cage changes. For my second study, I think I may need to exclude 13% of the data for one of my animals, and I will likely need to exclude some data for more than half of my animals.

Because I am planning to exclude the data from the affected sessions, I would really like to have some sort of corroboration for my committee. I need to be able to defend my decisions as part of the dissertation process. Could you provide some sort of confirmation for me? Did K[redacted] admit to adding additional food or was there any other substantiation?

I would really appreciate any assistance you can provide.

Best,
Shea

Figure E1. Cage change observations.

Appendix F

F. Email from ACU Interim Director Detailing Dates of Cage Changes

From: [redacted]
Sent: Friday, February 09, 2018 2:02 PM
To: [redacted]
Cc: [redacted]
Subject: RE: Cage Changes

Hi [redacted]

Thanks for talking to me on the phone about this so I could gain more insight into the situation. I will talk to K[redacted] first thing Monday when she returns about this. Here is the cage change data you requested. Looking at the data now I forgot that Z[redacted] had work restrictions from an injury that started mid-October and he was only checking the room from that point forward due to his restrictions but K[redacted] was to performing the cage changes, due to that I added the data from October to now.

October 2017

10/2 Z[redacted] changed cages
10/5 Z[redacted] changed cages
10/9 Z[redacted] changed cages
10/12 Z[redacted] changed cages
10/16 K[redacted] changed cages
10/19 K[redacted] Changed cages
10/23 K[redacted] changed cages
10/26 K[redacted] changed cages
10/30 K[redacted] changed cages

November2017

11/2 T[redacted] changed cages
11/6 A[redacted] Changed cages
11/9 A[redacted] changed cages
11/13 K[redacted] Changed cages
11/16 K[redacted] changed cages
11/20 K[redacted] changed cages
11/27 K[redacted] changed cages
11/30 K[redacted] changed cages

December 2017

12/4 A[redacted] changed cages
12/7 K[redacted] changed cages
12/11 A[redacted] changed cages
12/14 K[redacted] changed cages
12/18 K[redacted] changed cages
12/21 Z[redacted] changed cages
12/26 K[redacted] changed cages
12/28 K[redacted] changed cages

January 2018

1/4 K[redacted] changed cages
1/8 K[redacted] changed cages
1/11 K[redacted] changed cages
1/18 K[redacted] changed cages
1/22 K[redacted] changed cages
1/25 K[redacted] changed cages
1/29 K[redacted] changed cages

February 2018

2/1 K[redacted] changed cages
2/5 K[redacted] changed cages
2/8 K[redacted] changed cages

A[redacted]
Interim Director
University of Kansas
Animal Care Unit
[redacted]
[redacted] Office
[redacted] Cell
Research and compassion go hand in hand.

Figure F1. Dates of cage changes.